ISSN 2436-5173 (Online)

Metallomics Research

Vol. 1 / No. 1
October 2021

Japan Society for
Biomedical Research on Trace Elements

On the occasion of the first issue of *Metallomics Research*

Dear colleagues,

I would like to extend my heartfelt congratulations on the launching of the first issue of *Metallomics Research* as an international official journal of the Japan Society for Biomedical Research on Trace Elements.

The Japan Society for Biomedical Research on Trace Elements has published *Biomedical Research on Trace Elements* as its official journal since its establishment in 1990. However, the study of metals in biological systems has recently re-emerged to become an increasingly important area of research. Considering the current activities in this research field, we have decided to launch the new journal, which is open access with global peer reviewing.

The term "metallomics" was coined by Professor Hiroki Haraguchi, a previous director of our Society. As you may know, the term has been officially defined by the International Union of Pure and Applied Chemistry. Japan is the cradle of metallomics, and metallomics is disseminated around the world. Therefore, the launching of *Metallomics Research* is a great pleasure and pride of our Society. In addition, the 8th International Symposium on Metallomics (ISM-8) is scheduled in Japan in the summer of 2022. The first ISM was held in Japan in 2007 with Professor Haraguchi as chair. That this will be the second time for ISM to be held in Japan indicates that the research field of metallomics has reached its second and more mature phase. This is also the best timing to launch the journal.

The Japan Society for Biomedical Research on Trace Elements brings together researchers from diverse areas, including medicine, biology, toxicology, analytical chemistry, environmental science, pharmaceutical science, and so on. I expect that the publication of *Metallomics Research* would further stimulate the international activities of our Society.

Yasumitsu Ogra, Ph.D.
President
The Japan Society for Biomedical Research on Trace Elements

Metallomics Research

Vol. 1 / No. 1
October 2021
ISSN 2436-5173 (Online)

Japan Society for
Biomedical Research on Trace Elements

Index

Editorial Office

Seishinsha, co. Ltd.,
Japan society for Biomedical Research on Trace Elements
2-8-13 Fukashi, Matsumoto-shi, Nagano 390-0815, Japan
Tel: +81-263-32-2301
Fax: +81-263-36-4691
Editorial Office: brte-post@seisin.cc
URL: https://www.brte.org/
https://metallomicsresearch.brte.org/

Index

Regular article

Review https://metallomicsresearch.brte.org

Metallomics Research — Good Luck on New Publication

Hiroki Haraguchi

Nagoya University (Professor Emeritus)

Abstract

The Japan Society for Biomedical Research on Trace Elements decided to publish the new journal "Metallomics Research" from October, 2021, instead of their previous journal "Biomedical Research on Trace Elements" (BRTE). On this occasion, the history of trace element study in Japan and the progress of metallomics as integrated biometal science proposed about 20 years ago are reviewed. In the latter part of this review, basic concepts of metallomics research are discussed in relation to homeostasis and all-present theory, and finally it is considered that metallomics research has a mission to contribute to our humans and nature through the SDGs (Sustainable Development Goals), mainly with focusing on health science and environmental/green science as multidisciplinary science.

Key words: metallomics, metals in biology, health science, homeostasis, multidisciplinary science, all-elements present theory

Statements about COI: The author declares no conflict of interest associated with this manuscript.

1. Metals in biology

In 1969, the present author was employed as an assistant professor in the laboratory of Prof. Keiichiro Fuwa in the Department of Agricultural Chemistry, Faculty of Agriculture, the University of Tokyo. Prof. Fuwa had spent in the Medical School of Harvard University for 14 years, where he worked as the research staff with Prof. BL Vallee. Prof. Vallee was famous in the pioneer work of zinc physiology. In 1968, Prof. Fuwa came back to Japan, and he was responsible for the laboratory of Analytical Chemistry. There, he proposed to the laboratory members that "metals in biology" was the main research theme of his laboratory. "Metals in biology" was really new aspect to us, and gave great influences in our research life after that.

*Correspondence:
525-1-3-506, Shinano-machi, Totsuka-ku, Yokohama 244-0801, Japan (Home address).
Tel: +81 80 5883 4122
E-mail: haraguch@gmail.com

Received: September 1, 2021
Accepted: September 22, 2021
Released online: October 15, 2021

2. Progress of analytical atomic spectrometry

In 1974, Prof. Fuwa also held his position as the Division Head of Chemistry and Physics in the National Institute for Environmental Studies which was just newly established, and I moved to the same institute. As well known, those days our country had serious environmental pollution problems such as Minamata disease and Itai-Itai (Auch-Auch) disease caused by toxic metals such as mercury and cadmium. However, it was not so easy to analyze mercury, cadmium and other toxic metals sensitively and precisely, and we had to start to develop sensitive analytical instruments. Those days, atomic absorption

spectrometry (AAS) was the popular method for environmental analysis, but AAS was a tedious method for analyses of many elements in many samples, because AAS was the instrument for single element analysis. Then we tried to develop new analytical methods which allowed simultaneous multielement analysis using an inductively coupled argon plasma (ICP), "so-called" inductively coupled plasma atomic emission spectrometry (ICP-AES) and inductively coupled plasma mass spectrometry (ICP-MS). Both methods can analyze 40-50 elements simultaneously with the analytical sensitivity (detection limit) of ppb (10^{-9} g/ml) level for the former and ppt (10^{-12} g/l) level for the latter [1,2].

3. Japan Society for Biomedical Research on Trace Elements and Journal of "Biomedical Research on Trace Elements (BRTE)"

In 1984, the 1st Conference of International Society for Trace Element Research in Humans (ISTERH) was held by the effort of Dr. Prasad, Dr. Abdulla, Dr. Brewer, Dr. Fell, Dr. Parr, and Dr. Solomons in Palm Spring, California, USA. Prof. Issei Nomiyama (Jichi Medical University), who was one of participants from Japan in the 1st conference, invited the 2nd conference to Japan. Then, in 1989, the 2nd Conference (ISTERH) was held in Tokyo, under the chairmanship of Prof. Hiroshi Tomita (Nihon University). More than 1000 participants who were interested in trace element research related to medical and environmental sciences got-together in Tokyo from the world. After the conference the excellent proceedings over 500 pages was published by the edition of Prof. Tomita [3]. According to the proceedings, Prof. Prasado delivered the invited lecture entitled "Discovery of Human Zinc Deficiency and Marginal Deficiency of Zinc", and Prof. Tomita did "Zinc in Taste and Smell Disorders" [3]. In response to success of 2nd ISTERH, the Japanese scientists who participated the 2nd conference, decided to establish the Japan Society for Biomedical Research on Trace Elements in 1990. At the same time, the quarterly journal entitled "Biomedical Research on Trace Elements" (BRTE) was also launched by the Japan Society. The annual meetings of the society have been held every year around many places, and 31 volumes of BRTE have been published, where the original research papers and notes, reviews and other related information have been presented in each volume. As the result, the society has been playing important roles as the platform for scientific information and mutual exchange of biomedical research concerned with trace elements in Japan until now. Many medical doctors joined as the members of the society, and they had hot discussion in the meetings. Then we could learn many practical matter and knowledge concerned with medical and clinical fields. All articles in BRTE can be seen in the J-STAGE, and so the activities of the society are not commented any more.

Here I would like to introduce unforgettable memory that I got in the society meeting. I could not remember when, but I could not forget Prof. Nomiyama's report provided in the executive board meeting. One day he reported the results of application of scientific grant in the executive board meeting. He was enthusiastic to organize the big research group of trace element research as the national project under the support of big scientific grant from the government in the early 1990s, but he failed after application several times. Most clear reason why he could not succeed in getting such a grant, he said, was that the definition of trace elements and their biological significance were incomprehensible in comparison to vitamins and hormones. In the Evaluation Committee for Grant, he got many comments that the function of each vitamin or hormone was known clearly, while the biological functions of trace elements were not elucidated clearly. "What are trace elements and how much are they useful for life?" This Nomiyama's report shocked to me, but it became the origin to explore some understandable and clear term instead of trace element.

About 10 years later, I got the Grant-in-Aid for Specially Promotion Research with the program of "Creation of New Science "Metallomics" for 2004-2006 (3 years term). This was the kind of national research project. In this project, terminology of metallomics was approved in the Evaluation Committee for Grant. At this moment, the Prof. Nomiyama's report described above was remembered, although he already died.

4. Proposal of "Metallomics" and after that

In January, 2004, at last, the first paper entitled with "Metallomics as Integrated Biometal Science" was published in JAAS (Journal of Analytical Atomic Spectrometry) from the Royal Society of Chemistry [4]. Thus the year 2004 was a memorial year for "metallomics" in science. Since many papers in various journals have been published and the international or domestic meetings have been often held, we can get easily the information about progress of metallomics from many sources nowadays. Also, I published the review articles about metallomics in the journals [5.6], and Ogra and Hirata published an excellent book

[7]. Thus I hesitated to write the review which was asked from the editorial office. After significant consideration, however, I made up my mind to write the present review, by adding the brief explanation about the Japan Society of Biomedical Research on Trace Elements and their journal BRTE in Section 3.

In late1990s, proteomics was emphasized on an emerging scientific field after genomics. Omics-science such as genomics and proteomics were interested in interdisciplinary science to cell biology. Those days I was thinking the idea to take the position for metals in biology as a part of omics-science. One evening with drinking, I got inspiration of "metallomics" as the "metal-assisted biological function science" in early 2002. In 2002, fortunately, I had the chances to convey the idea "metallomics" in domestic seminar and international symposium. Then, actually the year of 2002 was the milestone for "metallomics".

In June, 2002, the present author gave the invited lecture in the Tokushima Seminar on Chemical Engineering held in Tokushima, Japan [8]. The title of the lecture in the seminar was "A Challenge to Pico-World and Metallomics: A New Frontier of Trace Element Chemistry" (in Japanese). In this seminar, I proposed the scientific term of "metallomics" for the first time. Since the Tokushima seminar was a memorial talk, the abstract of the presentation is cited below (translated). [8]

> *In recent years, the analytical detection sensitivities have been increasingly improved to pico (10^{-12}) gram in the absolute amount or sub-ppt (10^{-12} g/ml) level in the concentration, according to the development of ICP-MS. As a result, now we have a good chance to challenge the research on the pico-technology or pico-science, which may be called "Pico-World Science".*
>
> *Such a progress of analytical atomic spectrometry will lead to another interesting and important research on bio-trace elements in the biological systems including our "human beings" because all-elements including ultratrace elements might be contained in the biological systems. This concept is referred to as "Extended All Present Theory of the Elements". Furthermore, various trace elements play important roles in the biological systems, as metalloproteins and/or metalloenzymes. Then, now is the good time to challenge to trace element biochemistry to open our new scientific world "**metallomics**".*

The second chance was the International Symposium on Bio-Trace Elements 2002 (BITREL 2002) in autumn of the same year [9]. This symposium was held as the joint symposium of RIKEN and Yamanashi Institute of Environmental Sciences (YIES), for October 28-November 2, which was co-organized by Dr. Shuichi Enomoto in RIKEN and Dr. Yoshiyuki Seko in YIES. The present author delivered the invited lecture, entitled on "Trace Element Speciation for Metallomics". "Metallomics" was proposed as a new scientific term in English for the first time. As can be seen from the abstract in the Tokushima seminar [8], my first idea for metallomics came as the result of progress of analytical atomic spectrometry as well as the concept of the All Present Theory of the Elements derived from the idea for all elements analysis of all materials on earth. However, my idea was still under consideration at this moment. The followings are the abstract in the proceedings in BITREL 2002 [9].

> *In this paper, "metallomics" is newly proposed as a new scientific field in order to integrate the research fields related to bio-trace metals. Metallomics might be the scientific field of post-genomics and post-proteomics, where metal-containing compounds are defined as metallome, in a similar manner to genome in genomics and proteome in proteomics. Since the elucidation of the biological or physiological functions of metal-containing species in the biological systems is the main research target of metallomics, elemental speciation is important as one of analytical technologies to promote metallomics.*

In BITREL 2002, the distinguished scientists in the field of trace metal science were invited; they were Prof. Ryszard Lobinski (Warsaw University of Technology, Warsaw, Poland), Prof. Zhifang Chai (Institute of High Energy Physics, Chinese Academy of Science, Beijing, China), Prof. Wolfgang Maret (Harvard Medical School, USA; now Imperial College, London, UK), Prof. Bibudhendra Sarkar (University of Toronto, Ontario, Canada) and so forth.

The importance of speciation analysis (species analysis) of trace elements in the biological samples and biological systems was emphasized in the lecture, because trace elements (metals actually exist as the ionic forms in the biological systems) are contained in metalloproteins and/or metalloenzymes, and in particular trace elements play essential roles mostly as the active centers of metalloenzymes for biological and physiological functions. On the other hand, it is also known that metals and metalloids often cause seriously toxic or hazardous problems to humans and living organisms due to environmental pollution. These scientific fields including the functions of both essential and toxic trace metals have been generally called "trace element science", as will

be discussed in Section 10. The new scientific term of "metallomics" proposed in two symposiums achieved great response as the hot topics on the science community of trace metal science.

During BITREL 2002, Prof. Lobinski recommended me to submit a paper about metallomics to Journal of Analytical Atomic Spectrometry (JAAS), published from the Royal Society of Chemistry, UK, because the journal was just planning to publish the special issue on "Metals in Biology". Then, in 2004, my paper entitled on "Metallomics as integrated biometal science" was published in JAAS, which was analytical chemistry- or atomic spectrometry-oriented journal. Since the following abstract of the paper in JAAS [4] was the first proposal of metallomics in the scientific journal and gave significant suggestion for future direction of metallomics research, the abstract of the article is cited below [4].

> *In this paper, "metallomics"is proposed as a new scientific field in order to integrate the research fields related to biometal. Metallomics should be a scientific field in symbiosis with genomics and proteomics, because syntheses and metabolic functions of genes, (DNA and RNA) and proteins cannot be performed without the aid of various metal ions and metalloenzymes. In metallomics, metalloproteins, metalloenzymes and other metal-containing biomolecules are defined as"metallomes", in a similar manner to genomes in genomics as well as proteomes in proteomics. Since the identification of metallomes and the elucidation of their biological or physiological functions in the biological systems are main research targets of metallomics, chemical speciation for specific identification of bioactive metallomes is one of the most important analytical technologies to establish as the integrated bio-metal science.*

(Note: In this abstract [4], "*metallomes*" was used as common noun, but it might be my mistake. It is better to use metallome as collective noun because a scientific term of "metallome" is now used for an entirety of bioactive metal and metalloid species.)

5. International Symposium on Metallomics (ISM)

Metallomics had been receiving great attention as the newly emerging scientific field after publication of the above paper in 2004. According to the recommendation of many scientists, the International Symposium on Metallomics 2007 (ISM 2007) was held in Nagoya for November 28-December 1, 2007, as the first symposium on metallomics, which was organized by Haraguchi, chairman as well as by Profs. Kazuo Suzuki, Hiromu Sakurai and Naoki Furuta, vice-chairmen. This symposium was supported by IUPAC (International Union of Pure and Applied Chemistry), Chemical Society of Japan, Nagoya City and other academic societies and companies. In this symposium, about 350 scientists participated and more than 250 lectures and posters were presented [10]. The Proceedings of ISM 2007 was also published as the special issue of Pure and Applied Chemistry from IUPAC in 2008 [11].

In the International Advisory Board meeting of ISM 2007, Haraguchi summarized that ISM 2007 was a successful symposium, and proposed that the symposium would be held regularly in every 2 years around the world, to promote metallomics as an emerging science field in future. This proposal was approved unanimously in the advisory board meeting.

After Nagoya, ISMs have been held at Cincinnati, USA, Munster, Germany, Oviedo, Spain, Beijing, China, Vienna, Austria,

Table 1. | The years, conference place and organizers of the International Symposium on Metallomics (ISM)

	Year	Place	Organizers
1	2007	Nagoya, Japan	H. Haraguchi
2	2009	Cincinnati, USA	J. Caruso, G. Hiefje
3	2011	Munster, Germany	U. Karst, M. Sperling
4	2013	Oviedo, Spain	A. Sanz-Medel
5	2015	Beijing, China	Z. Chai. X. Zhang
6	2017	Vienna, Austria	G. Köllensperger
7	2019	Warsaw, Poland	R. Lobinski. L. Ruzik
8	2021*	Kanazawa, Japan (*scheduled*)	Y. Ogra

* The 8th ISM is scheduled during July 11-14, 2022 in Kanazawa, Japan.

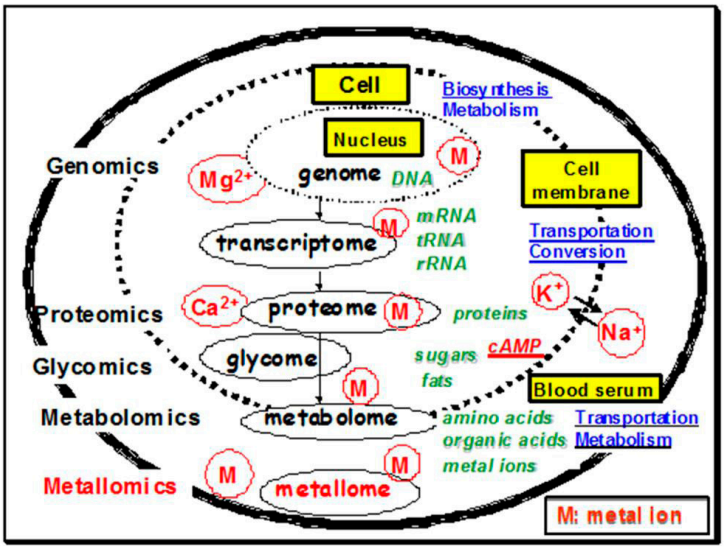

Fig. 1. Simplified model of biological system, showing the relationship of *omics*-science [4,18]. The continuous line outside indicates biological organ and/or whole body, while the dotted line inside does each biological cell.

and Warsaw, Poland. The 8th ISM is scheduled at Kanazawa, Japan, in 2022. All the past International Seminars are listed in **Table 1**. By the way, the summary reports of the ISMs held above have been presented on Metallomics [12-14]. It was sad that Prof. JA Caruso who organized the second ISM and the first editor-in-chief of Metallomics journal passed away in November, 2015.

In addition, in Japan the Metallomics Research Forum has been held every even-number year since 2008 as the domestic meeting. Some selected papers presented in the Metallomics Research Forum were reported as the themed issue in journal Metallomics [15,16].

6. Publication of the journal "METALLOMICS" from RCS

It was a surprising and great news that the academic journal of "Metallomics-Integrated Bimetal Science (now "**Metallomics**") was launched in January, 2009, from RSC [17]. Until now 13 volumes of Metallomics have been distributed, in which many excellent research and review papers have been presented. It should be highly evaluated that the publication of Metallomics has prompted progress of metallomics researches as multidisciplinary science.

In 2021, the publisher of Metallomics was transferred to the Oxford University Press from RCS.

7. "Metallomics Research"; New journal from the Japan Society for Biomedical Research on Trace Elements

The Japan Society for Biomedical Research on Trace Elements decided to change the old journal of "Biomedical Research on Trace Elements (BRTE)" to a new journal "**Metallomics Research**". Old journal was of a mixed-language (Japanese and English) style, including the information of society events. New journal, which is an international, open access, peer-reviewed journal including research papers, notes and reviews written only in English, will be launched from October, 2021. Prof. Yasumitsu Ogra (Chiba University), the present president of the society, and Prof. Masahiro Kawahara (Musashino University), the present Journal Editor-in-Chief, have made up their mind to accelerate research activities in biometals not only in Japan as well as in the world. Then, they asked me to write a review article about the history, activities, international symposium, and the perspectives of metallomics, maybe, because I coined the concept of "metallomics", as mentioned before. First of all, it is hoped that **Metallomics Research** will play a role of the platform to promote biomedical science developed by the Japan Society for Biomedical Research on Trace Elements since 1990.

8. A simplified model of the biological system

Fig. 1 is a schematic diagram of simplified model of the biological system [4,18], which is illustrated in order to get an insight into the scientific aspects of metallomics. In the figure, the dotted line (inside) and continuous line (outside) indicate a biological cell unit and an organ/whole body, respectively. Biological fluids (e.g., blood serum) are circulating between cell membrane and organ. Some biological species and their functions in the biological system are also indicated in **Fig. 1**. As is known, biological cells containing various microorgans (organelles) are composed of numerous internal structures, so that the cell structures in

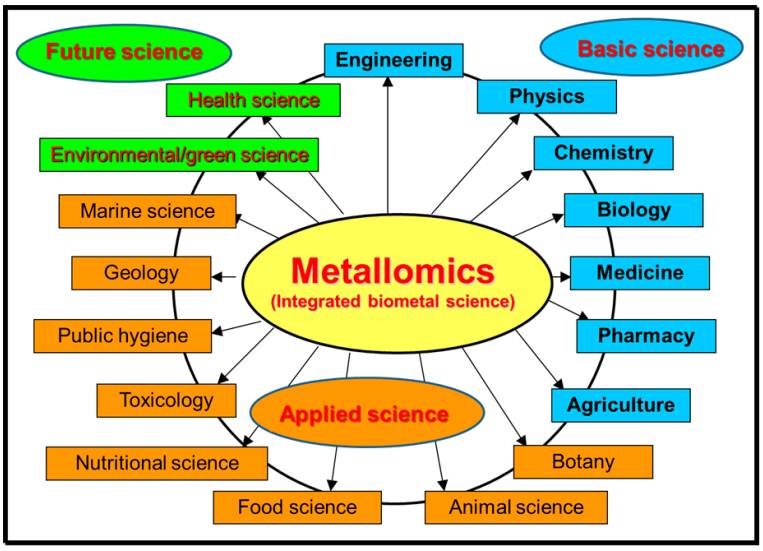

Fig. 2. Correlation map of metallomics as multidisciplinary science consisted of various scientific fields [23].

the biological system (either in prokaryotes or in eukaryotes) are complicated assemblies, but their functions are well organized.

On the left hand side of the simplified model shown in **Fig. 1**, the omics-science such as genomics, proteomics and metabollomics are depicted along with metallomics to indicate their research areas in the biological system. Such a simplified model also helps to understand the relationship of metallomics with genomics, proteomics and other omics-sciences (for example, metabolomics and glycomics). As is well known, genomics deals with the genetic information of DNAs and RNAs encoded as the sequences of nucleic bases. The entirety of DNAs and RNAs are generally called "genome", which preserve the information to synthesize proteins, to control protein structures and to regulate the protein functions. A large number of proteins are distributed inside and outside the cells as well as in membranes, and they work as enzymes for synthesis and metabolism of various biological substances inside the cells. It is well known, for example, that DNAs and RNAs are synthesized by DNA polymerase and RNA polymerase, which are zinc enzymes. Since various proteins play essential roles to regulate and maintain the life system through biosyntheses and metabolisms, proteomics as protein science has been also receiving great attention as post-genome science linked with genomics.

In addition, many biological substances as well as metal ions are transported inside and outside the cells through membranes. In general, since material conversion is actively occurring inside cells and also in cell membranes, such scientific field for material conversion and transportation/exclusion processes through the cells are now called "metabolomics" [19]. Biological substances such as amino acids, organic acids and metal-binding biomaterials produced in metabolism are defined "metabolome" in a similar manner to genome in genomics.

As can be seen from **Fig. 1**, metal ions are ubiquitously distributed inside and outside cells to assist the physiological/biological functions of genome, transcriptome, proteome, glycome and metabolome, maybe, with strong interactions and/or weak interactions. Here, strong interactions mean covalent bond formations between metal ions and biomaterials such as metalloproteins, while weak interactions do labile bond formations or ion-pair formations like in the case of Mg ion and phosphate groups in DNA or in the case of Ca ion and carboxyl groups in proteins. It is desirable to refer to the excellent literatures [4,20-22] in order to understand the functions of metal ions in the biological systems.

9. Multidisciplinary science for metallomics research

Metallomics is integrated biometal science, and so a variety of science fields are concerned with each other. In another words, metallomics is really multidisciplinary and/or interdisciplinary science. These situations are illustrated in **Fig.2**, where metallomics is illustrated in the center. Health science and environmental/green science should be performed as the main research purposes in metallomics, and so they are shown as future science in **Fig. 2**. Many individual academic fields as basic science and applied science are arranged around metallomics, as can be seen in **Fig. 2**. Although the academic fields in **Fig. 2** are conveniently arranged, biometal research is carried out based on biochemical and/or biological/physiological science. Then it should be stressed here that all these science fields are cooperated as multidisciplinary research.

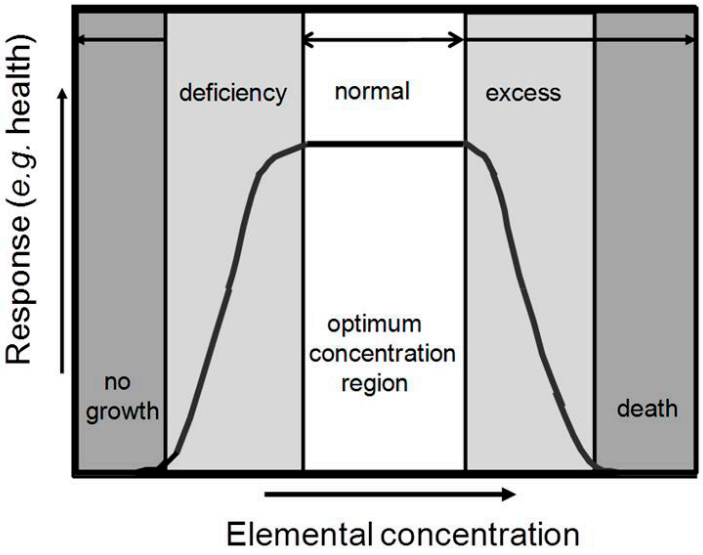

Fig. 3. The dose response curve of biological system [24].
The figure is illustrated as the response curve of elemental concentration *versus* response (*e.g.*, health condition). The optimum concentration corresponds to the homeostasis level.

10. Essentiality and toxicity of the elements

In analytical chemistry, the elements in the concentration ranges of 100-1%, 1-0.01%, 0.01-0.0001% and below 0.0001% are defined as major, minor, trace and ultratrace elements, respectively. Since 0.0001% is equal to 1 ppm (part per million), trace elements are corresponding to those in the concentration range of 1-100 ppm. It is noted here that, in medical and biological sciences, ultratrace elements are usually not distinguished from trace elements, and thus, the elements whose concentrations less than 100 ppm are called trace elements hereafter.

In trace element chemistry, the terms of essential elements and toxic (or hazardous) elements are often used, when the biological effects of the elements are discussed. In such cases, the biological effects of the elements on the biological systems (humans, animals, plants and microorganisms) are generally explained as the response of biological systems to the dose of the elements (generally through nutrients, foods, chemicals and so forth). The dose response curve is schematically shown in **Fig. 3**, where the concentration of the element as a dose is taken on the horizontal axis and the biological response is taken on the vertical axis. In the figure, the health condition is taken as the marker of the dose response of the element. As the biological response except for health, body height or weight, growth rate of microorganisms, plant growth, other medical indices and so forth are considered in the response curve, where the upper position of the curve indicates the better health condition (more normal). It is well known that the response curve in the biological systems generally shows a trapezoid-shaped curve, as is seen in **Fig. 3**.

In such a biological response curve in the trapezoid-shape, three regions such as deficiency region, normal region and excess region are usually observed, when the element concentration is increased from the lower to the higher (from the left to the right in **Fig. 3**). The normal region (the central region) is called the optimum concentration region, where our health is physiologically or functionally maintained to be normal or optimum, without any disease or allergic symptoms. This region is corresponding to the homeostasis level in biology. In the future research in health science, it is desirable that the homeostasis levels of various metals are evaluated in the biological systems (body, organ, cell, blood, and microorgan) for optimum regulation.

The deficiency region is lower in the concentration than the normal region, where some diseases due to deficiency are often caused because of the lack of specific nutrient supply, for example, like iron deficiency and vitamin deficiency. That is, when the nutrient supply becomes too smaller, various diseases or less growth are caused seriously. In the extreme case, for example, microorganism such as Escherichia coli (*E.coli*) does not grow, if the zinc concentration is below 1 ppb.

On other hand, the higher dose than the homeostasis level is called the excess region. In this region the excess amounts of the elements cause serious damages or dysfunctions to the biological systems, and such effects become fatal in the extreme cases. The typical examples are the environmental issues where serious adverse effects are caused by the environmental pollution due to toxic elements or hazardous chemicals. It should be carefully noticed that any element causes some toxic effects on the biological systems due to over-dose of nutrients (elements), as in the right-hand side of **Fig. 3**. If an element causes some adverse effect or disease due to the smaller amount of dose, that element is called highly toxic element. It should be also noticed that acute toxicity or chronic toxicity are often observed, depending on the elements or chemicals.

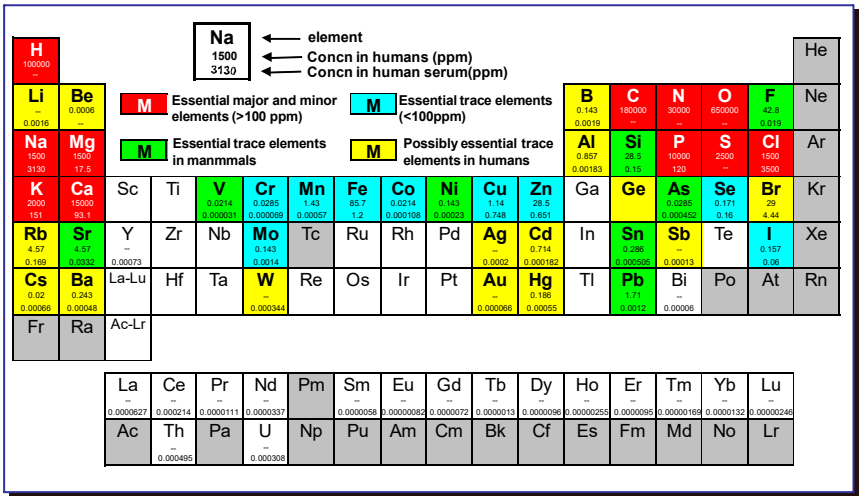

Fig. 4. Periodic table, which shows essential major and minor elements, essential trace elements and possibly essential trace elements in humans and animals.

According to definition of essential element, there are two types of essential elements. First, when the element is found in bioactive molecules such as Fe in hemoglobin, Zn in carboxypeptidase, and Se in glutathione peroxidase, Fe, Zn and Se are of course essential elements. Second, when the deficiency observed as physiological dysfunctions or abnormal diseases is recovered to the normal condition by adding dietary supplement containing a specific element, the element contained in supplement is considered as essential element.

Essential elements known in humans and mammals are summarized in the periodic table shown in **Fig. 4**. It can be seen in **Fig.4** that not only trace elements but also major and minor elements recognize as essential element in the biological systems. Essential trace elements should be elucidated by examining the response curves shown in **Fig. 3**. On the other hand, major and minor elements mainly consist of body structures of humans and mammals. In this sense, major and minor elements are indispensable, i.e., essential, in humans and animals. The situations are the same as plants and other biological systems.

According to **Fig. 4**, 11 elements (H, C, N, O, Na, Mg, P, S, Cl, K, Ca) are essential major and minor elements, which consist of whole body structures of the living organisms (biological systems) on earth. It is known that 8 elements (Cr, Mn, Fe, Co, Cu, Zn, Se, Mo, I) are essential trace elements known for humans, and 7 elements (F, Si, V, Ni, As, Sr, Sn, Pb) are essential trace elements proved for experimental mammals. It is interesting that the elements shown in yellow color boxes in **Fig. 4** are appreciated as possibly essential trace elements, among which Cd and Hg usually known as toxic or hazardous elements are included. One possibility is that their deficiencies or homeostasis levels have not been examined yet. Therefore, since possible essentialities of such elements have not been elucidated so far, further extensive research on their essentiality and physiological functions as biological trace elements may be required in the future.

As for the interpretation of essential and non-essential elements, Maret published the interesting article considering essential and non-essential elements in the biological periodic table [23]. His consideration is very similar to that discussed in this Section 10. The abstract in his article is cited below, as reference.

> *A significant number of chemical elements are either essential for life with known functions, or present in organisms with poorly defined functional outcomes. We do not know all the essential elements with certainty and we know even less about the functions of apparently non-essential elements. In this article, I discuss a basis for a biological periodic system of the elements and that biochemistry should include the elements that are traditionally part of inorganic chemistry and not only those that are in the purview of organic chemistry. A biological periodic system of the elements needs to specify what "essential" means and to which biological species it refers. It represents a snapshot of our present knowledge and is expected to undergo further modifications in the future. An integrated approach of biometal sciences called metallomics is required to understand the interactions of metal ions, the biological functions that their chemical structures acquire in the biological system, and how their usage is fine-tuned in biological species and in populations of species with genetic variations.*

11. Extended All-Elements Present Theory

In 1936, I. Noddack published the article entitled "Concerning the ubiquitous nature of the chemical elements" (the original title in Germany was "Über die Allgegenwart der chemischen Elemente") in ANGEWANDTE CHEMIE and suggested that "all elements in the periodic table supposed to be present in all rocks and minerals on earth" [24]. Prof. P. Kuroda supported the Noddack's idea (hypothesis) of ubiquitous presence of all elements in geological samples in his book "The Origin of the Chemical Elements and the Okhlo Phenomenon", published in 1982 [25], and he named the Noddack's concept "the All-Present Theory of the Elements".

In 1930s, the number of the elements detected in minerals were limited because the analytical methods available in those days, such as flame emission spectrometry, arc/spark emission spectrometry, electrochemical methods and so forth, were not sensitive enough to detect the low-abundant elements. Therefore, many scientists thought that the elements whose concentrations were unknown were not contained in the samples of interest. Nevertheless, Noddack believed that the existence of all elements in all geochemical samples might be proved, when the sensitive analytical techniques for trace analysis would be advanced in the future.

These days, according to great progress in analytical methodology, as mentioned earlier, almost all elements are able to be determined or detected not only in geochemical samples, but also in the biological and environmental samples. Since 1990, thus, the Haraguchi's research group in Nagoya University challenged all-elements analyses of various samples collected from the atmosphere, lithosphere, hydrosphere, biosphere, and urbanosphere (urban area); for example, they were airborne particulate matter, rocks, seawater and lake/river water, biological samples from humans and plants, and bottom/fly ashes collected from the waste incinerators [1,4,8,22]. Based on the experimental results, Haraguchi proposed a new concept of "the Extended All-Present Theory of the Elements" [1], as summarized below;

> *The elements contained in rocks and minerals are dissolved into water because of the weathering processes on earth, and plants growing in soil absorb the elements dissolved in water for nutrition, and then animals ingest plants for food, and humans drink water and ingest plants and animals as food because humans are at the top of food chain. Consequently, it is obvious to consider that plants and animals, even their organs and blood, contain all elements through the elemental cycles on earth. In another words, the All-Present Theory of the Element is true not only for rocks and minerals, but also for all materials including all biological systems on earth. This concept indicates that all elements in the periodic table are ubiquitously present even in all biological systems, such as animals, plants, and microorganisms as well as humans.*

Haraguchi is further thinking that the final goal of the All-Elements Present Theory is to prove the existence of all elements in single biological cells. This concept, that is, "the presence of all elements in single biological cell" is called "cell microcosm" [4]. If cell microcosm is scientifically elucidated for the living biological cells, such knowledge may provide great influence to the study on chemical revolution in whole universe including earth. This is the dream of the present author.

All elements analysis of salmon egg cells was challenged in order to examine the concept of cell microcosm, *i.e.*, all-elements presence in single biological cell. The analytical results are not shown in this article, but they can be seen in the references [22]. In the experiment, natural/artificial radioactive elements and rare gas elements were not measured because the specific experimental facilities for protection from harmful radioactivity were required for analyses of radioactive elements and the specific gas sampling systems as well as the skillful gas treatment techniques were necessary in rare gas analysis. As a result, 78 elements in the periodic table were the target of all-elements analysis in the standard laboratory.

The analytical results for 72 elements were experimentally obtained, where the metallic and metalloid elements were measured by ICP-AES and low resolution- ICP-QMS, and nonmetallic elements such as H, C, N, and O were determined by the conventional elemental analysis method. Finally, 65 elements among 78 could be determined and other 7 elements (Li, F, Zr, Nb, Hf, Ir, Bi) were just detected because of their low abundances in salmon egg cell [22]. Rhodium, Te, Ta and Re were not able to be determined or detected at this moment, maybe because of their extremely low concentrations in salmon egg cells. However, these elements except for F were detected by HR (high resolution)-ICP-MS in the recent experiments.

Many interesting facts can be found from the analytical results. For example, Fe, Zn, Cu, Co, Mn, Se and P provided the bio-accumulation factors larger than 10,000 [22], which indicate that these elements in salmon egg cell were enriched by 10,000-fold compared to those in seawater.

12. Research trends and subjects of metallomics

Finally research trends, research subjects and perspective of metallomics should be reviewed in this manuscript. However, such works are beyond the limit of capacity and ability of the present author. Then, the following two tables are shown with small comments here.

Table 2 is the top-20 ranked articles in the literatures, in which metallomics is used as the keyword. This table is summarized by referring to "current contents connect" in the Web of Science from Thomson Reuters. The original article of metallomics published in 2004 is still ranked at No.6. This year is the beginning of metallomics. As a whole, it seems that the researches listed in the ranking in **Table 2** reflect the present research trends. The largest interest is drug design and chemotherapy, where the compounds of ruthenium, platinum, copper and other metals are the targets in anti-cancer drugs. The research concerned with the role of metal dyshomeostasis in Alzheimer's disease may be interesting, but difficult research problems must be solved. The work in terms of zinc transporters by Fukada and Kambe is ranked at No.18, which is highly appreciated, and it is expected to be developed furthermore in the future. Anyway, it is recommended to read all the articles listed in **Table 2**, which are at the forefront of metallomics research.

Table 3 is the research subjects considered for metallomics research. Although the different research subjects were listed in the original paper [4], the list shown **Table 3** is corrected this time, because a variety of advanced research works/results have been achieved along with progress of analytical technologies after about 20 years since 2002. However, this list was made for personal use. It is desired to develop a list of research subjects especially for biomedical science as the recommended or approved version by the society for innovation in metallomics research.

Finally, the books published so far are listed as reference [7,27-29].

13. Summary

On the occasion of publication of a new journal Metallomics Research, the history of the Japan Society of for Biomedical Research on Trace Elements and its journal Biomedical Research on Trace Elements (BRTE) were looked back in order to consider publication program in the society. Since metallomics is relatively new science field, the background of proposal, international symposiums, journal publication Metallomics from RSC (presently Oxford University Press), and achievement as science were also reviewed as reference. In the future, it is hoped that metallomics will be developed as the multidiciplinary science focusing around health science and environmental science, and it is expected that new journal Metallomics Research will play an important role as the international version.

Acknowledgement

The author expresses his sincere thanks to Professors Masahiro Kawahara and Yasumitsu Ogra for their giving me the opportunity to write the present review.

Table 2. | The Top-20 ranked articles in the literatures, in which *metallomics* is used as a key word.

	Authors and titles of articles	Times of citation[a)]
1	Levina A, Mitra A, Lay, PA: Recent developments in ruthenium anticancer drugs. METALLOMICS 1: 458-470, 2009.	464
2	Todd RC, Lippard SJ: Inhibition of transcription by platinum antitumor compounds. METALLOMICS 1: 280-291, 2009.	366
3	Szpunar J: Advances in analytical methodology for bioinorganic speciation analysis: metallomics, metalloproteomics and heteroatom-tagged proteomics and metabolomics. Analyst 130: 442-465, 2005.	331
4	Roman M, Jitaru P, Barbante C: Selenium biochemistry and its role for human health. METALLOMICS 6: 25-54, 2014.	321
5	Berners-Price SJ, Filipovska A: Gold compounds as therapeutic agents for human diseases. METALLOMICS 3: 863-873, 2011.	312
6	Haraguchi H: Metallomics as integrated biometal science. Journal of Analytical Atomic Spectrometry 19: 5-14, 2004.	299
7	Colvin RA, Holmes WR, Fontaine CP, Maret W: Cytosolic zinc buffering and muffling: Their role in intracellular zinc homeostasis. METALLOMICS 2: 306-317, 2010.	282
8	Khan MAK, Wang FY: MERCURY-SELENIUM COMPOUNDS AND THEIR TOXICOLOGICAL SIGNIFICANCE: TOWARD A MOLECULAR UNDERSTANDING OF THE MERCURY-SELENIUM ANTAGONISM. EMVIRONMENTAL TOXICOGY AND CHEMISRY 28: 1567-1577, 2009.	276
9	Denoyer D, Masaldan S, Fontaine SL, Cater MA: Targeting copper in cancer therapy: 'Copper That Cancer'. METALLOMICS 7: 1459-1476, 2015.	272
10	Arita A. Costa M: Epigenetics in metal carcinogenesis: nickel, arsenic, chromium and cadmium. METALLOMICS 1: 222-228, 2009.	252
11	Kell DB, Pretorius E: Serum ferritin is an important inflammatory disease marker, as it is mainly a leakage product from damaged cells. METALLOMICS 6: 748-773, 2014.	248
12	Mounicou S, Szpunar J, Lobinski R: Metallomics: the concept and methodology. CHEMICAL SOCIETY REVIER 38: 1119-1138, 2009.	243
13	Gautier A, Cisnetti F: Advances in metal-carbene complexes as potent anti-cancer agents. METALLOMICS 4: 23-32, 2012.	228
14	Bonda DJ, Lee HG, Jeffrey A Blair JA, Zhu XW, Perry G, Smith MA: Role of metal dyshomeostasis in Alzheimer's disease. METALLOMICS 3: 267-270, 2011.	220
15	Lobinski R, Moulin C, Ortega R: Imaging and speciation of trace elements in biological environment. BIOCHEMIE 88: 1591-1604, 2006.	199
16	Dupont CL, Grass G, Rensing C: Copper toxicity and the origin of bacterial resistance-new insights and applications. METALLOMICS 3: 1109-1118, 2011.	183
17	Raliya R, Nair R, Chavalmane S, Wanga WN, Biswas P: Mechanistic evaluation of translocation and physiological impact of titanium dioxide and zinc oxide nanoparticles on the tomato (Solanum lycopersicum L.) plant. METALLOMICS 7: 1584-1594, 2015.	180
18	Fukada T, Kambe T: Molecular and genetic features of zinc transporters in physiology and pathogenesis. METALLOMICS 3: 662-674, 2011.	177
19	Duncan C, White AR: Copper complexes as therapeutic agents. METALLOMICS 4:127-138, 2012.	177
20	Darrah TH, Prutsman-Pfeiffer JJ, Poreda RJ, Campbell ME, Hauschka PV, Hannigan RE: Incorporation of excess gadolinium into human bone from medical contrast agents. METALLOMICS 1: 479-488, 2009.	171

a) Times of citation were referred to "current contents connect" in the Web of Science of Thomson Reuters on August 25, 2021.

Table 3. | Research subjects in metallomics.

1) Homeostasis study of the elements in the biological fluids, cell, organs etc.
2) Search and identification of metalloproteins and metalloenzymes
3) Bioimaging research for spatial distributions of metals
4) Correlation of structures and functions of metallome (metal-binding molecules)
5) Elucidation of reaction mechanisms of metalloenzymes
6) Metabolisms of metal-containing biomolecules (metabolome and metabolites)
7) Medical diagnosis of health and disease related to metallome
8) Design of inorganic drugs for chemotherapy
9) Toxicology and environmental science
10) Chemical evolution of the living systems and organisms on earth (universe)

References

[1] Haraguchi H: Multielement profiling analyses of biological, geochemical, and environmental samples as studied by analytical atomic spectrometry. Bull Chem Soc Jpn 72: 1163-1186, 1999.

[2] Haraguchi H, Furuta N: Analytical Atomic Spectrometry in Japan over Last 25 Years. J Anal At Spectrom 25: 1371-1377, 2010.

[3] Tomita H (ed.): Trace Elements in Clinical Medicine. Proceedings of the Second Meeting of the International Society for Trace Element Research in Humans (ISTERH), Springer-Verlag, August 28-September 1, Tokyo, 1989.

[4] Haraguchi H: Metallomics as integrated biometal science. J Anal At Spectrom 19: 5-14, 2004.

[5] Haraguchi H: New Development of Chemical Speciation Analysis for Metallomics Research. Biomed Res Trace Elem 16: 217-232, 2005. (in Japanese)

[6] Haraguchi H: Metallomics: the history over the last decade and a future outlook. Metallomics 9: 1001-1013, 2017.

[7] Ogra Y, Hirata T (ed.): Metallomics: Recent Analytical Techniques and Applications. Springer, Tokyo, 2017.

[8] Haraguchi H: A Challenge to Pico-World and Metallomics: A New Frontier of Trace Element Chemistry. The invited lecture in the Tokushima Seminar on Chemical Engineering 2002 (The English-written abstract was translated from the Japanese one).

[9] Haraguchi H. Matsuura H: Trace Element Speciation for Metallomics. S. Enomoto, Y. Seko (ed.) Proceedings of the International Symposium on Bio-trace Elements 2002 (BITREL 2002), The Institute of Physical and Chemical Research (RIKEN), Wako, pp 3-8, 2002.

[10] Haraguchi H: Preface–The International Symposium on Metallomics 2007 (ISM 2007). Pure Appl Chem 80: iv-iv, 2008.

[11] Haraguchi H (ed.): Proceedings of the International Symposium on Metallomics 2007 (ISM 2007). Pure Appl Chem (Special Issue of IUPAC) 80: 2565-2750, 2008.

[12] Caruso JA: 2009 international symposium on metallomics. Metallomics 2: 103, 2010.

[13] Sperling M: The third international symposium on metallomics 2011. Metallomics 3: 1263-1264, 2011.

[14] Montes-Bayon M, Bettmer J: 4th international symposium on metallomics 2013. 6: 187-188, 2014.

[15] Haraguchi H: Metallomjics in Japan. Metallomics 3: 648-649, 2011.

[16] Ogra Y, Himeno S: Metallomjics in Japan. Metallomics 5: 415-416, 2013.

[17] Caruso JA, O'Coonr N: Mettalomics: Integrating research related to biometals - a journal for an emerging community. Metallomics 1: 14-16, 2009.

[18] Lobinski R, Becker JS, Haraguchi H, Sarkar B: Metallomics: Guidelines for terminology and critical evaluation of analytical chemistry approaches (IUPAC Technical Report). Pure Appl Chem 82: 493-504, 2010.

[19] Dunn WB, Ellis DI: Metabolomics: current analytical platforms and methodologies, Trends Anal Chem 24: 285-294, 2005.

[20] Bowen HJM: Trace element chemistry. Academic, New York, 1973.

[21] Williams RJP, Frausto da Silva JJR: The natural selection of the chemical elements. Clarendon, Oxford, 1996.

[22] Haraguchi H, Ishii A, Hasegawa T, Matsuura H, Umemura T: Metallomics Study on All-Elements Analysis of Salmon Egg Cell and Fractionation Analysis of Metals in Cell Cytoplasm. Pure Appl Chem 80: 2595-2608, 2008.

[23] Maret W: The Metals in the Biological Periodic System of the Elements. Int J Mol Sci 17: 1-8, 2016.

[24] Noddack I: Concerning the ubiquitous nature of the chemical elements. Angew Chem 47: 835, 1936.

[25] Kuroda P: The origin of the chemical elements and the Oklo phenomenon. Springer, Berlin, 1982.

[26] Katsuki F, Hokura A, Iwahata D, Ikuma T, Oguri S, Haraguchi H: Multielement determination of major-to-ultratrace elements in cherry samples by ICP-MS and ICP-AES after acid digestion. Bunseki Kagaku 47: 835-844, 1998. (in Japanese)

[27] Lucia B (ed.): Metallomics and the Cell. Springer, Berlin, 2013.

[28] Maret W: Metallomics: A Primer of Integrated Biometal Sciences. Imperial College Press, London, 2016.

[29] Arruda MAZ (ed.): Metallomics-The Science of Biometals. Springer, Berlin, 2018.

Review https://metallomicsresearch.brte.org

Role of ferroptosis in nanofiber-induced carcinogenesis

Shinya Toyokuni[1,2], Fumiya Ito[1] and Yashiro Motooka[1]

[1]Department of Pathology and Biological Responses, Nagoya University Graduate School of Medicine, 65 Tsurumai-cho, Showa-ku, Nagoya 464-8550, Japan

[2]Center for Low-temperature Plasma Sciences, Nagoya University, Furo-cho, Chikusa-ku, Nagoya 464-8603, Japan

Abstract

Biopersistent nanofibers with specified physical dimension are unexpected human carcinogens whether they are natural or synthetic. Asbestos, a natural fibrous mineral, is classified as a definite human carcinogen (IARC Group 1) to cause malignant mesothelioma (MM) and lung cancer. Multi-walled carbon nanotube of 50 nm-diameter was defined in 2014 as a possible carcinogen (IARC Group 2B) toward MM, fortunately with no authorized patients thus far. Carcinogenic mechanism of asbestos has been a mystery for a long time. It is now recognized that asbestos goes through lung parenchyma by collecting hemoglobin-derived iron to reach pleural cavity, which takes several decades. Iron-loaded asbestos can induce oxidative damage directly to mesothelial cells, carcinogenesis-target cells lining somatic cavities. Recently, it was clarified that surrounding stromal environment are as important for mesothelial carcinogenesis. The novel concept here is ceaseless ferroptosis of macrophages, which forms a Fe(II)-dependent stromal mutagenic milieu indirectly for mesothelial cells and indeed is a revised understanding of frustrated phagocytosis. Deposition of foreign materials eventually causes iron accumulation *in situ* due to the innate characteristic of preserving iron inside cells. Nanofiber-induced carcinogenesis may be involved in other human carcinogenesis, including ovarian cancer. Alternatively, iron excess can be an optimal target of cancer prevention and cancer treatment.

Key words: asbestos, mesothelioma, ferroptosis, macrophage, iron, carbon nanotube

Statements about COI: The authors declare no conflict of interest associated with this manuscript.

*Correspondence:
Shinya Toyokuni, MD, PhD; Department of Pathology and Biological Responses, Nagoya University Graduate School of Medicine, 65 Tsurumai-cho, Showa-ku, Nagoya, Japan.
Tel: +81 52 744 2086; **Fax:** +81 52 744 2091;
E-mail: toyokuni@med.nagoya-u.ac.jp

Received: August 17, 2021
Accepted: September 8, 2021
Released online: October 15, 2021

Abbreviations:

DMT1	divalent metal transporter 1
EV(s)	extracellular vesicle(s)
IARC	International Agency for Research on Cancer
IRE	iron-responsive element
IRP(s)	iron-regulatory protein(s)
MM	malignant mesothelioma
MWCNT	multi-walled carbon nanotube
NCOA4	nuclear receptor coactivator 4
PCBP1/2	poly-repeated cytidine-binding protein 1/2
UTR	untranslated region

Introduction

Cancer is one of the leading causes of human mortality all over the world (https://www.who.int/data/gho/data/themes/mortality-and-global-health-estimates). Whereas molecular carcinogenic mechanism of each human cancer is diversely different and unidentified in most of the cases [1], some of the environmental carcinogenesis reveals unequivocally significant epidemiological association, including ionizing radiation with leukemia [2] and asbestos exposure with malignant mesothelioma (MM) [3].

Asbestos is a natural fibrous mineral, which has been used in the human history since 2,500 B.C. due to its resistance to heat, acid and friction, such as in pottery and sacred cremation garments for the Egyptian pharaohs [4]. After the industrial revolution period, wide use of asbestos started worldwide because of the economical merits of mining [5], which continued till epidemiologist recognized the association between asbestos exposure and MM or lung cancer [6]. MM has been and is a rare tumor [7] in that the tumor retains the characteristics of thin and flat mesothelial cells which line somatic cavities and decrease the friction-derived heat by producing hyaluronic acid [8]. We have ~2,000 new patients yearly in Japan (https://www.mhlw.go.jp/toukei/saikin/hw/jinkou/tokusyu/chuuhisyu17/dl/chuuhisyu.pdf) in comparison to ~120,000 new lung cancer patients. Historically, prolonged average human life was essential for the recognition of this tumor due to an extremely long incubation period of 30~40 years after asbestos exposure, which has been a long-time mystery [9]. After the recognition of all the asbestos as a definite human carcinogen (Group 1) by the International Agency for Research on Cancer (IARC) in 1987 [5], scientists have lost interest in the mechanistic elucidation for a while. Of note, asbestos is negative for Ames test [10].

In Japan, asbestos issue was reminded in 2005 when Kubota shock occurred by newspaper report [11], when inhabitants near the asbestos factory obtained a high incidence of MM. Even now the prognosis of MM is quite poor because of the difficulty in diagnosing the early stage of MM [12]. It is established that carcinogenicity of asbestos fibers depends on its high affinity for histones and hemoglobin-derived iron. Indeed, asbestos (ferruginous) body found in the lung parenchyma of those people exposed to high amounts of asbestos supports this mechanism, thus generating physical scissors for cutting genomic DNA via the Fenton reaction [3, 9] (**Figure 1**). Size (3 nm ~ 5 μm in diameter) [13] and length as an aspect ratio (fiber length/diameter) of > 3 were important to reach alveolar space and this needle-like structure with biopersistence was essential to reach pleural and sometimes peritoneal cavities eventually.

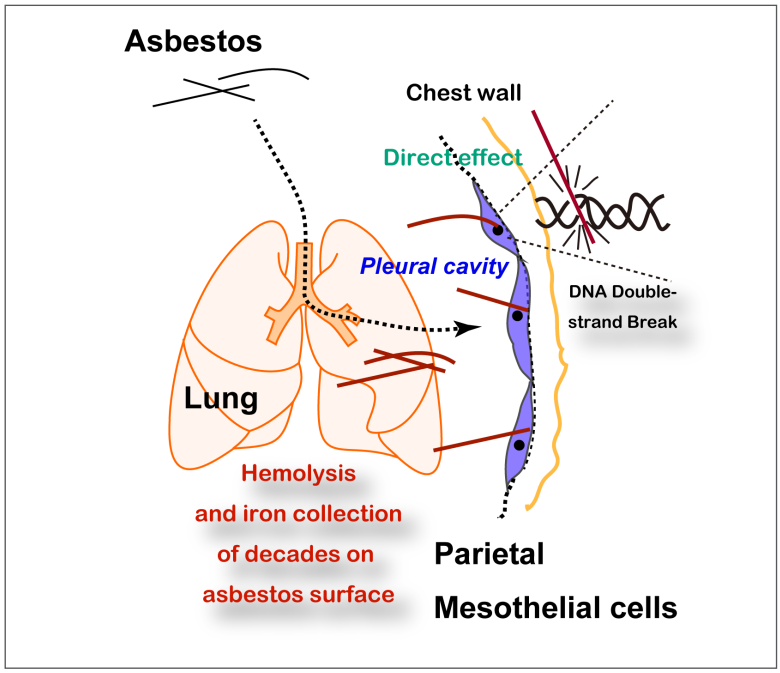

Figure 1. **Current understanding of the mechanism of asbestos-induced mesothelial carcinogenesis in humans.**
Note that a few decades are required for asbestos fibers to go through lung parenchyma to the pleural cavity. Asbestos fibers have hemolytic activity and high affinity for hemoglobin, thus accumulating massive amounts of iron on its surface (red fibers in the figure) to cause DNA double-strand breaks via Fenton reaction in parietal mesothelial cells, targets for carcinogenesis (direct effect). Refer to text for details.

Iron metabolism revised

No life on the earth can live without iron from bacteria to humans [14, 15]. There are recent advancements in the understanding of iron metabolism in higher animals, which started from transferrin/ferritin system, iron transporters (DMT1, ferroportin, etc.) [16], posttranscriptional regulation (IRE-IRPs system) and IRP2/FBXL5-ubiquitin-proteasome system [17, 18].

The recent noteworthy new concepts in iron metabolism would be ferritinophagy [19, 20], cytosolic iron chaperones [21] and ferritin secretion via IRE-IRP/CD63-regualted extracellular vesicles [22]. All of these suggest that intracellular iron levels are strictly regulated not to abandon but efficiently reuse iron and to maintain the iron in a safe non-catalytic fashion. Ferritinophagy

is ferritin-specific autophagic process directed by nuclear receptor coactivator 4 (NCOA4) to release iron from ferritin cores into lysosomes [23]. Poly(rC)-binding protein 1 and 2 (PCBP1/2) has been first reported as intranuclear RNA-binding proteins but are now recognized as mutually exclusive cytosolic iron chaperones [24-26]. Only PCBP1 can load Fe(II) to ferritin cores whereas PCBP2 play a role in other intracellular Fe(II) deliveries [27, 28]. Theoretically, PCBP1/2 carries 3 molecule of Fe(II) in non-catalytic manner [21]. In general, PCBP1 works as tumor suppressor gene [29] and PCBP2 as oncogene [30]. The last one is quite new reported in 2021. We discovered a canonical IRE in the 5'-untranslated region (UTR) of CD63 mRNA responsible for regulating its expression in response to increased iron. We showed that under iron-loading, intracellular ferritin is transferred via NCOA4 to CD63(+) extracellular vesicles (EVs) that are then secreted. Such iron-dependent secretion of the major iron storage protein ferritin is performed through CD63(+) EVs [22].

Ferroptosis

Ferroptosis is a recently defined regulated necrosis. The characteristic in this cell death mode is the dependence on catalytic Fe(II) leading to lipid peroxidation [18, 31]. This was first reported on *H-ras* mutated fibrosarcoma cells with the use of erastin, an inhibitor for cystine/glutamate antiporter (SLC7A11), resulting in decrease in reduced GSH as an antioxidant [32]. The current revised concept of ferroptosis is the imbalance between Fe and S (-SH; sulfhydryls) in favor of iron, causing Fenton-reaction [18]. Iron is one of the most basic elements of the cell, working as cofactors in enzymes, such as ribonucleotide reductase (DNA synthesis), cytochrome oxidase (energy production) and catalase (antioxidant), and hemoglobin in higher species. Thus, every cell tries to maintain the amounts of iron, and bacterial and fungal infections might be a fight to obtain iron for the continued growth of those invaders [15].

It is worth mentioning here that there is no mechanisms to abandon iron from an individual in higher species except for bleeding though Fe(II) can be secreted extracellularly via ferroportin [25, 33]. Accordingly, accumulated iron or decreased antioxidant systems results in ferroptosis. Cancer cells collects iron for persistent proliferation [34-36]. Thus, it is not hard to imagine that cancer cells specifically fall into ferroptosis when the overused antioxidant pathway is squeezed with certain chemicals [1]. Furthermore, autophagic process promotes ferroptosis via ferritin degradation [37] whereas ferritinophagy inhibition via NCOA4 deficiency in the heart mitigates the development of pressure overload-induced dilated cardiomyopathy [38].

Novel mechanism in asbestos-induced mesothelial carcinogenesis

Mesothelial cells are the major target cells in asbestos-induced carcinogenesis. Thus, the research has been performed to clarify how asbestos causes genotoxicity on mesothelial cells directly. However, we recently recognized that the surrounding microenvironment is as important for mesothelial carcinogenesis, based on animal model experiments [39]. In this peritoneal injection model in rats, we noticed after 1 month of injection that virtually all the asbestos fibers are inside the macrophages, which formed granuloma, a foreign body reaction.

Granuloma formation is a specific inflammation mainly of macrophages to confine uncontrollable materials/agents within those barriers, whether they are independent species or man-made synthetic materials (**Figure 2**). Macrophages are phagocytic and antigen-presenting cells. Furthermore, they play a central role in iron metabolism, especially regarding iron recovery from dead or dying cells. We found that asbestos due to its specified physical dimension kills macrophages consistently at first via lysosomal-dependent cell death and finally ferroptosis, which generates Fe(II)-dependent mutagenic stromal milieu, causing β-catenin induction in mesothelial cells [39]. This is an indirect effect to mesothelial cells and may be a revised understanding of frustrated phagocytosis [40].

Carbon nanotubes

Carbon nanotube was discovered with electron microscopic observation in 1991 [41]. This is a synthetic material, consisting exclusively of carbon and with a tubular structure of a few nanometer (single-walled) to several hundred nanometers (multi-walled) in diameter. This material has been and is used for numerous industrial purposes, such as in lithium battery and liquid crystal film, based on its physical nature of rigidity, electrophilicity and heat conductivity [42, 43].

However, its similarity to asbestos fibers in physical dimension was questioned in the early 2,000's, and thus we worked on this issue. We found that diameter of carbon nanotube is the most critical risk factor, where multi-walled carbon nanotube (MWCNT)

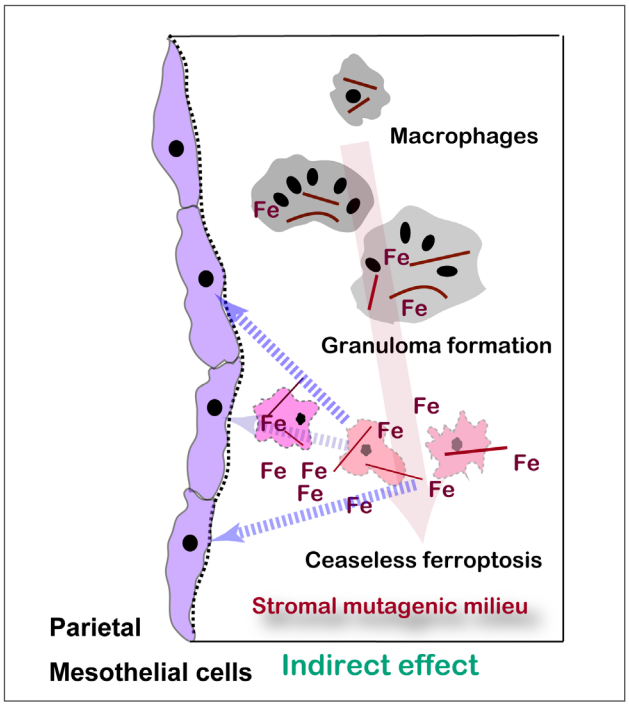

Figure 2. Stromal mutagenic milieu generated by ceaseless macrophage ferroptosis.
Mesothelial cells have phagocytic activity and asbestos fibers in the somatic cavity are eventually transferred to stromal tissue supporting the somatic walls, where macrophages take up the fibers coated with hemoglobin-derived iron. Macrophages try to accommodate all the asbestos fibers by making granuloma, a collection of macrophages with multinucleated giant cells. However, many of the macrophages die through ferroptosis because they cannot cope with the disposal of these thin and long fibers. Finally, abundant iron is released to the stroma of somatic wall, which constitutes the mutagenic milieu for the surface-lining mesothelial cells (indirect effect).

of ~50 nm-diameter was most carcinogenic to mesothelial cells in rat intraperitoneal injection studies [44] and that MWCNT of ~15 nm-diameter was not carcinogenic to mesothelial cells even after > 3 years of observation [45]. The interesting point was that carbon nanotubes have a high affinity not only for histone and hemoglobin but also for transferrin, an iron transporting protein in the serum, and that only MWCNT of -50 nm could go into mesothelial cells [46]. There observations suggest that excess iron play a role in MWCNT-associated mesothelial carcinogenesis. This is strongly confirmed with the similar genetic alterations observed in the rat and human MMs between asbestos origin [47-49] and MWCNT of 50 nm-diameter origin [44], where homozygous deletion of *p16*^{Ink4a} tumor suppressor gene was the most prominent . Indeed, we believe that deletion of *p16*^{Ink4a} tumor suppressor gene is a marker of Fenton reaction-induced carcinogenesis [35, 50], based on the studies of ferric nitrilotriacetate (Fe-NTA)-induced renal carcinogenesis model (**Table 1**). Regarding Fe-NTA-induced renal carcinogenesis,

Table 1. Similarities and differences among three *wild-type* animal models causing cancer through excess iron.
Fe-NTA, ferric nitrilotriacetate; *ip*, intraperitoneal; MWCNT, multi-walled carbon nanotube. Refer to text for details.

Models	Fe-NTA	Asbestos (chrysotile, crocidolite and amosite)	MWCNT of 50-nm diameter
Species	Rat, mouse	Rat, mouse	Rat, mouse
Injection	*ip*, 3~5 times a week/10-12 weeks	*ip*, 1~3 times	*ip*, 1~3 times
Major pathology	Repeated Fenton reaction in the renal proximal tubules	Direct action to mesothelial cells with prolonged foreign body reaction (ceaseless ferroptosis of macrophages)	Direct action to mesothelial cells with prolonged foreign body reaction
Origin of excess iron	Fe-NTA itself	Asbestos itself (crodidolite, amosite), hemolysis (chrysotile) and affinity to hemoglobin	Affinity to hemoglobin and transferrin
Induced cancer	Renal cell carcinoma; 50% of pulmonary metastasis in rats	Malignant mesothelioma	Malignant mesothelioma
Major target gene	Homozygous deletion of *16*^{ink4a} tumor suppressor gene	Homozygous deletion of *16*^{ink4a} tumor suppressor gene	Homozygous deletion of *16*^{ink4a} tumor suppressor gene
References	[15, 50, 71, 72]	[49, 73]	[44, 46]

refer to other published reviews [15, 51].

Recently, Tim4 was identified as a receptor for MWCNT in macrophages leading to granuloma formation [52, 53]. It was recently reported that Tim4+ macrophages sequester and impair proliferation of CD8+ T cells [54] whereas TIM4 expression by dendritic cells mediates uptake of tumor-associated antigens and anti-tumor responses [55]. Whether persistent ferroptosis of macrophages is at work for mesothelial carcinogenesis requires further investigation. We have to stress here that no definite MM case has been reported thus far in terms of carbon nanotubes. We believe that this depends on early recognition (IARC Group 2B) [56] and the efforts on the industry side to avoid the use of high-risk carbon nanotubes and to develop the large-scale automated systems to minimize human exposure. The continued use of MWCNT in industry and in material science, even for the robotic systems [57], is very different from the asbestos case and we can declare that this is one of the successful examples of experimental pathology using animal models and regulatory science.

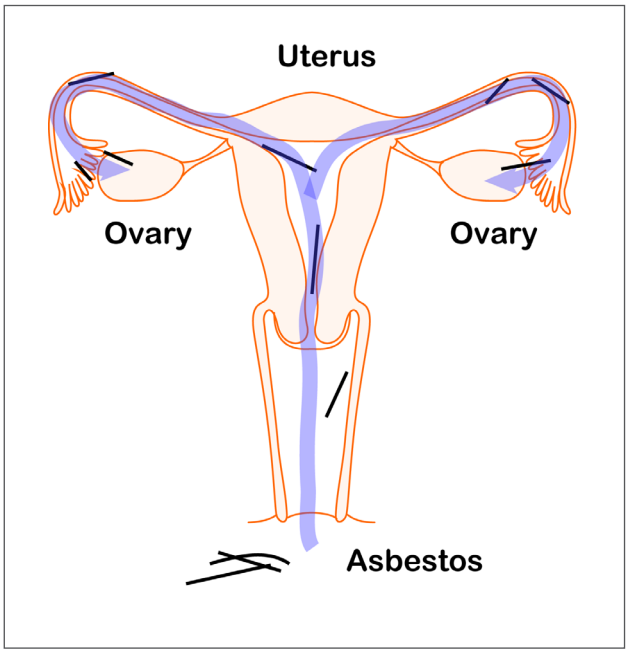

Figure 3. Possible pathway of asbestos fibers reaching ovaries in humans.
Asbestos and other nanofibers may exist in the vulva of reproductive-age women as contaminants of family laundry or cosmetic applications. Liquid flow from vulva, vagina, uterine cavity, oviduct to ovary may carry these fibers to ovarian epithelial cells. Refer to text for details.

Ovarian carcinogenesis

Another example we suspect for nanofiber-induced carcinogenesis accompanied by excess iron is ovarian carcinogenesis. Endometriosis is a female disease of reproductive age where endometrium exists outside of uterine cavity, leading to iron excess due to monthly bleeding. In the case of ovarian endometriosis, this iron excess is established as a risk for adenocarcinoma, especially clear cell carcinoma and endometrioid adenocarcinoma, in addition to menstrual pain and infertility [58, 59]. In addition to this, fibrous materials, including asbestos, are suspected to be carcinogenic to ovarian epithelial cells. There are two points that are true but not well recognized: 1) there is a pathway in women through vagina, endometrium, oviduct to ovary [60-62], which happens at fertilization; 2) frequent use of baby power, including talc and some amounts of asbestos, may be epidemiologically associated with ovarian cancer [63, 64] though it is still controversial [65, 66] (**Figure 3**). We believe that this is an important question to be explored to prevent ovarian carcinogenesis.

Conclusion

Biopersistent fibrous materials may provide humans with unexpected risk of cancer, depending on its physical parameters and exposure route. This is closely associated with the general response of our cells against foreign materials to collect/recover iron as much as possible and to deplete iron in the extracellular space. Alternatively, if the macrophages cannot accommodate or scavenge these fibrous materials and die through ferroptosis, mutagenic stromal milieu is generated [39]. Finally, it is important to recognize that iron excess can be a target for cancer prevention [67, 68] and also for cancer therapy [18, 69, 70], including non-thermal plasma.

Declaration of competing interest

The authors declare no conflict of interest to present.

Acknowledgments

This work was supported, in part, by JST CREST (Grant Number JPMJCR19H4), JSPS Kakenhi (Grant Number JP19H05462 and JP20H05502) and Research Grant of the Princess Takamatsu Cancer Research Fund (19-251).

References

[1] Toyokuni S, Ito F, Yamashita K, Okazaki Y, Akatsuka S: Iron and thiol redox signaling in cancer: An exquisite balance to escape ferroptosis. Free Radic Biol Med 108: 610-626, 2017.

[2] Leuraud K, Richardson DB, Cardis E, Daniels RD, Gillies M, et al.: Risk of cancer associated with low-dose radiation exposure: comparison of results between the INWORKS nuclear workers study and the A-bomb survivors study. Radiat Environ Biophys 60: 23-39, 2021.

[3] Toyokuni S: Iron addiction with ferroptosis-resistance in asbestos-induced mesothelial carcinogenesis: Toward the era of mesothelioma prevention. Free Radic Biol Med 133: 206-215, 2019.

[4] Oury TD, Sporn TA, Roggli VL (eds): Pathology of Asbestos-Associated Diseases, Third edition, Springer, Berlin/Heidelberg, 2014.

[5] IARC, WHO, Asbestos (chrysotile, amosite, crocidolite, tremolite, actinolite, and anthophyllite), IARC Monographs on the Evaluation of Carcinogenic Risks to Humans. A Review of Human Carcinogens; Part C: Arsenic, Metals, Fibres, and Dusts, Lyon, France, 2012, pp. 219-309.

[6] Wagner JC, Sleggs CA, Marchand P: Diffuse pleural mesothelioma and asbestos exposure in North Western Cape Province. Br J Ind Med 17: 260-271, 1960.

[7] Alpert N, van Gerwen M, Taioli E: Epidemiology of mesothelioma in the 21st century in Europe and the United States, 40 years after restricted/banned asbestos use. Transl Lung Cancer Res 9: S28, 2020.

[8] Husain AN, Colby T, Ordonez N, Krausz T, Attanoos R, et al.: Guidelines for pathologic diagnosis of malignant mesothelioma: 2012 update of the consensus statement from the International Mesothelioma Interest Group. Arch Pathol Lab Med 137: 647-667, 2012.

[9] Toyokuni S: Mechanisms of asbestos-induced carcinogenesis. Nagoya J Med Sci 71: 1-10, 2009.

[10] Clift MJD, Raemy DO, Endes C, Ali Z, Lehmann AD, et al.: Can the Ames test provide an insight into nano-object mutagenicity? Investigating the interaction between nano-objects and bacteria. Nanotoxicology 7: 1373-1385, 2013.

[11] 79 Kubota workers killed by asbestos over 26 years (2005.06.30), The Daily Yomiuri, 2005.

[12] Asciak R, George V, Rahman NM: Update on biology and management of mesothelioma. Eur Respir Rev 30: 200226, 2021.

[13] Witschi HR, Last JA: Toxic responses of the respiratory system. Casarett and Doull's toxicology: the basic science of poisons. 6th ed. New York: McGraw-Hill Book Co 515-534, 2001.

[14] Toyokuni S: Iron-induced carcinogenesis: the role of redox regulation. Free Radic Biol Med 20: 553-566, 1996.

[15] Toyokuni S: The origin and future of oxidative stress pathology: From the recognition of carcinogenesis as an iron addiction with ferroptosisresistance to non-thermal plasma therapy. Pathol Int 66: 245-259, 2016.

[16] Yanatori I, Kishi F: DMT1 and iron transport. Free Radic Biol Med 133: 55-63, 2019.

[17] Toyokuni S: Role of iron in carcinogenesis: Cancer as a ferrotoxic disease. Cancer Sci 100: 9-16, 2009.

[18] Toyokuni S, Yanatori I, Kong Y, Zheng H, Motooka Y, et al.: Ferroptosis at the crossroads of infection, aging and cancer. Cancer Sci 111: 2665-2671, 2020.

[19] Mancias JD, Wang XX, Gygi SP, Harper JW, Kimmelman AC: Quantitative proteomics identifies NCOA4 as the cargo receptor mediating ferritinophagy. Nature 509: 105-109, 2014.

[20] Masaldan S, Clatworthy SAS, Gamell C, Meggyesy PM, Rigopoulos AT, et al.: Iron accumulation in senescent cells is coupled with impaired ferritinophagy and inhibition of ferroptosis. Redox Biol 14: 100-115, 2018.

[21] Yanatori I, Richardson DR, Toyokuni S, Kishi F: The new role of poly (rC)-binding proteins as iron transport chaperones: Proteins that could couple with inter-organelle interactions to safely traffic iron. Biochim Biophys Acta Gen Subj 1864: 129685, 2020.

[22] Yanatori I, Richardson DR, Dhekne HS, Toyokuni S, Kishi F: CD63 is Regulated by Iron via the IRE-IRP System and is Important for Ferritin Secretion by Extracellular Vesicles. Blood 2021 doi: 10.1182/blood.2021010995 (in press).

[23] Mancias JD, Wang X, Gygi SP, Harper JW, Kimmelman AC: Quantitative proteomics identifies NCOA4 as the cargo receptor mediating ferritinophagy. Nature 509: 105-109, 2014.

[24] Yanatori I, Yasui Y, Tabuchi M, Kishi F: Chaperone protein involved in transmembrane transport of iron. Biochem J 462: 25-37, 2014.

[25] Yanatori I, Richardson DR, Imada K, Kishi F: Iron export through the transporter Ferroportin 1 is modulated by the iron chaperone PCBP2. J Biol Chem 291: 17303-17318, 2016.

[26] Yanatori I, Richardson DR, Toyokuni S, Kishi F: The iron chaperone poly(rC)-binding protein 2 forms a metabolon with the heme oxygenase 1/cytochrome P450 reductase complex for heme catabolism and iron transfer. J Biol Chem 292: 13205-13229, 2017.

[27] Shi HF, Bencze KZ, Stemmler TL, Philpott CC: A cytosolic iron chaperone that delivers iron to ferritin. Science 320: 1207-1210, 2008.

[28] Philpott CC, Jadhav S: The ins and outs of iron: Escorting iron through the mammalian cytosol. Free Radic Biol Med 133: 112-117, 2019.

[29] Zhang X, Di C, Chen Y, Wang J, Su R, et al.: Multilevel regulation and molecular mechanism of poly (rC)-binding protein 1 in cancer.

FASEB J 34: 15647-15658, 2020.

[30] Chen C, Lei J, Zheng Q, Tan S, Ding K, et al.: Poly(rC) binding protein 2 (PCBP2) promotes the viability of human gastric cancer cells by regulating CDK2. FEBS Open Bio 8: 764-773, 2018.

[31] Stockwell BR, Friedmann Angeli JP, Bayir H, Bush AI, Conrad M, et al.: Ferroptosis: A Regulated Cell Death Nexus Linking Metabolism, Redox Biology, and Disease. Cell 171: 273-285, 2017.

[32] Dixon SJ, Lemberg KM, Lamprecht MR, Skouta R, Zaitsev EM, et al.: Ferroptosis: an iron-dependent form of nonapoptotic cell death. Cell 149: 1060-1072, 2012.

[33] Drakesmith H, Nemeth E, Ganz T: Ironing out Ferroportin. Cell Metab 22: 777-87, 2015.

[34] Toyokuni S: Novel aspects of oxidative stress-associated carcinogenesis. Antioxid Redox Signal 8: 1373-1377, 2006.

[35] Toyokuni S: Mysterious link between iron overload and CDKN2A/2B. J Clin Biochem Nutr 48: 46-49, 2011.

[36] Ito F, Nishiyama T, Shi L, Mori M, Hirayama T, et al.: Contrasting intra- and extracellular distribution of catalytic ferrous iron in ovalbumin-induced peritonitis. Biochem Biophys Res Commun 476: 600-6, 2016.

[37] Hou W, Xie Y, Song X, Sun X, Lotze MT, et al.: Autophagy promotes ferroptosis by degradation of ferritin. Autophagy 12: 1425-1428, 2016.

[38] Ito J, Omiya S, Rusu MC, Ueda H, Murakawa T, et al.: Iron derived from autophagy-mediated ferritin degradation induces cardiomyocyte death and heart failure in mice. Elife 10: e62174, 2021.

[39] Ito F, Yanatori I, Maeda Y, Nimura K, Ito S, et al.: Asbestos conceives Fe(II)-dependent mutagenic stromal milieu through ceaseless macrophage ferroptosis and beta-catenin induction in mesothelium. Redox Biol 36: 101616, 2020.

[40] Stanton MF, Wrench C: Mechanisms of mesothelioma induction with asbestos and fibrous glass. J Natl Cancer Inst 48: 797-821, 1972.

[41] Iijima S: Helical Microtubules of Graphitic Carbon. Nature 354: 56-58, 1991.

[42] Endo M, Strano MS, Ajayan PM, Potential applications of carbon nanotubes, Carbon nanotubes, Springer 2008, pp. 13-62.

[43] Zhang Q, Huang JQ, Qian WZ, Zhang YY, Wei F: The Road for Nanomaterials Industry: A Review of Carbon Nanotube Production, Post-Treatment, and Bulk Applications for Composites and Energy Storage. Small 9: 1237-1265, 2013.

[44] Nagai H, Okazaki Y, Chew S, Misawa N, Yamashita Y, et al.: Diameter of multi-walled carbon nanotubes is a critical factor in mesothelial injury and subsequent carcinogenesis. Proc Natl Acad Sci U S A 108: E1330-1338, 2011.

[45] Nagai H, Okazaki Y, Chew SH, Misawa N, Miyata Y, et al.: Intraperitoneal administration of tangled multiwalled carbon nanotubes of 15 nm in diameter does not induce mesothelial carcinogenesis in rats. Pathol Int 63: 457-462, 2013.

[46] Wang Y, Okazaki Y, Shi L, Kohda H, Tanaka M, et al.: Role of hemoglobin and transferrin in multi-wall carbon nanotube-induced mesothelial injury and carcinogenesis. Cancer Sci 107: 250-257, 2016.

[47] Cheng JQ, Jhanwar SC, Klein WM, Bell DW, Lee WC, et al.: p16 alterations and deletion mapping of 9p21-p22 in malignant mesothelioma. Cancer Res 54: 5547-5551, 1994.

[48] Xio S, Li D, Vijg J, Sugarbaker DJ, Corson JM, et al.: Codeletion of p15 and p16 in primary malignant mesothelioma. Oncogene. 11: 511-515, 1995.

[49] Jiang L, Akatsuka S, Nagai H, Chew SH, Ohara H, et al.: Iron overload signature in chrysotile-induced malignant mesothelioma. J Pathol 228: 366-377, 2012.

[50] Akatsuka S, Yamashita Y, Ohara H, Liu YT, Izumiya M, et al.: Fenton reaction induced cancer in wild type rats recapitulates genomic alterations observed in human cancer. PLoS ONE 7: e43403, 2012.

[51] Okada S: Iron-induced tissue damage and cancer: The role of reactive oxygen free radicals. Pathol Int 46: 311-332, 1996.

[52] Nakayama M: Macrophage recognition of crystals and nanoparticles. Front Immunol 9: 103, 2018.

[53] Omori S, Tsugita M, Hoshikawa Y, Morita M, Ito F, et al.: Tim4 recognizes carbon nanotubes and mediates phagocytosis leading to granuloma formation. Cell Rep 34: 108734, 2021.

[54] Chow A, Schad S, Green MD, Hellmann MD, Allaj V, et al.: Tim-4(+) cavity-resident macrophages impair anti-tumor CD8(+) T cell immunity. Cancer Cell 39: 973-988 e9, 2021.

[55] Caronni N, Piperno GM, Simoncello F, Romano O, Vodret S, et al.: TIM4 expression by dendritic cells mediates uptake of tumor-associated antigens and anti-tumor responses. Nat Commun 12: 2237, 2021.

[56] Grosse Y, Loomis D, Guyton KZ, Lauby-Secretan B, El Ghissassi F, et al.: Carcinogenicity of fluoro-edenite, silicon carbide fibres and whiskers, and carbon nanotubes. Lancet Oncol 15: 1427-1428, 2014.

[57] Sealy C: Carbon nanotubes bring a new touch to robotics. Nano Today 10: 672-673, 2015.

[58] Pearce CL, Templeman C, Rossing MA, Lee A, Near AM, et al.: Association between endometriosis and risk of histological subtypes of ovarian cancer: a pooled analysis of case-control studies. Lancet Oncol 13: 385-94, 2012.

[59] Kajiyama H, Suzuki S, Yoshihara M, Tamauchi S, Yoshikawa N, et al.: Endometriosis and cancer. Free Radic Biol Med 133: 186-192, 2018.

[60] Langseth H, Johansen BV, Nesland JM, Kjaerheim K: Asbestos fibers in ovarian tissue from Norwegian pulp and paper workers. Int J Gynecol Cancer 17: 44-9, 2007.

[61] Johnson KE, Popratiloff A, Fan Y, McDonald S, Godleski JJ: Analytic comparison of talc in commercially available baby powder and in pelvic tissues resected from ovarian carcinoma patients. Gynecol Oncol 159: 527-533, 2020.

[62] Slomovitz B, De Haydu C, Taub M, Coleman RL, Monk BJ: Asbestos and ovarian cancer: examining the historical evidence. Int J Gynecol Cancer 31: 122-128, 2021.

[63] O'Brien KM, Tworoger SS, Harris HR, Anderson GL, Weinberg CR, et al.: Association of powder use in the genital area with risk of ovarian cancer. JAMA 323: 49-59, 2020.

[64] Johnson KE, Popratiloff A, Fan Y, McDonald S, Godleski JJ: Analytic comparison of talc in commercially available baby powder and in pelvic tissues resected from ovarian carcinoma patients. Gynecol Oncol 159: 527-533, 2020.

[65] McDonald SA, Fan Y, Welch WR, Cramer DW, Godleski JJ: Migration of Talc From the Perineum to Multiple Pelvic Organ Sites. Am J Clin Pathol 152: 590-607, 2019.

[66] Goodman JE, Kerper LE, Prueitt RL, Marsh CM: A critical review of talc and ovarian cancer. J Toxicol Environ Health B Crit Rev 23: 183-213, 2020.

[67] Nagai H, Okazaki Y, Chew SH, Misawa N, Yasui H, et al.: Deferasirox induces mesenchymal-epithelial transition in crocidolite-induced mesothelial carcinogenesis in rats. Cancer Prev Res 6: 1222-30, 2013.

[68] Ohara Y, Chew SH, Shibata T, Okazaki Y, Yamashita K, et al.: Phlebotomy as a preventive measure for crocidolite-induced mesothelioma in male rats. Cancer Sci 109: 330-339, 2018.

[69] Shi L, Ito F, Wang Y, Okazaki Y, Tanaka H, et al.: Non-thermal plasma induces a stress response in mesothelioma cells resulting in increased endocytosis, lysosome biogenesis and autophagy. Free Radic Biol Med 108: 904-917, 2017.

[70] Jiang L, Zheng H, Lyu Q, Hayashi S, Sato K, et al.: Lysosomal nitric oxide determines transition from autophagy to ferroptosis after exposure to plasma-activated Ringer's lactate. Redox Biol 43: 101989, 2021.

[71] Ebina Y, Okada S, Hamazaki S, Ogino F, Li JL, et al.: Nephrotoxicity and renal cell carcinoma after use of iron- and aluminum- nitrilotriacetate complexes in rats. J Natl Cancer Inst 76: 107-113, 1986.

[72] Li JL, Okada S, Hamazaki S, Ebina Y, Midorikawa O: Subacute nephrotoxicity and induction of renal cell carcinoma in mice treated with ferric nitrilotriacetate. Cancer Res 47: 1867-1869, 1987.

[73] Nagai H, Ishihara T, Lee WH, Ohara H, Okazaki Y, et al.: Asbestos surface provides a niche for oxidative modification. Cancer Sci 102: 2118-2125, 2011.

Metallomics Research 2021 (1) #MR202105

Review https://metallomicsresearch.brte.org

Corticosteroid receptor-mediated synaptic Zn^{2+} dynamics in the hippocampus and its significance

Miki Suzuki, Haruna Tamano, Atsushi Takeda*

School of Pharmaceutical Sciences, University of Shizuoka, 52-1 Yada, Suruga-ku, Shizuoka 422-8526, Japan

Summary

Neuronal Zn^{2+} homeostasis is closely linked with not only cognitive function but also cognitive decline, while there is no hormone involved in zinc homeostasis unlike calcium homeostasis. Extracellular Zn^{2+} dynamics is modified by extracellular levels of glucocorticoids and glutamate, which are linked with stress response. Extracellular glucocorticoid signal is transmitted via not only glucocorticoid receptors but also mineralocorticoid receptors. Membrane corticosteroid receptors dynamically modifies synaptic Zn^{2+} dynamics in the hippocampus. Synaptic plasticity, i.e., long-term potentiation (LTP), which is a cellular mechanism of memory, is affected by rapid intracellular Zn^{2+} dysregulation via membrane corticosteroid receptor activation in the CA1; Corticosterone rapidly induces the increase in intracellular Zn^{2+} via membrane corticosteroid receptor activation, and decreases phosphorylated CaMKII level, resulting in attenuating CA1 LTP. The mechanism of intracellular Zn^{2+} dysregulation is different between membrane mineralocorticoid and glucocorticoid receptor-mediated signaling. In contrast, corticosterone-induced intracellular Ca^{2+} dysregulation is less crucial for affecting CA1 LTP. The basal concentration (~100 pM) of intracellular Zn^{2+} is much lower than that (~100 nM) of intracellular Ca^{2+}. Therefore, the precise mechanism is required to regulate intracellular Zn^{2+} homeostasis because of more critical neurotoxicity of Zn^{2+}. This review summarizes the physiological significance of intracellular Zn^{2+} homeostasis focused on signaling of corticosterone and glutamate in the extracellular compartment.

Key words: Zn^{2+}, membrane corticosteroid receptor, glucocorticoid, hippocampus, stress

Statements about COI: All authors do not have any known or potential conflict of interest including any financial, personal or other relationships with other people or organizations within three years of beginning the submitted work that could inappropriately influence, or be perceived to influence, their work.

*Correspondence:
School of Pharmaceutical Sciences, University of Shizuoka, 52-1 Yada, Suruga-ku, Shizuoka 422-8526, Japan
Tel: +81-54-264-5893
E-mail: takedaa@u-shizuoka-ken.ac.jp

Received: August 30, 2021
Accepted: September 29, 2021
Released online: October 15, 2021

Introduction

Zrt-Irt-like proteins (ZIPs) are involved in the transport of Zn^{2+} into the cytoplasm, while the zinc transporter (ZnT) family is involved in the transport of Zn^{2+} out of the cytoplasm. ZIPs and ZnTs serve to regulate Zn^{2+} homeostasis in the living body including the brain [1-3]. The basal concentrations of extracellular Zn^{2+} and intracellular Zn^{2+} are approximately 10 nM [4] and 100 pM (**Fig. 1B**) [5,6], respectively, in the brain, while the basal concentrations of extracellular Ca^{2+}

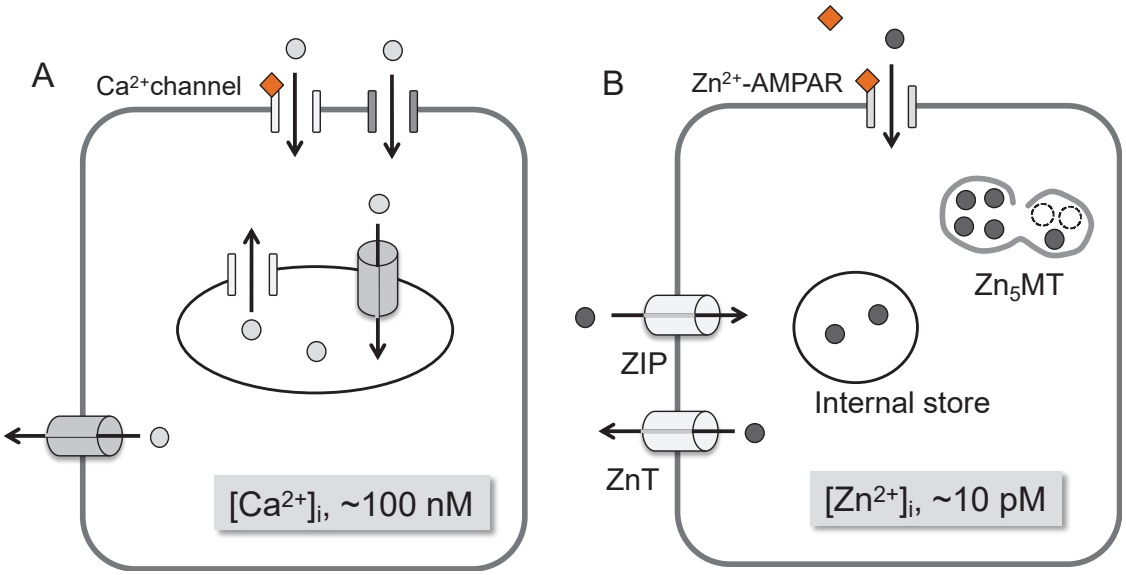

Figure 1. **Intracellular buffering systems of Ca^{2+} and Zn^{2+}**

A The influx of extracellular Ca^{2+} is dynamically induced through Ca^{2+} channels for intracellular Ca^{2+} signaling, while the basal concentration of intracellular Ca^{2+} is strictly regulated by the efflux of cytosol Ca^{2+} to the extracellular compartment and the reuptake of cytosol Ca^{2+} into the Ca^{2+} stores.

B The influx of extracellular Zn^{2+} is also dynamically induced through Zn^{2+}-permeable GluR2-lacking AMPA receptors (Zn^{2+}-AMPAR) for intracellular Zn^{2+} signaling. While the basal concentration of intracellular Zn^{2+} is regulated by the Zn^{2+}-buffering system, i.e., Zn^{2+} transporters (ZIPs and ZnTs), MTs, and internal stores containing Zn^{2+}, the mechanism is poorly understood.

and intracellular Ca^{2+}, which are 1.3 mM and 100 nM (**Fig. 1A**), respectively, are much higher than of extracellular Zn^{2+} and intracellular Zn^{2+}, resulting in much less attention paid to Zn^{2+} than Ca^{2+} to understand brain function and brain dysfunction. For understanding synaptic function, for example, no attention has been paid to Zn^{2+} in the extracellular compartment; Zn^{2+} is not added to artificial cerebrospinal fluid (ACSF), i.e., the brain extracellular medium widely used for *in vitro* and *in vivo* experiments. Not only neuronal excitation but also synaptic plasticity such as long-term potentiation (LTP), a cellular mechanism of memory, are modified in brain slices bathed in ACSF without Zn^{2+} where the original neurophysiology may be modified [7,8].

In the brain, approximately 80% of zinc is zinc metalloproteins. Approximately 20% is histochemically reactive as determined by Timm's sulfide-silver staining and concentrated in the synaptic vesicles of a subclass of glutamatergic neuron [9]. The latter serves as a signal factor, free Zn^{2+}, in both the intracellular and extracellular compartments. Synaptic Zn^{2+} dynamically functions in conjunction with synaptic activity, i.e., glutamatergic synapse activity in the limbic system including the hippocampus [10,11]. Synaptic Zn^{2+} plays a key role in not only cognitive function but also cognitive decline. However, there is no hormone involved in zinc homeostasis unlike calcium homeostasis. Extracellular Zn^{2+} dynamics, which is linked with intracellular Zn^{2+} homeostasis, is dynamically modified by the changes in extracellular circumstances. Dietary zinc deficiency activates the hypothalamo-pituitary-adrenocortical (HPA) system and increases glucocorticoid secretion from the adrenal cortex [12]. Extracellular levels of glucocorticoids modify extracellular Zn^{2+} dynamics followed by modifying intracellular Zn^{2+} level [13]. Extracellular levels of glucocorticoids and glutamate, which are linked with stress response, affects not only intracellular Ca^{2+} homeostasis but also intracellular Zn^{2+} homeostasis.

This review summarizes the physiological significance of intracellular Zn^{2+} homeostasis focused on signaling of corticosterone and glutamate in the extracellular compartment.

Intracellular buffering of Ca^{2+} and Zn^{2+}

Vulnerability to Ca^{2+} dysregulation is facilitated with brain aging [14-16]. Ca^{2+} dysregulation is not ubiquitous in the brain, and has been observed in specific cell populations and areas. For example, the expression of L-type Ca^{2+} channels is age-relatedly

elevated in hippocampal pyramidal cells [17]. *N*-Methyl-*D*-aspartate (NMDA) receptor function is age-relatedly reduced in the frontal cortex and the hippocampus [18], suggesting that a compensatory mechanism is induced in the process of brain aging to regulate the availability of intracellular Ca^{2+} signaling. On the other hand, intracellular Ca^{2+} buffering is involved not only in cognitive function but also in cognitive decline, and is weakened with brain aging (**Fig. 1A**) [15].

To regulate the availability of intracellular Zn^{2+} signaling, a compensatory mechanism is also induced in the process of brain aging. The zinc concentration in presynaptic vesicles is reduced by the decrease in ZnT3 protein with aging [19,20], while the extracellular zinc concentration is age-relatedly increased in the hippocampus [21]. Intracellular Zn^{2+} buffering is also involved not only in cognitive function but also in cognitive decline. However, the Zn^{2+}-buffering system is more poorly understood than the Ca^{2+}-buffering system (**Fig. 1**). Weakened intracellular Ca^{2+} buffering, with a net decrease in the Ca^{2+}-buffering capacity, is linked with both normal aging [15] and neurological disorders such as AD [22].

The Zn^{2+}-buffering system is composed of Zn^{2+} transporters (ZIPs and ZnTs), Zn^{2+}-binding proteins such as metallothioneins (MTs), internal stores containing Zn^{2+}, and Ca^{2+}-permeable channels, which is dynamically linked with synaptic excitation (**Fig. 1B**). Judging from the increased concentration of extracellular Zn^{2+} [21], it is estimated that intracellular Zn^{2+} buffering is modified in the aged brain of rats [23]. The characteristics (easiness) of extracellular Zn^{2+} influx may lead to reduced intracellular Zn^{2+}-buffering capacity in the aged dentate gyrus, which represents weakened intracellular Zn^{2+} buffering [23]. Because MT synthesis in the hippocampus is induced even in aged rats, it is estimated that MT-mediated Zn^{2+}-buffering capacity is not significantly different between young and aged hippocampus [24]. MTs are of benefit to maintaining intracellular Zn^{2+} homeostasis under acute changes in intracellular Zn^{2+} concentration [24].

Corticosteroid receptor-mediated synaptic Zn^{2+} dynamics in the hippocampus

The HPA system is activated after exposure to stress followed by increase in glucocorticoid secretion from the adrenal cortex [25-27]. Glucocorticoids pass through the brain barrier system and modulate cognitive activity bidirectionally [28-30]. Under stressful circumstances, glucocorticoids are excessively and/or persistently secreted and considered a major factor for stress-related memory disorders [31,32]. Glucocorticoids (corticosterone in rodents) act on via both mineralocorticoid and glucocorticoid receptors, which exist on the plasma membrane and in the cytosolic compartment. Many of glucocorticoid actions require time to lead to changes in gene expression (>15–30 min), while glucocorticoids have rapid non-genomic actions via the membrane-bound receptors [33].

The hippocampus is enriched with mineralocorticoid and glucocorticoid receptors and is a target area under stressful circumstances. Glucocorticoids facilitate glutamate release from the neuron terminals via the rapid action of membrane mineralocorticoid receptors [34,35]. On the basis of the evidence on co-release of glutamate and Zn^{2+} from a subclass of glutamatergic neurons, i.e., zincergic neurons, it is estimated that glucocorticoids facilitate Zn^{2+} release from zincergic neuron terminals under stressful conditions [36] and that Zn^{2+} accumulation in the extracellular compartment plays a key role for cognitive decline in cooperation with glutamate accumulation in the extracellular compartment [36-38].

Synaptic plasticity, i.e., long-term potentiation (LTP) has been extensively studied in the hippocampus [39]. The entorhinal cortex is connected with the hippocampus and both areas play a key role for cognitive performance (**Fig. 2**). In the hippocampal CA1, pyramidal cells are innervated by the non-zincergic perforant pathway from the entorhinal cortex and also by zincergic Schaffer collateral from the hippocampal CA3 pyramidal cells (**Fig. 2**). Zn^{2+} released from Schaffer collateral is required to induce LTP at the Schaffer collateral-CA1 pyramidal cell synapses in the CA1 (**Fig. 3 and 4**) [40], while excess Zn^{2+} release attenuates the LTP [41]. In contrast, Zn^{2+} released from internal stores is required to induce LTP at the perforant pathway-CA1 pyramidal cell synapses in the CA1 (**Fig. 3 and 4**) [42]. Extracellular Zn^{2+} preferentially passes through Ca^{2+}- and Zn^{2+}-permeable GluR2-lacking α-amino-3-hydroxy-5-methyl-4-isoxazolepropionate (AMPA) receptors followed by intracellular Zn^{2+} dysregulation (toxicity) when glutamate accumulates in the extracellular compartment of the CA1, resulting in neurodegeneration including cognitive decline [43-46]. Extracellular glutamate-mediated cognitive decline, which is induced by stimulation with high K^+, is linked with intracellular Zn^{2+} dysregulation, but not intracellular Ca^{2+} dysregulation [47]. In 6-hydroxydopamine-induced Parkinson's disease in rats, nigral dopaminergic degeneration is also induced by intracellular Zn^{2+} dysregulation, but not intracellular Ca^{2+} dysregulation [48]. Ca^{2+}- and Zn^{2+}-permeable GluR2-lacking AMPA receptors are more closely linked with intracellular Zn^{2+} toxicity than intracellular Ca^{2+} toxicity [49,50], because the basal concentration of intracellular Zn^{2+} is much lower.

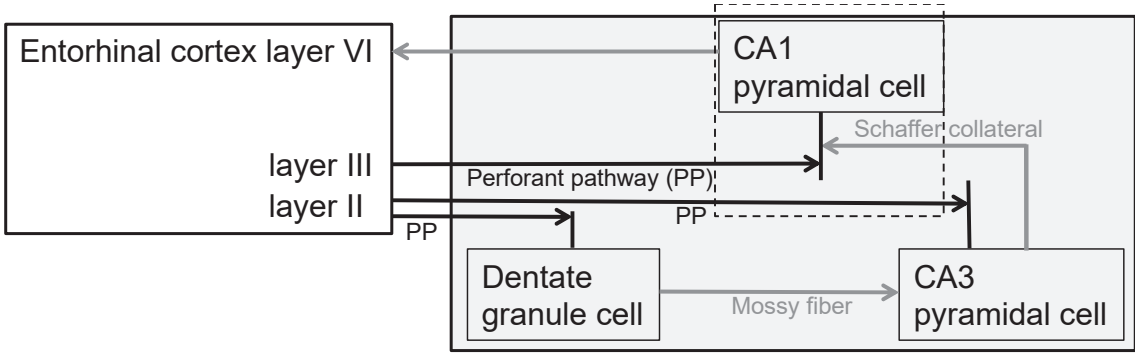

Figure 2. **The hippocampus is connected with the entorhinal cortex via the perforant pathway**
Mossy fiber and Schaffer collateral (the grey arrow) are zincergic and perforant pathway is non-zincergic.

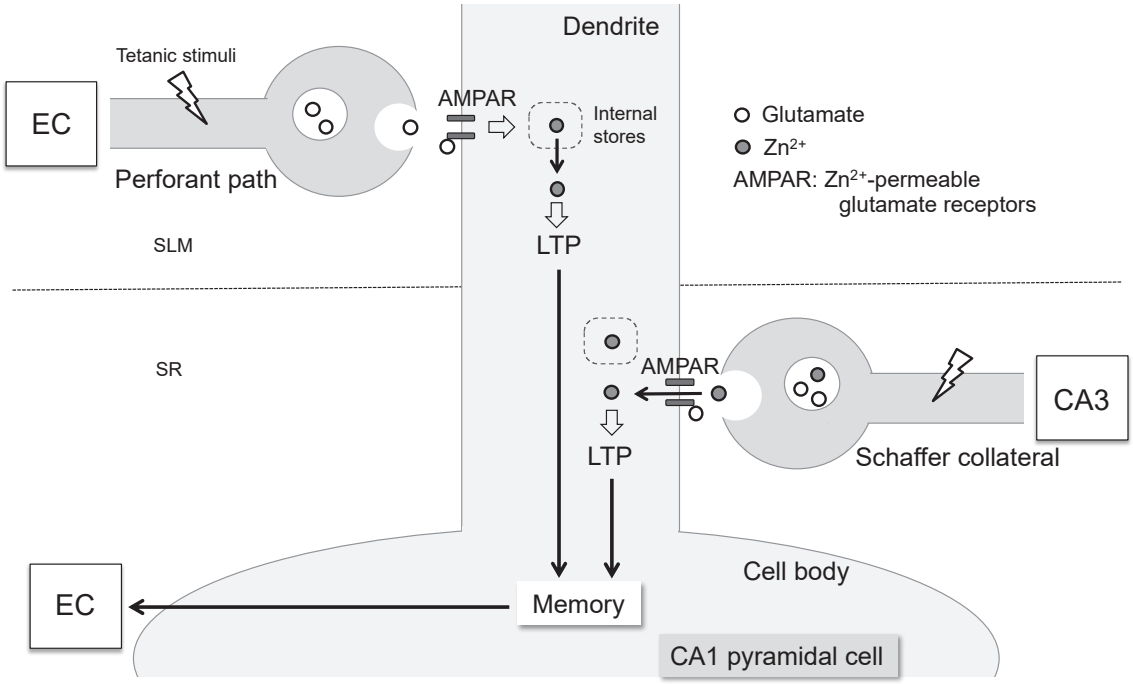

Figure 3. **Intracellular Zn^{2+} signaling is required for both perforant pathway LTP and Schaffer collateral LTP followed by hippocampus-dependent memory.**
The figure represents the area surrounded by the dotted line of Fig. 2. At perforant pathway synapses, Ca^{2+} signaling via NMDA receptor activation might be involved in Zn^{2+} release from the internal stores, which is required for perforant pathway LTP. At Schaffer collateral synapses, in contrast, transsynaptic Zn^{2+} influx through Zn^{2+}-permeable GluR2-lacking AMPA receptors is required for Schaffer collateral LTP. EC, entorhinal cortex; SLM, stratum lacunosum-moleculare; SR, stratum radiatum.

Acute stress induces a rapid corticosterone rise in the hippocampus of rats and impairs memory formation [51,52]. Non-genomic actions, especially via membrane mineralocorticoid receptor activation, are involved in the impairment of memory retrieval [53-55]. Although intracellular Zn^{2+} dysregulation is induced by excess signaling of extracellular glutamate, there has been no evidence on the relationship between synaptic Zn^{2+} dynamics and membrane corticosteroid receptors. We postulated that rapid modification of synaptic Zn^{2+} dynamics is linked with membrane corticosteroid receptors and leads to in vivo aberrant synaptic plasticity [38].

In the CA1, rapid changes in CA1 pyramidal cell function emerge via presyanptic and postsynaptic membrane mineralocorticoid receptors: corticosterone increases glutamate release probability pre-synaptically and causes a suppression in potassium current

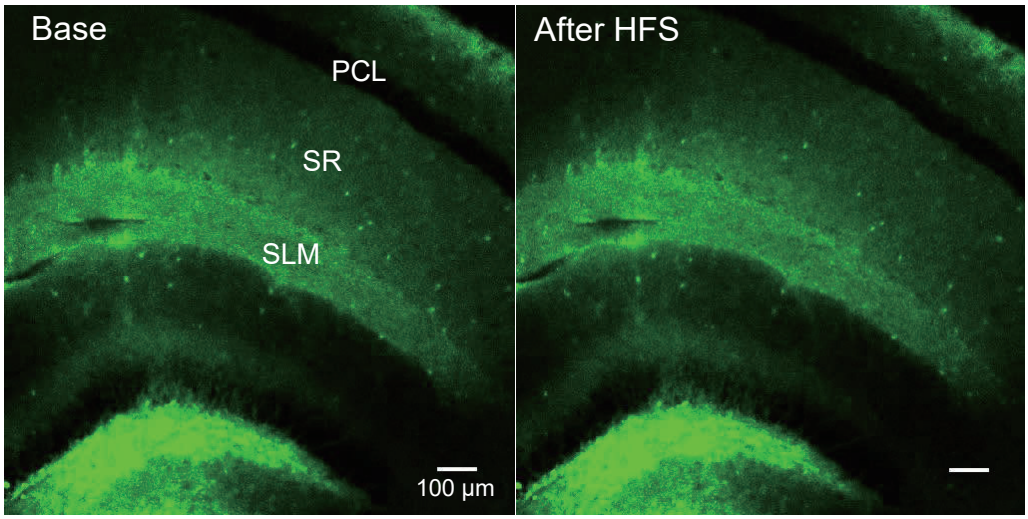

Figure 4. **Intracellular Zn^{2+} imaging in hippocampal CA1**
The basal level of intracellular Zn^{2+} in the CA1, which represents the area surrounded by the dotted line of Fig. 2, is imaged with intracellular ZnAF-2. Intracellular Zn^{2+} increases even in the stratum lacunosum-moleculare (SLM) where the perforant pathway connects with CA1 pyramidal cells after high-frequency stimulation (HFS) to induce LTP (Fig. 3). PCL, pyramidal cell layer; SLM, stratum lacunosum-moleculare; SR, stratum radiatum.

post-synaptically, leading to enhanced CA1 pyramidal cell excitability [56]. Corticosterone-induced increase in extracellular Zn^{2+}, which is linked with Schaffer collateral excitation, induces the subsequent attenuation of Schaffer collateral LTP in vivo [38]. Corticosterone-induced increase in extracellular Zn^{2+} may lead to intracellular Zn^{2+} dysregulation. In rat brain slices, corticosterone-induced rapid increases in extracellular and intracellular Zn^{2+} are canceled in the presence of spironolactone, a mineralocorticoid receptor antagonist that canceled corticosterone-induced attenuation of CA1 LTP. Corticosterone rapidly increases Zn^{2+} release from the Schaffer collateral via membrane mineralocorticoid receptor activation and then increases intracellular Zn^{2+} in CA1 pyramidal cells probably via Zn^{2+}-permeable GluR2-lacking AMPA receptor activation, resulting in the attenuated CA1 LTP (**Fig. 5B**). On the other hand, mifepristone, a glucocorticoid receptor antagonist, which canceled corticosterone-induced attenuation of CA1 LTP, also canceled corticosterone-induced rapid increase in intracellular Zn^{2+}, but not extracellular Zn^{2+}, suggesting that the short-term block of corticosterone-induced increase in intracellular Zn^{2+} with mifepristone is also benefit to canceling of the attenuated CA1 LTP. The mechanism of intracellular Zn^{2+} dysregulation is different between membrane mineralocorticoid and glucocorticoid receptor-mediated signaling (**Fig. 5B**). Corticosterone-induced rapid increase in intracellular Ca^{2+} is blocked by spironolactone, but not by mifepristone, suggesting that corticosterone-induced rapid intracellular Ca^{2+} dysregulation is less crucial for affecting CA1 LTP than rapid intracellular Zn^{2+} dysregulation.

Synaptic Zn^{2+} and Ca^{2+}/calmodulin-dependent protein kinase II (CaMKII)

Corticosterone regulates AMPA receptors trafficking including Zn^{2+}-permeable GluR2-lacking AMPA receptors and facilitates LTP in the hippocampus [57-60]. Newly synthesized LTP-related proteins can be captured at new binding sites via CaMKII, a key molecule for LTP, for structural synapse enlargement, sustaining the potentiated state for a long term. The location of CaMKII is crucial for the construction of the potentiated state [61,62]. The interplay between the kinase and structural functions of CaMKII is important for defining a time window permissive for synaptic plasticity [63]. It is estimated that Zn^{2+} concentrates in the postsynaptic density (PSD) via intracellular Zn^{2+} signaling after LTP induction, which can be linked with membrane mineralocorticoid and glucocorticoid receptor activation (**Fig. 5A**), and is able to influence the recruitment of ProSAP/Shank proteins to PSDs in a family member-specific manner during the course of synaptogenesis and structural plasticity [64,65]. Intracellular Zn^{2+} concentration might reach a few nanomolar for synaptic plasticity.

Total and phosphorylated CaMKII are increased in the hippocampal CA1 after CA1 LTP induction [66,67]. In contrast, chronic stress decreases basal levels of phosphorylated CaMKII and then attenuates LTP induction [68]. It is possible that Zn^{2+}

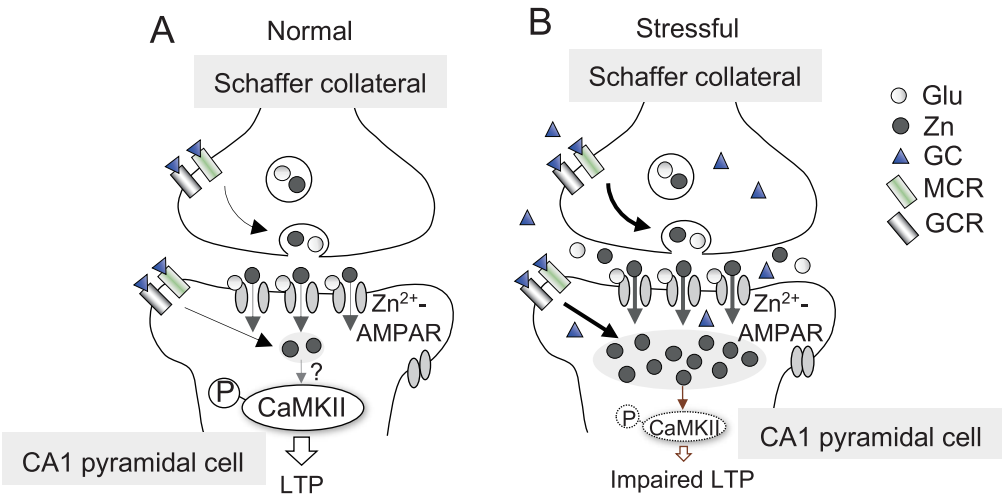

Figure 5. Schematic diagram on bidirectional synaptic Zn^{2+} dynamics via membrane corticosteroid receptor-mediated signaling in LTP induction

A The release of glutamate and Zn^{2+} is increased from Schaffer collateral by learning behavior and the increase is accelerated by glucocorticoid (GC): Presynaptic activation of membrane mineralocorticoid receptors (MCR) increases the release probability followed by the influx of extracellular Zn^{2+} through Zn^{2+}-permeable GluR2-lacking AMPA receptors (Zn^{2+}-AMPAR). Postsynaptic membrane corticosteroid receptors are also involved in the increase in intracellular Zn^{2+} in CA1 pyramidal cells followed by LTP (left).

B After exposure to stress, intracellular Zn^{2+} is excessively increased in CA1 pyramidal cells according to the bold arrows; presynaptic membrane mineralocorticoid receptors and postsynaptic membrane corticosteroid receptors, which are excessively activated, induce intracellular Zn^{2+} dysregulation followed by impaired LTP via the decrease in phosphorylated CaMKII (right). GCR, glucocorticoid receptor.

can directly modulate CaMKII activity for synaptic plasticity (**Fig. 5A**). At high micromolar concentrations (~400 μM), Zn^{2+} turns CaMKII into an increased mobility form on SDS-PAGE in vitro [69], while it is improbable in vivo. Intracellular Zn^{2+} concentration may reach low nanolmolar (~10 nM), an estimated concentration of extracellular Zn^{2+}, under the perfusion with $ZnCl_2$ and corticosterone prior to LTP induction, while the concentration may be neurotoxic [70].

Under stressful condition, on the other hand, corticosterone decreases the basal levels of phosphorylated CaMKII and the decreases are canceled by co-perfusion with CaEDTA, an extracellular Zn^{2+} chelator, or spironolactone, suggesting that the rapid influx of extracellular Zn^{2+} induced by corticosterone via presynaptic activation of membrane mineralocorticoid receptors into CA1 pyramidal cells leads to the decrease in the basal level of phosphorylated CaMKII (**Fig. 5B**).

Perspective

The basal concentration of intracellular Zn^{2+} is approximately 1000 times lower than that of intracellular Ca^{2+}, resulting in more critical neurotoxicity of Zn^{2+}. We need to understand the precise mechanism on regulation of intracellular Zn^{2+} homeostasis, i.e., the Zn^{2+}-buffering system under physiological and pathological conditions [71,72].

References

[1] Dufner-Beattie J, Kuo YM, Gitschier J, Andrews GK: The adaptive response to dietary zinc in mice involves the differential cellular localization and zinc regulation of the zinc transporters ZIP4 and ZIP5. J Biol Chem 279: 49082-49090, 2004.

[2] Cousins RJ, Liuzzi JP, Lichten LA: Mammalian zinc transport, trafficking, and signals. J Biol Chem 281: 24085-24089, 2006.

[3] Fukada T, Kambe T. Molecular and genetic features of zinc transporters in physiology and pathogenesis. Metallomics 3: 662-674, 2011.

[4] Frederickson CJ, Giblin LJ, Krezel A, McAdoo DJ, Muelle RN, Zeng Y, Balaji RV, Masalha R, Thompson RB, Fierke CA: Concentrations of extracellular free zinc (pZn)e in the central nervous system during simple anesthetization, ischemia and reperfusion. Exp Neurol 198: 285-293, 2006.

[5] Sensi SL, Canzoniero LMT, Yu SP, Ying HS, Koh JY, Kerchner GA, Choi DW: Measurement of intracellular free zinc in living cortical neurons: routes of entry. J Neurosci 15: 9554-9564, 1997.

[6] Colvin RA, Bush AI, Volitakis I, Fontaine CP, Thomas D, Kikuchi K, Holmes WR. Insights into Zn^{2+} homeostasis in neurons from experimental and modeling studies. Am. J. Physiol. Cell Physiol., 294, C726-742, 2008.

[7] Tamano H, Nishio R, Shakushi Y, Sasaki M, Koike Y, Osawa M, Takeda A: In vitro and in vivo physiology of low nanomolar concentrations of Zn^{2+} in artificial cerebrospinal fluid. Sci Rep 7: 42897, 2017.

[8] Takeda A, Tamano H: Significance of low nanomolar concentration of Zn^{2+} in artificial cerebrospinal fluid. Mol Neurobiol 54: 2477-2482, 2017.

[9] Frederickson CJ: Neurobiology of zinc and zinc-containing neurons. Int Rev Neurobiol 31: 145-238, 1989.

[10] Takeda A, Nakamura M, Fujii H, Tamano H: Synaptic Zn^{2+} homeostasis and its significance. Metallomics 5: 417-423, 2013.

[11] Tamano H, Takeda A: Age-dependent modification of intracellular Zn^{2+}-buffering in the hippocampus and its impact. Biol Pharm Bull 42: 1070-1075, 2019.

[12] Takeda A, Tamano H, Kan F, Itoh H, Oku N: Anxiety-like behavior of young rats after 2-week zinc deprivation. Behav Brain Res 177: 1-6, 2007.

[13] Takeda A, Tamano H: Insight into zinc signaling from dietary zinc deficiency. Brain Res Rev 62: 33-44, 2009.

[14] Foster TC: Calcium homeostasis and modulation of synaptic plasticity in the aged brain. Aging Cell 6: 319-325, 2007.

[15] Kumar A, Bodhinathan K, Foster TC: Susceptibility to calcium dysregulation during brain aging. Front Aging Neurosci 1: 2, 2009.

[16] Toescu EC, Vreugdenhil M: Calcium and normal brain ageing. Cell Calcium 47: 158-164, 2010.

[17] Thibault O, Landfield PW: Increase in single L-type calcium channels in hippocampal neurons during aging. Science 272: 1017-1020, 1996.

[18] Zamzow DR, Elias V, Shumaker M, Larson C, Magnusson KR: An increase in the association of GluN2B containing NMDA receptors with membrane scaffolding proteins was related to memory declines during aging. J Neurosci 33: 12300-12305, 2013.

[19] Adlard PA, Parncutt JM, Finkelstein DI, Bush AI: Cognitive loss in zinc transporter-3 knock-out mice: a phenocopy for the synaptic and memory deficits of Alzheimer's disease? J Neurosci 30: 1631-1636, 2010.

[20] Lee JY, Kim JS, Byun HR, Palmiter RD, Koh JY: Dependence of the histofluorescently reactive zinc pool on zinc transporter-3 in the normal brain. Brain Res 1418: 12-22, 2011.

[21] Takeda A, Koike Y, Osawa M, Tamano H: Characteristic of extracellular Zn^{2+} influx in the middle-aged dentate gyrus and its involvement in attenuation of LTP. Mol Neurobiol 55: 2185-2195, 2018.

[22] Berridge MJ: Dysregulation of neural calcium signaling in Alzheimer disease, bipolar disorder and schizophrenia. Prion 7: 2-13, 2013.

[23] Takeda A, Tamano H, Murakami T, Nakada H, Minamino T, Koike Y: Weakened intracellular Zn^{2+}-buffering in the aged dentate gyrus and its involvement in erasure of maintained LTP. Mol Neurobiol 55: 3856-3865, 2018.

[24] Takeda A, Tamano H, Hashimoto W, Kobuchi S, Suzuki H, Murakami T, Tempaku M, Koike Y, Adlard PA, Bush AI: Novel defense by metallothionein induction against cognitive decline: from amyloid $\beta_{1\text{-}42}$-induced excess Zn^{2+} to functional Zn^{2+} deficiency. Mol Neurobiol 55: 7775-7788, 2018.

[25] Tamano H, Kan F, Oku N, Takeda A: Ameliorative effect of Yokukansan on social isolation-induced aggressive behavior of zinc-deficient young mice. Brain Res Bull 83; 351-355, 2010.

[26] Nicolaides NC, Kyratzi E, Lamprokostopoulou A, Chrousos GP, Charmandari E: Stress, the stress system and the role of glucocorticoids. Neuroimmunomodulation 22: 6-19, 2015.

[27] Gjerstad JK, Lightman SL, Spiga F: Role of glucocorticoid negative feedback in the regulation of HPA axis pulsatility. Stress 21: 403-416, 2018.

[28] McEwen BS, Sapolsky RM: Stress and cognitive function. Curr Opin Neurobiol 5: 205-216, 1995.

[29] Kim J, Yoon KS: Stress: Metaplastic effects in the hippocampus. Trends Neurosci 21: 505-509, 1998.

[30] Kim JJ, Diamond DM: The stressed hippocampus, synaptic plasticity and lost memories. Nat Rev Neurosci 3: 453-462, 2002.

[31] McEwen BS Bowles NP, Gray JD, Hill MN, Hunter RG, Karatsoreos IN, Nasca C: Mechanisms of stress in the brain. Nat Neurosci 18: 1353-1363, 2015.

[32] Joëls M, de Kloet ER: The brain mineralocorticoid receptor: A saga in three episodes. J Endocrinol 234: T49-T66, 2017.

[33] Evanson NK, Herman JP, Sakai RR, Krause ER: Nongenomic actions of adrenal steroids in the central nervous system. J Neuroendocrinol 22: 846-861, 2010.

[34] Karst H, Berger S, Turiault M, Tronche F, Schutz G, Joels M: Mineralocorticoid receptors are indispensable for nongenomic modulation of hippocampal glutamate transmission by corticosterone. Proc Natl Acad Sci SSA 102: 19204-19207, 2005.

[35] Joëls M, Karst H, DeRijk R, de Kloet ER: The coming out of the brain mineralocorticoid receptor. Trends Neurosci 31: 1-7, 2008.

[36] Takeda A, Suzuki M, Tamano H, Takada S, Ide K, Oku K: Involvement of glucocorticoid-mediated Zn^{2+} signaling in attenuation of hippocampal CA1 LTP by acute stress. Neurochem Int 60: 394-399, 2012.

[37] Sandi C: Glucocorticoids act on glutamatergic pathways to affect memory processes. Trends Neurosci 34: 165-176, 2011.

[38] Suzuki M, Sato Y, Tamura K, Tamano H, Takeda A: Rapid intracellular Zn^{2+} dysregulation via membrane corticosteroid receptor activation affects in vivo CA1 LTP. Mol Neurobiol 56: 1356-1365, 2019.

[39] Lynch MA: Long-Term Potentiation and Memory. Physiol Rev 84: 87-136, 2004.

[40] Takeda A, Suzuki M, Tempaku M, Ohashi K, Tamano H: Influx of Extracellular Zn^{2+} Into the Hippocampal Ca1 Neurons Is Required for Cognitive Performance Via Long-Term Potentiation. Neuroscience 304: 209-216, 2015.

[41] Takeda A, Takada S, Nakamura M, Suzuki M, Tamano H, Ando M, Oku N: Transient Increase in Zn^{2+} in Hippocampal CA1 Pyramidal Neurons Causes Reversible Memory Deficit. PLoS One 6: e28615, 2011.

[42] Tamano H, Nishio R, Takeda A: Involvement of intracellular Zn^{2+} signaling in LTP at perforant pathway-CA1 pyramidal cell synapse. Hippocampus 27: 777-783, 2017.

[43] Frederickson CJ, Koh JY, Bush AI: The neurobiology of zinc in health and disease. Nat Rev Neurosci 6: 449-462, 2005.

[44] Kwak S, Weiss JH: Calcium-permeable AMPA channels in neurodegenerative disease and ischemia. Curr Opin Neurobiol 16: 281-287, 2006.

[45] Weiss JH: Ca permeable AMPA channels in diseases of the nervous system. Front Mol Neurosci 4: 42, 2011.

[46] Takeda A, Koike Y, Osawa M, Tamano H: Characteristic of extracellular Zn^{2+} influx in the middle-aged dentate gyrus and its involvement in attenuation of LTP. Mol Neurobiol 55: 2185-2195, 2018.

[47] Takeda A, Tamano H, Hisatsune M, Murakami T, Nakada H, Fujii H: Maintained LTP and memory are lost by Zn^{2+} influx into dentate granule cells, but not Ca^{2+} influx. Mol Neurobiol 55: 1498-1508, 2018.

[48] Tamano H, Nishio R, Morioka H, Takeda A: Extracellular Zn^{2+} influx into nigral dopaminergic neurons plays a key role for pathogenesis of 6-hydroxydopamine-induced Parkinson's disease in rats. Mol Neurobiol 56: 435-443, 2019.

[49] Tamano H, Morioka H, Nishio R, Takeuchi A, Takeda A: AMPA-induced extracellular Zn^{2+} influx into nigral dopaminergic neurons causes movement disorder in rats. NeuroToxicology 69: 23-28, 2018.

[50] Nakajima S, Saeki N, Tamano H, Nishio R, Katahira M, Takeuchi A, Takeda A: Age-related vulnerability to nigral dopaminergic degeneration in rats via Zn^{2+}-permeable GluR2-lacking AMPA receptor activation. NeuroToxicology 83: 69-76, 2021.

[51] Tronche C, Piérard C, Coutan M, Chauveau F, Liscia P, Béracochéa D: Increased stress-induced intra-hippocampus corticosterone rise associated with memory impairments in middle-aged mice. Neurobiol Learn Mem 93: 343-351, 2009.

[52] Chauveau F, Tronche C, Piérard C, Liscia P, Drouet I, Coutan M, Béracochéa D: Rapid stress-induced corticosterone rise in the hippocampus reverses serial memory retrieval pattern. Hippocampus 20: 196-207, 2010.

[53] Sajadi AA, Samaei SA, Rashidy-Pour A: Intra-hippocampal microinjections of anisomycin did not block glucocorticoid-induced impairment of memory retrieval in rats: An evidence for non-genomic effects of glucocorticoids. Behav Brain Res 173: 158-162, 2006.

[54] Khaksari M, Rashidy-Pour A, Vafaei AA: Central mineralocorticoid receptors are indispensable for corticosterone-induced impairment of memory retrieval in rats. Neuroscience 149: 729-738, 2007.

[55] Dorey R, Piérard C, Shinkaruk S, Tronche C, Chauveau F, Baudonnat M, Béracochéa D: Membrane Mineralocorticoid but not Glucocorticoid Receptors of the Dorsal Hippocampus Mediate the Rapid Effects of Corticosterone on Memory Retrieval. Neuropsychopharmacology 36: 2639-2649, 2011.

[56] Olijslagers JE, De Kloet ER, Elgersma Y, Van Woerden GM, Joëls M, Karst K: Rapid changes in hippocampal CA1 pyramidal cell function via pre- as well as postsynaptic membrane mineralocorticoid receptors. Eur J Neurosci 27: 2542-2550, 2008.

[57] De Kloet ER, Oitzl MS, Joëls M: Stress and cognition: Are corticosteroids good or bad guys? Trends Neurosci 22: 422-426, 1999.

[58] Martin S, Henley JM, Holman D, Zhou M, Wiegert O, van Spronsen M, Joëls M, Hoogenraad CC, Krugers HJ: Corticosterone alters AMPAR mobility and facilitates bidirectional synaptic plasticity. PLoS One, 4: e4714, 2009.

[59] Conboy L, Sandi C: Stress at Learning Facilitates Memory Formation by Regulating AMPA Receptor Trafficking Through a Glucocorticoid Action. Neuropsychopharmacology 35: 674-685, 2010.

[60] Whitehead G, Jo J, Hogg EL, Piers T, Kim DH, Seaton G, Seok H, Bru-Mercier G, Son GH, Regan P, Hildebrandt L, Waite E, Kim BC, Kerrigan TL, Kim K, Whitcomb DJ, Collingridge GL, Lightman SL, Cho K: Acute stress causes rapid synaptic insertion of Ca^{2+} -permeable AMPA receptors to facilitate long-term potentiation in the hippocampus. Brain 136: 3753-6375, 2013.

[61] Lee SJ, Escobedo-Lozoya Y, Szatmari EM, Yasuda R: Activation of CaMKII in single dendritic spines during long-term potentiation. Nature 458: 299-304, 2009.

[62] Halt AR, Dallapiazza RF, Zhou Y, Stein IS, Qian H, Juntti S, Wojcik S, Brose N, Silva AJ, Hell JW: CaMKII bind- ing to GluN2B is critical during memory consolidation. EMBO J 31: 1203-1216, 2012.

[63] Kim K, Lakhanpal G, Lu HE, Khan M, Suzuki A, Hayashi MK, Narayanan R, Luyben TT, Matsuda T, Nagai T, Blanpied TA, Hayashi Y, Okamoto K: A Temporary Gating of Actin Remodeling during Synaptic Plasticity Consists of the Interplay between the Kinase and Structural Functions of CaMKII. Neuron 87: 813-826, 2015.

[64] Grabrucker AM, Knight MJ, Proepper C, Bockmann J, Joubert M, Rowan M, Nienhaus GU, Garner CC, Bowie JU, Kreutz MR, Gundelfinger ED, Boeckers TM: Concerted action of zinc and ProSAP/Shank in synaptogenesis and synapse maturation. EMBO J 30: 569-581, 2011.

[65] Tao-Cheng JH, Toy D, Winters CA, Reese TS, Dosemeci A: Zinc Stabilizes Shank3 at the Postsynaptic Density of Hippocampal Synapses. PLoS One 11: e0153979, 2016.

[66] Ouyang Y, Rosenstein A, Kreiman G, Schuman EM, Kennedy MB: Tetanic Stimulation Leads to Increased Accumulation of Ca^{2+}/Calmodulin-Dependent Protein Kinase II via Dendritic Protein Synthesis in Hippocampal Neurons. J Neurosci 19: 7823-7833, 1999.

[67] Racaniello M, Cardinale A, Mollinari C, D'Antuono M, De Chiara G, Tancredi V, Merlo D: Phosphorylation Changes of CaMKII, ERK1/2, PKB/Akt Kinases and CREB Activation during Early Long-Term Potentiation at Schaffer Collateral-CA1 Mouse Hippocampal Synapses. Neurochem Res 35: 239-246, 2010.

[68] Gerges NZ, Aleisa AM, Schwarz LA, Alkadhi KA: Reduced basal CaMKII levels in hippocampal CA1 region: Possible cause of stress-induced impairment of LTP in chronically stressed rats. Hippocampus 14: 402-410, 2004.

[69] Lengyel I, Fieuw-Makaroff S, Hall AL, Sim AT, Rostas JA, Dunkley PR: Modulation of the phosphorylation and activity of calcium/calmodulin-dependent protein kinase II by zinc. J Neurochem 75: 594-605, 2000.

[70] Takeda A, Tamano H: Impact of synaptic Zn^{2+} dynamics on cognition and its decline. Int J Mol Sci 18: 2411, 2017.

[71] Kawahara M, Kato-Negishi M, Tanaka KI: Amyloids: Regulators of Metal Homeostasis in the Synapse. Molecules 25: 1441, 2020.

[72] Sato Y, Takiguchi M, Tamano H, Takeda A: Extracellular Zn^{2+}-dependent amyloid-$\beta_{1\text{-}42}$ neurotoxicity in Alzheimer's disease pathogenesis. Biol Trace Elem Res 199: 53-61, 2021.

Metallomics Research 2021 (1) #MR202109

Review https://metallomicsresearch.brte.org

Non-malignant diseases associated with environmental arsenic exposure in Taiwan, Chile, and Bangladesh

Seiichiro Himeno[1, 2, *], Khaled Hossain[3]

[1]Showa University, School of Pharmacy, Tokyo, 142-8555, Japan
[2]Tokushima Bunri University, Faculty of Pharmaceutical Sciences, Tokushima, 770-8514, Japan
[3]University of Rajshahi, Department of Biochemistry and Molecular Biology, Rajshahi 6205, Bangladesh

Abstract

Extensive epidemiological studies in Taiwan, Chile, and Bangladesh have shown that chronic arsenic exposure is associated with increased incidence and prevalence of skin lesions, cancers, as well as non-malignant disorders such as hypertension, diabetes mellitus, cardiovascular diseases, and respiratory diseases. However, the underlying mechanisms of how arsenic facilitates vascular disorders and diabetes remained unclear. To understand biochemical mechanisms related to arsenic-induced non-malignant diseases, we have examined the relationships between disease-related blood biomarkers and arsenic exposure levels in the arsenic-contaminated area in the western region of Bangladesh. In this review, we presented a summary of the findings of our studies in Bangladesh and discussed their significances in comparison with epidemiological observations in Taiwan and Chile. We have identified arsenic-induced changes in the biomarkers reflecting oxidative stress, inflammation, dyslipidemia, vasoconstriction, monocyte adhesion, and angiogenesis, all related to promoting atherosclerosis and hypertension. Determinations of glucose intolerance, serum insulin and creatinine, and lean body mass suggested a potential role of arsenic-induced skeletal muscle atrophy and its association with insulin resistance. Respiratory function tests and measurements of serum immunoglobulin E and cytokines showed that arsenic-induced T helper 2 (Th2)-dominant immunomodulation might predispose to developing Th2-high type asthma. Thus, the investigation of disease-related biomarkers allowed us to provide novel insight into biochemical mechanisms of arsenic-associated increases in non-malignant diseases.

Key words: arsenic, Bangladesh, atherosclerosis, diabetes mellitus, asthma, cardiovascular disease, biomarker

Statements about COI: The authors declare no conflict of interest associated with this manuscript.

*Correspondence:
Showa University, School of Pharmacy, 1-5-8, Hatanodai, Shinagawa-ku, Tokyo, 142-8555, Japan.
Tel: +81-3-3784-8196
E-mail: himenos@pharm.showa-u.ac.jp

Received: September 11, 2021
Accepted: November 06, 2021
Released online: December 01, 2021

Abbreviations:

BFD, black foot disease; BMI, body mass index; COPD, chronic obstructive pulmonary disease; CRP, C-reactive protein; CVD, cardiovascular disease; DBP, diastolic blood pressure; DM, diabetes mellitus; FBG, fasting blood glucose; FEV1, forced expiratory volume in one second; FEV6, forced expiratory volume in six second; FVC, forced vital capacity; GTT, glucose tolerance test; HDL, high-density lipoprotein; HEALS, the Health Effects of Arsenic Logitudinal Study; HOMA-IR, homeostasis model assessment-insulin resistance; ICAM-1, intercellular adhesion

molecule-1; IFN-γ, interferron-γ; IgE, immunoglobulin E; IGT, impaired glucose tolerance; IL, interleukin; LBM, lean body mass; LDL, low-density lipoprotein; LOX-1, lectin-like oxidized LDL receptor-1; MMP, matrix metalloprotease; NO, nitric oxide; NOX2, NADPH oxidase 2; OR, Odds ratio; oxLDL, oxidized low-density lipoprotein; RAO, reversible airway obstruction; senescence-associated secretory phenotypes, SASP; SBP, systolic blood pressure; SMR, standardized mortality ratios; sTM, soluble thrombomodulin; Th2, T helper 2; TNF-α, tumor necrosis factor-α; VCAM-1, vascular cell adhesion molecule-1; VEGF, vascular endothelial growth factor

1. Introduction

Since ancient times, arsenic has long been known as a poison and used for purposes such as assassination because of its colorless, tasteless, and odorless nature. Today, however, arsenic has become an environmental pollutant harming people globally. Arsenic pollution occurs mainly from groundwater naturally contaminated by the arsenic leached from the earth's crust, contrasting with other toxic metals, such as cadmium, mercury, and lead, originating mainly from mines and industrial products and wastes. Health hazards due to groundwater-derived arsenic have been reported in Taiwan, Bangladesh, India, China, and Mongolia in Asia and Chile, Argentina, and Mexico in Central and South America. It is estimated that more than 200 million people worldwide are exposed to arsenic from drinking water containing arsenic over 10 μg/L, the permissible limit set by WHO [1].

Health hazards caused by chronic arsenic exposure include skin lesions, such as hyperpigmentation, depigmentation and keratosis, and cancers of the skin, liver, lung, bladder, and kidneys [2,3]. Chronic arsenic exposure is also linked to non-malignant diseases such as cardiovascular diseases (CVDs) [4], diabetes mellitus (DM) [5], and respiratory diseases [6]. However, the causal relationships between arsenic exposure and these common diseases and the underlying mechanisms have yet to be clarified because many confounding factors are involved in these lifestyle-related diseases.

Although arsenic contamination is a global issue, Taiwan, Chile, and Bangladesh have suffered from particularly severe arsenic-related health problems, including non-malignant diseases, each having different modes of arsenic exposure and disease development. In the southwestern region in Taiwan, exposure to extremely high concentrations of arsenic from well-water for a long time caused a severe peripheral vascular disorder called black foot disease. In a city in Chile, tap water contamination by arsenic occurred from 1958 to 1970. More than 40 years' follow-up studies in Chile have demonstrated delayed health effects on CVDs, DM, and respiratory functions even after arsenic contamination had ceased. In Bangladesh, where more than eight million tube-wells have been installed throughout the country, an unprecedented scale exposure to arsenic has occurred and is continuing.

We have been investigating the health effects of chronic arsenic exposure among the residents in arsenic-contaminated areas in western Bangladesh, focusing on non-malignant diseases. This review will discuss possible mechanisms underlying arsenic-induced non-malignant diseases based on our human studies in Bangladesh. First, we briefly describe the findings of other epidemiological studies on the effects of chronic arsenic exposure on non-malignant diseases in Taiwan and Chile. It will clarify the similarities and differences among the three countries, including dose levels, exposure durations, and the effects of confounding factors such as obesity. Although arsenic exposure similarly elevated the risks of CVDs and DM in the three countries, detailed mechanistic approaches have not been fully achieved in Taiwan or Chile because arsenic exposure had occurred more than 50 years ago (**Fig. 1**). In Bangladesh, where exposure to arsenic is still ongoing, we were able to use blood biomarkers to examine the mechanisms by which arsenic increases the risks of non-malignant diseases.

2. Black foot disease in Taiwan

Arsenic-induced black foot disease (BFD) occurred in the coastal area north of Tainan City in southwestern Taiwan (**Fig. 1**). BFD was found among the people using artesian wells to pump up the groundwater from 120-180 m depth, which contained high concentrations of arsenic [7]. They began to use the deep-well groundwater in the 1920s because the groundwater from shallow wells (12-18 m depth) was salty in this coastal area. The average arsenic concentration in the groundwater collected from the BFD-endemic area in 1959 was 780 μg/L, ranging from 350 to over 1050 μg/L [8]. The incidence of BFD peaked during 1956-1960, indicating that exposure to high-level arsenic for more than 30 years resulted in developing BFD [9].

BFD is a peripheral vascular disease with characteristic blackened skin of the lower limbs, which eventually progresses to ulceration and gangrene in the toes and feet, forcing many patients to have their toes and feet amputated. BFD patients also showed typical symptoms of arsenic poisoning, including skin pigmentation and keratosis. A 15-year follow-up study of 789 BFD

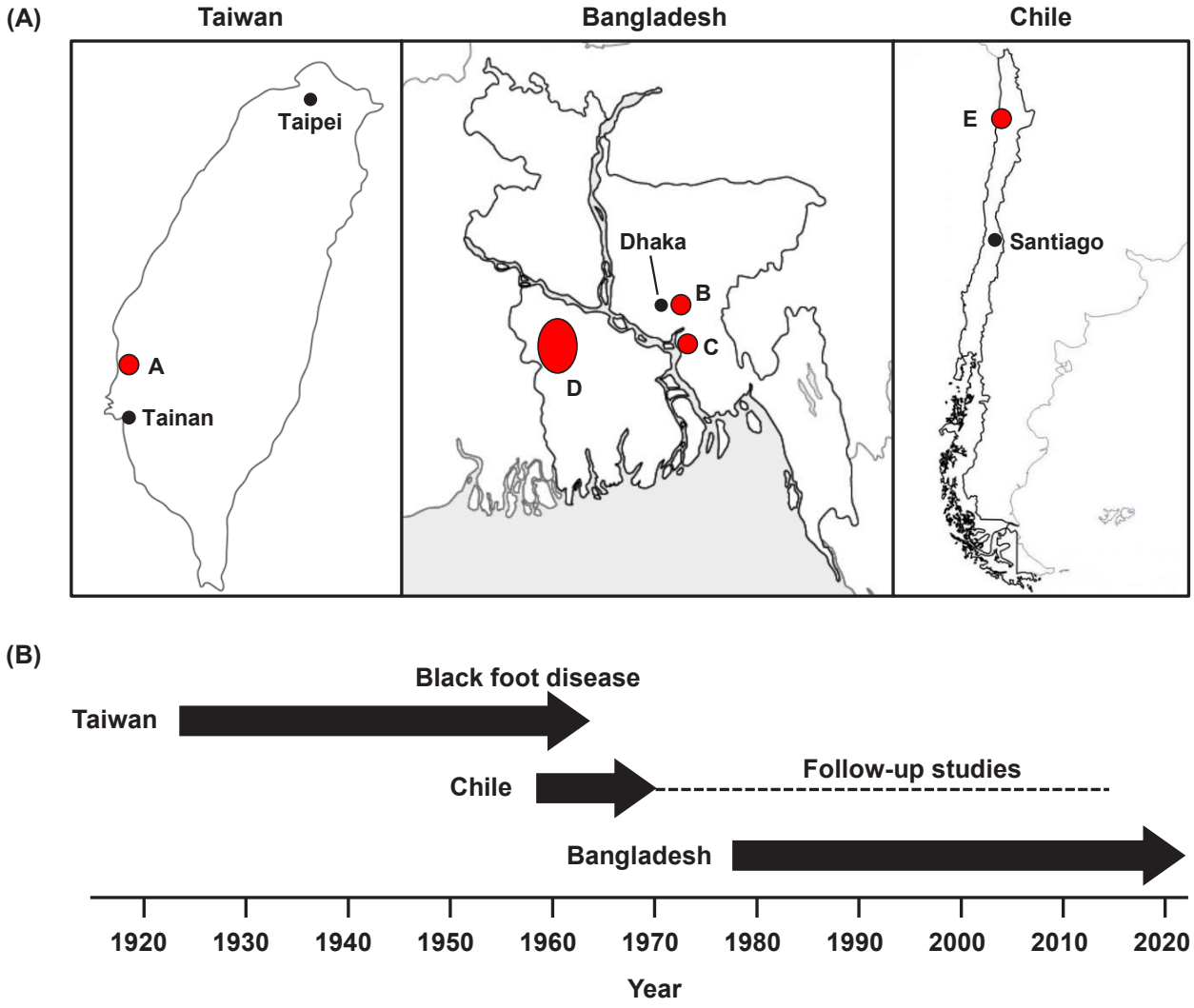

Fig. 1. **(A)** Maps of Taiwan, Bangladesh, and Chile. A, The black foot disease-endemic area in Taiwan; B, Araihazar, C, Matlab, and D, our research areas in Bangladesh; E, Antofagasta in Chile.
(B) Roughly estimated duration of arsenic contamination in Taiwan, Chile, and Bangladesh.

patients showed that the standardized mortality ratios (SMRs) for skin, lung, bladder, and liver cancers were 4.5, 2.8, 2.6, and 2.5, respectively, compared to the general population in Taiwan [10]. The SMRs of peripheral vascular disease and cardiovascular disease were 3.5 and 1.6, respectively. The prevalence of ischemic heart disease increased dose-dependently in the BFD-endemic areas [11]. The elevated prevalence of DM [12,13] and hypertension [14] was also found in the BFD-endemic area compared with the non-endemic area. Thus, many cancerous and non-cancerous diseases, currently recognized as arsenic-related diseases, had already been observed in the BFD-endemic area in Taiwan [7].

Pathological examination of the amputated parts of extremities from 51 BFD patients provided insight into the etiology of BFD [7,15]. Notably, histopathological manifestations of all BFD patients were similar to the well-known peripheral arterial diseases; 70% of the patients exhibited symptoms similar to arteriosclerosis obliterans, and 30% did thromboangiitis obliterans. Arteriosclerosis obliterans are characterized by blood vessel occlusion due to extensive accumulation of atherosclerotic plaques, causing limited blood flow to the lower extremities and, eventually, necrosis and gangrene of the toes and feet. Thromboangiitis obliterans is another type of peripheral arterial disease characterized by inflammation of the artery walls, causing the development of clots and eventually the occlusion of blood vessels in the toes and fingers. Although thromboangiitis obliterans is not directly related to atherosclerosis, examinations of the autopsy cases, who had thromboangiitis obliterans, showed extensive atherosclerosis in the arteries of the other organs [7]. Thus, both types of BFDs are occlusive vascular diseases with the extensive formation of

atherosclerosis-related clots, leading to necrosis and gangrene of the lower limbs.

Based on histopathological observations of BFD, arsenic is thought to cause vascular lesions such as atherosclerosis and inflammation of blood vessels. Diabetes and hypertension are also the risk factors driving arteriosclerosis obliterans; terminally ill diabetic patients may develop arteriosclerosis obliterans, resulting in amputating the lower limbs, even without arsenic contamination. Because the prevalence of DM and hypertension was high in the BFD-endemic area [12-14], the arsenic-induced peripheral arterial lesions might have been further accelerated by DM and hypertension.

Since the overt BFD has been rarely observed in the other arsenic-contaminated areas than Taiwan, it was initially speculated that additional unknown factors unique to this region of Taiwan might be involved in this rare disease. However, many human and experimental studies have provided evidence of atherosclerotic changes caused by arsenic exposure [16,17]. In Taiwan, the high concentrations (780 μg/L on average) of arsenic in water and the long duration of exposure (20-30 years) might have caused BFD, the severest case of atherosclerotic and inflammatory vascular lesions. However, the mechanisms of how arsenic caused atherosclerosis, hypertension, and DM in humans remained unclarified.

3. Long-term follow-up studies in Chile

In the South American countries, including Chile, arsenic leaching from volcanic rocks of the Andes Mountains has caused contamination of rivers, lakes, and groundwater. Particularly, in Antofagasta city in northern Chile (**Fig. 1**), significant health problems occurred due to the contamination of the municipal tap water that used arsenic-contaminated river water as a water source. Residents were exposed to about 860 μg/L arsenic via tap water for 12 years from 1958 to 1970. In 1971, a facility for removing arsenic was installed in the water supply system, and the exposure to high concentrations of arsenic ended [18,19]. Since there was no alternative water source, most residents in Antofagasta consumed the tap water containing approximately the same concentration of arsenic during the same period. Such a unique situation has offered a rare opportunity to conduct epidemiological studies with a certainty of information on arsenic exposure levels and durations.

The follow-up studies on the residents in Antofagasta, especially those born between 1958 and 1970, have demonstrated that arsenic exposure *in utero* and early childhood increased the incidences of cancers and non-malignant diseases 20-40 years later [18, 19]. The age-adjusted mortality rates from ischemic heart disease, especially acute myocardial infarction, were increased in males in the arsenic-contaminated regions more than 20 years after the cessation of high-level arsenic exposure [20]. SMRs for acute myocardial infarction among the people born in 1950-1957 were highest at the age of 40-49, and those born in 1958-1970 were highest at the age of 30-39. These results suggest that high-level arsenic exposure *in utero* or early childhood increased the risk of mortality from myocardial infarction even 20-30 years after the cessation of arsenic exposure.

A case-control study conducted in 2007-2010 showed that higher levels of arsenic exposure elevated the risk of hypertension [21]. The relationship between DM and arsenic exposure was also examined using the same data sources. The odds ratios (ORs) for DM after adjustment for sex, age, and BMI were higher in the highest arsenic exposure group than the low exposure group in tertiles [22]. However, the BMI-stratified analysis showed a significant increase in the OR of DM by arsenic exposure only in the group with BMI >30. These results suggest that arsenic exposure potentiated the risk of DM, which is primarily associated with obesity.

Early-life exposure to arsenic also caused increased mortality from bronchiectasis, the end-stage pulmonary disease with abnormal bronchial dilatation and epithelial inflammation. Mortality from bronchiectasis at the age of 30-49 years among the residents born in Antofagasta between 1958 and 1970 was markedly higher than the mortality in the general population in Chile [23]. The residents born in Antofagasta during 1958-1970 showed elevated prevalences of shortness of breath, persistent cough, and persistent sputum when examined during 2009-2011 [24]. The prevalence of asthma and chronic bronchitis slightly increased but was not statistically significant. The FVC (forced vital capacity) in non-smokers in the residents of Antofagasta was lower than that in the uncontaminated area [25]. However, the BMI-stratified analysis showed that only the non-smokers with BMI >30 showed significantly lowered FVC.

Thus, decades-long follow-up studies in Antofagasta, Chile, have demonstrated that early-life exposure to arsenic increased the risk of cancers, CVDs, DM, and respiratory diseases in later life. In addition, confounding effects of obesity on arsenic-associated diseases have been observed.

4. A large-scale arsenic poisoning in Bangladesh

Bangladesh has undergone an unprecedented scale of arsenic poisoning. Since the country's independence in 1971, a tremendous number (finally more than 8 million) of tube-wells have been installed with the support of UNICEF to provide pathogen-free water instead of surface water from ponds and rivers. Owing to these wells, the incidence of waterborne diseases had decreased. However, nationwide groundwater contamination with arsenic was recognized in the 1990s. Arsenic-contaminated groundwater over 50 μg/L arsenic (the limit set by the Bangladesh government) has been found in 61 out of 64 districts in Bangladesh [26], and the population exposed to arsenic was estimated to be more than 35 million [27]. Due to the difficulties in installing arsenic removal equipment in millions of wells and the low coverage of tap water, especially in rural areas, a large population is still obliged to use arsenic-contaminated well-water. The prevalence of lifestyle-related disorders such as hypertension and DM is high in the arsenic-contaminated areas in Bangladesh, where obesity is low, almost nobody drinks alcohol due to religious reasons, and women do not smoke.

Two large-scale prospective cohort studies have been carried out to examine the health effects of chronic arsenic exposure in Bangladesh. In Matlab, located 53 km southeast of Dhaka (**Fig. 1**), the International Centre for Diarrheal Disease Research, Bangladesh (icddr, b) has maintained a Health and Demographic Surveillance System covering 142 villages since 1966. Arsenic concentrations in half of the wells in Matlab were higher than 150 μg/L, and about 40% were in a range of 150-500 μg/L [27]. In Araihazar, located close to Dhaka (**Fig. 1**), approximately 12,000 residents have participated in the Health Effects of Arsenic Longitudinal Study (HEALS) since 2000 [28]. Arsenic concentrations in about 80% of the wells in Araihazar were less than 180 μg/L, representing low-to-moderate level arsenic exposure. Studies conducted in the two areas have provided extensive findings regarding the effects of chronic arsenic exposure on skin lesions, cancers, and non-malignant diseases [29,30].

Since 2009, we have started studying the health effects of arsenic exposure in the western region of Bangladesh, including Jessore, Chuadanga, and Kushtia districts (**Fig. 1**). Several hundred km from big cities like Dhaka, these rural areas were largely left out of groundwater mitigation, and most residents continue to use arsenic-contaminated groundwater with average concentrations of 170-190 μg/L ranging from low to high (up to about 1,000 μg/L) levels [16,31,32]. Naogaon district in the northwestern part was included as a non-endemic low-arsenic area. Because the villages to be surveyed are scattered over a large area, we took a cross-sectional approach. The total number of participants was small initially but increased gradually during the past ten years to more than 800 [33].

Unlike Taiwan and Chile, arsenic exposure is still ongoing, especially in rural areas like our study areas in Bangladesh. This situation has rendered us opportunities to examine the changes of disease-related biomarkers induced by the recent exposure to arsenic. In Bangladesh, groundwater is also used for rice-field irrigation, and the per capita rice consumption is very high. Hence, determining water arsenic concentrations in each well is insufficient to assess the individual arsenic exposure levels. To overcome this problem, we measured arsenic concentrations in the residents' hair and nails, which reflect relatively long-term arsenic intake [34,35], in addition to their drinking water. We have attempted to examine dose-response relationships between these individual-level arsenic exposure indicators and the changes in biomarkers for various diseases to clarify the mechanisms underlying arsenic-induced disease development in humans. The results of our studies thus far published [16,31-33,36-46] are summarized in **Table 1**.

5. Changes in biomarkers related to CVDs by arsenic exposure

Prospective cohort studies conducted in Matlab in Bangladesh have reported that arsenic exposure increased mortality from CVDs [47,48]. Another cohort study among the participants in HEALS has also shown that arsenic exposure increased mortality from ischemic heart disease and other forms of heart diseases [49]. Prevalence of hypertension was increased dose-dependently by arsenic exposure in Matlab [50]. A seven-year follow-up study among the participants in HEALS showed that age-dependent increases in blood pressure were accelerated by arsenic exposure [51]. Our studies have also shown that the average levels of SBP and DBP and the prevalence of hypertension among the subjects in the arsenic-contaminated areas were significantly higher than those in the non-contaminated area [16,31,32,39,42].

As a blood biomarker for hypertension, we focused on endothelin-1, a vasoconstrictor secreted from vascular endothelial cells. Since the half-life of endothelin-1 in the blood is very short, we measured the plasma levels of its precursor, Big-endothelin-1, which has a longer half-life in the blood. We found that plasma levels of Big-endothelin-1 were higher among the subjects in the

arsenic-contaminated areas than those in the non-contaminated area and significantly higher in hypertensive than in normotensive individuals [31]. Arsenic concentrations in drinking water, hair, and nails all showed significant positive correlations (r >0.4) with plasma Big-endothelin-1 concentrations. It is known that blood endothelin-1 levels reflect abnormalities in vascular endothelial cells and are elevated in patients with CVDs and DM [52,53]. Our results suggest that arsenic exposure enhanced secretion of endothelin-1 from the damaged vascular endothelial cells, contributing to the elevation of blood pressure.

We next investigated the relationships between arsenic exposure indicators and the concentrations of blood lipids, inflammation markers, and soluble forms of adhesion molecules related to atherosclerosis [16]. We found that plasma levels of triglycerides and total cholesterol were not increased by arsenic exposure. However, oxidized LDL (OxLDL) levels were increased, HDL levels were decreased, and the ratios of OxLDL/HDL were increased in an arsenic concentration-dependent manner, suggesting the involvement of reactive oxygen species (ROS) induced by arsenic. We also found that plasma levels of C-reactive protein (CRP), an indicator of inflammation, and circulating adhesion molecules, such as soluble VCAM-1 (sVCAM-1) and sICAM-1, were elevated dose-dependently by arsenic exposure. The reduced levels of HDL, which has antioxidant properties, may fail to suppress LDL oxidation and OxLDL accumulation in macrophages [54]. These results suggest that arsenic accelerates the initiation process of atherosclerosis via enhancing oxidative stress and inflammation and activating circulating monocytes' adhesion to endothelial cells and transmigration to the intima (**Fig. 2**).

Based on our results and recent evidence on the processes of atherosclerosis supporting our results [55-66], we propose the mechanisms of arsenic-induced vascular damages as illustrated in **Fig. 2**. Arsenic was shown to activates NADPH oxidase 2 (NOX2) in vascular endothelial cells, promoting ROS formation [55,56]. ROS-induced OxLDL activates endothelial cells via binding to LOX-1, the receptor for OxLDL expressed in endothelial cells [57,58] in addition to the engulfment by intimal macrophages. The internalization of OxLDL via LOX-1 plays a crucial role in initiating atherosclerosis by activating various downstream genes in endothelial cells, including VCAM-1, ICAM-1, endothelin-1, and CRP, with concomitant production of ROS [59-62]. The secreted endothelin-1 and CRP, in turn, enhance the expression of LOX-1 and increases OxLDL uptake

Table 1. | Lists of biomarkers and their changing tendencies dependent on arsenic exposure in our studies in western Bangladesh

Blood biomarkers	Changes caused by arsenic exposure	Ref.
Choline esterase	Choline esterase ↓	36
Lactate dehydrogenase (LDH)	LDH ↑	37
Alanine succinate transferase (AST), Alanine lactate transferase (ALT)	AST ↑, ALT ↑	38
Big endothelin-1 (precursor of endothelin-1)	Big endothelin-1 ↑	31
Triglyceride, Total cholesterol, LDL, HDL, Oxidized LDL (OxLDL), C-reactive protein (CRP), sVCAM-1, sICAM-1	OxLDL ↑, HDL ↓, OxLDL/HDL ratio ↑, CRP ↑, sVCAM-1 ↑, sICAM-1 ↑	16
Uric acid	Uric acid ↑	39
Vascular endothelial growth factor (VEGF)	VEGF ↑	40
Matrix metalloproteases (MMP)	MMP-2 ↑, MMP-9 ↑	41
Long interspersed nuclear element-1 (LINE-1)	Methylation of LINE-1 ↓	42
sThrombomodulin (sTM)	sTM ↑	32
Fasting blood glucose (FBG), 2h-blood glucose at glucose tolerance test	FBG ↑, 2h-blood glucose ↑ Odds ratio of hyperglycemia ↑ in females	43
Brain-derived neurotrophic factor (BDNF)	Cognitive function test ↓, BDNF ↓	44
Total IgE	FEV1 ↓, FEV1/FEV6 ↓, Reversible airway obstruction ↑, Asthma-like symptoms ↑, Total IgE ↑	33
FBG, Insulin, Creatinine	FBG ↑, Insulin ↑, HOMA-IR ↑, Creatinine ↓, Lean body mass ↓	45
IL-4, IL-5, IL-13, IFN-γ, TNF-α, Eotaxin	IL-4 ↑, IL-5 ↑, IL-13 ↑, Eotaxin ↑	46

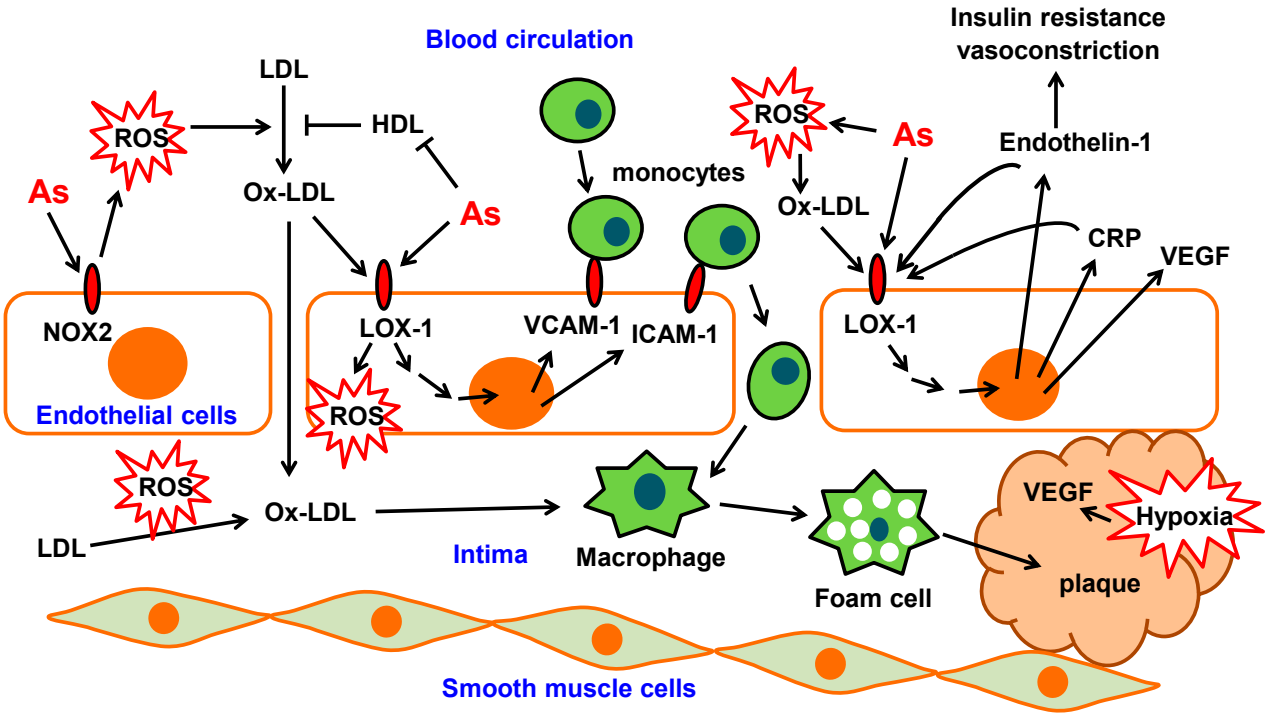

Fig. 2. Vascular events involved in arsenic-induced endothelial damages and their relations to recently found mechanisms of atherosclerosis development. Details are explained in the text.

and downstream gene expression, forming a reinforcing loop [61,63,64]. Notably, treatment of cultured endothelial cells with arsenic was shown to increase the expression of LOX-1, thereby accelerating the binding of OxLDL to LOX-1 and downstream pathways [65]. Another experimental study showed that the administration of arsenic to mice enhanced ROS-mediated expression of VCAM-1 in endothelial cells [66]. We have determined plasma levels of Big-endothelin-1, the precursor to endothelin-1, as a vasoconstrictor in our previous study [31]. However, recent evidence has shown that endothelin-1 plays a broader role in developing both atherosclerosis and hypertension.

We also examined other biomarkers related to vascular disorders and CVDs, including vascular endothelial growth factor (VEGF), matrix metalloprotease-2 (MMP-2), MMP-9, uric acid, and soluble thrombomodulin (sTM). It is known that VEGF and MMPs play critical roles in cancer cell infiltration and invasion, and angiogenesis in cancer tissue [67,68]. VEGF has also been shown to promote angiogenesis within atherogenic plaques and cause plaque instability in advanced atherosclerosis [69,70]. Intraplaque VEGF expression is induced by hypoxia in the advanced plaques [69], but the OxLDL-LOX-1 interaction also upregulates VEGF expression in endothelial cells [71] (**Fig. 2**). MMP-2 and MMP-9 contribute to the degradation of the extracellular matrix, leading to remodeling of the vasculature and instability of plaques [72]. We found that arsenic exposure dose-dependently increased serum VEGF, MMP-2, and MMP-9 levels among our study subjects in the arsenic-contaminated areas [40,41]. These results suggest that either arsenic directly upregulated the expression and production of these molecules, contributing to advancing atherosclerosis, or that the elevations of these molecules in serum merely reflected the consequences of arsenic-induced advancement of atherosclerosis. Furthermore, the elevated serum VEGF, MMP-2, and MMP-9 levels may partly reflect arsenic-induced cancer cell infiltration, if any.

Because blood levels of uric acid and sTM are known to be elevated in patients with vascular disorders [73-75], we also determined the concentrations of these circulating molecules. Under physiological conditions, uric acid plays the role of antioxidant, but higher levels of uric acid promote ROS formation in endothelial cells and induce endothelin-1 expression [75]. We found plasma uric acid levels among our study subjects in the arsenic-contaminated areas were higher than those in the non-contaminated area [39]. Hypertensive individuals showed higher levels of plasma uric acid than normotensive individuals in the

arsenic-contaminated areas, suggesting the association of uric acid with vascular dysfunctions. Thrombomodulin at the surface membrane of endothelial cells plays an antithrombotic role, but the serum levels of sTM reflect the proteolytic degradation of thrombomodulin due to endothelial damages [76]. The serum levels of sTM were shown to be elevated in patients with peripheral vascular diseases [73,74]. We found that serum levels of sTM were elevated among our study subjects in the arsenic-contaminated areas with significant correlations with blood pressure and serum levels of sVCAM-1 and sICAM-1 [32].

Thus, examining the vascular lesion-related blood biomarkers allowed us to find dose-dependent changes in these biomarkers by arsenic exposure. All these data suggest that arsenic is a vascular toxicant affecting the expression of various target molecules related to hypertension and atherosclerosis in endothelial cells.

6. Arsenic-induced DM and insulin resistance

A link between arsenic exposure and DM has been observed in Taiwan, Chile, Mexico, India, and Bangladesh. Previous studies in Bangladesh have shown that fasting blood glucose (FBG) or HbA1c levels were elevated by arsenic exposure [77-79]. A study conducted among the participants of HEALS failed to show significant associations of arsenic exposure with HbA1c levels, possibly due to the low-to-moderate arsenic concentrations in the well-water (most of them <300 μg/L) in this area [80].

In our study, a glucose tolerance test (GTT) was carried out in addition to FBG determination [43]. We divided the subjects into tertile of low (<10.6 μg/L), moderate (10.6 – 168 μg/L), and high (168 – 1000 μg/L) exposure groups based on water arsenic concentration. Both FBG and the blood glucose levels 2 hr after the loading of 75 g glucose increased significantly as the arsenic exposure levels increased, suggesting an impaired glucose tolerance (IGT). DM was diagnosed based on GTT results according to the WHO's criteria. The ORs of DM were 3.00 (1.39-6.45) in the moderate and 3.63 (1.7-7.76) in the high arsenic exposure group after adjustment for sex, age, BMI, and smoking status. Similar associations were observed with hair and nail arsenic concentrations. Sex showed significant confounding effects on the associations, and the prevalences of hyperglycemia and IGT were higher in females than in males.

IGT is caused by either reduced insulin secretion or elevated insulin resistance; the latter generally develops at the initiation phase among most patients with type 2 DM. However, the mechanisms underlying arsenic-related DM remain elusive. Both possibilities that arsenic causes pancreatic damage, leading to reduced insulin secretion, and that arsenic disturbs insulin signaling in glucose-uptaking tissues, causing insulin resistance, have been proposed and argued [5,81]. We, therefore, determined serum insulin concentrations among the subjects who participated in the previous DM study [43]. Based on serum insulin concentrations, HOMA-IR, an indicator of insulin resistance, and HOMA-β, an indicator of decreased pancreatic function, were calculated. We found that serum insulin and HOMA-IR levels were significantly higher in the high arsenic exposure group than in the low exposure group [45]. Even the moderate exposure group showed significant increases in serum insulin and HOMA-IR levels in females. For the first time, these results provided evidence indicating that arsenic-induced hyperglycemia and DM are primarily related to elevated insulin resistance among the populations exposed to moderate-to-high levels of arsenic.

Further analyses of serum biomarkers enabled us to find the involvement of skeletal muscle atrophy as a possible cause for developing insulin resistance by arsenic exposure. Initially, we measured serum creatinine levels to see if DM caused kidney damages. However, almost none of the subjects showed an increase in serum creatinine concentration. Instead, serum creatinine concentrations decreased dose-dependently by arsenic exposure [45]. Consistent with our results, another study in Bangladesh also reported that serum creatinine levels among the residents in the arsenic-contaminated area were lower than those in the non-contaminated area [82]. Under conditions with no renal dysfunction, serum creatinine levels generally reflect skeletal muscle mass [83]. We also found that the levels of lean body mass (LBM), another surrogate marker for skeletal muscle mass, were significantly lower in the high exposure group than the low exposure group. The dose-dependent decreases in serum creatinine and LBM levels suggest that chronic arsenic exposure might have caused skeletal muscle atrophy.

We also found an inverse association of skeletal muscle mass with insulin resistance. When the subjects were divided into tertiles based on their serum creatinine or LBM levels, FBG and HOMA-IR levels increased with decreased serum creatinine and LBM levels [45]. These results suggest that arsenic-induced skeletal muscle atrophy is a likely cause of inducing insulin resistance. Although there were no sex differences in arsenic-induced reduction in skeletal muscle mass, the contributions of the muscle mass loss to the increases in FBG and HOMA-IR levels were more evident in females than males [45]. The higher risk of hyperglycemia in females observed in our previous study [43] may be explained, at least partly, by the higher sensitivity

of females to the effects of skeletal muscle atrophy on insulin sensitivity.

Skeletal muscle, the largest tissue in the body, plays a vital role in absorbing postprandially increased blood glucose. The interaction of DM and sarcopenia, the conditions of skeletal muscle loss and weakness with advanced aging, is currently attracting global attention [84]. Many clinical studies have been concerned about the worsening of diabetic symptoms by aging-associated sarcopenia. On the other hand, several prospective cohort studies have reported that the individuals with low serum creatinine levels at the beginning or those whose serum creatinine levels declined during the study period showed an increased risk of developing DM later, suggesting the role of skeletal muscle reduction in initiating DM [83,85-89]. Because our study on the association of muscle mass and insulin resistance is cross-sectional, we could not conclude that skeletal muscle mass atrophy is a preceding event causing insulin resistance. However, the average ages of our study subjects were below 40 [43,45], suggesting a lower possibility of aging-related sarcopenia. Furthermore, experimental studies have shown that arsenic affected the regeneration of the muscle [90] and mitochondrial morphology and functions of the muscle in mice [91], supporting our human studies. Our study highlighted the novel role of muscle as a target organ of arsenic toxicity and its relation to insulin resistance.

Skeletal muscle is also a target of endothelin-1. Endothelin-1 suppresses glucose uptake in skeletal muscle [92] and induces insulin resistance in skeletal muscle [93,94]. Since the high-level glucose is known to cause elevated production of endothelin-1 in endothelial cells [95], hyperglycemia may further facilitate endothelin-1-induced insulin resistance in skeletal muscle. Thus, the elevation of blood endothelin-1 levels among the arsenic-exposed individuals, which we found in our previous study [31], may be associated with multiple events, including hypertension, atherosclerosis, and skeletal muscle-related insulin resistance (**Fig. 2**).

7. Arsenic-induced respiratory dysfunctions involving immunomodulation

In Bangladesh, the incidence of respiratory symptoms, such as repeated cough, breathing problems, or blood in their sputum, increased in the arsenic-exposed subjects who participated in HEALS [96]. The respiratory functions determined by spirometric measures such as FEV1 (forced expiratory volume in one second) and FVC were also decreased by arsenic exposure among the participants in HEALS exposed to low-to-moderate level arsenic [97].

Since many people in our study areas also showed respiration difficulties, we conducted respiratory function tests using a portable spirometer (Hi-checker) and interviews regarding respiratory symptoms [33]. FEV6 was used as a surrogate for FVC. Reduction in FEV1/FEV6 suggests obstructive lung diseases, such as chronic obstructive pulmonary disease (COPD) and asthma. Although discriminating COPD and asthma has many difficulties in clinical settings, the recovery of FEV1 more than 12% after dosing a bronchodilator is internationally used as the indicator of reversible airway obstruction (RAO), a characteristic feature of asthma. We, therefore, examined the frequencies of airway obstruction (FEV1/FEV6 <0.73), RAO (FEV1/FEV6 <0.73 plus FEV1 recovery >12% by bronchodilator), and the presence of all four asthma-like symptoms (repeated cough, wheezing, shortness of breath, and chest tightness). Of 842 subjects participating in our study, 97, 70, and 87 showed airway obstruction, RAO, and all four asthma-like symptoms, respectively. The ORs of the airway obstruction, RAO, and asthma-like symptoms in moderate and high arsenic exposure groups were 1.94 and 3.65, 1.76 and 3.81, and 2.04 and 3.69, respectively, compared to the low exposure group (referent). The dose-dependent increases in the ORs of the RAO and asthma-like symptoms suggest that arsenic exposure is likely to enhance the risk of airway obstruction, especially asthma [33].

Asthma is not a single entity disease but includes multiple phenotypes and mechanistic pathways (endotypes). Our study showed that the average concentration of serum IgE in the subjects showing RAO was about two times higher than the rest of the study participants, suggesting a possibility of allergic (atopic) asthma [33]. Allergic asthma overlaps with the Th2-high endotype, the major type of asthma that involves the activation of Th2 cytokines and Th2-related inflammatory cascades in the airway [98,99]. When allergens are recognized by dendric cells in the lung, naïve CD4+ T cells differentiate to the Th2 phenotype and secrete Th2 cytokines such as IL-4, IL-5, and IL-13 [100]. IL-4 and IL-13 activate the switching of B cells to plasma cells producing IgE, and IgE activates mast cells, leading to enhanced histamine secretion. IL-5 stimulates the maturation of eosinophils in the bone marrow and facilitates the recruitment of eosinophils to the airway, resulting in elevated inflammation in the lung [101]. Eotaxin (CCL11), a chemokine, also promotes recruiting eosinophils and Th2 cells to the site of inflammation in the airway [102].

Hence, we determined serum levels of Th1 cytokines, IFN-γ and TNF-α, and Th2 cytokines, IL-4, IL-5, and IL-13 among the subjects in the previous asthma study [33]. We also determined serum levels of eotaxin. Results showed that serum levels of IL-4, IL-5, IL-13, and eotaxin among the residents in the arsenic-contaminated areas were significantly higher than those in

the non-contaminated area [46]. In contrast, serum levels of IFN-γ and TNF-α were similar between arsenic-exposed and non-exposed subjects. When the subjects with RAO and without RAO were compared, the subjects with RAO had higher serum levels of IL-4, IL-5, IL-13, and eotaxin. These results suggest that arsenic exposure altered the Th1/Th2 balance toward Th2 dominance, predisposing the arsenic-exposed subjects to develop Th2-high type asthma.

8. Conclusions and future perspectives

Extensive epidemiological studies in Taiwan and Chile have demonstrated the associations between arsenic exposure and the increased risk of non-malignant diseases such as DM, CVDs, and respiratory diseases. However, the mechanisms underlying arsenic-induced increases in the risks of these diseases have remained unclear. We have explored biochemical mechanisms by examining the dose-response relationships between disease-related biomarkers and individuals' arsenic exposure indicators. Our studies have provided novel insights into biochemical mechanisms of arsenic-related development of hypertension, atherosclerosis, insulin resistance, DM, and respiratory diseases.

The inter-disease and inter-organ communications in the pathogenesis of DM, hypertension, and CVDs have recently been studied extensively. DM promotes atherosclerosis [103], insulin resistance exacerbates CVDs [104], and muscle fat infiltration develops insulin resistance and CVDs [105,106]. The vasculature is the central place for these interactions mediated by OxLDL, LOX-1, endothelin-1, VEGF, MMPs, and adhesion and inflammatory molecules. Our findings suggest that arsenic plays multiple roles in accelerating the interactions of these complex networks, facilitating atherosclerosis, hypertension, insulin resistance, and DM. However, many other pieces of this puzzle have yet to be investigated. For example, vascular constriction and relaxation depend on the balance of endothelin-1 and vasodilator, NO [107], but NO's contribution has not been elucidated in our study area. We found that skeletal muscle is a novel target of arsenic toxicity [45], but more detailed mechanisms causing insulin resistance via arsenic-related muscle atrophy should be elucidated. Effects of arsenic on muscle quality, such as ectopic lipid accumulation by fat infiltration [105,106], in addition to muscle quantity, need to be investigated. The Th2-dominant immunomodulation by arsenic exposure, which we found as a possible predisposing factor for developing asthma [46], may also be involved in other arsenic-associated diseases such as skin lesions and even cancers.

CVDs are considered a disease of premature aging of the vasculature [108, 109], and muscular atrophy is a clear reflection of aging [110]. In our studies, the increased blood pressure and atherosclerosis-related biomarkers and the reduced skeletal muscle mass were found in the participants whose average age was below 40 years [16,31,45]. In another study, we conducted cognitive function tests, initially developed for the elderly, among the arsenic-exposed adults with an average age below 40 years and found an arsenic concentration-dependent decrease in cognitive function [44]. Thus, there is a possibility that accelerated aging by arsenic exposure is the fundamental underlying mechanism of arsenic-induced increases in CVDs, DM, and muscle-related dysfunctions. Future studies may be necessary to measure the biomarkers for premature aging, such as senescence-associated secretory phenotypes (SASP) factors [111].

It should be argued here about the relationship between obesity and arsenic-induced DM or hypertension. Indeed, obesity is the primary risk factor for hypertension, atherosclerosis, DM, and CVDs. However, the average percentage of obesity (BMI >30) in Bangladesh in 2016 was 3.6%, while those in Chile, Mexico, and the USA are 28.0, 28.9, and 36.2, respectively [112], where the associations of arsenic exposure with DM and CVDs have been extensively investigated [20-22,113,114]. In Chile, the risk of DM was increased by early-life arsenic exposure only in the obese (BMI >30) people [22], suggesting that arsenic is a potentiating factor for the primarily obesity-associated DM. Even in Bangladesh, obesity has increased (1.0%, 1.9%, and 3.6% in 1996, 2006, and 2016, respectively) [112]. However, the participants of our studies in rural areas had an average BMI of 20-21 constantly during the past ten years [36,45], and only 1.6% of them showed BMI >30 [115]. The OR of hyperglycemia was increased even after adjusting BMI [43]. Thus, the confounding effects of obesity on analyzing the association of arsenic exposure with DM and hypertension may be minimal in Bangladesh, particularly the rural areas like our study area. Nevertheless, ectopic fat accumulation in the muscle or abdominal adipose tissues needs to be explored even among the Bangladesh populations with low BMI. Recent studies have implied that skeletal muscle atrophy is linked to intramuscular fat infiltration, which may be the ultimate cause for promoting insulin resistance [105,106].

The studies in Chile have demonstrated that arsenic exposure *in utero* and early childhood is crucial for developing cancers and non-cancer diseases in adulthood [18,19]. In Bangladesh, health hazards due to arsenic contamination of groundwater were

detected in the 1990s. However, long-term monitoring of arsenic concentrations in well-water at Matlab showed that arsenic concentrations began to increase in the 1970s [27]. It is necessary to identify the participants in our studies subjected to early-life exposure to arsenic and examine their disease development.

Our studies have limitations caused by the cross-sectional approach itself. We have shown the associations of arsenic exposure levels with the changes in biomarkers and pathological conditions, but these results are insufficient to prove cause-effect relationships. We have proposed several new hypotheses from our cross-sectional studies, such as that arsenic decreases muscle mass and increases insulin resistance or that arsenic causes a Th2 shift and promotes the development of asthma. These hypotheses require further scientific validation by future epidemiological and experimental studies.

Fundings

This work was partially supported by two JSPS KAKENHI grants [No. 16H05834 and No. 19H01081] in Japan, and the two grants from the Ministry of Science and Technology, Government of the People's Republic of Bangladesh [grant number: 39.009.006.01.00.042.2012-2013/ES-21/558 and 2007-2008/BS-135/176/1(5)].

References

[1] Naujokas MF, Anderson B, Ahsan H, Aposhian HV, Graziano JH, Thompson C, Suk WA: The broad scope of health effects from chronic arsenic exposure: update on a worldwide public health problem. Environ Health Perspect 121(3): 295-302. 2013.

[2] IARC Working group on the evaluation of carcinogenic risks to humans: Some drinking-water disinfectants and contaminants, including arsenic. IARC Monogr Eval Carcinog Risks Hum 84: 1-477, 2004.

[3] Karagas MR, Gossai A, Pierce B, Ahsan H: Drinking water arsenic contamination, skin lesions, and malignancies: A systematic review of the global evidence. Curr Environ Health Rep 2(1): 52-68, 2015.

[4] Moon K, Guallar E, Navas-Acien A: Arsenic exposure and cardiovascular disease: an updated systematic review. Curr Atheroscler Rep 14(6): 542-555, 2012.

[5] Navas-Acien A, Silbergeld EK, Streeter RA, Clark JM, Burke TA, Guallar E: Arsenic exposure and type 2 diabetes: a systematic review of the experimental and epidemiological evidence. Environ Health Perspect 114(5): 641-648, 2006.

[6] Sanchez TR, Powers M, Perzanowski M, George CM, Graziano JH, Navas-Acien A: A meta-analysis of arsenic exposure and lung function: Is there evidence of restrictive or obstructive lung disease? Curr Environ Health Rep 5(2): 244-254, 2018.

[7] Jean JS, Bundschur CJ, Chen CJ, Guo HR, Liu CW, Lin TF, Chen YH (eds) The Taiwan crisis: a showcase of the global arsenic problem. CRC Press, London, 2010.

[8] Wang CH. Cause of blackfoot disease: Arsenic in artesian well water. Jean JS, Bundschur CJ, Chen CJ, Guo HR, Liu CW, Lin TF, Chen YH (eds) The Taiwan crisis: a showcase of the global arsenic problem. CRC Press, London, 2010, 61-71.

[9] Tseng CH: Blackfoot disease and arsenic: a never-ending story. J Environ Sci Health C Environ Carcinog Ecotoxicol Rev 23(1): 55-74, 2005.

[10] Chen CJ, Wu MM, Lee SS, Wang JD, Cheng SH, Wu HY: Atherogenicity and carcinogenicity of high-arsenic artesian well water. Multiple risk factors and related malignant neoplasms of blackfoot disease. Arteriosclerosis 8(5): 452-460, 1988.

[11] Tseng CH, Chong CK, Tseng CP, Hsueh YM, Chiou HY, Tseng CC, Chen CJ: Long-term arsenic exposure and ischemic heart disease in arseniasis-hyperendemic villages in Taiwan. Toxicol Lett 137(1-2): 15-21, 2003.

[12] Lai MS, Hsueh YM, Chen CJ, Shyu MP, Chen SY, Kuo TL, Wu MM, Tai TY: Ingested inorganic arsenic and prevalence of diabetes mellitus. Am J Epidemiol 139(5): 484-492, 1994.

[13] Tseng CH, Tai TY, Chong CK, Tseng CP, Lai MS, Lin BJ, Chiou HY, Hsueh YM, Hsu KH, Chen CJ: Long-term arsenic exposure and incidence of non-insulin-dependent diabetes mellitus: a cohort study in arseniasis-hyperendemic villages in Taiwan. Environ Health Perspect 108(9): 847-851, 2000.

[14] Chen CJ, Hsueh YM, Lai MS, Shyu MP, Chen SY, Wu MM, Kuo TL, Tai TY: Increased prevalence of hypertension and long-term arsenic exposure. Hypertension 25(1): 53-60, 1995.

[15] Wang CH. History of blackfoot disease. Jean JS, Bundschur CJ, Chen CJ, Guo HR, Liu CW, Lin TF, Chen YH (eds) The Taiwan crisis: a showcase of the global arsenic problem. CRC Press, London, 2010, 49-59.

[16] Karim MR, Rahman M, Islam K, Mamun AA, Hossain S, Hossain E, Aziz A, Yeasmin F, Agarwal S, Hossain MI, Saud ZA, Nikkon F, Hossain M, Mandal A, Jenkins RO, Haris PI, Miyataka H, Himeno S, Hossain K: Increases in oxidized low-density lipoprotein and other inflammatory and adhesion molecules with a concomitant decrease in high-density lipoprotein in the individuals exposed to arsenic in Bangladesh. Toxicol Sci 135(1): 17-25, 2013.

[17] States JC, Srivastava S, Chen Y, Barchowsky A: Arsenic and cardiovascular disease. Toxicol Sci 107(2): 312-323, 2009.

[18] Smith AH, Marshall G, Liaw J, Yuan Y, Ferreccio C, Steinmaus C: Mortality in young adults following in utero and childhood exposure to arsenic in drinking water. Environ Health Perspect 120(11): 1527-1531, 2012.

[19] Steinmaus CM, Ferreccio C, Romo JA, Yuan Y, Cortes S, Marshall G, Moore LE, Balmes JR, Liaw J, Golden T, Smith AH: Drinking water arsenic in northern chile: high cancer risks 40 years after exposure cessation. Cancer Epidemiol Biomarkers Prev 22(4): 623-630, 2013.

[20] Yuan Y, Marshall G, Ferreccio C, Steinmaus C, Selvin S, Liaw J, Bates MN, Smith AH: Acute myocardial infarction mortality in comparison with lung and bladder cancer mortality in arsenic-exposed region II of Chile from 1950 to 2000. Am J Epidemiol 166(12): 1381-1391, 2007.

[21] Hall EM, Acevedo J, López FG, Cortés S, Ferreccio C, Smith AH, Steinmaus CM: Hypertension among adults exposed to drinking water arsenic in Northern Chile. Environ Res 153: 99-105, 2017.

[22] Castriota F, Acevedo J, Ferreccio C, Smith AH, Liaw J, Smith MT, Steinmaus C: Obesity and increased susceptibility to arsenic-related type 2 diabetes in Northern Chile. Environ Res 167: 248-254, 2018.

[23] Smith AH, Marshall G, Yuan Y, Ferreccio C, Liaw J, von Ehrenstein O, Steinmaus C, Bates MN, Selvin S: Increased mortality from lung cancer and bronchiectasis in young adults after exposure to arsenic in utero and in early childhood. Environ Health Perspect 114(8): 1293-1296, 2006.

[24] Steinmaus C, Ferreccio C, Acevedo J, Balmes JR, Liaw J, Troncoso P, Dauphiné DC, Nardone A, Smith AH: High risks of lung disease associated with early-life and moderate lifetime arsenic exposure in northern Chile. Toxicol Appl Pharmacol 313: 10-15, 2016.

[25] Nardone A, Ferreccio C, Acevedo J, Enanoria W, Blair A, Smith AH, Balmes J, Steinmaus C: The impact of BMI on non-malignant respiratory symptoms and lung function in arsenic exposed adults of Northern Chile. Environ Res 158: 710-719, 2017.

[26] Hossain K, Hasibuzzaman MM, Himeno S. Characteristics and health effects of arsenic exposure in Bangladesh. Yamauchi H, Sun G (eds) Arsenic contamination in Asia. Biological effects and preventive measures. Springer Nature, Singapore, 2019, 43-60.

[27] Rahman M, Vahter M, Wahed MA, Sohel N, Yunus M, Streatfield PK, El Arifeen S, Bhuiya A, Zaman K, Chowdhury AM, Ekström EC, Persson LA: Prevalence of arsenic exposure and skin lesions. A population based survey in Matlab, Bangladesh. J Epidemiol Community Health 60(3): 242-248, 2006.

[28] Ahsan H, Chen Y, Parvez F, Argos M, Hussain AI, Momotaj H, Levy D, van Geen A, Howe G, Graziano J: Health Effects of Arsenic Longitudinal Study (HEALS): description of a multidisciplinary epidemiologic investigation. J Expo Sci Environ Epidemiol 16(2): 191-205, 2006.

[29] Yunus M, Sohel N, Hore SK, Rahman M: Arsenic exposure and adverse health effects: a review of recent findings from arsenic and health studies in Matlab, Bangladesh. Kaohsiung J Med Sci 27(9): 371-376, 2011.

[30] Chen Y, Parvez F, Gamble M, Islam T, Ahmed A, Argos M, Graziano JH, Ahsan H: Arsenic exposure at low-to-moderate levels and skin lesions, arsenic metabolism, neurological functions, and biomarkers for respiratory and cardiovascular diseases: review of recent findings from the Health Effects of Arsenic Longitudinal Study (HEALS) in Bangladesh. Toxicol Appl Pharmacol 239(2): 184-192, 2009.

[31] Hossain E, Islam K, Yeasmin F, Karim MR, Rahman M, Agarwal S, Hossain S, Aziz A, Al Mamun A, Sheikh A, Haque A, Hossain MT, Hossain M, Haris PI, Ikemura N, Inoue K, Miyataka H, Himeno S, Hossain K: Elevated levels of plasma Big endothelin-1 and its relation to hypertension and skin lesions in individuals exposed to arsenic. Toxicol Appl Pharmacol 259(2): 187-194, 2012.

[32] Hasibuzzaman MM, Hossain S, Islam MS, Rahman A, Anjum A, Hossain F, Mohanto NC, Karim MR, Hoque MM, Saud ZA, Miyataka H, Himeno S, Hossain K: Association between arsenic exposure and soluble thrombomodulin: A cross sectional study in Bangladesh. PLoS One 12(4): e0175154, 2017.

[33] Siddique AE, Rahman M, Hossain MI, Karim Y, Hasibuzzaman MM, Biswas S, Islam MS, Rahman A, Hossen F, Mondal V, Banna HU, Huda N, Hossain M, Sultana P, Nikkon F, Saud ZA, Haque A, Nohara K, Xin L, Himeno S, Hossain K: Association between chronic arsenic exposure and the characteristic features of asthma. Chemosphere 246: 125790, 2020.

[34] Karagas MR, Morris JS, Weiss JE, Spate V, Baskett C, Greenberg ER: Toenail samples as an indicator of drinking water arsenic exposure. Cancer Epidemiol Biomarkers Prev 5(10): 849-852, 1996.

[35] Gault AG, Rowland HA, Charnock JM, Wogelius RA, Gomez-Morilla I, Vong S, Leng M, Samreth S, Sampson ML, Polya DA: Arsenic in hair and nails of individuals exposed to arsenic-rich groundwaters in Kandal province, Cambodia. Sci Total Environ 393(1): 168-176, 2008.

[36] Ali N, Hoque MA, Haque A, Salam KA, Karim MR, Rahman A, Islam K, Saud ZA, Khalek MA, Akhand AA, Hossain M, Mandal A, Karim MR, Miyataka H, Himeno S, Hossain K: Association between arsenic exposure and plasma cholinesterase activity: a population based study in Bangladesh. Environ Health 9: 36, 2010.

[37] Karim MR, Salam KA, Hossain E, Islam K, Ali N, Haque A, Saud ZA, Yeasmin T, Hossain M, Miyataka H, Himeno S, Hossain K: Interaction between chronic arsenic exposure via drinking water and plasma lactate dehydrogenase activity. Sci Total Environ 409(2): 278-283, 2010.

[38] Islam K, Haque A, Karim R, Fajol A, Hossain E, Salam KA, Ali N, Saud ZA, Rahman M, Rahman M, Karim R, Sultana P, Hossain M, Akhand AA, Mandal A, Miyataka H, Himeno S, Hossain K: Dose-response relationship between arsenic exposure and the serum enzymes for liver function tests in the individuals exposed to arsenic: a cross sectional study in Bangladesh. Environ Health 10: 64, 2011.

[39] Huda N, Hossain S, Rahman M, Karim MR, Islam K, Mamun AA, Hossain MI, Mohanto NC, Alam S, Aktar S, Arefin A, Ali N, Salam

KA, Aziz A, Saud ZA, Miyataka H, Himeno S, Hossain K: Elevated levels of plasma uric acid and its relation to hypertension in arsenic-endemic human individuals in Bangladesh. Toxicol Appl Pharmacol 281(1): 11-18, 2014.

[40] Rahman M, Al Mamun A, Karim MR, Islam K, Al Amin H, Hossain S, Hossain MI, Saud ZA, Noman AS, Miyataka H, Himeno S, Hossain K: Associations of total arsenic in drinking water, hair and nails with serum vascular endothelial growth factor in arsenic-endemic individuals in Bangladesh. Chemosphere 120: 336-342, 2015.

[41] Islam MS, Mohanto NC, Karim MR, Aktar S, Hoque MM, Rahman A, Jahan M, Khatun R, Aziz A, Salam KA, Saud ZA, Hossain M, Rahman A, Mandal A, Haque A, Miyataka H, Himeno S, Hossain K: Elevated concentrations of serum matrix metalloproteinase-2 and -9 and their associations with circulating markers of cardiovascular diseases in chronic arsenic-exposed individuals. Environ Health 14: 92, 2015.

[42] Hossain K, Suzuki T, Hasibuzzaman MM, Islam MS, Rahman A, Paul SK, Tanu T, Hossain S, Saud ZA, Rahman M, Nikkon F, Miyataka H, Himeno S, Nohara K: Chronic exposure to arsenic, LINE-1 hypomethylation, and blood pressure: a cross-sectional study in Bangladesh. Environ Health 16(1): 20, 2017.

[43] Paul SK, Islam MS, Hasibuzzaman MM, Hossain F, Anjum A, Saud ZA, Haque MM, Sultana P, Haque A, Andric KB, Rahman A, Karim MR, Siddique AE, Karim Y, Rahman M, Miyataka H, Xin L, Himeno S, Hossain K: Higher risk of hyperglycemia with greater susceptibility in females in chronic arsenic-exposed individuals in Bangladesh. Sci Total Environ 668:1004-1012, 2019.

[44] Karim Y, Siddique AE, Hossen F, Rahman M, Mondal V, Banna HU, Hasibuzzaman MM, Hosen Z, Islam MS, Sarker MK, Nikkon F, Saud ZA, Xin L, Himeno S, Hossain K: Dose-dependent relationships between chronic arsenic exposure and cognitive impairment and serum brain-derived neurotrophic factor. Environ Int 131: 105029, 2019.

[45] Mondal V, Hosen Z, Hossen F, Siddique AE, Tony SR, Islam Z, Islam MS, Hossain S, Islam K, Sarker MK, Hasibuzzaman MM, Liu LZ, Jiang BH, Hoque MM, Saud ZA, Xin L, Himeno S, Hossain K: Arsenic exposure-related hyperglycemia is linked to insulin resistance with concomitant reduction of skeletal muscle mass. Environ Int 143: 105890, 2020.

[46] Rahman A, Islam MS, Tony SR, Siddique AE, Mondal V, Hosen Z, Islam Z, Hossain MI, Rahman M, Anjum A, Paul SK, Hossen F, Sarker MK, Hossain S, Salam KA, Haque A, Hoque MA, Saud ZA, Xin L, Sumi D, Himeno S, Hossain K: T helper 2-driven immune dysfunction in chronic arsenic-exposed individuals and its link to the features of allergic asthma. Toxicol Appl Pharmacol 420: 115532, 2021.

[47] Sohel N, Persson LA, Rahman M, Streatfield PK, Yunus M, Ekström EC, Vahter M: Arsenic in drinking water and adult mortality: a population-based cohort study in rural Bangladesh. Epidemiology 20(6): 824-830, 2009.

[48] Rahman M, Sohel N, Yunus M, Chowdhury ME, Hore SK, Zaman K, Bhuiya A, Streatfield PK: A prospective cohort study of stroke mortality and arsenic in drinking water in Bangladeshi adults. BMC Public Health 14: 174, 2014.

[49] Chen Y, Graziano JH, Parvez F, Liu M, Slavkovich V, Kalra T, Argos M, Islam T, Ahmed A, Rakibuz-Zaman M, Hasan R, Sarwar G, Levy D, van Geen A, Ahsan H: Arsenic exposure from drinking water and mortality from cardiovascular disease in Bangladesh: prospective cohort study. BMJ 342: d2431, 2011.

[50] Rahman M, Tondel M, Ahmad SA, Chowdhury IA, Faruquee MH, Axelson O: Hypertension and arsenic exposure in Bangladesh. Hypertension 33(1): 74-78, 1999.

[51] Jiang J, Liu M, Parvez F, Wang B, Wu F, Eunus M, Bangalore S, Newman JD, Ahmed A, Islam T, Rakibuz-Zaman M, Hasan R, Sarwar G, Levy D, Slavkovich V, Argos M, Scannell Bryan M, Farzan SF, Hayes RB, Graziano JH, Ahsan H, Chen Y: Association between arsenic exposure from drinking water and longitudinal change in blood pressure among HEALS cohort participants. Environ Health Perspect 123(8): 806-812, 2015.

[52] Böhm F, Pernow J: The importance of endothelin-1 for vascular dysfunction in cardiovascular disease. Cardiovasc Res 76(1): 8-18, 2007.

[53] Schneider JG, Tilly N, Hierl T, Sommer U, Hamann A, Dugi K, Leidig-Bruckner G, Kasperk C: Elevated plasma endothelin-1 levels in diabetes mellitus. Am J Hypertens 15(11): 967-972, 2002.

[54] Negre-Salvayre A, Dousset N, Ferretti G, Bacchetti T, Curatola G, Salvayre R: Antioxidant and cytoprotective properties of high-density lipoproteins in vascular cells. Free Radic Biol Med 41(7): 1031-1040, 2006.

[55] Smith KR, Klei LR, Barchowsky A: Arsenite stimulates plasma membrane NADPH oxidase in vascular endothelial cells. Am J Physiol Lung Cell Mol Physiol 280(3): L442-L449, 2001.

[56] Ellinsworth DC: Arsenic, reactive oxygen, and endothelial dysfunction. J Pharmacol Exp Ther 353(3): 458-464, 2015.

[57] Chen M, Masaki T, Sawamura T: LOX-1, the receptor for oxidized low-density lipoprotein identified from endothelial cells: implications in endothelial dysfunction and atherosclerosis. Pharmacol Ther 95(1): 89-100, 2002.

[58] Kattoor AJ, Goel A, Mehta JL: LOX-1: Regulation, signaling and its role in atherosclerosis. Antioxidants (Basel) 8(7): 218, 2019.

[59] Yurdagul A Jr, Sulzmaier FJ, Chen XL, Pattillo CB, Schlaepfer DD, Orr AW: Oxidized LDL induces FAK-dependent RSK signaling to drive NF-κB activation and VCAM-1 expression. J Cell Sci 129(8): 1580-1591, 2016.

[60] Niemann B, Rohrbach S, Catar RA, Muller G, Barton M, Morawietz H: Native and oxidized low-density lipoproteins stimulate endothelin-converting enzyme-1 expression in human endothelial cells. Biochem Biophys Res Commun 334(3): 747-753, 2005.

[61] Stancel N, Chen CC, Ke LY, Chu CS, Lu J, Sawamura T, Chen CH: Interplay between CRP, atherogenic LDL, and LOX-1 and its

potential role in the pathogenesis of atherosclerosis. Clin Chem 62(2): 320-327, 2016.

[62] Nishimura S, Akagi M, Yoshida K, Hayakawa S, Sawamura T, Munakata H, Hamanishi C. Oxidized low-density lipoprotein (ox-LDL) binding to lectin-like ox-LDL receptor-1 (LOX-1) in cultured bovine articular chondrocytes increases production of intracellular reactive oxygen species (ROS) resulting in the activation of NF-kappaB. Osteoarthritis Cartilage. 2004 Jul;12(7):568-76.

[63] Morawietz H, Duerrschmidt N, Niemann B, Galle J, Sawamura T, Holtz J: Induction of the oxLDL receptor LOX-1 by endothelin-1 in human endothelial cells. Biochem Biophys Res Commun 284(4): 961-965, 2001.

[64] Li L, Roumeliotis N, Sawamura T, Renier G: C-reactive protein enhances LOX-1 expression in human aortic endothelial cells: relevance of LOX-1 to C-reactive protein-induced endothelial dysfunction. Circ Res 95(9): 877-883, 2004.

[65] Hossain E, Ota A, Karnan S, Damdindorj L, Takahashi M, Konishi Y, Konishi H, Hosokawa Y: Arsenic augments the uptake of oxidized LDL by upregulating the expression of lectin-like oxidized LDL receptor in mouse aortic endothelial cells. Toxicol Appl Pharmacol 273(3): 651-658, 2013.

[66] Lemaire M, Negro Silva LF, Lemarié CA, Bolt AM, Flores Molina M, Krohn RM, Smits JE, Lehoux S, Mann KK: Arsenic exposure increases monocyte adhesion to the vascular endothelium, a pro-atherogenic mechanism. PLoS One 10(9): e0136592, 2015.

[67] Apte RS, Chen DS, Ferrara N: VEGF in signaling and disease: Beyond discovery and development. Cell 176(6): 1248-1264, 2019.

[68] Deryugina EI, Quigley JP: Matrix metalloproteinases and tumor metastasis. Cancer Metastasis Rev 25(1): 9-34, 2006.

[69] Sluimer JC, Gasc JM, van Wanroij JL, Kisters N, Groeneweg M, Sollewijn Gelpke MD, Cleutjens JP, van den Akker LH, Corvol P, Wouters BG, Daemen MJ, Bijnens AP: Hypoxia, hypoxia-inducible transcription factor, and macrophages in human atherosclerotic plaques are correlated with intraplaque angiogenesis. J Am Coll Cardiol 51(13): 1258-1265, 2008.

[70] Camaré C, Pucelle M, Nègre-Salvayre A, Salvayre R: Angiogenesis in the atherosclerotic plaque. Redox Biol 12: 18-34, 2017.

[71] Dandapat A, Hu C, Sun L, Mehta JL: Small concentrations of oxLDL induce capillary tube formation from endothelial cells via LOX-1-dependent redox-sensitive pathway. Arterioscler Thromb Vasc Biol 27(11): 2435-2442, 2007.

[72] Li T, Li X, Feng Y, Dong G, Wang Y, Yang J: The role of matrix metalloproteinase-9 in atherosclerotic plaque instability. Mediators Inflamm 2020: 3872367, 2020.

[73] Blann AD, Seigneur M, Steiner M, Boisseau MR, McCollum CN: Circulating endothelial cell markers in peripheral vascular disease: relationship to the location and extent of atherosclerotic disease. Eur J Clin Invest 27(11): 916-921, 1997.

[74] Igari K, Kudo T, Toyofuku T, Inoue Y: The relationship between endothelial dysfunction and endothelial cell markers in peripheral arterial disease. PLoS One 11(11): e0166840, 2016.

[75] Yu W, Cheng JD: Uric acid and cardiovascular disease: An update from molecular mechanism to clinical perspective. Front Pharmacol 11: 582680, 2020.

[76] Conway EM: Thrombomodulin and its role in inflammation. Semin Immunopathol 34(1): 107-125, 2012.

[77] Rahman M, Tondel M, Ahmad SA, Axelson O: Diabetes mellitus associated with arsenic exposure in Bangladesh. Am J Epidemiol 148(2): 198-203, 1998.

[78] Islam R, Khan I, Hassan SN, McEvoy M, D'Este C, Attia J, Peel R, Sultana M, Akter S, Milton AH: Association between type 2 diabetes and chronic arsenic exposure in drinking water: a cross sectional study in Bangladesh. Environ Health 11: 38, 2012.

[79] Pan WC, Seow WJ, Kile ML, Hoffman EB, Quamruzzaman Q, Rahman M, Mahiuddin G, Mostofa G, Lu Q, Christiani DC: Association of low to moderate levels of arsenic exposure with risk of type 2 diabetes in Bangladesh. Am J Epidemiol 178(10): 1563-1570, 2013.

[80] Chen Y, Ahsan H, Slavkovich V, Peltier GL, Gluskin RT, Parvez F, Liu X, Graziano JH: No association between arsenic exposure from drinking water and diabetes mellitus: a cross-sectional study in Bangladesh. Environ Health Perspect 118(9): 1299-1305, 2010.

[81] Castriota F, Rieswijk L, Dahlberg S, La Merrill MA, Steinmaus C, Smith MT, Wang JC: A state-of-the-science review of arsenic's effects on glucose homeostasis in experimental models. Environ Health Perspect 128(1): 16001, 2020.

[82] Nabi AH, Rahman MM, Islam LN: Evaluation of biochemical changes in chronic arsenic poisoning among Bangladeshi patients. Int J Environ Res Public Health 2(3-4): 385-393, 2005.

[83] Bao X, Gu Y, Zhang Q, Liu L, Meng G, Wu H, Xia Y, Shi H, Wang H, Sun S, Wang X, Zhou M, Jia Q, Song K, Niu K: Low serum creatinine predicts risk for type 2 diabetes. Diabetes Metab Res Rev 34(6): e3011, 2018.

[84] Mesinovic J, Zengin A, De Courten B, Ebeling PR, Scott D: Sarcopenia and type 2 diabetes mellitus: a bidirectional relationship. Diabetes Metab Syndr Obes 12: 1057-1072, 2019.

[85] Hu H, Nakagawa T, Honda T, Yamamoto S, Okazaki H, Yamamoto M, Miyamoto T, Eguchi M, Kochi T, Shimizu M, Murakami T, Tomita K, Ogasawara T, Sasaki N, Uehara A, Kuwahara K, Kabe I, Mizoue T, Sone T, Dohi S, Japan Epidemiology Collaboration on Occupational Health Study Group: Low serum creatinine and risk of diabetes: The Japan Epidemiology Collaboration on Occupational Health Study. J Diabetes Investig 10(5): 1209-1214, 2019.

[86] Kashima S, Inoue K, Matsumoto M, Akimoto K: Low serum creatinine is a type 2 diabetes risk factor in men and women: The Yuport

Health Checkup Center cohort study. Diabetes Metab 43(5): 460-464, 2017.

[87] Harita N, Hayashi T, Sato KK, Nakamura Y, Yoneda T, Endo G, Kambe H: Lower serum creatinine is a new risk factor of type 2 diabetes: the Kansai healthcare study. Diabetes Care 32(3): 424-426, 2009.

[88] Takeuchi M, Imano H, Muraki I, Shimizu Y, Hayama-Terada M, Kitamura A, Okada T, Kiyama M, Iso H: Serum creatinine levels and risk of incident type 2 diabetes mellitus or dysglycemia in middle-aged Japanese men: a retrospective cohort study. Vet Rec *6*(1): e000492, 2018.

[89] Moon JS, Lee JE, Yoon JS: Variation in serum creatinine level is correlated to risk of type 2 diabetes. Endocrinol Metab (Seoul) 28(3): 207-213, 2013.

[90] Yen YP, Tsai KS, Chen YW, Huang CF, Yang RS, Liu SH: Arsenic inhibits myogenic differentiation and muscle regeneration. Environ Health Perspect 118(7): 949-956, 2010.

[91] Ambrosio F, Brown E, Stolz D, Ferrari R, Goodpaster B, Deasy B, Distefano G, Roperti A, Cheikhi A, Garciafigueroa Y, Barchowsky A: Arsenic induces sustained impairment of skeletal muscle and muscle progenitor cell ultrastructure and bioenergetics. Free Radic Biol Med 74: 64-73, 2014.

[92] Shemyakin A, Salehzadeh F, Böhm F, Al-Khalili L, Gonon A, Wagner H, Efendic S, Krook A, Pernow J: Regulation of glucose uptake by endothelin-1 in human skeletal muscle in vivo and in vitro. J Clin Endocrinol Metab 95(5): 2359-2366, 2010.

[93] Shemyakin A, Salehzadeh F, Esteves Duque-Guimaraes D, Böhm F, Rullman E, Gustafsson T, Pernow J, Krook A: Endothelin-1 reduces glucose uptake in human skeletal muscle in vivo and in vitro. Diabetes 60(8): 2061-2067, 2011.

[94] Horinouchi T, Hoshi A, Harada T, Higa T, Karki S, Terada K, Higashi T, Mai Y, Nepal P, Mazaki Y, Miwa S: Endothelin-1 suppresses insulin-stimulated Akt phosphorylation and glucose uptake via GPCR kinase 2 in skeletal muscle cells. Br J Pharmacol 173(6): 1018-1032, 2016.

[95] Padilla J, Carpenter AJ, Das NA, Kandikattu HK, López-Ongil S, Martinez-Lemus LA, Siebenlist U, DeMarco VG, Chandrasekar B: TRAF3IP2 mediates high glucose-induced endothelin-1 production as well as endothelin-1-induced inflammation in endothelial cells. Am J Physiol Heart Circ Physiol 314(1): H52-H64, 2018.

[96] Parvez F, Chen Y, Brandt-Rauf PW, Slavkovich V, Islam T, Ahmed A, Argos M, Hassan R, Yunus M, Haque SE, Balac O, Graziano JH, Ahsan H: A prospective study of respiratory symptoms associated with chronic arsenic exposure in Bangladesh: findings from the Health Effects of Arsenic Longitudinal Study (HEALS). Thorax 65(6): 528-533, 2010.

[97] Parvez F, Chen Y, Yunus M, Olopade C, Segers S, Slavkovich V, Argos M, Hasan R, Ahmed A, Islam T, Akter MM, Graziano JH, Ahsan H: Arsenic exposure and impaired lung function. Findings from a large population-based prospective cohort study. Am J Respir Crit Care Med 188(7): 813-819, 2013.

[98] Fahy JV: Type 2 inflammation in asthma--present in most, absent in many. Nat Rev Immunol 15(1): 57-65, 2015.

[99] Papi A, Brightling C, Pedersen SE, Reddel HK: Asthma. Lancet 391(10122): 783-800, 2018.

[100] Lambrecht BN, Hammad H, Fahy JV: The cytokines of asthma. Immunity 50(4): 975-991, 2019.

[101] Nakagome K, Nagata M: Involvement and possible role of eosinophils in asthma exacerbation. Front Immunol 9: 2220, 2018.

[102] Mattes J, Foster PS: Regulation of eosinophil migration and Th2 cell function by IL-5 and eotaxin. Curr Drug Targets Inflamm Allergy 2(2): 169-174, 2003.

[103] Shah MS, Brownlee M: Molecular and cellular mechanisms of cardiovascular disorders in diabetes. Circ Res 118(11): 1808-1829, 2016.

[104] Laakso M, Kuusisto J: Insulin resistance and hyperglycaemia in cardiovascular disease development. Nat Rev Endocrinol 10(5): 293-302, 2014.

[105] Miljkovic I, Cauley JA, Wang PY, Holton KF, Lee CG, Sheu Y, Barrett-Connor E, Hoffman AR, Lewis CB, Orwoll ES, Stefanick ML, Strotmeyer ES, Marshall LM; Osteoporotic Fractures in Men (MrOS) Research Group: Abdominal myosteatosis is independently associated with hyperinsulinemia and insulin resistance among older men without diabetes. Obesity (Silver Spring) 21(10): 2118-2125, 2013.

[106] Miljkovic I, Kuipers AL, Cauley JA, Prasad T, Lee CG, Ensrud KE, Cawthon PM, Hoffman AR, Dam TT, Gordon CL, Zmuda JM; Osteoporotic Fractures in Men Study Group: Greater skeletal muscle fat infiltration is associated with higher all-cause and cardiovascular mortality in older men. J Gerontol A Biol Sci Med Sci 70(9): 1133-1140, 2015.

[107] Tousoulis D, Kampoli AM, Tentolouris C, Papageorgiou N, Stefanadis C: The role of nitric oxide on endothelial function. Curr Vasc Pharmacol 10(1): 4-18, 2012.

[108] Costantino S, Paneni F, Cosentino F: Ageing, metabolism and cardiovascular disease. J Physiol 594(8): 2061-2073, 2016.

[109] McCarthy CG, Wenceslau CF, Webb RC, Joe B: Novel contributors and mechanisms of cellular senescence in hypertension-associated premature vascular aging. Am J Hypertens 32(8): 709-719, 2019.

[110] Larsson L, Degens H, Li M, Salviati L, Lee YI, Thompson W, Kirkland JL, Sandri M: Sarcopenia: Aging-related loss of muscle mass and function. Physiol Rev 99(1): 427-511, 2019.

[111] Okamura K, Suzuki T, Nohara K: Gestational arsenite exposure augments hepatic tumors of C3H mice by promoting senescence in F1 and F2 offspring via different pathways. Toxicol Appl Pharmacol 408: 115259, 2020.

[112] Ritchie H, Roser M: Obesity. Published online at OurWorldInData.org. Retrieved from: 'https://ourworldindata.org/obesity' [Online Resource] 2017.

[113] Del Razo LM, García-Vargas GG, Valenzuela OL, Castellanos EH, Sánchez-Peña LC, Currier JM, Drobná Z, Loomis D, Stýblo M: Exposure to arsenic in drinking water is associated with increased prevalence of diabetes: a cross-sectional study in the Zimapán and Lagunera regions in Mexico. Environ Health 10: 73, 2011.

[114] Gribble MO, Howard BV, Umans JG, Shara NM, Francesconi KA, Goessler W, Crainiceanu CM, Silbergeld EK, Guallar E, Navas-Acien A: Arsenic exposure, diabetes prevalence, and diabetes control in the Strong Heart Study. Am J Epidemiol 176(10): 865-874, 2012.

[115] Sarker MK, Tony SR, Siddique AE, Karim MR, Haque N, Islam Z, Islam MS, Khatun M, Islam J, Hossain S, Saud ZA, Miyataka M, Sumi D, Barchowsky A, Himeno S, Hossain K: Secondary methylation capacity is inversely associated with arsenic exposure-related muscle mass reduction, Int J Environ Res Public Health 18: 9730, 2021.

Metallomics Research 2021 (1) #MR202104

Review https://metallomicsresearch.brte.org

Neurotoxicity of aluminum and its link to neurodegenerative diseases

Masahiro Kawahara*, Ken-ichiro Tanaka, Midori Kato-Negishi

Department of Bio-Analytical Chemistry, Faculty of Pharmacy, Research Institute of Pharmaceutical Sciences, Musashino University, Tokyo 202-8585, Japan.

Abstract

Aluminum (Al) is the third most abundant element in the earth's crust. However, because of its specific chemical properties, Al is not essential for life, and it exerts various adverse effects on plants, animals, and humans. In particular, Al is a widely recognized neurotoxin. The association between Al and neurodegenerative diseases including Alzheimer's disease, amyotrophic lateral sclerosis and Parkinson's disease dementia in the Kii Peninsula and Guam has been suspected. However, controversy has persisted for several decades. Based on recent epidemiological, analytical, and toxicological studies, we review the detailed characteristics of Al neurotoxicity and revisit its link to Alzheimer's disease and other diseases. The daily intake of Al and its bioavailability linked with adverse effects on human health are also described.

Key words: aluminum, Alzheimer's disease, bioavailability, iron, neurotoxicity

Statements about COI: All authors declare that there are no conflicts of interests.

1. Introduction

Aluminum (Al) is the third most abundant element in the earth's crust and is widely distributed throughout the environment. Materials containing Al (*e.g.*, clay, glass, and alum) have been used for centuries. In this context, Al is considered to be an old and well-known metal. However, Al was first isolated as an element in 1827, and its use as a silvery metal began only after 1886. Because Al is light, nonmagnetic, malleable, and ductile, it has widespread and important uses in industrial applications and manufacturing of consumer products. From this perspective, Al is a new metal.

Al is widely distributed throughout the environment and eluted from soils by acid rain. Al can enter the human body through foods, cooking utensils, pharmacological agents (such as antacids, antiperspirants, medicine for hyperphatemia, and vaccines), occupational exposure such as use as a leather tanning agent, a component of hemodialysis solution and drinking water after purification with Al coagulants such as aluminum sulphate or polynuclear hydroxyaluminum chloride (PAC)[1].

Despite its widespread distribution throughout the environment, Al is not essential for life, and there is no known biological reaction that requires Al. In contrast, Al is a well-established neurotoxin. As a component of hemodialysis solution or pharmacological compounds, Al causes dialysis encephalopathy in hemodialysis patients[2]. In the environment, Al is eluted from soils by acid rain and

*Correspondence:
Masahiro KAWAHARA, Ph.D.
Department of Bio-Analytical Chemistry, Faculty of Pharmacy, Musashino University
1-1-20 Shinmachi, Nishitokyo-shi, Tokyo 202-8585, Japan
Tel and Fax: +81-42-468-8299
E-mail: makawa@musashino-u.ac.jp

Received: August 27, 2021
Accepted: November 22, 2021
Released online: December 15, 2021

causes toxicity to plants and fishes. Furthermore, Al has been linked to various neurodegenerative disorders including Alzheimer's disease (AD), amyotrophic lateral sclerosis (ALS), and Parkinson's disease dementia (PDD) in the Kii Peninsula and Guam, Gulf-war syndrome, and autism spectrum disorder (ASD)[3-6].

In particular, a crucial link has been established between Al and AD. AD was first reported in 1906 and now accounts for approximately 60% of senile dementia cases. The pathological hallmarks of AD are the deposition of β-amyloid protein (AβP) as extracellular senile plaques and the presence of phosphorylated tau protein in intracellular neurofibrillary tangles (NFTs)[7]. It has been suggested that the risk factors of AD are age, sex, family history, apolipoprotein E phenotype, head trauma, and Al exposure[8]. The hypothesis that Al is an environmental contributor to the pathogenesis of AD, termed the "aluminum hypothesis", was proposed in the 1960s based on various neurotoxicological, analytical, and epidemiological findings [9-12]. Despite these findings, the aluminum hypothesis has been the subject of much debate and criticism for several decades[13]. Great progress has been made in AD research and Al toxicology research during this period, particularly in epidemiological findings about drinking water contaminated with Al and occupational exposure of Al, accumulation of Al in the AD brain, implication of Al in the conformational changes of AβP, and characteristics of Al-induced neurotoxicity. Therefore, it is good time to review Al neurotoxicty, especially based on new findings.

In this review, we focus on the neurotoxicity of Al based on its chemical properties and revisit the significance of Al in the pathogenesis of AD. We describe the daily intake of Al and its bioavailability and association with human health, particularly in infants.

2. Chemical characteristics of Al and its effects on the central nervous system

Despite its environmental abundance, Al is not an essential element and has no known function that is crucial for living organisms. This may be because of several specific chemical characteristics of Al[14].

Al exhibits only one oxidation state, Al^{3+}. In acidic solutions with pH < 4, Al^{3+} exists as the soluble octahedral hexahydrate $Al(H_2O)_6^{3+}$. In neutral solutions, Al^{3+} forms an insoluble hydroxide, $Al(OH)_3$; thus, the concentration of free Al^{3+} under physiological conditions is usually very low. In alkaline solutions with pH > 9.6, Al^{3+} exists as the soluble tetrahedral $Al(OH)_4^-$. This chemistry suggests that a low level of Al is present in the seawater from the era when life first evolved. Indeed, the concentration of Al in the earth's crust, which is termed as the lithospheric abundance of Al, is 82,000 ppm[15]. Meanwhile, the concentration of Al in the human body, the biospheric abundance, is only 0.9 ppm. Thus, the biospheric/lithospheric ratio of Al (approximately 1.1×10^{-5}) is extremely low compared with that of other essential elements such as calcium (Ca: 0.35), iron (Fe: 1.5×10^{-3}), and zinc (Zn: 0.44).

Al^{3+} has affinity for negatively charged, oxygen-donor ligands and strongly binds to inorganic and organic phosphates, carboxylate, and deprotonated hydroxyl groups. By this mechanism, Al^{3+} can bind to DNA and RNA and influence the expression of various genes such as those coding for neurofilament, tubulin, neuron specific enolase, mitochondrial cytochrome oxidase, nerve growth factor, and brain derived neurotrophic factor (BDNF)[11,16]. Lukiw *et al.* reported that nanomolar levels of Al^{3+} were sufficient to influence neuronal gene expression[17]. Al^{3+} also binds to the phosphate groups of nucleoside di- and triphosphates, such as ATP, and inhibits hexokinase, phosphofructokinase, and glucose-6-phosphate dehydrogenase[18], and therefore, Al^{3+} influences energy metabolism. Al also influences the functions of other protein kinases and phosphatases such as protein kinase C and Ca^{2+}/calmodulin-dependent protein kinase[11,19]. Interestingly, Al inhibits dephosphorylation of tau, the main component of AD-NFTs[20].

Al^{3+} has a very low ligand exchange rate compared with other metal ions. For example, the ligand exchange rate of magnesium (Mg^{2+}) is 10^5 times higher compared with that of Al^{3+}, and that of Ca^{2+} is 10^8 times greater. Therefore, Al cannot participate in Ca^{2+}- or Mg^{2+}-related enzymatic reactions and inhibits numerous enzymes with Mg^{2+} and/or Ca^{2+} cofactors. Because of its low ligand exchange rate, Al has a prolonged half-life in the body. Once it enters the brain, Al is retained and semi-permanently accumulates.

Meanwhile, there have been studies suggesting that Al affects the synaptic transmission *via* the mechanism related to Ca^{2+}. It has been reported that Al^{3+} inhibits various enzymes that regulate neurotransmitter synthesis, such as catecholamine o-methyl transferase, tyrosine hydroxylase, dopamine β-hydroxylase, choline acetyl transferase, tyrosine hydroxylase, and glutamate decarboxylase[11]. Moreover, Al inhibits various ion channels and neurotransmitter receptors including sodium (Na^+) channels,

potassium (K^+) channels, voltage-gated Ca^{2+} channels, N-methyl-D-aspartate-type glutamate receptors, and receptors of catecholamine-related neurotransmitters[21]. By the inhibition of neurotransmitter synthesis and receptors including voltage-gated Ca^{2+} channels, Al^{3+} impairs synaptic transmission and Ca^{2+} homeostasis.

Al^{3+} has similar characteristics to Fe^{3+} and binds to Fe-binding proteins such as transferrin and Fe chelators such as deferoxamine. Therefore, Al^{3+} affects Fe homeostasis and Fe-induced expression of various genes containing iron responsive elements (IREs) in their mRNA. Furthermore, Al^{3+} stimulates Fe-induced lipid peroxidation and causes oxidative damage *in vitro* and *in vivo*[22,23]. Increasing evidence suggests that Al acts as a pro-oxidant and induces reactive oxygen species (ROS) production, although Al is a non-redox-active metal[24-27]. It is also notable that co-exposure to Al and 6-hydroxydopamine, a model compound of Parkinson's disease, enhanced the auto-oxidation-induced oxidative stress in brain mitochondrial preparations[28].

As mentioned above, Al has been used as a leather tanning agent for many centuries, since Al^{3+} strongly binds to proteins, causing cross-linking and finally inducing conformational changes. Because Al^{3+} has strong positive charges with a relatively small ionic radius compared with other metal ions (such as Ca^{2+}, Zn^{2+}, and Na^+), Al^{3+} firmly binds to metal-binding amino acids (histidine [His], tyrosine [Tyr], and arginine [Arg]) and phosphorylated amino acids. The strong binding of Al^{3+} to phosphorylated amino acids promotes the self-aggregation of highly phosphorylated cytoskeletal proteins such as neurofilaments and microtubule associated proteins. Furthermore, Al inhibits proteolytic degradation of AβP by cathepsin D[28]. Thus, Al induces the accumulation of AβP as well as cytoskeleton proteins including neurofilaments, tau, and microtubule associated protein 2. The details of this process are discussed in section 4-1.

Because of these chemical properties, Al^{3+} reportedly influences the expression of various genes crucial for brain function and participates in more than 200 biologically important reactions[9,11]. These include processes crucial for brain functions, such as axonal transport, synaptic transmission, phosphorylation or dephosphorylation of proteins, protein degradation, and inflammatory responses. **Fig. 1** summarizes the effects of Al on the central nervous system. Once Al passes through the blood brain barrier and enters the brain by binding with transferrin and/or citrate (Ctr), it induces various adverse effects. Al binds to the phosphates of DNA/RNA and inhibits expression of various genes. It also perturbs Fe homeostasis and affects Fe-related gene expression. Al influences numerous enzymes including kinases, phosphatases, and enzymes that require Ca^{2+} and/or magnesium Mg^{2+} as a cofactor. Al impairs mitochondrial energy producing pathways by binding to ATP and by inducing the generation of ROS. Al also induces endoplasmic reticulum (ER) stress. Furthermore, Al causes cross-linking of and conformational changes in proteins and finally induces the accumulation of proteins including AβP, neurofilaments, and tau.

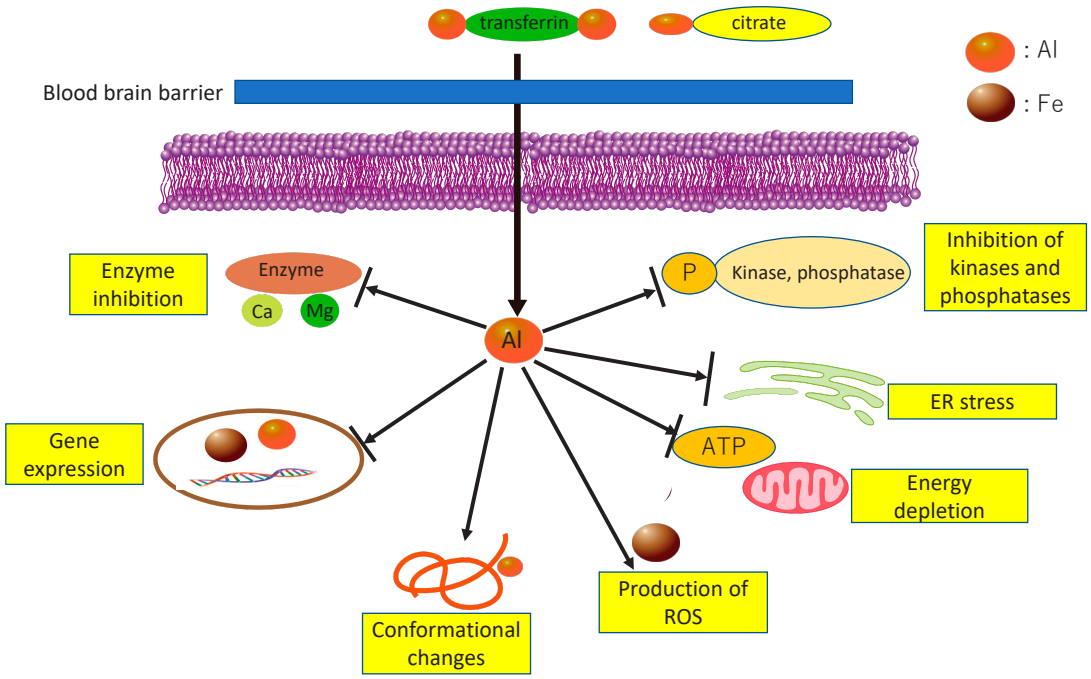

Fig. 1. **Effects of aluminum (Al) on the central nervous system.**
Al causes numerous adverse effects on the central nervous system. Details are shown in the text.

3. Neurotoxicity of Al

3-1. Al neurotoxicity *in vitro*

Because Al possesses these specific chemical characteristics, Al impairs various crucial neurological functions and eventually causes death of neurons and glial cells. We have reported that chronic application of $AlCl_3$ to primary cultured cortical neurons induced the accumulation of tau protein and AβP and the impairment of synapse formation, which are similar to the pathological changes observed in AD[30]. To explore the molecular mechanisms of Al neurotoxicity, its chemical speciation, namely, the types of ligands that coexist with Al and their concentrations, must be considered. The lability, stability, and hydrophobicity of Al compounds are dependent on the counterions because Al^{3+} easily forms insoluble $Al(OH)_3$ in aqueous solutions at physiological pH values[31].

Al binds to maltol (3-hydroxy-2-methyl-4-pyrone) and forms the hydrolytically stable complex termed aluminum maltolate ($Al(malt)_3$)[32]. It has been reported that the toxicity of $Al(malt)_3$ is higher than those of other Al compounds. We have examined the viability of primary cultured neurons after exposure to identical concentrations of four Al compounds, including the simple salt of Al^{3+} ($AlCl_3$), a relatively stable and hydrophilic complex (aluminum lactate ($Al(lac)_3$)), and two lipophilic Al species ($Al(malt)_3$ and aluminum acetylacetonate ($Al(acac)_3$)) [33]. $Al(acac)_3$ and $Al(malt)_3$ exhibited higher toxicity than $AlCl_3$ or $Al(lac)_3$. We have also demonstrated that $Al(malt)_3$ induced synaptic loss and death in primary cultured rat hippocampal neurons and that BDNF attenuated its toxicity[34]. $Al(malt)_3$ inhibits the increase in the intracellular Ca^{2+} level induced by BDNF, but it does not influence the increase in the intracellular Ca^{2+} level induced by KCl or glutamate[35]. Based on these results, it is possible that depletion of neurotrophic factors and disruption of Ca^{2+} homeostasis may be involved in $Al(malt)_3$-induced neuronal death.

$Al(malt)_3$ has been used as a convenient tool to investigate the molecular mechanisms of Al neurotoxicity. $Al(malt)_3$ reportedly causes apoptotic cell death by inducing an inflammatory response in neuronal cell model such as PC12 cells and SH-SY5Y cells[36]. $Al(malt)_3$ induces mitochondrial oxidative stress[37] and ER stress *via* PERK-Elf2a signaling pathway[38] in SH-SY5Y cells. Recent studies suggested that $Al(malt)_3$ also triggers non-apoptotic cell death including ferroptosis in PC12 cells[39] and necroptosis in SH-SY5Y cells [40].

Another crucial feature of the chemical speciation of Al is pH-dependent polymerization. As the pH increases, Al readily forms polynuclear hydroxy-Al complexes. In solutions at pH 5, aluminum tridecamer (Al_{13}; $[AlO_4Al_{12}(OH)_{24}(H_2O)_{12}]^{7+}$) is a dominant species[41], as shown in **Fig.2A**. In soils in which the pH has been decreased by acid rain, the eluted Al causes toxicity to plants and fishes. Al_{13} formed in the soil was reported to be more toxic to the growth of plant roots than monomeric Al^{3+} [42]. It is hypothesized that Al_{13} binds to the phosphate groups in the cell membrane and thereby inhibits various cellular functions[43]. Al_{13} has been shown to form in synaptosomes incubated under neutral pH conditions[44]. Al_{13} might exist in our environment, since polynuclear hydroxyaluminum chloride (PAC) is widely used in the water purification process in Japan[1].

We have developed a pulse-exposure method by which cultured neurons can be exposed to chemically-identified Al species[45]. Using ^{27}Al-NMR, we have confirmed that Al^{3+}, Al_{13}, and $Al(malt)_3$ are stable in 100 mM HEPES buffer (pH 7.0). Cultured neurons were exposed to solutions of monomeric Al^{3+}, Al_{13}, and $Al(malt)_3$ in this condition. After 1 h, the buffer was replaced with usual culture media, and the incubation was continued. At 14 days after the pulse exposure (200 μM for 1 h), Al_{13}-exposed neurons as well as $Al(malt)_3$-exposed neurons exhibited significantly decreased cell viability compared with those exposed to Al^{3+} (**Fig.2B**). Use of this technique with primary cultured neurons will provide a convenient tool to investigate the neurotoxicity of chemically-identified Al species.

3-2. Al neurotoxicity *in vivo*

Al also causes neurodegeneration in experimental animals and impairs various brain functions related to learning, memory, and behavior. Intracerebral administration of Al induces epilepsy in experimental animals, which have been used as models for epilepsy research [46]. Increasing evidence suggests that chronic administration of Al compounds in diets or drinking water causes various detrimental effects in experimental animals. Oral administration of $AlCl_3$ for 7 days caused neurobehavioral changes, increased oxidative stress, and decreased acetylcholine esterase and neurotransmitter levels of aged rats[47]. Exposure to $AlCl_3$ in drinking water caused long-term memory impairment and influenced BDNF gene expression in rats[48]. Al reportedly induces dendritic spine loss, ultrastructural changes in synapses, spatial memory deficits, and decreased emotional reactivity in rats [49,50]. Al also impairs long-term potentiation (LTP), which is a form of synaptic information storage and a paradigm of memory mechanisms in rats[51]. Zhang *et al.* demonstrated that chronic exposure to $AlCl_3$ in drinking water for 90 days caused

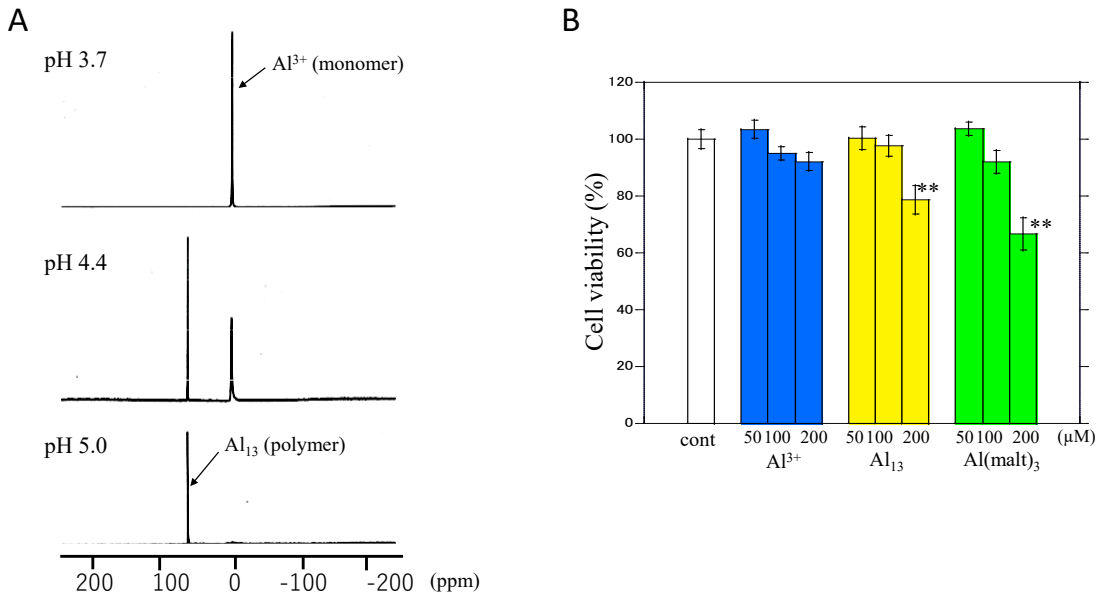

Fig. 2. **Chemical speciation of aluminum (Al) and its neurotoxicity**

A: ^{27}Al-nuclear magnetic resonance (NMR) spectrum of Al solutions at different pH values.
The NMR spectra of 10 mM solutions of Al at pH 3.7 (a), pH 4.4 (b), and pH 5.0 (c) were recorded using a GX-400 (Hitachi, Tokyo Japan). The standard peak (0 ppm) was adjusted according to $Al(NO_3)_3$. The arrow indicates the peak corresponding to Al_{13} at 63.5 ppm. The data are modified from Ref No.45 with permission.

B: The viability of cultured neurons after pulse-exposure to Al
After 14 days of pulse-exposure to 50–200 μM monomeric Al^{3+} (monomer), Al_{13}, or $Al(malt)_3$, the cell viability was examined using the WST-1 method. Data are expressed as means±SEM. * $p<0.05$, ** $p<0.01$. The data are modified from Ref No.45 with permission.

apoptotic death in the hippocampus *via* the IL-1β/JNK signaling pathway, neurobehavioral changes, and changes in synaptic plasticity in rats[52]. Al also impairs hippocampal neurogenesis in infant mice as well as in adult mice[53,54].

3-3. Al neurotoxicity in humans

An association between Al poisoning and memory disorder in humans was first reported in 1921[55]. Later, Al was found to cause dialysis encephalopathy in hemodialysis patients because Al is present in dialysis solution or in pharmacological compounds as treatments for hyperphosphatemia[2]. Al induces various dialysis-related disorders, including osteomalacia (Al bone disease), microcytic anemia, and β_2-microglobulin-associated amyloidosis in dialysis patients[56]. Although the use of Al-containing agents in dialysis patients is prohibited in many countries, recent studies suggest an association between the serum Al level and the risk of uremic pruritus and increased mortality in chronic hemodialysis patients[57,58].

In 1988, in Camelford (Cornwall, U.K.), drinking water was accidentally contaminated by Al, and more than 20,000 people were exposed to high levels of Al for several days. Residents who were exposed to Al exhibited various symptoms related to cerebral impairment such as inability to concentrate, short-term memory loss, and poor psychomotor performance in a 10-year follow-up study[59]. Exley and Esiri demonstrated the deposition of high amounts of Al in the brain of a resident who was exposed to Al and died 15 years later[60]. This 58-year-old woman exhibited unspecified neurological symptoms and a rare form of sporadic cerebral amyloid angiopathy that was characterized by AβP deposition in blood vessels. Al-specific fluorescence microscopy along with congo red staining exhibited co-localization of Al and AβP in the brain of this patient[61]. Another case study of a resident who died 26 years after the incident exhibited similar characteristics to AD patients such as deposition of AβP and phosphorylated tau as well as increased Al in senile plaques[62]. An increased Al level was also observed in the hippocampus of another resident who suffered from epilepsy[63]. Mold *et al.* observed the intracellular accumulation of Al in inflammatory cells and glial cells in the brain of the other resident who suffered cerebral amyloid angiopathy [64]. These studies indicate that short-term exposure to Al can cause prolonged accumulation of Al in the human brain for many years and may finally cause various neurological symptoms.

4. Link between Al and Alzheimer's disease

4-1. Al and the amyloid cascade hypothesis in AD

The link between Al and AD is supported on many findings, beginning in 1965 with the finding of Klatzo *et al.* that the intracerebral administration of Al to rabbits induced the neurofibrillary degeneration and the appearance of tangle-like structures that were similar to the NFTs found in the brains of AD patients[10]. Moreover, Crapper *et al.* reported an increased level of Al in the brains of AD patients[65]. In the 1970s, Al was found to cause dementia in dialysis patients (dialysis encephalopathy) as mentioned above[2].

Although the precise causes of AD are still under investigation, numerous biochemical, toxicological, cell biological, and genetic studies have supported the "amyloid cascade hypothesis", namely, that the accumulation of AβP and its neurotoxicity play a central role in the pathogenesis of AD[66,67]. AβP is a small peptide consisting of 39–43 amino acid residues that is secreted after cleavage of the amyloid precursor protein (APP) N-terminus by β-APP cleaving enzyme (BACE) and intramembrane cleavage of its C-terminus by γ-secretase[7].

It is widely accepted that conformational changes of AβP induced by oligomerization enhance its neurotoxicity. Approaches using size-exclusion chromatography, gel electrophoresis, and atomic force microscopy have demonstrated that the soluble oligomers of AβP are synaptotoxic and neurotoxic[66].

Considering that AβP is secreted in the cerebrospinal fluid of young individuals as well as in older adults and in AD patients[68], factors that accelerate or inhibit its oligomerization may play essential roles in the pathogenesis of AD. Several factors such as peptide concentration, pH and composition of solvents, and temperature can influence the oligomerization process[67]. Interestingly, rodent (rats or mice) AβP exhibits less of a tendency to oligomerize than primate (humans or monkeys) AβP *in vitro*, and accumulation of AβP is rarely observed in the brains of rodents compared with primates[69]. The amino acid sequences of human and rodent AβP are similar; rodent AβP differs from primate AβP by only three amino acids (Arg^{5}, Tyr^{10}, and His^{13}) as shown in **Fig.3**. Considering that these three amino acids have the ability to bind metals, trace elements including Al^{3+} are of particular interest as potential acceleratory factors and might play important roles in the accumulation of AβP in the human brain.

Exley *et al.* firstly demonstrated by circular dichroism spectroscopy that Al induces a conformational change in the first 40 amino acid residues of AβP (AβP(1-40))[70]. Al has also been shown to promote the oligomerization of ^{125}I-labeled AβP(1-40), and Fe and Zn have shown similar effects[71]. Using immunoblotting and high-performance liquid chromatography, we found that Al remarkably enhances the oligomerization of AβP(1-40) compared with other metals, including Zn^{2+}, Fe^{3+}, copper (Cu^{2+}), and cadmium (Cd^{2+})[72,73]. Al-oligomerized AβP(1-40) was sodium dodecyl sulfate-stable, but it could be re-dissolved by adding deferoxamine, an Al chelator.

Other metal ions such as Zn^{2+}, Cu^{2+}, and manganese (Mn^{2+}) induced oligomerization of AβP[74-76]. However, the characteristics (size, morphology) of AβP oligomers formed in the presence of Al, Zn Cu, and Fe were different according to atomic force microscopy images[77]. Sharma *et al.* reported that Zn-oligomerized AβPs were less toxic than Cu-oligomerized AβPs[78]. For the comparison of the toxic effects of Al-oligomerized AβPs to that of Zn- oligomerized AβPs, we exposed Al-oligomerized and Zn- oligomerized AβPs to cultured hippocampal neurons[33]. After 4 days, Al-oligomerized AβPs bound tightly to the surface of cultured neurons and formed fibrillar deposits, meanwhile Zn-oligomerized AβPs were rarely observed. These results suggest that Al-oligomerized AβPs have a strong affinity for membrane surfaces of neurons and undergo minimal degradation by proteases. Indeed, Al has been shown to inhibit the degradation of AβP as a result of conformational changes. Meanwhile, AβP coupled with Al is more toxic than AβP alone, causing membrane disruption and perturbation of neural Ca^{2+} homeostasis and mitochondrial respiration[79]. Bolognin *et al.* demonstrated that Al-oligomerized AβPs induced overproduction of APP and tau, but AβP oligomers that were formed in the presence of other metals (Cu, Fe, and Zn) did not[80].

Increasing evidence suggests that chronic application of Al resulted in accumulation of AβP in cultured neurons from the rat cerebral cortex, neuroblastoma cells, and other neuronal cells[81-84]. Pratico *et al.* found that orally administered Al caused a marked increase in the amount of AβP in both its secreted and accumulated forms and increased deposition of senile plaques in AD model mice transfected with the human APP gene (Tg2576)[85]. These results are consistent with other studies demonstrating that oral Al intake induces AβP accumulation in the brain and impairs spatial learning and memory in AD model mice[86].

Furthermore, other recent studies have demonstrated the accumulation of AβP in brains of Al-intoxicated rats[87-89]. Al also induced other characteristics of AD pathogenesis such as neuronal death, synaptical changes, and memory disorders[90-93].

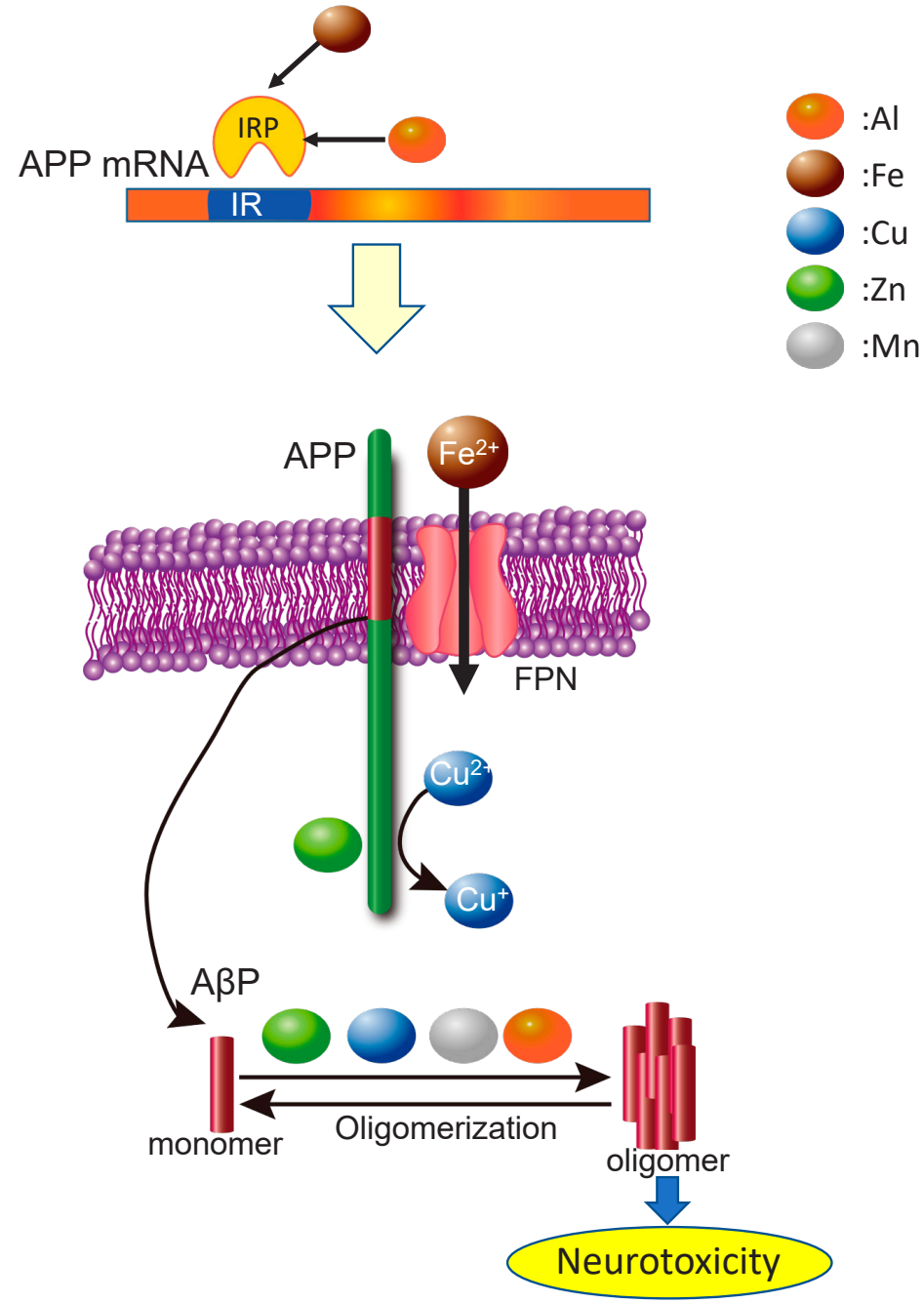

Fig. 3. **Effects of aluminum (Al) on the expression of amyloid precursor protein (APP) and the oligomerization of β-amyloid protein (AβP)**
Al can implicate in the expression of APP, the production of AβP, the neurotoxicity of AβP, and contributes to the pathogenesis of AD.
FPN :ferroportin, colored circles represent metals.

Therefore, Al-induced animal model has been used as a model for AD, and several substances were reportedly effective in the prevention of Al-induced neurotoxicity[94,95].

Al has been reported to bind and cause conformational changes in other AD-related proteins, including APP[96], tau protein, and paired helical filament-tau protein[97], and in proteins related to other diseases such as α-synuclein (*PDD and dementia with Lewy bodies (DLB)*)[98-100], islet amyloid peptide (IAPP) (*diabetes mellitus*)[101,102], ABri (*familial British dementia*)[103], ataxin 3 (*spinocerebellar ataxia type 3*)[104], and β_2-microglobulin (*dialysis-related arthropathy*)[105]. As shown in **Table 1**, Al also binds to neurofilament or to albumin and other serum proteins such as trypsin, transferrin, lactoglobulin[106]. Recent lines of evidence suggest that diverse human disorders including several neurodegenerative diseases may arise from the misfolding and aggregation of underlying proteins[107].

This concept of "conformational disease (protein misfolding diseases)" may explain the common mechanism that underlies various disorders. Under this concept, AD, prion diseases, and dementia with Lewy bodies (PDD) are categorized as conformational diseases. Considering that proteins including AβP, α-synuclein, and human IAPP are also related to conformational diseases, Al-induced conformational changes of these proteins might be associated with other neurodegenerative diseases.

Table 1. | Al-induced conformational changes of proteins

Disease-related proteins
Alzheimer's disease
AβP[1-40]: *DAEFRHDSGYEVHHQKLVFFAEDVGSNKGAIIGLMVGGVV*
AβP[1-42]: *DAEFRHDSGYEVHHQKLVFFAEDVGSNKGAIIGLMVGGVVIA*
AβP[25-35]:*GSNKGAIIGLMV*
AβP[1-16]: *DAEFRHDSGYEVHHQK*
APP
Tau or hyperphosphorylated tau (PHF-tau)
Parkinson's disease and other diseases with Lewy body
α-synuclein (NACP)
Type 2 diabetes mellitus
Islet amyloid protein (Human amylin):
KCNTATCATQRLANFLVHSSNNFGAILSSTNVGSNTY
Pro islet amyloid polypeptide (Pro IAPP)
Familial British dementia
ABri: *ASNCPAIRHPGNKPAVGTLICSRTVKKNIIGGN*
Spinocerebellar ataxia
Ataxin 3
Dialysis-related arthropathy
β_2-microglobulin
Non-disease related proteins
neurofilament
human serum albumin (HSA)
bovine serum albumin (BSA)
milk β-lactoglobulin (β-LG)
Hen Egg-white lysozyme
trypsin and trypsin inhibitor
transferrin

Al also influences the production of AβP *via* the expressions of APP and disrupts Fe homeostasis. APP is a metal-binding protein and is involved in the regulation of metal homeostasis at synapses[108]. APP possesses Cu and/or Zn binding sites at its N-terminus. APP has also been implicated in Fe^{2+} efflux along with ferroportin. Moreover, Fe controls APP expression because its mRNA possesses an IRE domain. The concentration of free Fe^{2+}, which causes formation of toxic free radicals, is generally regulated by the expression of Fe-binding proteins such as ferritin or transferrin through the IRE/iron regulatory protein (IRP) network[109]. Under Fe-deficient conditions, IRP binds to the IRE. As the concentration of free Fe^{2+} increases, the binding of Fe to IRP causes down-regulation of transferrin and up-regulation of ferritin, and the amount of free Fe^{2+} is thereby decreased. Rogers *et al.* found that APP mRNA contains an IRE domain, and their expression is regulated by Fe[110]. Other disease-related genes such as α-synuclein and prion protein also possess an IRE domain[111]. Because Al and Fe share similar chemical characteristics, Al^{3+} reportedly binds to IRP[112,113], and therefore, Al can influence the expression of Fe-binding proteins with IREs in their mRNA, resulting in elevation of the Fe concentration. Al also influences Fe uptake in cultured neurons and glial cells[114]. Indeed, Al reportedly induces elevated APP expression in experimental animals[115,116]. There have been other studies which suggested that Fe homeostasis is implicated in AD pathogenesis. A Fe-related gene, transferrin C2, was revealed to be a risk factor for AD[117], and Imagawa *et al.* reported that Fe supplementation was effective for recovery of cognitive function of familiar AD[118]. Thus, the interactions between Al and Fe may be central to the pathogenesis of AD. **Figure 3** also exhibits the effects of Al on the expression of APP, the secretion of AβP, and its oligomerization. APP is a Zn and/or Cu-binding protein and is implicating in the regulation of metal homeostasis such as controlling Fe^{2+} efflux with ferroportin (FPN) at synapse. Abnormal APP expression induced by Al leads to the disruption of metal homeostasis and the increased amount of AβP. Normally, secreted AβP is degraded by various proteases. However, AβP that is aggregated in the presence of trace metals, including Al, Zn, Cu, and Mn, is resistant to proteases and accumulates in the brain. The oligomerized AβPs can be easily incorporated into membranes and cause neuronal death. Al and other metals may participate in these degenerative processes and could be linked to the pathogenesis of Alzheimer's disease.

4-2. Accumulation of Al in the AD brain

The accumulation of Al in the brain of AD patients supports the association about Al and AD pathogenesis. After the finding of Crapper *et al.*[65], similar results supporting elevated Al in AD brains were reported[119-122], as well as the controversy results[123]. However, prior studies examining Al have been controversial because Al contamination of tissue samples can easily occur during fixation and staining. Thus, quantitative analysis of non-fixed and freshly frozen tissues is necessary. Andrási et al. reported higher Al and lower Mg and P in AD brain[124]. Although several studies have claimed that Al is absent in senile plaques or NFTs[125], this may be caused by limitations of their analytical methods in detecting low levels of Al. Bouras *et al.* used highly sensitive laser microprobe mass analysis (LAMMA) with non-fixed brain samples and reported accumulation of Al in NFT-bearing neurons of AD brains[126]. Accumulation of Al in both senile plaques and NFTs has been reported in renal failure patients[127]. Yumoto *et al.* analyzed Al using energy-dispersive X-ray spectroscopy combined with transmission electron microscopy (TEM-EDX), a method that yields a high resolution and has a low detection limit[128]. Their detailed analysis demonstrated that Al was present in cores of senile plaques at a concentrations of 35–50 ppm. They also demonstrated the co-localization of Al and Fe in the nucleus of AD brains[129]. Exley and coworkers demonstrated Al deposition colocalized with amyloid plaques and NFTs in the brains of familial AD patients using Al-specific fluorescence microscopy[130,131]. They also investigated the amount of Al in the brains of patients with various neurodegenerative diseases and found elevated Al levels in patients with sporadic AD, familial AD, ASD, and multiple sclerosis compared with controls[132]. Lukiw *et al.* reported the increased Al content in brains of AD patients by 36-year multicenter study[133]. Recent meta-analysis of 34 studies demonstrated the significantly higher Al in brain, serum, and cerebrospinal fluid of AD patients[134].

4-3. Epidemiology of Al and dementia

The reported risk factors of AD include age, gender, family history, apolipoprotein E polymorphism, head trauma, and Al. Among them, Al in drinking water has been a focus of study since 1989 when Martyn *et al.* reported a high incidence of AD in areas with high levels of Al in the drinking water in England and Wales[135]. After this initial report, a considerable number of studies provided evidence to support an association between AD and Al in drinking water[136]. McLachlan *et al.* found that an elevated risk of histopathologically verified AD is associated with the consumption of high concentrations of Al in drinking water[137]. Rondeau *et al.* demonstrated that high daily intake of Al was correlated with an increased risk of dementia or cognitive

decline in a 15-year-follow-up French cohort study[138]. A meta-analysis of eight cohort and case-control studies with a total of 10,567 individuals suggests that the chronic exposure to Al has an association with increased risk of AD[139]. Bagepally *et al.* conducted a meta-analysis of 16 studies investigating the relationship of Al with dementia that included one high quality study and 13 moderate quality studies with almost 22,000 participants[140]. Among them, one high quality study and six moderate quality studies found an association between increased Al levels in drinking water and increased dementia risk. A recent study using the Canadian Study of Health and Aging cohort data suggested an increased, although not significant, association of Al in drinking water with AD risk [141].

Considering that the amount of Al consumed in drinking water is approximately 5% of the total daily intake, it is possible that some factors that prevent or accelerate Al absorption may be present in drinking water. Silicate (Si) in water was reported to interact with Al and prevent Al toxicity in fishes. In a French cohort study, the relationship between Al and cognitive impairment was suggested to be influenced by the Si concentration[142]. Cognitive impairment among women was correlated with low Si concentrations in drinking water[143]. Meanwhile, fluoride (F) binds to Al, and aluminum fluoride (AlF_3) possesses various biological functions. Al and F in drinking water have been demonstrated to be risk factors for dementia in both men and women in Scotland[144].

Several studies have indicated that occupational exposure to Al induces adverse effects on human memory. The longitudinal study suggests a chronic Al exposure among Al workers in China can damage cognitive functions including episodic memory and that higher plasma Al level is associated with the mild cognitive impairments[145]. Shang *et al.* demonstrated by their cross-sectional study that increased Al and lithium (Li) and decreased Zn levels in plasma are related to cognitive impairment in Al workers[146]. Furthermore, plasma Al levels were associated with cognitive performance in Al-exposed workers in China[147]. Mohammed *et al.* demonstrated an association of plasma Al and tau levels and cognitive dysfunction in Al foundry workers[148]. Miners that inhaled Al dust exhibited increased mortality from AD, although the increase was not statistically significant[149]. A 55-year-old woman who was exposed to Al-containing paints and had a high serum Al level exhibited movement disorders (tremors of the hands and head, polyminimyoclonus, and dystonic posturing of the hands) and symptoms of dementia[150].

Considering these increasing new lines of evidence regarding Al, it is difficult to agree with the early criticisms of the aluminum hypothesis. Although the precise mechanism underlying AD pathogenesis remains elusive, the significance of Al in the pathogenesis of AD needs to be revisited.

5. Al and human health

5-1. Intake, bioavailability, and excretion of Al

Neurotoxicological, analytical, and epidemiological studies have demonstrated that Al is toxic to the central nervous system and causes dementia when it enters the brain, even though the link between Al and AD is controversial. Therefore, the Al levels in the body and brain are crucial to consider when determining the risk of Al to human health. The primary source of Al in humans is food. In general, the Al levels in most foods are low and vary within a wide range, although the concentration of Al in several plants are very high. The daily intake of Al is estimated to be 10-20 mg/day[151]. Contamination from food additives such as baking powder or from cooking utensils accounts for a considerable part of Al intake. The National Food Administration in Sweden reported in 1992 that the daily intake of Al in Sweden was estimated to be 13 mg[152]. Since baking powder contains Al, cakes or breads used baking powder contribute much in Al intake. The use of Al utensils was estimated to increase the Al intake by approximately 2 mg/day. As other sources of Al, Al is present in the drinking water because it is used as a coagulant in the water treatment process. Respiratory absorption of Al is important, although it is difficult to estimate. Atmospheric fine particulate matter (PM2.5) contains much Al, and rats exposed to PM2.5 dust reportedly exhibited an elevated Al level in the cerebral cortex[153].

In 1989, a joint Food and Agriculture Organization/World Health Organization Expert Committee on Food Additives (JECFA) recommended a provisional tolerable weekly intake (PTWI) of 7.0 mg/kg body weight of Al. In 2007, this was changed to 1.0 mg/kg body weight because of its potential effects on the reproductive system and the developing nervous system. However, it was estimated that several foods contained much amount of Al and exceeded this PTWI value when the food consumed by a 16-kg infant. In 2011, this PTWI value was further changed to 2.0 mg/kg body weight[154].

5-2. The bioavailability and biological fate of Al

The absorption rate of metals including Al by the gastrointestinal tract is low and widely varies. Thus, the bioavailability of Al, namely, the amount of Al that is absorbed in the gastrointestinal tract and transported to the brain through the blood brain barrier, is crucial for human health. The lack of appropriate radioactive isotopes of Al has made it difficult to study on Al bioavailability. However, the analyses using accelerator mass spectrometry and ^{26}Al, a non-radioactive isotope of Al, have advanced this area of study[155]. Using this approach, it became clear that a small amount of Al (approximately less than 1%) is absorbed from food *via* the gastrointestinal pathway; however, this amount is influenced by various factors including individual differences, age, pH, stomach contents, chemical speciation of Al, and coexisting substances[156]. For example, the absorption of Al hydroxide ($Al(OH)_3$), a main component of antacids, is much lower than that of Al citrate. The coexistence of organic ligands such as citric acid or maltol promotes the absorption of Al, while Si prevents its absorption. Although the consumption of tea greatly contributes to the daily intake of Al, the Al in tea infusion is adsorbed at a low level[157]. It is possible that Al eluted from cooking utensils is highly bioavailable because the stopping of the use of Al utensils has decreased serum Al levels[158]. Fe, which possesses similar chemical characteristics to Al, in the utensils is reportedly also easily adsorbed[159,160]. Arabi *et al.* demonstrated that mice exposed to boiled water from old Al cookware exhibited cytotoxic and genotoxic changes[161]. The rate of Al absorption is increased in older people, patients with Down's syndrome, and patients with AD[162].

Once absorbed from the gastrointestinal tract, Al rapidly appears in the blood, and approximately 80% of Al is transported by binding to transferrin, a Fe transporter protein; the remaining Al binds to albumin and citrate[163]. Approximately 50% of Al in the serum is excreted in the urine through the kidneys. Thus, high Al levels are observed in the bodies of patients with renal failure or kidney disease. Additionally, half of the Al amount is accumulated in the bone. A small, but considerable amount of Al can cross the blood brain barrier, possibly through the transferrin-receptor pathway or monocarboxylate transporters, and enter the brain. Then, Al remains in the brain and accumulates semi-permanently[136,164]. Kobayashi *et al.* reported that intraperitoneally or orally administered ^{26}Al was transferred to the brain and the amount of Al in the brain was not changed after 35 days, although Al in the serum disappeared rapidly[165]. The amount of Al in human bodies increases in age-dependent manner, although other trace elements don't[166]. Thus, it is possible that the brain has little ability to eliminate Al. **Figure 4** summarizes the biological fate of Al from various sources.

5-3. Iatrogenic exposure to Al

The Al present in medications has a crucial effect on human health because of its high bioavailability. A considerable amount of contamination is present in total parenteral nutrition (TPN). Al in TPN solutions is completely absorbed and enters the blood. Although a part of Al in the blood is excreted from the kidneys, some patients receiving TPN solutions have renal failure. In particular, the renal functions of infants have not been fully developed, and infants are considered to be more susceptible to Al in TPN. The accumulation of Al in bones of patients receiving TPN has been reported. Bishop *et al.* reported that preterm infants who received TPN containing high concentrations of Al had lower mental development scores than age-matched infants who received TPN with low Al levels[167]. Based on these findings, The U.S. Food and Drug Administration (FDA), North American Society for Pediatric Gastroenterology and Nutrition, and other societies have recommended reduction of Al contamination in TPN solutions. The FDA published a final rule requiring the concentration of Al in TPN solutions to be labeled by 2000, and the rule has been in effect from 2003[168]. In Japan, the method for determination of Al in TPN solutions was added to the Japanese Pharmacopoeia in 2006.

Another source of Al for infants is milk and formula[169]. High levels of Al are found in infant formulas. Yumoto *et al.* demonstrated that ^{26}Al administered to mother rats was transported to the brain of suckling infants through maternal milk suggesting that it would happen in humans [170]. In fact, Ma *et al.* reported that higher concentrations of Al in nails of infants were associated with low fine motor score[171].

A large amount of Al is present in antacids, and therefore, continuous exposure of patients with renal failure or kidney diseases to Al-containing antacids may increase their risk of encephalopathy. In 2002, the Japanese Ministry of Health, Labour and Welfare recommended that patients on dialysis or with renal failure should not use Al-containing antacids.

Al compounds, such as $Al(OH)_3$ or Al phosphate, are widely used as adjuvants in various vaccines. Using the ^{26}Al technique, Al in vaccines was shown to be absorbed and appeared in serum and other tissues of rats after intramuscular injection[172]. Weisser investigated the increase in serum Al levels and accumulation of Al in the bones of rats after intramuscular injection of

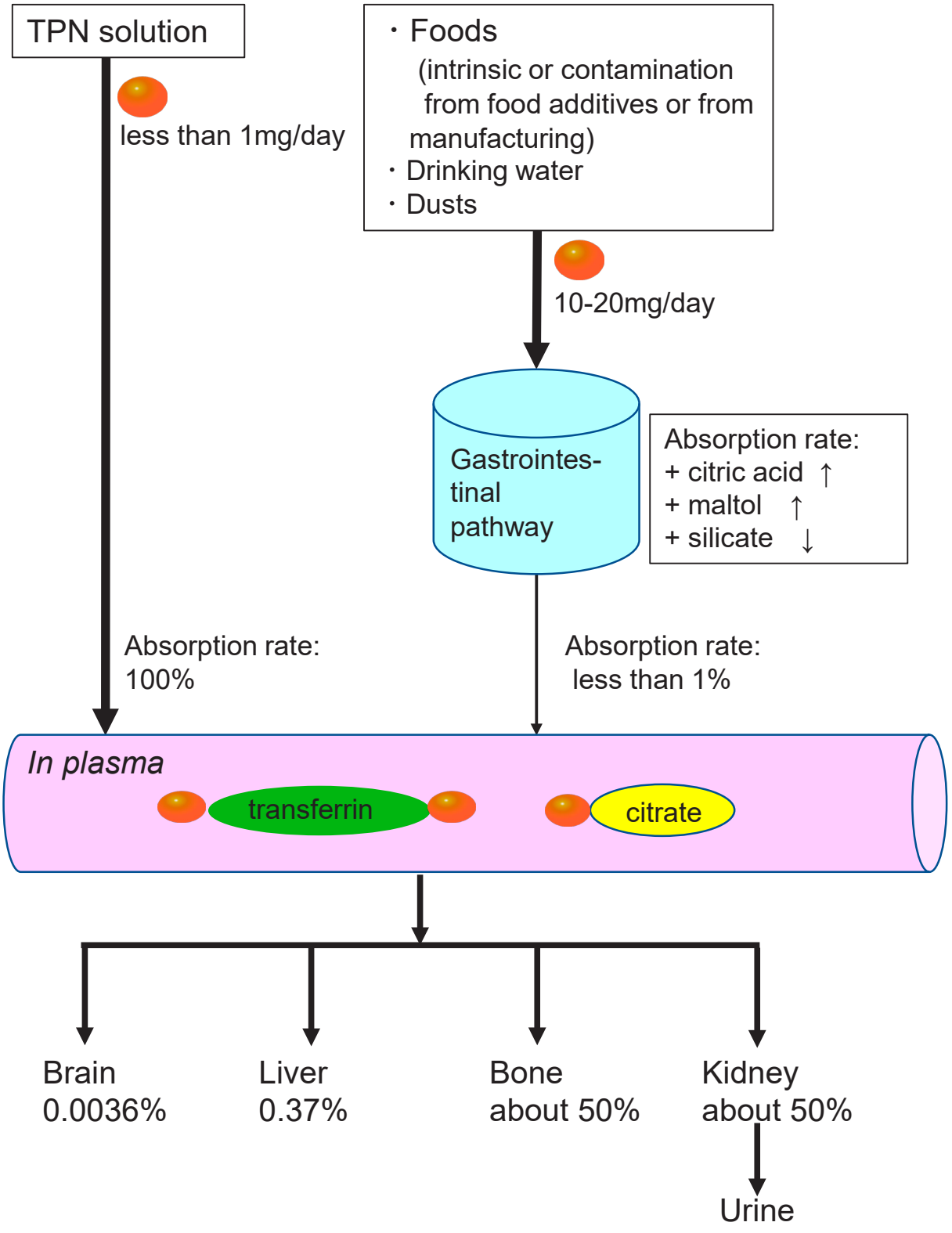

Fig. 4. **Intake and bioavailability of aluminum (Al)**
The daily intake of Al is estimated to be 10–20 mg from intrinsic foods and contamination by food additives or utensils. In general, the gastrointestinal absorption rate is less than 1%. However, this rate varies in individuals and is largely influenced by age, pH, stomach contents, chemical speciation of Al, and coexistence of substances such as silicic acid. Once Al enters the blood flow, a small but considerable amount of Al passes through the blood brain barrier, enters the brain, and accumulates throughout the lifetime. The absorption rates were obtained from Ref. No. 163.

vaccines with Al adjuvants[173]. An association between Al-containing vaccines and Gulf War Syndrome and other diseases has been suspected[174]. Gulf War Syndrome is a multi-system disorder afflicting many veterans of the 1990–1991 Gulf War.

Petrik *et al.* demonstrated that subcutaneous injection of $Al(OH)_3$ caused apoptotic death of motor neurons and impaired motor functions of mice in addition to producing Al deposition in motor neurons[175]. Furthermore, the link between Al adjuvants and autism spectrum disorders (ASD) has been discussed for many years[176]. High Al concentrations are observed in the brains of ASD patients[132]. Considering that infants receive much more Al from vaccines than other sources, the risk of Al-containing vaccines should be revisited.

6. Conclusion

Al is widely accepted as a neurotoxin and can cause cognitive deficiency and dementia when it enters the brain. Growing analytical, toxicological, and epidemiological studies support a link between Al and AD. Moreover, Al can affect infants, older adults, and patients with impaired renal functions and can cause severe health problems in these populations. Because Al is not excreted from the brain and accumulates for the long-term, unnecessary exposure to Al should be avoided. The link between Al and neurodegenerative diseases may provide a seed for the treatments/prevention of the diseases. The characteristics of Al neurotoxicity are complex, and further detailed research is necessary, particularly in relation to its bioavailability, cellular effects, metabolism, and metal-metal interactions.

Acknowledgements:

This work was partially supported by a Grant-in-Aid for Scientific Research from the Ministry of Education, Culture, Sports, Science and Technology of Japan (JSPS Kakennhi Grant numbers JP18K06669 and JP17H03197). We thank Kobayashi, N. for technical assistance. We thank Lisa Kreiner, PhD, from Edanz (https://www.jp.edanz.com/ac) for editing a draft of this manuscript.

References

[1] Wang P, Ding S, An G, Qu R, Liu X, Fang C, Chu W: Removal of disinfection by-product precursors by Al-based coagulants: A comparative study on coagulation performance. J Hazard Mater 420:126558, 2021.

[2] Alfrey AC, LeGendre GR, Kaehny WD: The dialysis encephalopathy syndrome: Possible aluminium intoxication. New Engl J Med 294:184-188, 1976.

[3] Kawahara M and Kato-Negishi M: Link between aluminum and the pathogenesis of Alzheimer's disease: the integration of the aluminum and amyloid cascade hypotheses. Int J Alzheimer Dis 276393, 2011.

[4] Shiraki H and Yase Y: Amyotrophic lateral sclerosis and Parkinsonism-dementia in the Kii peninsula: comparison with the same disorders in Guam and with Alzheimer's disease. Handbook of Clinical Neurology 15:273-300, 1991.

[5] Shaw CA, Tomljenovic L: Aluminum in the central nervous system (CNS): toxicity in humans and animals, vaccine adjuvants, and autoimmunity. Immunol Res 56:304-16, 2013.

[6] Sulaiman R, Wang M, Ren X: Exposure to aluminum, cadmium, and mercury and autism spectrum disorder in children: a systematic review and meta-analysis. Chemical Research in Toxicology 33:2699-2718, 2020.

[7] Selkoe DJ: The molecular pathology of Alzheimer's disease. Neuron 6:487-498, 1991.

[8] Armstrong RA: Risk factors for Alzheimer disease. Folia Neuropathol 57:87-105, 2019.

[9] McLachlan DR: Aluminium and the risk for Alzheimer's disease. Environmetrics 6:233-275, 1995.

[10] Klatzo I, Wisniewski H, Streicher E: Experimental production of neurofibrillary degeneration I. Light microscopic observation. J Neuropathol Exp Neurol 24:187-199, 1965.

[11] Kawahara M: Effects of aluminum on the nervous system and its possible link with neurodegenerative diseases. J Alzheimer Disease 8:171-182, 2005.

[12] Exley C: Aluminum should now be considered a primary etiological factor in Alzheimer's disease. Journal of Alzheimer's Disease Reports, 1:23-25, 2017.

[13] Lidsky TI: Is the Aluminum Hypothesis dead? J Occup Environ Med 56:S73-9, 2014.

[14] Martin RB 1997. Chemistry of aluminum in the central nervous system. Yasui M, et al. (eds): Mineral and Metal Neurotoxicology. CRC Press, N.Y., pp75-81, 1997.

[15] Exley C: A biogeochemical cycle for aluminium? J Inorg Biochem 97:1-7, 2003.

[16] Johnson VJ, Sharma RP: Aluminum disrupts the pro-inflammatory cytokine/neurotrophin balance in primary brain rotation-mediated aggregate cultures: possible role in neurodegeneration. Neurotoxicology 24:261-8, 2003.

[17] Lukiw WJ, LeBlanc HJ, Carver LA, McLachlan DR, Bazan NG: Run-on gene transcription in human neocortical nuclei. Inhibition by nanomolar aluminum and implications for neurodegenerative disease. J Mol Neurosci 11:67-78, 1998.

[18] Zatta P, Lain E, Cagnolini C: Effects of aluminum on activity of krebs cycle enzymes and glutamate dehydrogenase in rat brain homogenate. Eur J Biochem 267:3049-55, 2000.

[19] Julka D, Gill KD: Involvement of altered cytoskeletal protein phosphorylation in aluminum-induced CNS dysfunction. J Biochem Toxicol 11:227-33, 1996.

[20] Yamamoto H, Saitoh Y, Yasugawa S, Miyamoto E: Dephosphorylation of tau factor by protein phosphatase 2A in synaptosomal cytosol fractions, and inhibition by aluminum. J Neurochem 55:683-90, 1990.

[21] Kanazirska M, Vassilev PP, Birzon SY, Vassilev PM: Voltage-dependent effect of Al^{3+} on channel activities in hippocampal neurons. Biochem Biophys Res Commun 232:84-7, 1997.

[22] Kaneko N, Sugioka T, Sakurai H: Aluminum compounds enhance lipid peroxidation in liposomes: insight into cellular damage caused by oxidative stress. J Inorg Biochem 101:967-75, 2007.

[23] Oteiza PI: A mechanism for the stimulatory effect of aluminum on iron-induced lipid peroxidation. Arch Biochem Biophys 308:374-9, 1994.

[24] Ogasawara Y, Ohata E, Sakamoto T, Ishii K, Takahashi H, Tanabe S: A model of aluminum exposure associated with lipid peroxidation in rat brain. Biol Trace Elem Res 96:191-201, 2003.

[25] Han S, Lemire J, Appanna VP, Auger C, Castonguay Z, Appanna VD: How aluminum, an intracellular ROS generator promotes hepatic and neurological diseases: the metabolic tale. Cell Biol Toxicol 29:75-84, 2013.

[26] Kumar V, Gill KD: Oxidative stress and mitochondrial dysfunction in aluminium neurotoxicity and its amelioration: a review. Neurotoxicology 41:154-66, 2014.

[27] Exley C: The pro-oxidant activity of aluminum. Free Radic Biol Med. 36:380-7, 2004.

[28] Sánchez-Iglesias S, Méndez-Alvarez E, Iglesias-González J, Muñoz-Patiño A, Sánchez-Sellero I, Labandeira-García JL, Soto-Otero R: Brain oxidative stress and selective behavior of aluminium in specific areas of rat brain: potential effects in a 6-OHDA-induced model of Parkinson's disease. J Neurochem 109:879-88, 2009.

[29] Sakamoto T, Saito H, Ishii K, Takahashi H, Tanabe S, Ogasawara Y: Aluminum inhibits proteolytic degradation of amyloid beta peptide by cathepsin D: a potential link between aluminum accumulation and neuritic plaque deposition. FEBS Lett 580:6543-9, 2006.

[30] Kawahara M, Muramoto K, Kobayashi K, Kuroda Y: Functional and morphological changes in cultured neurons of rat cerebral cortex induced by long-term application of aluminum. Biochem Biophys Res Commun 189:1317-1322, 1992.

[31] Zatta PF, Cervellin D, Zambenedetti P: Effects of the aluminium speciation on the morphology of rabbit erythrocytes: a toxicological model. Toxicol In Vitro 12:287-93, 1998.

[32] Fontana L, Perazzolo M, Stella MP, Tapparo A, Corain B, Favarato M, Zatta P: A long-term toxicological investigation on the effect of tris(maltolate) aluminum(III) in rabbits. Biol Trace Elem Res 31:183-91, 1991.

[33] Kawahara M, Kato M, kuroda Y: Effects of aluminum on the neurotoxicity of primary cultured neurons and on the aggregation of β-amyloid protein. Brain Res Bull 55:211-217, 2001.

[34] Kawahara M, Kato-Negishi M, Hosoda R, Imamura L, Tsuda M, Kuroda Y: Brain-derived neurotrophic factor protects cultured rat hippocampal neurons from aluminum maltolate neurotoxicity. Journal of Inorganic Biochemistry 97:124-131, 2003.

[35] Konoha K, Imamura L, Tsuda M, Kawahara M: Aluminum maltolate inhibits brain-derived neurotrophic factor induced intracellular free calcium elevations in cultured rat hippocampal neurons. Biomed Res Trace Elements 14:173-175, 2003.

[36] Bharathi MB, Justin-Thenmozhi A, Manivasagam T, Rather MA, Babu CS, Essa MM, Guillemin GJ: Amelioration of aluminum maltolate-induced inflammation and endoplasmic reticulum stress-mediated apoptosis by tannoid principles of emblica officinalis in neuronal cellular model. Neurotox Res 35:318-330, 2019.

[37] Wang H, Shao B, Yu H, Xu F, Wang P, Yu K, Han Y, Song M, Li Y, Cao Z: Neuroprotective role of hyperforin on aluminum maltolate-induced oxidative damage and apoptosis in PC12 cells and SH-SY5Y cells. Chem Biol Interact 299:15-26, 2019.

[38] Rizvi SHM, Parveen A, Ahmad I, Ahmad I, Verma AK, Arshad M, Mahdi MA: Aluminum activates PERK-EIF2α signaling and inflammatory proteins in human neuroblastoma SH-SY5Y cells. Biol Trace Elem Res 172:108-119, 2016.

[39] Cheng L, Liang R, Zhuang Li, Ren J, Yang S, Bai J, Niu Q, Yu H, Zhang H, Xia N, Liu H: Aluminum maltolate triggers ferroptosis in neurons: mechanism of action. Toxicol Mech Methods. 31:33-42, 2021.

[40] Zhang QL, Niu Q, Ji XL, Conti P, Boscolo P: Is necroptosis a death pathway in aluminum-induced neuroblastoma cell demise? Int J Immunopathol Pharmacol 21:787-96, 2008.

[41] Hiradate S, Taniguchi S and Sakurai K: Aluminum speciation in aluminum-silica solutions and potassium chloride extracts of acidic soils.

Soil Sci Soc Am J 62:630-636, 1998.

[42] Parker DR, Kinraide TB and Zelazny LW: On the phytotoxicity of polynuclear hydroxy-aluminum complexes. Soil Sci Soc Am J 53:789-796, 1989.

[43] Flaten TP, Garruto RM: Polynuclear ions in aluminum toxicity. J Theor Biol 156:129-32, 1992.

[44] Rao GV, Rao KS: Evidence for a hydroxy- aluminium polymer (Al_{13}) in synaptosomes. FEBSLett 311:49-50, 1992.

[45] Konoha K, Nagata T, Sadakane Y, Kawahara M: Neurotoxicity of aluminum hydroxyl polymer on primary cultured neurons of rat cerebral cortex. Biomed Res Trace Elements 18:395-399, 2007.

[46] Chusid JG, Pacella BL, Kopeloff LM, Kopeloff N: Chronic epilepsy in the monkey following multiple intracerebral injection of alumina cream. Proc Soc Exp Biol Med 78:53-4, 1951.

[47] Allagui MS, Feriani A, Saoudi M, Badraoui R, Bouoni Z, Nciri R, Murat JC, Elfeki A: Effects of melatonin on aluminium-induced neurobehavioral and neurochemical changes in aging rats. Food Chem Toxicol 70:84-93, 2014.

[48] Zhang L, Jin C, Lu X, Yang J, Wu S, Liu Q, Chen R, Bai C, Zhang D, Zheng L, Du Y, Cai Y: Aluminium chloride impairs long-term memory and downregulates cAMP-PKA-CREB signalling in rats. Toxicology 323:95-108, 2014.

[49] Qin X, Li L, Nie X, Niu Q: Effects of chronic aluminum lactate exposure on neuronal apoptosis and hippocampal synaptic plasticity in rats. Biol Trace Elem Res 197:571-579, 2020.

[50] Zhang L, Jin C, Liu Q, Lu X, Wu S, Yang J, Du Y, Zheng L, Cai Y: Effects of subchronic aluminum exposure on spatial memory, ultrastructure and L-LTP of hippocampus in rats. J Toxicol Sci 38:255-68, 2013.

[51] Li H, Xue X, Li L, Li Y, Wang Y, Huang T, Wang Y, Meng H, Pan B, Niu Q: Aluminum-induced synaptic plasticity impairment via PI3K-Akt-mTOR signaling pathway. Neurotox Res 37:996-1008, 2020.

[52] Zhang H, Wei M, Lu X, Sun Q, Wang C, Zhang J, Fan H: Aluminum trichloride caused hippocampal neural cells death and subsequent depression-like behavior in rats via the activation of IL-1β/JNK signaling pathway. Sci Total Environ 715:136942, 2020.

[53] Inohana M, Eguchi A, Nakamura M, Nagahara R, Onda N, Nakajima K, Saegusa Y, Yoshida T, Shibutani M: Developmental exposure to aluminum chloride irreversibly affects postnatal hippocampal neurogenesis involving multiple functions in mice. Toxicol Sci 164:264-277, 2018.

[54] Nam SM, Kim JW, Yoo DY, Jung HY, Choi JH, Hwang IK, Seong JK, Yoon YS: Reduction of adult hippocampal neurogenesis is amplified by aluminum exposure in a model of type 2 diabetes. J Vet Sci 17:13-20, 2016.

[55] Spofforth J, Edin lRC, Eng MRC: Case of aluminium poisoning. Lancet 1:1301, 1921.

[56] Chen Y, Tian X, Wang X: Advances in dialysis encephalopathy research: a review. Neurol Sci 39:1151-1159, 2018.

[57] Hsu CW, Weng CH, Chan MJ, Lin-Tan DT, Yen TH, Huang WH: Association between serum aluminum level and uremic pruritus in hemodialysis patients. Sci Rep 8:17251, 2018.

[58] Tsai MH, Fang YW, Liou HH, Leu JG, Lin BS: Association of serum aluminum levels with mortality in patients on chronic hemodialysis. Sci Rep 8:16729, 2018.

[59] Altmann P, Cunningham J, Dhanesha U, Ballard M, Thompson J, Marsh F: Disturbance of cerebral function in people exposed to drinking water contaminated with aluminium sulphate: retrospective study of the Camelford water incident. BMJ 319:807-11, 1999.

[60] Exley C, Esiri M: Severe cerebral congophilic angiopathy coincident with increased brain aluminium in a resident of Camelford, Cornwall, UK. Journal of Neurology Neurosurgery & Psychiatry 77:877-879, 2006.

[61] Exley C, Mold MJ: Imaging of aluminium and amyloid β in neurodegenerative disease. Heliyon 6:e03839, 2020.

[62] King A, Troakes C, Aizpurua M, Mirza A, Hodges A, Al-Sarraj S, Exley C; Unusual neuropathological features and increased brain aluminium in a resident of Camelford, UK. Neuropathol Appl Neurobiol 43:537-541, 2017.

[63] Mold M, Cottle J, Exley C: Aluminium in Brain Tissue in Epilepsy: A Case Report from Camelford. Int J Environ Res Public Health 16:2129, 2019.

[64] Mold M, Cottle J, King A, Exley C: Intracellular aluminium in inflammatory and glial cells in cerebral amyloid angiopathy: a case report. Int J Environ Res Public Health 16:1459, 2019.

[65] Crapper DR, Krishnan SS, Dalton AL: Brain aluminium distribution in Alzheimer's disease and experimental neurofibrillary degeneration. Scienece 180:511-513, 1973.

[66] Wirths O, Multhaup G, Bayer TA: A modified β-amyloid hypothesis: intraneuronal accumulation of the beta-amyloid peptide--the first step of a fatal cascade. J Neurochem 91:513-520, 2004.

[67] Sadakane Y, Kawahara M: Implications of metal binding and asparagine deamidation for amyloid formation. Int J Mol Sci 19:2449, 2018.

[68] Fukuyama R, Mizuno T, Mori S, Nakajima K, Fushiki S, Yanagisawa K: Age-dependent change in the levels of Aβ40 and Aβ42 in cerebrospinal fluid from control subjects, and a decrease in the ratio of Aβ42 to Aβ40 level in cerebrospinal fluid from Alzheimer's disease

patients. Eur Neurol 43:155-60, 2000.

[69] Dyrks T, Dyrks E, Masters CL, Beyreuther K: Amyloidogenicity of rodent and human β A4 sequences. FEBS letters 324:231-236, 1993.

[70] Exley C, Price NC, Kelly SM, Birchall JD: An interaction of β-amyloid with aluminium in vitro. FEBS letters 324:293-295, 1993.

[71] Mantyh PW, Ghilardi JR, Rogers S, DeMaster E, Allen CJ, Stimson ER, Maggio JE: Aluminum, iron, and zinc ions promote aggregation of physiological concentrations of β-amyloid peptide. J Neurochem 61:1171-4, 1993.

[72] Kawahara M, Muramoto K, Kobayashi K, Mori H, Kuroda Y: Aluminum promotes the aggregation of Alzheimer's β-amyloid protein in vitro. Biochem Biophys Res Commun 198:531-535, 1994.

[73] Kuroda Y and Kawahara M: Aggregation of amyloid β-protein and its neurotoxicity:enhancement by aluminum and other metals. Tohoku J Exp Med 174:263-268, 1994.

[74] Bush AI, Pettingell WH, Multhaup G, d Paradis M, Vonsattel JP, Gusella JF, Beyreuther K, Masters CL, Tanzi RE: Rapid induction of Alzheimer Aβ amyloid formation by zinc. Science 265:1464-1467, 1994.

[75] Atwood CS, Moir RD, Huang X, Scarpa RC, Bacarra NM, Romano DM, Hartshorn MA, Tanzi RE, Bush AI: Dramatic aggregation of Alzheimer Aβ by Cu(II) is induced by conditions representing physiological acidosis. J Biol Chem 273:12817-26, 1998.

[76] Wallin C, Kulkarni YS, Abelein A, Jarvet J, Liao Q, Strodel B, Olsson L, Luo J, Abrahams JP, Sholts SB, Roos PM, Kamerlin SCL, Gräslund A, Wärmländer S: Characterization of Mn(II) ion binding to the amyloid-β peptide in Alzheimer's disease. J Trace Elem Med Biol 8:183-193, 2016.

[77] Chen WT, Liao YH, Yu HM, Cheng IH, Chen YR: Distinct effects of Zn^{2+}, Cu^{2+}, Fe^{3+}, and Al^{3+} on amyloid-beta stability, oligomerization, and aggregation: amyloid-beta destabilization promotes annular protofibril formation. J Biol Chem 286:9646-56, 2011.

[78] Sharma AK, Pavlova ST, Kim J, Kim J, Mirica LM: The effect of Cu^{2+} and Zn^{2+} on the Aβ42 peptide aggregation and cellular toxicity. Metallomics 5:1529-36, 2013.

[79] Drago D, Cavaliere A, Mascetra N, Ciavardelli D, di Ilio C, Zatta P, Sensi SL: Aluminum modulates effects of beta amyloid(1-42) on neuronal calcium homeostasis and mitochondria functioning and is altered in a triple transgenic mouse model of Alzheimer's disease. Rejuvenation Res 11:861-71, 2008.

[80] Bolognin S, Zatta P, Lorenzetto E, Valenti MT, Buffelli M: β-Amyloid-aluminum complex alters cytoskeletal stability and increases ROS production in cortical neurons, Neurochem Int. 62:566-74, 2013.

[81] Kuroda Y, Kobayashi K, Ichikawa M, Kawahara M, Muramoto K: Application of long-term cultured neurons in aging and neurological research: aluminum neurotoxicity, synaptic degeneration and Alzheimer's disease. Gerontology 41:2-6, 1995.

[82] Guy SP, Seabright PJ, Day JP, Itzhaki TF: Uptake of aluminium by human neuroblastoma cells. Biochem Soc Trans 18:392-3, 1990.

[83] Li H, Liu Q, Xue X, Lu X, Song J, He C, Hao Y, Nie J, Zhang Q, Zhao Y, Pan B, Wang L, Niu Q: miR-29a/b1 Regulates BACE1 in aluminum-induced Aβ deposition in vitro. ACS Chem Neurosci, 2021. doi: 10.1021/acschemneuro.1c00444.

[84] Zhang T, Wang S, Niu Q: Effect of aluminum-maltolate on the content of Aβ protein and the expression of ApoER2, VLDLRs, and LRP1 in PC12-ApoE4 Cells. Neurotox Res 35:931-944, 2019.

[85] Praticò D, Uryu K, Sung S, Tang S, Trojanowski JQ, Lee VMY: Aluminum modulates brain amyloidosis through oxidative stress in APP transgenic mice. FASEB J 16:1138-40, 2002.

[86] Zhang QL, Jia L, Jiao X, Guo WL, Ji JW, Yang HL, Niu Q: APP/PS1 transgenic mice treated with aluminum: an update of Alzheimer's disease model. Int J Immunopathol Pharmacol 25:49-58, 2012.

[87] Promyo K, Iqbal F, Chaidee N, Chetsawang B: Aluminum chloride-induced amyloid β accumulation and endoplasmic reticulum stress in rat brain are averted by melatonin. Food Chem Toxicol 146:111829, 2020.

[88] Chavali DV, Agarwal M, Kumar V, Saxena B: Neuroprotective Effects of Ethyl Pyruvate against Aluminum Chloride-Induced Alzheimer's Disease in Rats via Inhibiting Toll-Like Receptor. J Mol Neurosci 70:836-850, 2020.

[89] Wang L, Hu J, Zhao Y, Lu X, Zhang Q, Niu Q: Effects of aluminium on β-amyloid (1-42) and secretases (APP-cleaving enzymes) in rat brain. Neurochem Res 39:1338-45, 2014.

[90] Song J: Animal model of aluminum-induced Alzheimer's disease. Adv Exp Med Biol, 1091:113-127, 2018.

[91] Wisniewski HM, Sturman JA, Shek JW: Aluminum chloride induced neurofibrillary changes in the developing rabbit a chronic animal model. Ann Neurol 8:479-90, 1980.

[92] Elizabeth MA, Samson P, Itohan OR: Histomorphological evaluations on the frontal cortex extrapyramidal cell layer following administration of N-Acetyl cysteine in aluminum induced neurodegeneration rat model. Metab Brain Dis 35:829-839, 2020.

[93] Bilgic Y, Demir EA, Bilgic N, Dogan H, Tutuk O, Tumer C: Detrimental effects of chia (Salvia hispanica L.) seeds on learning and memory in aluminum chloride-induced experimental Alzheimer's disease. Acta Neurobiol Exp (Wars) 78:322-331, 2018.

[94] Sharma DR, Wani WY, Sunkaria A, Kandimalla RJ, Sharma RK, Verma D, Bal A, Gill KD: Quercetin attenuates neuronal death against

aluminum-induced neurodegeneration in the rat hippocampus. Neuroscience. 324:163-76, 2016.

[95] Lin WT, Chen RC, Lu WW, Liu SH, Yang FY: Protective effects of low-intensity pulsed ultrasound on aluminum-induced cerebral damage in Alzheimer's disease rat model. Sci Rep. 5:9671, 2015.

[96] Chong YH, Suh YH: Aggregation of amyloid precursor proteins by aluminum in vitro. Brain Res 670:137-41, 1995.

[97] Murayama H, Shin RW, Higuchi J, Shibuya S, Muramoto T, Kitamoto T: Interaction of aluminum with PHFtau in Alzheimer's disease neurofibrillary degeneration evidenced by desferrioxamine-assisted chelating autoclave method. Am J Pathol 155:877-85, 1999.

[98] Paik SR, Lee JH, Kim DH, Chang CS, Kim J: Aluminum-induced structural alterations of the precursor of the non-Aβ component of Alzheimer's disease amyloid. Arch Biochem Biophys 344:325-34, 1997.

[99] Uversky VN, Li J, Fink AL: Metal-triggered structural transformations, aggregation, and fibrillation of human alpha-synuclein. A possible molecular link between Parkinson's disease and heavy metal exposure. J Biol Chem 276:44284-96, 2001.

[100] Ramis R, Ortega-Castro J, Vilanova B, Adrover M, Frau J: A systematic DFT study of some plausible Zn(II) and Al(III) interaction sites in N-terminally acetylated α-synuclein. J Phys Chem A 122:690-699, 2018.

[101] Su L, Lu C, Yan P, Zhang N, Cai S, Zhang G, Zhou X, Li B: The effect of aluminum ion on the aggregation of human islet amyloid polypeptide (11-28). Acta Biochim Biophys Sin (Shanghai) 49:355-360, 2017.

[102] Exley C, House E, Patel T, Wu L, Fraser PE: Human pro-islet amyloid polypeptide (Pro IAPP(1-48)) forms amyloid fibrils and amyloid spherulites in vitro. J Inorg Biochem 104:1125-9, 2010.

[103] Khan A, Ashcroft AE, Korchazhkina OV, Exley C: Metal-mediated formation of fibrillar ABri amyloid. J Inorg Biochem 98:2006-10, 2004.

[104] Ricchelli F, Fusi P, Tortora P, Valtorta M, Riva M, Tognon G, Chieregato K, Bolognin S, Zatta P: Destabilization of non-pathological variants of ataxin-3 by metal ions results in aggregation/fibrillogenesis. Int J Biochem Cell Biol 39:966-77, 2007.

[105] Chaussidon M, Netter P, Kessler M, Membre H, Fener P, Delons S, Albarède F: Dialysis-associated arthropathy: secondary ion mass spectrometry evidence of aluminum silicate in beta 2-microglobulin amyloid synovial tissue and articular cartilage. Nephron 65:559-63, 1993.

[106] Chanphai P, Kreplak L, Tajmir-Riahi HA: Al cation induces aggregation of serum proteins. J Pharm Biomed Anal 141:234-240, 2017.

[107] Carrell RW, Lomas DA: Conformational disease. Lancet 350:134-8, 1997.

[108] Kawahara M, Kato-Negishi M, Tanaka KI: Amyloids: regulators of metal homeostasis in the synapse. Molecules. 25: pii: E1441, 2020.

[109] Muckenthaler MU, Galy B, Hentze MW: Systemic iron homeostasis and the iron-responsive element/iron-regulatory protein (IRE/IRP) regulatory network. Annu Rev Nutr 28:197-213, 2008.

[110] Rogers JT, Randall JD, Cahill CM, Eder PS, Huang X, Gunshin H, Leiter L, et al.: An iron-responsive element type II in the 5'-untranslated region of the Alzheimer's amyloid precursor protein transcript. J Biol Chem 277:45518-28, 2002.

[111] Rogers JT, Cahill CM: Iron-responsive-like elements and neurodegenerative ferroptosis. Learn Mem 27:395-413,2020.

[112] Yamanaka K, Minato N, Iwai K: Stabilization of iron regulatory protein 2, IRP2, by aluminum. FEBS Lett 462:216-20, 1999.

[113] Oshiro S, Nozawa K, Hori M, Zhang C, Hashimoto Y, Kitajima S, Kawamura K: Modulation of iron regulatory protein-1 by various metals. Biochem Biophys Res Commun 290:213-8, 2001.

[114] Oshiro S, Kawahara M, Kuroda Y, Zhang C, Cai Y, Kitajima S, Shirao M: Glial cells contribute more to iron and aluminum accumulation but are more resistant to oxidative stress than neuronal cells. Biochim Biophys Acta 1502:405-414, 2000.

[115] Liang RF, Li WQ, Wang H, Wang JX, Niu Q: Impact of sub-chronic aluminium-maltolate exposure on catabolism of amyloid precursor protein in rats. Biomed Environ Sci. 26:445-52, 2013.

[116] Li XB, Zhang ZY, Yin LH, Schluesene HJ: The profile of β-amyloid precursor protein expression of rats induced by aluminum. Environ Toxicol Pharmacol 33:135-40, 2013.

[117] Namekata K, Imagawa M, Terashi A, Ohta S, Oyama F, Ihara Y: Association of transferrin C2 allele with late-onset Alzheimer's disease. Hum Genet 101:126-9, 1997.

[118] Imagawa M, Naruse S, Tsuji S, Fujioka A, Yamaguchi H: Coenzyme Q10, iron, and vitamine B6 in genetically-confirmed Alzheimer's disease. Lancet 340: 671, 1992.

[119] Crapper DR, Krishnan SS, Quittkat S: Aluminium, neurofibrillary degeneration and Alzheimer's disease. Brain 99:67-80, 1976.

[120] McDermott JR, Smith AI, Iqbal K, Wisniewski HM: Aluminium and Alzheimer's disease. Lancet. 2:710-1, 1977.

[121] Perl DP: Relationship of aluminum to Alzheimer's disease. Environ Health Perspect 63:149-53, 1985.

[122] Trapp GA, Miner GD, Zimmerman RL, Mastri AR, Heston LL. Aluminum levels in brain in Alzheimer's disease. Biol Psychiatry 13:709-18, 1978.

[123] Shore D and Wyatt RL: Aluminum and Alzheimer's disease. J Nerv Ment Dis 171:553-558, 1983.

[124] Andrási E, Páli N, Molnár Z, Kösel S: Brain aluminum, magnesium and phosphorus contents of control and Alzheimer-diseased patients.

J Alzheimers Dis. 7:273-84, 2005.

[125] Landsberg JP, McDonald B, Watt F: Absence of aluminium in neuritic plaque cores in Alzheimer's disease. Nature 360:65-69, 1992.

[126] Bouras C, Giannakopoulos P, Good PF, Hsu A, Hof PR, Perl DP: A laser microprobe mass analysis of brain aluminum and iron in dementia pugilistica: comparison with Alzheimer's disease. Eur Neurol 38:53-8, 1997.

[127] Candy JM, McArthur FK, Oakley AE, Taylor GA, Chen CP, Mountfort SA, Thompson JE, Chalker PR, Bishop HE, Beyreuther K, et al.: Aluminium accumulation in relation to senile plaque and neurofibrillary tangle formation in the brains of patients with renal failure. J Neurol Sci 107:210-8, 1992.

[128] Yumoto S, Kakimi S, Ohsaki A, Ishikawa A: Demonstration of aluminum in amyloid fibers in the cores of senile plaques in the brains of patients with Alzheimer's disease. J Inorg Biochem 103:1579-84, 2009.

[129] Yumoto S, Kakimi S, Ishikawa A: Colocalization of aluminum and iron in nuclei of nerve cells in brains of patients with Alzheimer's disease. J Alzheimers Dis 65:1267-1281, 2018.

[130] Mold M, Linhart C, Gómez-Ramírez J, Villegas-Lanau A, Exley C: Aluminum and amyloid-β in familial Alzheimer's Disease. J Alzheimers Dis 73:1627-1635, 2020.

[131] Mold MJ, O'Farrell A, Morris B, Exley C: Aluminum and tau in neurofibrillary tangles in familial Alzheimer's disease. J Alzheimers Dis Rep 5:283-294, 2021.

[132] Exley C, Clarkson E: Aluminium in human brain tissue from donors without neurodegenerative disease: A comparison with Alzheimer's disease, multiple sclerosis and autism. Sci Rep 10,7770, 2020.

[133] Lukiw WJ, Kruck TPA, Percy ME, Pogue AI, Alexandrov PN, Walsh WJ, et al.: Aluminum in neurological disease - a 36 year multicenter study. J Alzheimers Dis Parkinsonism 8:457, 2019.

[134] Virk SA, Eslick GD: Aluminum levels in brain, serum, and cerebrospinal fluid are higher in Alzheimer's disease cases than in controls: a series of meta-analyses. J Alzheimers Dis 47:629-38, 2015.

[135] Martyn CN, Barker DJ, Osmond C, Harris EC, Edwardson JA, Lacey RF: Geographical relation between Alzheimer's disease and aluminum in drinking water. Lancet 1, 59-62, 1989.

[136] Flaten TP: Aluminium as a risk factor in Alzheimer's disease, with emphasis on drinking water. Brain Res Bull 55:187-96, 2001.

[137] McLachlan DR, Bergeron C, Smith JE, Boomer D, Rifat SL: Risk for neuropathologically confirmed Alzheimer's disease and residual aluminum in municipal drinking water employing weighted residential histories. Neurology 46:401-405, 1996.

[138] Rondeau V, Jacqmin-Gadda H, Commenges D, Helmer C, Dartigues JF: Aluminum and silica in drinking water and the risk of Alzheimer's disease or cognitive decline: findings from 15-year follow-up of the PAQUID cohort. Am J Epidemiol 169:489-96, 2009.

[139] Wang Z, Wei X, Yang J, Suo J, Chen J, Liu X, Zhao X: Chronic exposure to aluminum and risk of Alzheimer's disease: a meta-analysis. Neurosci Lett 610:200-6, 2016.

[140] Bagepally BS, Balachandar R, Kalahasthi R, Tripathi R, Haridoss M: Association between aluminium exposure and cognitive functions: A systematic review and meta-analysis. Chemosphere 268:128831, 2021.

[141] Van Dyke N, Yenugadhati N, Birkett NJ, Lindsay J, Turner MC, Willhite CC, Krewski D: Association between aluminum in drinking water and incident Alzheimer's disease in the Canadian Study of Health and Aging cohort. Neurotoxicology 83:157-165, 2021.

[142] Rondeau V: A review of epidemiologic studies on aluminum and silica in relation to Alzheimer's disease and associated disorders. Rev Environ Health 17:107-21, 2002.

[143] Guyonnet SG, Andrieu S, Vellas B: The potential influence of silica present in drinking water on Alzheimer's disease and associated disorders. J Nutr Health Aging 11:119-24, 2007.

[144] Russ TC, Killin LOJ, Hannah J, Batty GD, Deary IJ, Starr JM: Aluminium and fluoride in drinking water in relation to later dementia risk. Br J Psychiatry 216:29-34, 2020.

[145] Lu XT, Xu SM, Zhang YW, Gao D, Yang H, Song J, Wang LP, Zhang QL, Shang N, Niu Q: Longitudinal study of the effects of occupational aluminium exposure on workers' cognition. Chemosphere 271:129569,2021.

[146] Shang N, Zhang L, Wang S, Huang T, Wang Y, Gao X, Xu S, Zhang J, Zhang L, Niu Q, Zhang Q: Increased aluminum and lithium and decreased zinc levels in plasma is related to cognitive impairment in workers at an aluminum factory in China: A cross-sectional study. Ecotoxicol Environ Saf 214: 112110, 2021.

[147] Xu SM, Zhang YW, Ju XF, Gao D, Yang H, Wang LP, Song J, Zhang QL, Shang N, Niu Q, Lu XT: Cross-sectional study based on occupational aluminium exposure population. Environ Toxicol Pharmacol 83:103581, 2021.

[148] Mohammed RS, Ibrahim W, Sabry D, El-Jaafary SI: Occupational metals exposure and cognitive performance among foundry workers using tau protein as a biomarker. Neurotoxicology 76:10-16, 2020.

[149] Peters S, Reid A, Fritschi L, de Klerk N, Musk AWB: Long-term effects of aluminium dust inhalation. Occup Environ Med 70:864-8, 2013.

[150] Reyes AJ, Ramcharan K, Giddings SL, Ramesar A, Arias ER, Rampersad F: Movement disorders and dementia in a woman with chronic aluminium toxicity: video-MRI imaging. Tremor Other Hyperkinet Mov (NY) 11:5, 2021.

[151] Greger JL: Dietary and other sources of aluminium intake. Ciba Found Symp 169: 26-35, 1992.

[152] Jorhem L, Haegglund G: Aluminium in foodstuffs and diets in Sweden. Z Lebensm Unters Forsch 194:38-42, 1992.

[153] Li Q, Liu H, Alattar M, Jiang S, Han J, Ma Y, Jiang C: The preferential accumulation of heavy metals in different tissues following frequent respiratory exposure to PM2.5 in rats. Sci Rep 5:16936, 2019.

[154] Aluminium. Evaluation of the joint FAO/WHO expert committee on food additives (JECFA):(https://apps.who.int/food-additives-contaminants-jecfa-database/chemical.aspx?chemID=298) at 2021 Aug25. WHO Report (TRS 996-JECFA 74/7).

[155] Priest ND, Talbot RJ, Austin JG, Day JP, King SJ, Fifield K, Cresswell RG: The bioavailability of ^{26}Al-labelled aluminium citrate and aluminium hydroxide in volunteers. Biometals 9:221-8, 1996.

[156] Edwardson JA, Moore PB, Ferrier IN, Lilley JS, Newton GWA, Barker J, Templar J, Day JP: Effect of silicon on gastrointestinal absorption of aluminium. Lancet 342: 211-212, 1993.

[157] Wu J, Zhou CY, Wong MK, Lee HK, Ong CN: Urine levels of aluminum after drinking tea. Biol Trace Elem Res 57:271-80, 1997.

[158] Lin JL, Yang YJ, Yang SS, Leu ML: Aluminum utensils contribute to aluminum accumulation in patients with renal disease. Am J Kidney Dis 30:653-8, 1997.

[159] Adish A, Esrey SA, Gyorkos TW, Jean-Baptiste J, Rojhani A: Fe Effect of consumption of food cooked in iron pots on iron status and growth of young children: a randomised trial. Lancet 353:712-6, 1999.

[160] Talley L, Woodruff BA, Seal A, Tripp K, Mselle LS, Abdalla F, Bhatia R, Mirghani Z: Evaluation of the effectiveness of stainless steel cooking pots in reducing iron-deficiency anaemia in food aid-dependent populations. Public Health Nutr 13:107-15, 2010.

[161] Alabi OA, Unuigboje MA, Olagoke DO, Adeoluwa YM: Toxicity associated with long term use of aluminum cookware in mice: A systemic, genetic and reproductive perspective. Mutat Res 861-862:503296, 2021.

[162] Moore PB, Edwardson JA: Gastrointestinal absorption of aluminum is increased in Down's syndrome. Biol Psychiatry 41:488-492, 1997.

[163] Jouhanneau P, Raisbeck GM, Yiou F, Lacour B, Banide H, Drueke TB: Gastrointestinal absorption, tissue retention, and urinary excretion of dietary aluminum in rats determined by using ^{26}Al. Clin Chem 43:1023-8, 1997.

[164] Day JP, Barker J, Evans LJ, Perks J, Seabright PJ, Ackrill P, Lilley JS, Drumm PV, Newton GW: Aluminum absorption studied by ^{26}Al tracer. Lancet 337:1345, 1991.

[165] Kobayashi K, Yumoto S, Nagai H, Hosoyama Y, Imamura M, Masuzawa S, Koizumi Y, Yamashita H: ^{26}Al tracer experiment by accelerator mass spectrometry and its application to the studies for amyotrophic lateral sclerosis and Alzheimer's disease. I. Proc Japan Acad Ser B 66:189-192, 1990.

[166] Markesbery WR, Ehmann WD, Alauddin M, Hossain TI: Brain trace element concentrations in aging. Neurobiol Aging 5:19-28, 1984.

[167] Bishop NJ, Morley R, Day JP, Lucas A: Aluminum neurotoxicity in preterm infants receiving intravenous-feeding solutions. New Eng J Med 336:1557-1561, 1997.

[168] Federal Register 68:32979-32981, 2003.

[169] Corkins MR, Committee on Nutrition: Aluminum effects in infants and children. Pediatrics, 144: e20193148, 2019.

[170] Yumoto S, Nagai H, Kobayashi K, Tamate A, Kakimi S, Matsuzaki H: ^{26}Al incorporation into the brain of suckling rats through maternal milk. J Inorg Biochem 97:155-60, 2003.

[171] Ma R, Yang K, Chen C, Mao X, Shen X, Jiang L, Ouyang F, Tian Y, Zhang J, Kahe K, Shanghai Birth Cohort: Early-life exposure to aluminum and fine motor performance in infants: a longitudinal study. J Expo Sci Environ Epidemiol 31:248-256, 2021.

[172] Flarend RE, Hem SL, White JL, Elmore D, Suckow MA, Rudy AC, Dandashli DA: In vivo absorption of aluminium-containing vaccine adjuvants using ^{26}Al. Vaccine 15:1314-8, 1997.

[173] Weisser, K., Göen, T., Oduro, J. D., Wangorsch, G., Hanschmann, K. M. O., & Keller-Stanislawski, B: Aluminium in plasma and tissues after intramuscular injection of adjuvanted human vaccines in rats. Archives of Toxicology, 93,2787–2796, 2019.

[174] Gherardi RK, Aouizerate J, Cadusseau J, Yara S, Authier FJ: Aluminum adjuvants of vaccines injected into the muscle: Normal fate, pathology and associated disease. Morphologie 100:85-94, 2016.

[175] Petrik MS, Wong MC, Tabata RC, Garry RF, Shaw CA: Aluminum adjuvant linked to Gulf War illness induces motor neuron death in mice. Neuromolecular Medicine 9:83-100, 2007.

[176] Boretti A: Reviewing the association between aluminum adjuvants in the vaccines and autism spectrum disorder. J Trace Elem Med Biol 66:126764, 2021.

Regular article https://metallomicsresearch.brte.org

Determination of Fifty Trace Element Contents in Normal and Goitrous Thyroid using a Combination of Instrumental Neutron Activation Analysis and Inductively Coupled Plasma Mass Spectrometry

Vladimir Zaichick

Department of Radionuclide Diagnostics, Medical Radiological Research Center, Obninsk, Russia

Abstract

Background: Nodular goiter (NG) is an internationally important health problem. The aim of this exploratory study was to evaluate whether significant changes in the thyroid tissue levels of fifty trace elements (TE) exist in the goitrous transformed thyroid.

Method: Thyroid tissue levels of fifty TE were prospectively evaluated in 46 patients with colloid NG and 105 healthy inhabitants. Measurements were performed using a combination of non-destructive and destructive methods: instrumental neutron activation analysis and inductively coupled plasma mass spectrometry, respectively. Tissue samples were divided into two portions. One was used for morphological study while the other was intended for TE analysis.

Results: It was found that contents of Ag, Al, Bi, Ce, Cr, Er, Fe, Hg, La, Li, Mn, Mo, Nd, Ni, Pr, Se, Sm, Tl, U, Y, and Zn in colloid NG tissue significantly increased whereas the levels of Cd, Ga, and Sn decrease in comparison with those in normal thyroid. Conclusion: There are considerable changes in TE contents in the goitrous tissue of thyroid.

Key words: Colloid nodular goiter, Intact thyroid, Trace elements, Biomarkers for goiter diagnosis, Instrumental neutron activation analysis, Inductively coupled plasma mass spectrometry

Statements about COI: The author declares that there is no conflict of interest.

Funding Sources: None.

*Correspondence:
Department of Radionuclide Diagnostics Medical Radiological Research Center
Korolyev St. 4, Obninsk, Kaluga Region, 249036, Russia
Tel: +7 48439 60289
E-mail: vzaichick@gmail.com

Received: Jun 10, 2021
Accepted: September 10, 2021
Released online: October 15, 2021

Introduction

No less than 10 % of the world population is affected by goiter detected during the examination and palpation and most of these thyroidal lesions are nodular goiters (NG) [1]. However, using ultrasonography NG can be detected in almost 70% of the general population [2]. NG is also known as endemic nodular goitre, simple goitre, nodular hyperplasia, nontoxic uninodular goitre or multinodular goiter [3]. NG is benign lesions; however, during clinical examination, they can mimic malignant tumors. NG can be hyperfunctioning, hypofunctioning, and normal functioning. Euthyroid NG is defined as a local enlargement of

thyroid without accompanying disturbance in thyroid function [3].

For over the 20th century, there was the dominant opinion that NG is the simple consequence of iodine (I) deficiency. However, it was found that NG is a frequent disease even in those countries and regions where the population is never exposed to I shortage [4]. Moreover, it was shown that I excess has severe consequences on human health and associated with the presence of thyroidal disfunctions and autoimmunity, NG and diffuse goiter, benign and malignant tumors of gland [5-8]. It was also demonstrated that besides the I deficiency and excess many other dietary, environmental, and occupational factors are associated with the NG incidence [9-11]. Among them a disturbance of evolutionary stable input of many trace elements (TE) in human body after industrial revolution plays a significant role in etiology of thyroidal disorders [12].

Besides I involved in thyroid function, other TE have also essential physiological functions such as maintenance and regulation of cell function, gene regulation, activation or inhibition of enzymatic reactions, and regulation of membrane function [13]. Essential or toxic (goitrogenic, mutagenic, carcinogenic) properties of TE depend on tissue-specific need or tolerance, respectively [13]. Excessive accumulation or an imbalance of the TE may disturb the cell functions and may result in cellular degeneration, death, benign or malignant transformation [13-15].

In our previous studies the complex of in vivo and in vitro nuclear analytical and related methods was developed and used for the investigation of I and other TE contents in the normal and pathological thyroid [16-22]. Level of I in the normal thyroid was investigated in relation to age, gender and some non-thyroidal diseases [23,24]. After that, variations of TE content with age in the thyroid of males and females were studied and age- and gender-dependence of some TE was observed [25-41]. Furthermore, a significant difference between some TE contents in normal and cancerous thyroid was demonstrated [42-47].

To date, the pathogenesis of NG has to be considered as multifactorial. The present study was performed to clarify the role of fifty TE in the maintenance of thyroid growth and goitrogenesis. Having this in mind, our first aim is to assess the silver (Ag), aluminum (Al), arsenic (As), gold (Au), boron (B), beryllium (Be), bismuth (Bi), cadmium (Cd), cerium (Ce), cobalt (Co), chromium (Cr), cesium (Cs), dysprosium (Dy), iron (Fe), erbium (Er), europium (Eu), gallium (Ga), gadolinium (Gd), mercury (Hg), holmium (Ho), iridium (Ir), lanthanum (La), lithium (Li), lutecium (Lu), manganese (Mn), molybdenum (Mo), niobium (Nb), neodymium (Nd), nickel (Ni), lead (Pb), palladium (Pd), praseodymium (Pr), platinum (Pt), rubidium (Rb), antimony (Sb), scandium (Sc), selenium (Se), samarium (Sm), tin (Sn), terbium (Tb), tellurium (Te), thorium (Th), titanium (Ti), thallium (Tl), thulium (Tm), uranium (U), yttrium (Y), ytterbium (Yb), zinc (Zn), and zirconium (Zr) mass fraction contents in NG tissue using a combination of non-destructive and destructive methods: instrumental neutron activation analysis with high resolution spectrometry of long-lived radionuclides (INAA-LLR) and inductively coupled plasma mass spectrometry (ICP-MS), respectively. INAA-LLR and ICP-MS are the most powerful multi-element analytical tools for TE analysis. Using INAA-LLR it is possible to determine about 10 TE in thyroid samples [29,30] and using ICP-MS - about 50 [35,41]. However, as a non-destructive method INAA-LLR does not need in a special sample preparation (only freeze-drying and homogenization). Therefore, this method is an ideal method for some TE analysis of precious biopsy samples. By comparison TE results obtained both two methods allows to control possible losses of TE or contaminations by TE during acid digestion of thyroid samples that needs for ICP-MS.

A further aim is to compare the levels of these fifty TE in the goitrous thyroid with those in normal gland of apparently healthy persons.

Materials and Methods

Samples

All patients suffered from NG (n=46, mean age M±SD was 48±12 years, range 30-64) were hospitalized in the Head and Neck Department of the Medical Radiological Research Centre. Thick-needle puncture biopsy of suspicious nodules of the thyroid was performed for every patient, to permit morphological study of thyroid tissue at these sites and to estimate their TE contents. For all patients the diagnosis has been confirmed by clinical and morphological results obtained during studies of biopsy and resected materials. Histological conclusion for all thyroidal lesions was the colloid NG.

Normal thyroids for the control group samples were removed at necropsy from 105 deceased (mean age 44±21 years, range 2-87), who had died suddenly. The majority of deaths were due to trauma. A histological examination in the control group was used to control the age norm conformity, as well as to confirm the absence of micro-nodules and latent cancer.

All studies were approved by the Ethical Committees of the Medical Radiological Research Centre (MRRC), Obninsk. All the procedures performed in studies involving human participants were in accordance with the ethical standards of the institutional and/or national research committee and with the 1964 Helsinki declaration and its later amendments, or with comparable ethical standards.

Sample preparation

All tissue samples were divided into two portions using a titanium scalpel [48]. One was used for morphological study while the other was intended for TE analysis. After the samples intended for TE analysis were weighed, they were freeze-dried and homogenized [49-51].

The pounded sample weighing about 5-10 mg (for biopsy) and 50-100 mg (for resected materials) was used for TE measurement by INAA-LLR. The samples for INAA-LLR were wrapped separately in a high-purity aluminum foil washed with rectified alcohol beforehand and placed in a nitric acid-washed quartz ampoule.

After INAA-LLR investigation the thyroid samples were taken out from the aluminum foils and used for ICP-MS. The samples were decomposed in autoclaves; 1.5 mL of concentrated HNO_3 (nitric acid at 65 %, maximum (max) of 0.0000005 % Hg; GR, ISO, Merck, Darmstadt, Germany) and 0.3 mL of H_2O_2 (pure for analysis) were added to thyroid samples, placed in one-chamber autoclaves (Ancon-AT2, Ltd., Moscow, Russia) and then heated for 3 h at 160–200 °C. After autoclaving, they were cooled to room temperature and solutions from the decomposed samples were diluted with deionized water (up to 20 mL) and transferred to plastic measuring bottles. Simultaneously, the same procedure was performed in autoclaves without tissue samples (only $HNO_3^+H_2O_2^+$ deionized water), and the resultant solutions were used as control samples.

Certified Reference Materials

To determine contents of the TE by comparison with a known standard, biological synthetic standards (BSS) prepared from phenol-formaldehyde resins were used [52]. In addition to BSS, aliquots of commercial, chemically pure compounds were also used as standards. For quality control, ten subsamples of the certified reference materials (CRM) IAEA H-4 Animal Muscle from the International Atomic Energy Agency (IAEA), and also five sub-samples INCT-SBF-4 Soya Bean Flour, INCT-TL-1 Tea Leaves and INCT-MPH-2 Mixed Polish Herbs from the Institute of Nuclear Chemistry and Technology (INCT, Warszawa, Poland) were analyzed simultaneously with the investigated thyroid tissue samples. All samples of CRM were treated in the same way as the thyroid tissue samples. Detailed results of this quality assurance program were presented in earlier publications [53-59].

Instrumentation and methods

A vertical channel of nuclear reactor was applied to determine the content of Ag, Co, Cr, Fe, Hg, Rb, Sb, Sc, Se, and Zn by INAA-LLR. The quartz ampoule with thyroid samples, standards, and CRM was soldered, positioned in a transport aluminum container and exposed to a 24-hour irradiation in a vertical channel with a neutron flux of $1.3 \cdot 10^{13}$ $n \cdot cm^{-2} \cdot s^{-1}$. Ten days after irradiation samples were reweighed and repacked.

The samples were measured for period from 10 to 30 days after irradiation. The duration of measurements was from 20 min to 10 hours subject to pulse counting rate. Spectrometric measurements were performed using a coaxial 98-cm^3 Ge (Li) detector and a spectrometric unit (NUC 8100, Hungary), including a PC-coupled multichannel analyzer. Resolution of the spectrometric unit was 2.9-keV at the ^{60}Co 1,332-keV line.

Sample aliquots were used to determine the content of Ag, Al, As, Au, B, Be, Bi, Cd, Ce, Co, Cr, Cs, Dy, Er, Eu, Ga, Gd, Hg, Ho, Ir, La, Li, Lu, Mn, Mo, Nb, Nd, Ni, Pb, Pd, Pr, Pt, Rb, Sb, Se, Sm, Sn, Tb, Te, Th, Ti, Tl, Tm, U, Y, Yb, Zn, and Zr by ICP-MS using a Thermo X7 ICP-MS (Thermo Elemental, USA). The TE concentrations in aqueous solutions were determined by the quantitative method using multi elemental calibration solutions ICP-MS-68A and ICP-AM-6-A produced by High-Purity Standards (Charleston, SC 29423, USA). Indium was used as an internal standard in all measurements.

Information detailing with the INAA-LLR and ICP-MS methods used and other details of the analysis was presented in our previous publication concerning TE contents in human prostate and scalp hair [53-59].

Computer programs and statistic

A dedicated computer program for INAA-LLR mode optimization was used [60]. All thyroid samples were prepared in duplicate, and mean values of TE contents were used. Mean values of TE contents were used in final calculation for the Ag, Co, Cr, Fe, Hg, Rb, Sb, Se, and Zn mass fractions measured by both two methods INAA-LLR and ICP-MS. Using Microsoft Office Excel, a summary of the statistics, including, arithmetic mean, standard deviation, standard error of mean, minimum and maximum values, median, percentiles with 0.025 and 0.975 levels was calculated for TE mass fractions. The difference in the results between two groups (normal and goitrous thyroid) was evaluated by the parametric Student's t-test and non-parametric Wilcoxon-Mann-Whitney *U*-test.

Results

The comparison of our results for the Ag, Co, Cr, Fe, Hg, Rb, Sb, Se, and Zn mass fractions (mg/kg, dry mass basis) in the normal human thyroid obtained by both INAA-LLR and ICP-MS methods is shown in **Table 1**.

Tables 2 and 3 present certain statistical parameters (arithmetic mean, standard deviation, standard error of mean, minimal and maximal values, median, percentiles with 0.025 and 0.975 levels) of the Ag, Al, As, Au, B, Be, Bi, Cd, Ce, Co, Cr, Cs, Dy, Er, Eu, Fe, Ga, Gd, Hg, Ho, Ir, La, Li, Lu, Mn, Mo, Nb, Nd, Ni, Pb, Pd, Pr, Pt, Rb, Sb, Sc, Se, Sm, Sn, Tb, Te, Th, Ti, Tl, Tm, U, Y, Yb, Zn, and Zr mass fractions in normal and goitrous thyroid tissue, respectively. The As, Au, Eu, Ho, Ir, Lu, Pd, Pt, Te, Th, Tm, Yb, and Zr mass fractions in normal thyroid samples were determined in a few samples. The possible upper limit of the mean (≤M) for these TE was calculated as the average mass fraction, using the value of the detection limit (DL) instead of the individual value when the latter was found to be below the DL:

$$\leq M = \left(\sum_{i}^{n_i} C_i + DL \cdot n_j \right) / n$$

where C_i is the individual value of the TE mass fraction in sample *-i*, n_i is number of samples with mass fraction higher than the DL, n_j is number of samples with mass fraction lower than the DL, and $n = n_i + n_j$ is number of samples that were investigated. The As, Dy, Er,Gd, Ho, Ir, Lu, Nb, Pd, Pt, Tb, Te, Ti, and Tm contents in all samples of goitrous thyroid were under DL.

The comparison of our results with published data for TE mass fraction in normal and goitrous thyroid [61-95] is shown in **Table 4 and 5,** respectively.

The ratios of means and the difference between mean values of Ag, Al, B, Be, Bi, Cd, Ce, Co, Cr, Cs, Fe, Ga, Hg, La, Li, Mn, Mo, Nd, Ni, Pb, Pr, Rb, Sb, Sc, Se, Sm, Sn, Tl, U, Y, and Zn mass fractions in normal and goitrous thyroid are presented in **Table 6**.

Discussion

Precision and accuracy of results

Since there were no significant differences in TE concentration obtained by two methods, the losses and contaminations of the elements through acid digestion can be negligible for at least nine TE presented in **Table 1**. Moreover, a good agreement of our results for the TE mass fractions with the certified values of CRM IAEA H-4 and CRM IAEA HH-1 [53-59] as well as the similarity of the means of the Ag, Co, Cr, Fe, Hg, Rb, Sb, Se, and Zn mass fractions in the normal human thyroid determined by both non-destructive INAA-LLR and destructive ICP-MS methods (**Table 1**) demonstrates an acceptable precision and accuracy of the results obtained in the study and presented in **Tables 2-6**.

Comparison with published data

Values obtained for Al, B, Cd, Cr, Cs, Dy, Er, Fe, Gd, Hg, Ho, Lu, Mn, Nb, Nd, Ni, Pb, Pr, Pt, Rb, Sb, Sc, Se, Sm, Tb, Th, Ti, Tm, Yb, Zn, and Zr contents in the normal human thyroid (**Table 4**) agree well with median of mean values reported by other researches [61-83]. The obtained means for Ag, Au, Co, Mo, Sn, Y, and U were almost one-three orders of magnitude lower median of previously reported means but inside the range of means (**Table 4**). The mean obtained for As, Be, Bi, Ce, Eu, Ga, La, Li, and Tl were also one-three orders of magnitude lower than the median of previously reported data and outside the range of previously reported means (under a minimal value of published means). The mean obtained for Te was five orders of

magnitude lower than the only reported result [83].

Data cited in **Table 4** also includes samples obtained from patients who died from different non-endocrine diseases. A number of values for TE mass fractions were not expressed on a dry mass basis by the authors of the cited references. However, we calculated these values using published data for water (75%) [75] and ash (4.16% on dry mass basis) [96] contents in thyroid of adults. No published data referring Ir and Pd contents of normal thyroid tissue were found.

In goitrous tissues (**Table 5**) our results were comparable with published data for Ag, Cd, Cr, Fe, Mn, Mo, Ni, Pb, Se, and Zn contents. The obtained means for Co and Ti were approximately one order of magnitude and for Rb and U two orders of magnitude lower median of previously reported means, herewith, means for Co and Ti were outside, while for Rb and U were inside the range of cited means (**Table 5**). Our result for As was some lower than the minimal published mean for this TE (**Table 5**). No published data referring Au, B, Be, Bi, Ce, Cs, Dy, Er, Eu, Ga, Gd, Hg, Ho, Ir, La, Li, Lu, Nb, Nd, Pd, Pr, Pt, Sc, Sm, Sn, Tb, Te, Tl, Tm, Y, Yb, and Zr contents of goitrous thyroid were found.

The ranges of means of TE content reported in the literature for normal and goitrous thyroid vary widely (**Tables 4 and 5**, respectively). This can be explained by a dependence of TE content on many factors, including the region of the thyroid, from which the sample was taken, age, gender, ethnicity, mass of the gland, and the goiter stage. Not all these factors were strictly controlled in cited studies. Another and, in our opinion, leading cause of inter-observer variability can be attributed to the accuracy of the analytical techniques, sample preparation methods, and inability of taking uniform samples from the affected tissues. It was insufficient quality control of results in these studies. In many reported papers tissue samples were ashed or dried at high temperature for many hours. In other cases, thyroid samples were treated with solvents (distilled water, ethanol, formalin etc). There is evidence that by use of these methods some quantities of certain TE are lost as a result of this treatment that concern not only such volatile halogen as Br, but also other TE investigated in the study [97,98].

Effect of goitrous transformation on trace element contents

From **Table 6**, it is observed that in goitrous tissue the mass fraction of Ag, Al, Bi, Ce, Cr, Er, Fe, Hg, La, Li, Mn, Mo, Nd, Ni, Pr, Se, Sm, Tl, U, Y, and Zn are higher than in normal tissues of the thyroid. The most increased (higher 3 times) group of TE was Ag (14.4), Bi (Bi), Er (7.9), Hg (21.7), Nd (3.4), Ni (5.9), Pr (3.7),Sm (3.3), U (3.3), and Y (4.4). In contrast, the mass fraction of Cd, Ga, and Sn are 39%, 34%, and 41%, respectively, lower. Thus, if we accept the TE contents in thyroid glands in the control group as a norm, we have to conclude that with a goitrous transformation the levels of Ag, Al, Bi, Ce, Cr, Er, Fe, Hg, La, Li, Mn, Mo, Nd, Ni, Pr, Se, Sm, Tl, U, Y, and Zn in affected thyroid tissue significantly increased whereas the levels of Cd, Ga, and Sn decrease.

Role of trace elements in goitrous transformation of the thyroid

Characteristically, elevated or reduced levels of TE observed in goitrous thyroid are discussed in terms of their potential role in the initiation and promotion of thyroid goiter. In other words, using the low or high levels of the TE in goitrous tissues researchers try to determine the goitrogenic role of the deficiency or excess of each TE in investigated organ. In our opinion, abnormal levels of many TE in tumor could be and cause, and also effect of malignant transformation. From the results of such kind studies, it is not always possible to decide whether the measured decrease or increase in TE level in pathologically altered tissue is the reason for alterations or vice versa.

Silver

Ag is a TE with no recognized trace metal value in the human body [99]. Ag in metal form and inorganic Ag compounds ionize in the presence of water, body fluids or tissue exudates. The silver ion Ag^{+} is biologically active and readily interacts with proteins, amino acid residues, free anions and receptors on mammalian and eukaryotic cell membranes [100]. Besides such the adverse effects of chronic exposure to Ag as a permanent bluish-gray discoloration of the skin (argyria) or eyes (argyrosis), exposure to soluble Ag compounds may produce other toxic effects, including liver and kidney damage, irritation of the eyes, skin, respiratory, and intestinal tract, and changes in blood cells [101]. More detailed knowledge of the Ag toxicity can lead to a better understanding of the impact on human health, including thyroid function.

Aluminum

The Al is not described as essential, because no biochemical function has been directly connected to it. At this stage of our

knowledge, there is no doubt that Al overload impacts negatively on human health, including the thyroid function [102]. Thus, the present study suggests that an excess of Al may be involved in the colloid NG etiology.

Bismuth

The Bi is the heaviest stable element. There is only limited information on Bi compounds effects and fate in the human body but Bi is seen as the least toxic trace metal for humans. It is widely used in medical applications for its good antibacterial properties [103]. Until now Bi is not considered a human goitro- or carcinogen. However, in recent publication Bi effects on thyroid function was shown [104]. Moreover, it was found that Bi replaces catalytic or structural metals such as iron, nickel and zinc in metalloproteins and the inorganic Bi derivatives can cause DNA single-strand breaks [105]. Thus, the present study suggests that an excess of Bi may be involved in the colloid NG etiology.

Cadmium

The Cd is well known as a category I carcinogen and mitochondria are considered to be the main intracellular targets for this trace metal. It was shown in many studies that Cd acts as a thyroid disrupter in both animals and humans [106]. Colloid cystic goiter, adenomatoid follicular hyperplasia with low-grade dysplasia and thyroglobulin hypo- and asecretion, and parafollicular cell diffuse and nodular hyperplasia and hypertrophy are often found in chronic Cd toxicity [107]. In the thyroid, Cd activates or stimulates the activity of various factors that increase cell proliferation and a reduction in normal apoptotic activity. In this connection our finding of lower Cd content in the goitrous thyroid is very astonishing.

Cerium, erbium, lanthanum, neodymium, praseodymium, samarium, and ittrium

The Ce, Er, La, Nd, Pr, Sm, and Y are rare earth elements (REEs). REEs are a series of 17 chemical elements. They include scandium (Sc), yttrium (Y), lanthanum (La) and the lanthanide series from Ce to lutetium (Lu), in the periodic table. Their adverse health effects, including toxicity affected embryogenesis, fertilization, cytogenetic and redox endpoints, are well known [108,109]. However, the available information is insufficient to ascertain the mutagenicity and carcinogenicity of lanthanides and their compounds. Thus, the present study suggests that an excess of lanthanides and their compounds may be involved in the colloid NG etiology.

Chromium

The Cr-compounds are cytotoxic, genotoxic, and carcinogenic in nature. Some Cr forms, including hexavalent chromium (Cr^{6+}), are toxicants known for their carcinogenic effect in humans. They have been classified as certain or probable carcinogens by the International Agency for Research on Cancer (IARC) [110]. Furthermore, it was found that an elevated intake of Cr may induce functional and cellular damage in animal and human thyroid [113,112]. Besides reactive oxygen species (ROS) generation, oxidative stress, and cytotoxic effects of Cr exposure, a variety of other changes like DNA damage, increased formation of DNA adducts and DNA-protein cross-links, DNA strand breaks, chromosomal aberrations and instability, disruption of mitotic cell division, chromosomal aberration, premature cell division, S or G2/M cell cycle phase arrest, and carcinogenesis also occur in humans or experimental test systems [113]. In this connection our finding of elevated Cr content in the goitrous thyroid confirms the role of this TE in the colloid NG etiology.

Iron

It is well known that Fe as TE is involved in many very important functions and biochemical reactions of human body. Fe metabolism is therefore very carefully regulated at both a systemic and cellular level [114,115]. Under the impact of age and multiple environmental factors the Fe metabolism may become dysregulated with attendant accumulation of this metal excess in tissues and organs, including thyroid [25,26,29-35]. Most experimental and epidemiological data support the hypothesis that Fe overload is a risk factor for benign and malignant tumors [116]. This goitrogenic and oncogenic effect could be explained by an overproduction of ROS and free radicals [117].

Gallium

Ga a group IIIa metal in the periodic system of elements, shares chemical properties with Fe. Ga is commonly used in industry and medicine. Data on the toxic potential of Ga are very limited [118]. Because there is a competition between Fe and Ga in biological systems [119], the lower level of Ga in the goitrous thyroid may be connected with the elevated Fe content in the affected gland.

Mercury

Hg is one of the most dangerous environmental pollutants [120]. The growing use of this metal in diverse areas of industry

has resulted in a significant increase of environment contamination and episodes of human intoxication. Hg has been classified as certain or probable carcinogen by the IARC [121]. For example, in Hg polluted area thyroid cancer incidence was almost 2 times higher than in in adjacent control areas [122].

Negative effects of Hg are due to the interference of this metal in cellular signaling pathways and protein synthesis during the period of development. Since it bonds chemically with the sulfur hydride groups of proteins, it causes damage to the cell membrane and decreases the amount of RNA [123]. Moreover, it was shown that Hg may be involved in four main processes that lead to genotoxicity: generation of free radicals and oxidative stress, action on microtubules, influence on DNA repair mechanisms and direct interaction with DNA molecules [124]. Thus, the present study suggests that an elevated level of Hg in thyroid may act as a goitrogen.

Lithium

The results of lifelong Li-poor nutrition of animals show that Li is essential to the fauna, and thus, to humans as well [125]. Li-poor nutrition has a negative influence on some enzyme activity, mainly the enzymes of the citrate cycle, glycolysis, and of nitrogen metabolism [125]. On the other hand, Li is widely used in medicine as a mood-stabilizing drug. Because of the active transport of Na^+/I^- ions, Li is accumulated in the thyroid gland at a concentration 3 - 4 times higher than that in the plasma. It can inhibit the formation of colloid in thyrocytes, change the structure of thyroglobulin, weaken the iodination of tyrosines, and disrupt their coupling [126]. In addition, it reduces the clearance of free thyroxine in the serum, thereby indirectly reducing the activity of 5-deiodinase type 1 and 2 and reducing the deiodination of these hormones in the liver [126]. All these actions may cause the development of goiter.

Manganese

Trace element Mn is a cofactor for numerous enzymes, playing many functional roles in living organisms. The Mn-containing enzyme, manganese superoxide dismutase (Mn-SOD), is the principal antioxidant enzyme which neutralizes the toxic effects of reactive oxygen species. It was speculated that Mn interferes with thyroid hormone binding, transport, and activity at the tissue level [127]. However, an overall comprehension of Mn homeostasis and physiology, which is not yet acquired, is mandatory to establish Mn exact role in the thyroid goiter etiology and metabolism.

Molybdenum

The Mo is an essential TE and part of a complex called molybdenum co-factor, which is required for three mammalian enzymes—xanthine oxidase, aldehyde oxidase and sulphite oxidase [128]. Mo-dependent enzymes operate in the oxidative system of thyroid epithelial cells and also play role in the release of T_3 from the thyroid gland. However, there is data that even a slight increase Mo in the diet may accelerate and/or promote the process of thyroid cell transformation, thus acting as a tumor-promoting agent rather than a carcinogen [129]. Thus, the present study suggests that an elevated level of Mo in thyroid may act as a goitrogen.

Nickel

The peripheral connection between inorganic Ni and autoimmune thyroid diseases was mentioned in the literature [130]. Moreover, well known that human exposure to highly nickel-polluted environments, such as those associated with nickel refining, electroplating, and welding, has the potential to produce thyroid diseases. The exact mechanisms of nickel-induced thyroid diseases are not known. However, there is data that Ni-induced oxidative stress triggers cell proliferation, a process of great significance for thyroid goiter and cancer [131].

Selinium

The high level of Se content found just in the colloid NG cannot be regarded as pure chance. The seleno-protein characterized as Se-dependent glutathione peroxidase (Se-GSH-Px) is involved in protecting cells from peroxidative damage. This enzyme may reduce tissue concentration of free radicals and hydroperoxides. It is particular important for the thyroid gland, because thyroidal functions involve oxidation of iodide, which is incorporated into thyreoglobulin, the precursor of the thyroid hormones. For oxidation of iodide thyroidal cells produce a specific thyroid peroxidase using of physiologically generated hydrogen-peroxide (H_2O_2) as a cofactor [132]. It follows that the thyroid parenchyma must be continuously exposed to a physiological generation of H_2O_2 and in normal conditions must be a balance between levels of Se (as Se-GSH-Px) and H_2O_2. Thus, it might be assumed that the elevated level of Se in colloid NG tissue reflects an increase in concentration of free radicals and hydroperoxides during goitrous transformation.

Tin

For last four decades it was concluded that tin in an adequate level has beneficial effects on plants, animals and humans [133]. Sn and especially organotin compounds generates a wide variety of biological functions connected with the immune system, brain nervous system and endocrine glands, including thyroid. Among other several processes the biological functions of organotin compounds appear to be due to the inhibition of the membrane-mediated signal transduction system leading to DNA synthesis via phospholipid turnover and Ca^{2+} mobilization, as well as the involvement in cell proliferation, necrosis or apoptosis [134]. Thus, the possible goitrogenic effects of Sn deficiency on the thyroid gland cannot be ruled out.

Thallium

The Tl is a ubiquitous natural metal considered as the most toxic among TE. Moreover, Tl is a suspected human carcinogen [135]. We can't exclude the role of Tl elevated level in the NG etiology.

Uranium

The U accumulates in thyroid and its content is about an order of magnitude greater than the average soft tissue level [136]. It is known that U exposure may affect thyroid health [137].

Zinc

The Zn is active in more than 300 proteins and over 100 DNA-binding proteins, including the tumor suppressor protein p53, a Zn-binding transcription factor acting as a key regulator of cell growth and survival upon various forms of cellular stress. p53 is mutated in half of human tumors and its activity is tightly regulated by metals and redox mechanisms. On the other hand, excessive intracellular Zn concentrations may be harmful to normal metabolism of cells [138]. By now much data has been obtained related both to the direct and indirect action of intracellular Zn on the DNA polymeric organisation, replication and lesions, and to its vital role for cell division [139]. Other actions of Zn have been also described. They include its action as a potent anti-apoptotic agent [140]. All these facts allowed us to speculate that age-related overload Zn content in female thyroid, as was found in our previous study [25,29,31,33], is probably one of the factors in etiology of thyroid goiter and malignant tumors. Therefore, the elevated Zn level in colloid NG in comparison with normal level, detected in this study, supports our hypothesis.

Trace element levels as goiter markers

Our findings show that mass fraction of Ag, Al, Bi, Cd, Ce, Cr, Er, Fe, Ga, Hg, La, Li, Mn, Mo, Nd, Ni, Pr, Se, Sm, Sn, Tl, U, Y, and Zn are significantly different in colloid NG as compared to normal thyroid tissues (**Table 6**). Thus, it is plausible to assume that levels of these TE in affected thyroid tissue can be used as goiter markers. However, this subject needs in additional studies.

Limitations

This study has several limitations. Firstly, analytical techniques employed in this study measure only fifty TE mass fractions. Future studies should be directed toward using other analytical methods which will extend the list of chemical elements investigated in normal and goitrous thyroid tissue. Secondly, the sample size of NG group was relatively small. It was not allow us to carry out the investigations of TE contents in NG group using differentials like gender, histological types of goiter, stage of disease, and dietary habits of healthy persons and patients with NG. Lastly, generalization of our results may be limited to Russian population. Despite these limitations, this study provides evidence on goiter-specific tissue Ag, Al, Bi, Cd, Ce, Cr, Er, Fe, Ga, Hg, La, Li, Mn, Mo, Nd, Ni, Pr, Se, Sm, Sn, Tl, U, Y, and Zn level alteration and shows the necessity the need to continue TE research of goitrous thyroid.

Conclusion

In this work, TE measurements were carried out in the tissue samples of normal thyroid and colloid NG using two instrumental analytical methods: non-destructive neutron activation analysis with high resolution spectrometry of long-lived radionuclides and inductively coupled plasma mass spectrometry. It was shown that the combination of these methods is an adequate analytical tool for the estimation of fifty TE contents in the tissue samples of human thyroid, including needle-biopsy cores. It was observed that in goitrous tissues content of Ag, Al, Bi, Ce, Cr, Er, Fe, Hg, La, Li, Mn, Mo, Nd, Ni, Pr, Se, Sm, Tl, U, Y, and Zn significantly increased whereas the levels of Cd, Ga, and Sn decrease in a comparison with the normal thyroid tissues. In our opinion, the data of presented study strongly imply that TE play a significant role in thyroid health and the etiology of colloid

NG. It was supposed that the found differences in levels of TE in affected thyroid tissue can be used as colloid NG markers.

Acknowledgements

The author is extremely grateful to Profs. Vtyurin BM and Medvedev VS, Medical Radiological Research Center, Obninsk, as well as to Dr. Choporov Yu, Head of the Forensic Medicine Department of City Hospital, Obninsk, for supplying thyroid samples. He is also grateful to Dr. Karandaschev V, Dr. Nosenko S, and Irina Moskvina from Institute of Microelectronics Technology and High Purity Materials, Chernogolovka, Russia, for their help in ICP-MS analysis.

Table 1. Comparison of the mean values (M±SEM) of the trace element mass fractions (mg/kg, on dry-mass basis) in the normal thyroid obtained by both NAA-LLR and ICP-MS methods

Element	NAA-LLR M_1	ICP-MS M_2	Δ, %
Ag	0.0151±0.0016	0.0122±0.0014	19.2
Co	0.0399±0.0030	0.0378±0.0031	5.3
Cr	0.539±0.032	0.451±0.033	16.3
Fe	225±11	221±12	1.8
Hg	0.0421±0.0041	0.0794±0.0114	-88.5
Rb	7.37±0.44	7.79±0.46	-5.7
Sb	0.111±0.008	0.079±0.008	28.8
Se	2.32±0.14	2.12±0.14	8.6
Zn	97.8±4.5	91.8±4.3	6.1

M – arithmetic mean, SEM – standard error of mean, $\Delta=[(M_1 - M_2)/M_1] \cdot 100\%$.

Table 2. Some statistical parameters of 50 trace element mass fraction (mg/kg, dry mass basis) in the normal thyroid (n=105)

Element	M	SD	SEM	Min	Max	Median	P 0.025	P 0.975
Ag	0.0133	0.0114	0.0013	0.00160	0.0789	0.0102	0.00187	0.0333
Al	10.5	13.4	1.8	0.80	69.3	6.35	1.19	52.9
As	≤0.0049	-	-	<0.003	0.0200	-	-	-
Au	≤0.0050	-	-	<0.002	0.0203	-	-	-
B	0.476	0.434	0.058	0.200	2.30	0.300	0.200	1.73
Be	0.00052	0.00060	0.00008	0.0001	0.0031	0.00030	0.0001	0.0022
Bi	0.0072	0.0161	0.0022	0.000300	0.100	0.00270	0.000500	0.0523
Cd	2.08	2.05	0.27	0.0110	8.26	1.37	0.113	7.76
Ce	0.0080	0.0080	0.0011	0.00100	0.0348	0.00475	0.00134	0.0293
Co	0.0390	0.0276	0.0031	0.0100	0.140	0.0285	0.0130	0.124
Cr	0.495	0.261	0.031	0.130	1.30	0.430	0.158	1.08
Cs	0.0245	0.0166	0.0022	0.00220	0.0924	0.0198	0.00667	0.0723
Dy	0.00122	0.00183	0.00025	0.000300	0.0121	0.000630	0.000300	0.00519
Er	0.000377	0.000367	0.000050	0.000100	0.00220	0.000275	0.000100	0.00110
Eu	≤0.00039	-	-	<0.0002	0.00190	-	-	-
Fe	222.8	89.5	9.6	52.0	474	222	67.8	425
Ga	0.0316	0.0156	0.0021	0.0100	0.0810	0.0295	0.0100	0.0700
Gd	0.00105	0.00109	0.00015	0.000400	0.00650	0.000600	0.000400	0.00425
Hg	0.0543	0.0373	0.0043	0.00700	0.151	0.0460	0.00983	0.150
Ho	≤0.00040	-	-	<0.0001	0.00420	-	-	-
Ir	≤00.00028	-	-	<0.0002	0.0010	-	-	-
La	0.00475	0.00461	0.00062	0.000400	0.0219	0.00270	0.000400	0.0171
Li	0.0208	0.0155	0.0022	0.00150	0.0977	0.0178	0.00412	0.0487
Lu	≤0.00020	-	-	<0.0001	0.00100	-	-	-
Mn	1.28	0.56	0.07	0.470	4.04	1.15	0.537	2.23
Mo	0.0836	0.0470	0.0062	0.0104	0.299	0.0776	0.0278	0.211
Nb	0.597	0.898	0.120	0.0130	3.77	0.188	0.0130	3.26
Nd	0.0041	0.0034	0.0004	0.00020	0.0165	0.0030	0.00064	0.0137
Ni	0.449	0.344	0.046	0.0740	1.80	0.330	0.120	1.39
Pb	0.233	0.246	0.033	0.0230	1.60	0.180	0.0328	0.776
Pd	≤0.022	-	-	<0.014	0.0700	-	-	-
Pr	0.00107	0.00086	0.00011	0.00010	0.00390	0.00073	0.00020	0.00350
Pt	≤0.00057	-	-	<0.00020	0.0138	-	-	-
Rb	7.54	3.65	0.39	1.21	22.6	6.84	3.54	17.4
Sb	0.0947	0.0692	0.0075	0.00470	0.308	0.0808	0.0117	0.279
Sc	0.0268	0.0329	0.0060	0.000200	0.0860	0.00640	0.000418	0.0860
Se	2.22	1.24	0.14	0.320	5.80	1.84	0.776	5.58
Sm	0.000507	0.000469	0.000064	0.000100	0.00210	0.000350	0.000100	0.00150
Sn	0.0777	0.0677	0.0091	0.00900	0.263	0.0550	0.00900	0.242
Tb	0.000198	0.000116	0.000016	0.0000800	0.000600	0.000150	0.000100	0.000470
Te	≤0.0057	-	-	<0.003	0.0185	-	-	-
Th	≤0.0032	-	-	<0.002	0.0100	-	-	-
Ti	3.50	3.53	0.47	0.440	14.5	2.30	0.602	13.0
Tl	0.000932	0.000511	0.000068	0.000100	0.00290	0.000900	0.000294	0.00216
Tm	≤0.00014	-	-	<0.0001	0.00040			
U	0.000443	0.000434	0.000059	0.000100	0.00260	0.00030	0.000100	0.00131
Y	0.00260	0.00234	0.00032	0.00100	0.0110	0.00170	0.00100	0.00942
Yb	≤0.00059	-	-	<0.0003	0.00570	-	-	-
Zn	94.8	39.6	4.2	7.10	215	88.9	34.9	196
Zr	≤0.081	-	-	<0.03	0.480	-	-	-

M – arithmetic mean, SD – standard deviation, SEM – standard error of mean, Min – minimum value, Max – maximum value, P 0.025 – percentile with 0.025 level, P 0.975 – percentile with 0.975 level.

Table 3. Some statistical parameters of 50 trace element mass fraction (mg/kg, dry mass basis) in the colloid nodular goiter (n=46)

Element	M	SD	SEM	Min	Max	Median	P 0.025	P 0.975
Ag	0.192	0.214	0.038	0.00200	0.842	0.102	0.00200	0.736
Al	27.1	24.7	5.3	6.60	95.1	20.5	6.92	85.2
As	<0.004	-	-	-	-	-	-	-
Au	0.0141	0.0152	0.0030	0.00300	0.0585	0.00800	0.00300	0.0551
B	5.50	17.8	3.8	0.900	85.2	1.00	0.953	43.1
Be	0.00072	0.00053	0.00011	0.000200	0.00200	0.000500	0.000200	0.00200
Bi	0.0585	0.0560	0.0130	0.00390	0.214	0.0433	0.00732	0.192
Cd	1.26	1.30	0.28	0.126	5.36	0.964	0.164	4.56
Ce	0.0186	0.0185	0.0040	0.00310	0.0696	0.0109	0.00340	0.0639
Co	0.0576	0.0282	0.0049	0.0150	0.147	0.0538	0.0163	0.128
Cr	1.18	1.38	0.24	0.144	7.30	0.659	0.200	4.47
Cs	0.0216	0.0232	0.0050	0.00760	0.114	0.0147	0.00793	0.0760
Dy	<0.005	-	-	-	-	-	-	-
Er	0.00299	0.00332	0.00100	0.00100	0.0138	0.00200	0.00100	0.0113
Eu	<0.001	-	-	-	-	-	-	-
Fe	449	597	92	62.0	2734	207	65.6	2623
Ga	0.0210	0.0080	0.0020	0.0100	0.0340	0.0200	0.0100	0.0328
Gd	<0.001	-	-	-	-	-	-	-
Hg	1.18	1.01	0.17	0.100	5.18	1.11	0.122	3.34
Ho	<0.0002	-	-	-	-	-	-	-
Ir	<0.0003	-	-	-	-	-	-	-
La	0.00990	0.00921	0.00200	0.00170	0.0356	0.00570	0.00199	0.0311
Li	0.0281	0.0117	0.0030	0.00730	0.0541	0.0259	0.00890	0.0530
Lu	<0.0002	-	-	-	-	-	-	-
Mn	1.77	1.13	0.23	0.450	5.50	1.60	0.516	4.12
Mo	0.183	0.121	0.026	0.0490	0.627	0.173	0.0511	0.437
Nb	<0.013	-	-	-	-	-	-	-
Nd	0.0139	0.0087	0.0020	0.00310	0.0331	0.0114	0.00326	0.0306
Ni	2.63	2.43	0.54	0.130	10.4	1.75	0.149	7.74
Pb	0.94	1.86	0.41	0.120	8.90	0.460	0.120	5.10
Pd	<0.012	-	-	-	-	-	-	-
Pr	0.00396	0.00359	0.00100	0.000530	0.0131	0.00360	0.000601	0.0125
Pt	<0.0002	-	-	-	-	-	-	-
Rb	9.50	4.23	0.50	2.50	22.1	9.05	3.41	19.6
Sb	0.127	0.113	0.019	0.00102	0.425	0.0865	0.0128	0.404
Sc	0.0196	0.0316	0.0060	0.000200	0.113	0.00655	0.000200	0.111
Se	3.54	3.31	0.56	0.860	13.8	2.37	1.02	12.8
Sm	0.00169	0.00156	0.00033	0.000400	0.00690	0.00100	0.000400	0.00522
Sn	0.0458	0.0384	0.0090	0.0143	0.172	0.0319	0.0154	0.142
Tb	<0.0001	-	-	-	-	-	-	-
Te	<0.007	-	-	-	-	-	-	-
Th	0.0074	0.0062	0.0010	0.00200	0.0210	0.00600	0.00200	0.0210
Ti	<0.4	-	-	-	-	-	-	-
Tl	0.00174	0.00093	0.00021	0.000520	0.00350	0.00155	0.000591	0.00345
Tm	<0.0003	-	-	-	-	-	-	-
U	0.00145	0.00053	0.00022	0.000820	0.00240	0.00130	0.000880	0.00230
Y	0.0113	0.0103	0.0030	0.00360	0.0346	0.00665	0.00360	0.0318
Yb	0.000246	0.000087	0.000024	0.000200	0.000400	0.000200	0.000200	0.000400
Zn	121	51	8	47.0	264	113	49.1	257
Zr	0.074	0.045	0.010	0.0310	0.205	0.0620	0.0310	0.174

M – arithmetic mean, SD – standard deviation, SEM – standard error of mean, Min – minimum value, Max – maximum value, P 0.025 – percentile with 0.025 level, P 0.975 – percentile with 0.975 level.

Table 4. Median, minimum and maximum value of means of trace element contents in the normal thyroid according to data from the literature in comparison with our results (mg/kg, dry mass basis)

Element	Published data [Reference]			This work
	Median of means (n)*	Min of means M or M±SD, (n)**	Max of means M or M±SD, (n)**	M±SD
Ag	0.25 (12)	0.000784 (16) [61]	1.20±1.24 (105) [62]	0.0133±0.0114
Al	33.6 (12)	0.33 (-) [63]	420 (25) [64]	10.5±13.4
As	0.068 (15)	0.0036 (131) [65]	500±48 (4) [66]	≤0.0049
Au	0.084 (3)	0.0014±0.0002 (10) [67]	<0.4 (-) [68]	≤0.0050
B	0.151 (2)	0.084 (1) [69]	0.46 (1) [69]	0.476±0.434
Be	0.042 (3)	0.000924(16) [61]	<0.12 (-) [68]	0.00052±0.00060
Bi	0.126 (4)	0.0339 (16) [61]	<0.4 (-) [68]	0.0072±0.0161
Cd	1.68 (20)	0.12 (131) [65]	47.6±8.0 (16) [70]	2.08±2.05
Ce	0.22 (1)	0.22 (59) [61]	0.22 (59) [61]	0.0080±0.0080
Co	0.306 (25)	0.016 (66) [71]	70.4±40.8 (14) [72]	0.039±0.028
Cr	0.69 (17)	0.088 (83) [73]	24.8±2.4 (4) [66]	0.49±0.25
Cs	0.066 (6)	0.0112±0.0109 (14) [74]	0.109±0.370 (48) [75]	0.025±0.017
Dy	0.00106 (1)	0.00106 (60) [61]	0.00106 (60) [61]	0.0012±0.0018
Er	0.00068 (1)	0.00068 (60) [61]	0.00068 (60) [61]	0.00038±0.00038
Eu	0.0036 (1)	0.0036 (60) [61]	0.0036 (60) [61]	≤0.00039
Fe	252 (21)	56 (120) [76]	3360 (25) [64]	223±90
Ga	0.273 (3)	<0.04 (-) [68]	1.7±0.8 (-) [77]	0.032±0.016
Gd	0.00256 (1)	0.00256 (59) [61]	0.00256 (59) [61]	0.00105±0.00015
Hg	0.08 (13)	0.0008±0.0002 (10) [67]	396±40 (4) [66]	0.054±0.037
Ho	0.00016 (1)	0.00016 (60) [61]	0.00016 (60) [61]	≤0.00040
Ir	-	-	-	≤0.00028
La	0.068 (3)	0.052 (59) [61]	<4.0 (-) [68]	0.0047±0.0046
Li	6.3 (2)	0.092 (-) [68]	12.6 (180) [78]	0.021±0.015
Lu	0.000224 (1)	0. 000224 (60) [61]	0. 000224 (60) [61]	≤0.00020
Mn	1.62 (40)	0.076 (83) [73]	69.2±7.2 (4) [66]	1.28±0.56
Mo	0.40 (11)	0.0288±0.0096 (39) [67]	516±292 (14) [72]	0.0836±0.047
Nb	<4.0 (1)	<4.0 (-) [68]	<4.0 (-) [68]	0.60±0.90
Nd	0.0108 (1)	0.0108 (60) [61]	0.0108 (60) [61]	0.0041±0.0034
Ni	0.44 (19)	0.0084 (83) [73]	33.6±3.6 (4) [66]	0.45±0.34
Pb	0.58 (25)	0.021 (83) [73]	68.8±6.8 (4) [66]	0.23±0.25
Pd	-	-	-	≤0.022
Pr	0.0034 (1)	0.0034 (59) [61]	0.0034 (59) [61]	0.00107±0.00086
Pt	0.00017 (1)	0.00017 (59) [61]	0.00017 (59) [61]	≤0.00057
Rb	7.8 (9)	≤0.85 (29) [67]	294±191 (14) [72]	7.5±3.7
Sb	0.15 (10)	0.040±0.003 (-) [79]	≤12.4 (-) [68]	0.095±0.069
Sc	0.009 (4)	0.0018±0.0003 (17) [80]	0.0135±0.0045 (10) [67]	0.0268±0.0329
Se	2.32 (21)	0.436 (40) [81]	756±680 (14) [72]	2.2±1.2
Sm	0.00216 (1)	0.00216 (60) [61]	0.00216 (60) [61]	0.00051±0.00047
Sn	0.67 (7)	0.0235 (16) [61]	-≤3.8 (17) [82]	0.078±0.068
Tb	0.000224 (1)	0.000224 (60) [61]	0.000224 (60) [61]	0.00020±0.00012
Te	109 (1)	109±82 (7) [83]	109±82 (7) [83]	≤0.0057
Th	0.00216 (42)	0.00044 (40) [81]	0.00528 (60) [61]	≤0.0032
Ti	1.42 (8)	0.084 (83) [73]	73.6±7.2 (4) [66]	3.5±3.5
Tl	<0.2 (2)	0.00138 (16) [61]	<0.4 (-) [68]	0.00093±0.00051
Tm	0.000124 (1)	0.000124 (60) [61]	0.000124 (60) [61]	≤0.00014
U	0.0060 (11)	0.00014 (66) [71]	0.428±0.143 (10) [67]	0.00044±0.00043
Y	<2.9 (2)	0.00225 (16) [61]	≤5.9 (17) [82]	0.0026±0.0023
Yb	0.00056 (1)	0.00056 (60) [61]	0.00056 (60) [61]	≤0.00059
Zn	110 (56)	2.1 (-) [63]	820±204 (14) [72]	95±40
Zr	<0.4 (3)	0.188 (60) [61]	<4.0 (-) [68]	≤0.082

M –arithmetic mean, SD – standard deviation, Min – minimum, Max – maximum, (n)* – number of all references, (n)** – number of samples.

Table 5. Median, minimum and maximum value of means of trace element contents in the thyroid nodular goiter according to data from the literature in comparison with our results (mg/kg, dry mass basis)

Element	Published data [Reference]			This work
	Median of means (n)*	Min of means M or M±SD, (n)**	Max of means M or M±SD, (n)**	M±SD
Ag	0.21 (4)	0.098±0.042 (19) [84]	2.56 (167) [85]	0.192±0.199
Al	3.84 (6)	2.45 (123) [86]	840 (25) [64]	27.3±23.6
As	0.0045 (3)	0.0044 (41) [81]	68±52 (11) [72]	<0.004
Au	-	-	-	0.0166±0.0194
B	-	-	-	4.65±15.0
Be	-	-	-	0.00090±0.00113
Bi	-	-	-	0.0706±0.0845
Cd	1.24 (4)	0.125±0.006 (64) [87]	1.72±0.13 (9) [88]	1.55±1.68
Ce	-	-	-	0.0181±0.0176
Co	0.67 (12)	0.110±0.003 (64) [87]	62.8±22.4 (11) [72]	0.0576±0.0324
Cr	3.66 (5)	0.72 (51) [89]	25.2 (25) [64]	1.17±1.19
Cs	-	-	-	0.0320±0.0471
Dy	-	-	-	<0.005
Er	-	-	-	0.00303±0.00328
Eu	-	-	-	<0.001
Fe	390 (5)	128±52 (13) [90]	4848±3056 (11) [72]	430±566
Ga	-	-	-	0.0211±0.0081
Gd	-	-	-	<0.001
Hg	-	-	-	1.15±1.04
Ho	-	-	-	<0.0002
Ir	-	-	-	<0.0003
La	-	-	-	0.00939±0.00882
Li	-	-	-	0.0295±0.0151
Lu	-	-	-	<0.0002
Mn	2.64 (21)	0.352 (130) [65]	34.9 (101) [91]	1.81±1.41
Mo	0.39 (4)	0.094-0.145 (77) [84]	512±16 (11) [72]	0.193±0.121
Nb	-	-	-	<0.013
Nd	-	-	-	0.0134±0.0075
Ni	1.00 (9)	0.404 (41) [81]	19.7±20.5 (11) [72]	2.89±2.52
Pb	0.76 (9)	0.156±0.156 (13) [88]	8.08±6.00 (514) [92]	1.31±2.27
Pd	-	-	-	<0.012
Pr	-	-	-	0.00389±0.00335
Pt	-	-	-	<0.0002
Rb	436 (2)	7,0 (10) [80]	864±148 (11) [72]	9.50±4.23
Sb	0.63 (1)	0.15 (1) [93]	1.10 (1) [93]	0.121±0.108
Sc	-	-	-	0.0239±0.0383
Se	2.60 (8)	0.248 (41 [81]	174±116 (11) [72]	3.20±2.92
Sm	-	-	-	0.00171±0.00181
Sn	-	-	-	0.0516±0.0399
Tb	-	-	-	<0.0001
Te	-	-	-	<0.007
Th	0.00026 (1)	0.00026 (41) [81]	0.00026 (41) [81]	0.0104±0.0155
Ti	4.12 (2)	2.69 (-) [94]	16.4±25.2 (514) [92]	<0.4
Tl	-	-	-	0.00190±0.00109
Tm	-	-	-	<0.0003
U	0.202 (4)	0.00052 130) [65]	0.280±0.256 (51) [92]	0.00116±0.00059
Y	-	-	-	0.0110±0.0108
Yb	-	-	-	0.000275±0.000133
Zn	146 (25)	22.4 (130) [65]	1236±560 (2) [95]	117.7±48.7
Zr	-	-	-	0.0733±0.0444

M –arithmetic mean, SD – standard deviation, Min – minimum, Max – maximum, (n)* – number of all references, (n)** – number of samples.

Table 6. Differences between mean values (M±SEM) of trace element mass fractions (mg/kg, dry mass basis) in normal thyroid and colloid nodular goiter

Element	Thyroid tissue				Ratio
	Norm n=105	Goiter n=46	Student's t-test $p\leq$	U-test p	Goiter to Norm
Ag	0.0133±0.0013	0.192±0.038	**<0.000046**	**≤0.01**	14.4
Al	10.5±1.8	27.1±5.3	**0.0058**	**≤0.01**	2.58
B	0.476±0.058	5.50±3.8	0.200	>0.05	11.6
Be	0.00052±0.00008	0.00072±0.00011	0.165	>0.05	1.38
Bi	0.0072±0.0022	0.0585±0.0130	**0.00088**	**≤0.01**	8.13
Cd	2.08±0.27	1.26±0.28	**0.038**	**≤0.01**	0.61
Ce	0.0080±0.0011	0.0186±0.0040	**0.018**	**≤0.01**	2.33
Co	0.0390±0.0031	0.0576±0.0049	**0.0021**	**≤0.01**	1.48
Cr	0.495±0.031	1.18±0.24	**0.0088**	**≤0.01**	2.38
Cs	0.0245±0.0022	0.0216±0.0050	0.595	>0.05	0.88
Er	0.000377±0.000050	0.00299±0.00100	**0.0014**	**≤0.01**	7.93
Fe	222.8±9.6	449±92	**0.019**	**≤0.01**	2.02
Ga	0.0316±0.0021	0.0210±0.0020	**0.0014**	**≤0.01**	0.66
Hg	0.0543±0.0043	1.18±0.17	**<0.00000016**	**≤0.01**	21.7
La	0.00475±0.00062	0.00990±0.00200	**0.025**	**≤0.01**	2.08
Li	0.0208±0.0022	0.0281±0.0030	**0.037**	**≤0.01**	1.35
Mn	1.28±0.07	1.77±0.23	**0.048**	**≤0.01**	1.38
Mo	0.0836±0.0062	0.183±0.026	**0.0010**	**≤0.01**	2.19
Nd	0.0041±0.0004	0.0139±0.0020	**0.0010**	**≤0.01**	3.39
Ni	0.449±0.046	2.63±0.54	**0.00076**	**≤0.01**	5.85
Pb	0.233±0.033	0.94±0.41	0.098	>0.05	4.03
Pr	0.00107±0.00011	0.00396±0.00100	**0.0020**	**≤0.01**	3.70
Rb	7.54±0.39	9.50±0.50	0.108	>0.05	1.26
Sb	0.0947±0.0075	0.127±0.019	0.126	>0.05	1.34
Sc	0.0268±0.0060	0.0196±0.0060	0.387	>0.05	0.73
Se	2.22±0.14	3.54±0.56	**0.028**	**≤0.01**	1.59
Sm	0.000507±0.000064	0.00169±0.00033	**0.0037**	**≤0.01**	3.33
Sn	0.0777±0.0091	0.0458±0.0090	**0.013**	**≤0.01**	0.59
Tl	0.000932±.000068	0.00174±0.00021	**0.0012**	**≤0.01**	1.87
U	0.000443±0.000059	0.00145±0.00022	**0.0044**	**≤0.01**	3.27
Y	0.00260±0.00032	0.0113±0.0030	**0.014**	**≤0.01**	4.35
Zn	94.8±4.2	121±8	**0.0053**	**≤0.01**	1.28

M – arithmetic mean, SEM – standard error of mean, Statistically significant values are in **bold**.

References

[1] Carlé A, Krejbjerg A, Laurberg P: Epidemiology of nodular goitre. Influence of iodine intake. Best Pract Res Clin Endocrinol Metab 28(4): 465-479, 2014.

[2] Kant R, Davis A, Verma V: Thyroid nodules: Advances in evaluation and management. Am Fam Physician 102(5): 298-304, 2020.

[3] Hoang VT, Trinh CT: A review of the pathology, diagnosis and management of colloid goitre. Eur Endocrinol 16(2): 131-135, 2020.

[4] Derwahl M, Studer H: Multinodular goitre: 'much more to it than simply iodine deficiency'. Baillieres Best Pract Res Clin Endocrinol Metab 14(4): 577-600, 2000.

[5] Zaichick V: Iodine excess and thyroid cancer. J Trace Elements in Experimental Medidicne 11(4): 508-509, 1998.

[6] Zaichick V, Iljina T: Dietary iodine supplementation effect on the rat thyroid ^{131}I blastomogenic action. In: Die Bedentung der Mengen- und Spurenelemente. 18. Arbeitstangung. Friedrich-Schiller-Universität, Jena, 1998, 294-306.

[7] Kim S, Kwon YS, Kim JY, Hong KH, Park YK: Association between Iodine Nutrition Status and Thyroid Disease-Related Hormone in Korean Adults: Korean National Health and Nutrition Examination Survey VI (2013-2015). Nutrients 11(11): 2757, 2019.

[8] Vargas-Uricoechea P, Pinzón-Fernández MV, Bastidas-Sánchez BE, Jojoa-Tobar E, Ramírez-Bejarano LE, Murillo-Palacios J: Iodine status in the colombian population and the impact of universal salt iodization: a double-edged sword? J Nutr Metab 2019: 6239243, 2019.

[9] Stojsavljević A, Rovčanin B: Impact of essential and toxic trace metals on thyroid health and cancer: A review. Expo Health 2021. https://doi.org/10.1007/s12403-021-00406-8.

[10] Fahim YA, Sharaf NE, Hasani IW, Ragab EA, Abdelhakim HK: Assessment of thyroid function and oxidative stress state in foundry workers exposed to lead. J Health Pollut 10(27): 200903, 2020.

[11] Liu M, Song J, Jiang Y, Lin Y, Peng J, Liang H, Wang C, Jiang J, Liu X, Wei W, Peng J, Liu S, Li Y, Xu N, Zhou D, Zhang Q, Zhang J: A case-control study on the association of mineral elements exposure and thyroid tumor and goiter. Ecotoxicol Environ Saf 208: 111615, 2021.

[12] Zaichick V: Medical elementology as a new scientific discipline. J Radioanal Nucl Chem 269: 303-309, 2006.

[13] Moncayo R, Moncayo H: A post-publication analysis of the idealized upper reference value of 2.5 mIU/L for TSH: Time to support the thyroid axis with magnesium and iron especially in the setting of reproduction medicine. BBA Clin 7: 115–119, 2017.

[14] Beyersmann D, Hartwig A: Carcinogenic metal compounds: recent insight into molecular and cellular mechanisms. Arch Toxicol 82(8): 493-512, 2008.

[15] Martinez-Zamudio R, Ha HC: Environmental epigenetics in metal exposure. Epigenetics 6(7): 820-827, 2011.

[16] Zaĭchik VE, Raibukhin YuS, Melnik AD, Cherkashin VI: Neutron-activation analysis in the study of the behavior of iodine in the organism. Med Radiol (Mosk) 15(1): 33-36, 1970.

[17] Zaĭchik VE, Matveenko EG, Vtiurin BM, Medvedev VS: Intrathyroid iodine in the diagnosis of thyroid cancer. Vopr Onkol 28(3): 18-24, 1982.

[18] Zaichick V, Tsyb AF, Vtyurin BM: Trace elements and thyroid cancer. Analyst 120(3): 817-821, 1995.

[19] Zaichick VYe, Choporov YuYa: Determination of the natural level of human intra-thyroid iodine by instrumental neutron activation analysis. J Radioanal Nucl Chem 207(1): 153-161, 1996.

[20] Zaichick V: *In vivo* and *in vitro* application of energy-dispersive XRF in clinical investigations: experience and the future. J Trace Elements in Experimental Medidicne 11(4): 509-510, 1998.

[21] Zaichick V, Zaichick S: Energy-dispersive X-ray fluorescence of iodine in thyroid puncture biopsy specimens. J Trace Microprobe Tech 17(2): 219-232, 1999.

[22] Zaichick V: Relevance of, and potentiality for in vivo intrathyroidal iodine determination. Ann N Y Acad Sci 904: 630-632, 2000.

[23] Zaichick V, Zaichick S: Normal human intrathyroidal iodine. Sci Total Environ 206(1): 39-56, 1997.

[24] Zaichick V: Human intrathyroidal iodine in health and non-thyroidal disease. In: New aspects of trace element research (Eds: M.Abdulla, M.Bost, S.Gamon, P.Arnaud, G.Chazot). Smith-Gordon, London, and Nishimura, Tokyo, 1999, 114-119.

[25] Zaichick V, Zaichick S: Age-related changes of some trace element contents in intact thyroid of females investigated by energy dispersive X-ray fluorescent analysis. Trends Geriatr Healthc 1(1): 31-38, 2017.

[26] Zaichick V, Zaichick S: Age-related changes of some trace element contents in intact thyroid of males investigated by energy dispersive X-ray fluorescent analysis. MOJ Gerontol Ger 1(5): 00028, 2017.

[27] Zaichick V, Zaichick S: Age-related changes of Br, Ca, Cl, I, K, Mg, Mn, and Na contents in intact thyroid of females investigated by neutron activation analysis. Curr Updates Aging 1: 5.1, 2017.

[28] Zaichick V, Zaichick S: Age-related changes of Br, Ca, Cl, I, K, Mg, Mn, and Na contents in intact thyroid of males investigated by neutron activation analysis. J Aging Age Relat Dis 1(1): 1002, 2017.

[29] Zaichick V, Zaichick S: Age-related changes of Ag, Co, Cr, Fe, Hg, Rb, Sb, Sc, Se, and Zn contents in intact thyroid of females investigated by neutron activation analysis. J Gerontol Geriatr Med 3: 015, 2017.

[30] Zaichick V, Zaichick S: Age-related changes of Ag, Co, Cr, Fe, Hg, Rb, Sb, Sc, Se, and Zn contents in intact thyroid of males investigated by neutron activation analysis. Curr Trends Biomedical Eng Biosci 4(4): 555644, 2017.

[31] Zaichick V. and Zaichick S: Effect of age on chemical element contents in female thyroid investigated by some nuclear analytical methods. MicroMedicine 6(1): 47-61, 2018.

[32] Zaichick V, Zaichick S: Neutron activation and X-ray fluorescent analysis in study of association between age and chemical element contents in thyroid of males. Op Acc J Bio Eng Bio Sci 2(4): 202-212, 2018.

[33] Zaichick V, Zaichick S: Variation with age of chemical element contents in females' thyroids investigated by neutron activation analysis and inductively coupled plasma atomic emission spectrometry. J Biochem Analyt Stud 3(1): 1-10, 2018.

[34] Zaichick V, Zaichick S: Association between age and twenty chemical element contents in intact thyroid of males. SM Gerontol Geriatr Res 2(1): 1014, 2018.

[35] Zaichick V, Zaichick S: Associations between age and 50 trace element contents and relationships in intact thyroid of males. Aging Clin Exp Res 30(9): 1059-1070, 2018.

[36] Zaichick V, Zaichick S: Possible role of inadequate quantities of intra-thyroidal bromine, rubidium and zinc in the etiology of female subclinical hypothyroidism. EC Gynaecology 7(3): 107-115, 2018.

[37] Zaichick V, Zaichick S: Possible role of inadequate quantities of intra-thyroidal bromine, calcium and magnesium in the etiology of female subclinical hypothyroidism. Int Gyn and Women's Health 1(3): IGWHC.MS.ID.000113, 2018.

[38] Zaichick V, Zaichick S: Possible role of inadequate quantities of intra-thyroidal cobalt, rubidium and zinc in the etiology of female subclinical hypothyroidism. Womens Health Sci J 2(1): 000108, 2018.

[39] Zaichick V, Zaichick S: Association between female subclinical hypothyroidism and inadequate quantities of some intra-thyroidal chemical elements investigated by X-ray fluorescence and neutron activation analysis. Gynaecology and Perinatology 2(4): 340-355, 2018.

[40] Zaichick V, Zaichick S: Investigation of association between the high risk of female subclinical hypothyroidism and inadequate quantities of twenty intra-thyroidal chemical elements. Clin Res: Gynecol Obstet 1(1): 1-18, 2018.

[41] Zaichick V, Zaichick S: Investigation of association between the high risk of female subclinical hypothyroidism and inadequate quantities of intra-thyroidal trace elements using neutron activation and inductively coupled plasma mass spectrometry. Acta Scientific Medical Sciences 2(9): 23-37, 2018.

[42] Zaichick V. Zaichick S: Trace element contents in thyroid cancer investigated by energy dispersive X-ray fluorescent analysis. American Journal of Cancer Research and Reviews 2: 5, 2018.

[43] Zaichick V, Zaichick S: Trace element contents in thyroid cancer investigated by instrumental neutron activation analysis. J Oncol Res 2(1): 1-13, 2018.

[44] Zaichick V, Zaichick S: Variation in selected chemical element contents associated with malignant tumors of human thyroid gland. Cancer Studies 2(1): 2, 2018.

[45] Zaichick V, Zaichick S: Twenty chemical element contents in normal and cancerous thyroid. Int J Hematol Blo Dis 3(2): 1-13, 2018.

[46] Zaichick V, Zaichick S: Levels of chemical element contents in thyroid as potential biomarkers for cancer diagnosis (a preliminary study). J Cancer Metastasis Treat 4: 60, 2018.

[47] Zaichick V, Zaichick S: Fifty trace element contents in normal and cancerous thyroid. Acta Scientific Cancer Biology 2(8): 21-38, 2018.

[48] Zaichick V, Zaichick S: Instrumental effect on the contamination of biomedical samples in the course of sampling. The Journal of Analytical Chemistry 51(12): 1200-1205, 1996.

[49] Zaichick V, Zaichick S: A search for losses of chemical elements during freeze-drying of biological materials. J Radioanal Nucl Chem 218(2): 249-253, 1997.

[50] Zaichick V, Tsislyak YuV: A simple device for bio-sample lyophilic drying. Lab Delo 2: 109-110, 1978.

[51] Zaichick V, Tsislyak YuV: A modified adsorptive and cryogenic lyophilizer for biosamples freeze-drying. Lab Delo 2: 100-101, 1981.

[52] Zaichick V: Applications of synthetic reference materials in the medical Radiological Research Centre. Fresenius J Anal Chem 352: 219-223, 1995.

[53] Zaichick S, Zaichick V: The effect of age on Ag, Co, Cr, Fe, Hg, Sb, Sc, Se, and Zn contents in intact human prostate investigated by neutron activation analysis. J Appl Radiat Isot 69: 827-833, 2011.

[54] Zaichick V, Zaichick S: INAA application in the assessment of Ag, Co, Cr, Fe, Hg, Rb, Sb, Sc, Se, and Zn mass fraction in pediatric and young adult prostate glands. J Radioanal Nucl Chem 298(3): 1559-1566, 2013.

[55] Zaichick V, Zaichick S: Relations of the Al, B, Ba, Br, Ca, Cl, Cu, Fe, K, Li, Mg, Mn, Na, P, S, Si, Sr, and Zn mass fractions to morphometric parameters in pediatric and nonhyperplastic young adult prostate glands. BioMetals 27(2): 333-348, 2014.

[56] Zaichick S, Zaichick V, Nosenko S, Moskvina I: Mass fractions of 52 trace elements and zinc trace element content ratios in intact human prostates investigated by inductively coupled plasma mass spectrometry. Biol Trace Elem Res 149(2): 171-183, 2012.

[57] Zaichick V, Zaichick S: Use of neutron activation analysis and inductively coupled plasma mass spectrometry for the determination of trace elements in pediatric and young adult prostate. AJAC 4: 696-706, 2013.

[58] Zaichick V, Zaichick S: Use of INAA and ICP-MS for the assessment of trace element mass fractions in adult and geriatric prostate. J Radioanal Nucl Chem 301(2): 383-397, 2014.

[59] Zaichick S, Zaichick V: The effect of age and gender on 37 chemical element contents in scalp hair of healthy humans. Biol Trace Elem Res 134(1): 41-54, 2010.

[60] Korelo AM, Zaichick V: Software to optimize the multielement INAA of medical and environmental samples. In: Activation Analysis in Environment Protection. Joint Institute for Nuclear Research, Dubna, Russia, 1993, 326-332.

[61] Zhu H, Wang N, Zhang Y, Wu Q, Chen R, Gao J, Chang P, Liu Q, Fan T, Li J, Wang J, Wang J: Element contents in organs and tissues of Chinese adult men. Health Phys 98(1): 61-73, 2010.

[62] Vlasova ZA: Dynamics of trace element contents in thyroid gland in connection with age and atherosclerosis. Proceedings of the Leningrad Institute of Doctor Advanced Training, 80: 135-144, 1969.

[63] Kortev AI, Dontsov GI, Lyascheva AP: Bioelements and a human pathology. Middle-Ural publishing-house, Sverdlovsk, Russia, 1972.

[64] Kamenev VF: About trace element contents in thyroid of adults. In: Trace Elements in Agriculture and Medicine. Buryatia publishing-house, Ulan-Ude, 1963, 12-16.

[65] Stojsavljević A, Rovčanin B, Krstić D, Borković-Mitić S, Paunović I, Kodranov I, Gavrović-Jankulović M, Manojlović D: Evaluation of trace metals in thyroid tissues: Comparative analysis with benign and malignant thyroid diseases. Ecotoxicol Environ Saf 183: 109479, 2019.

[66] Reddy SB, Charles MJ, Kumar MR, Reddy BS, Anjaneyulu Ch, Raju GJN, Sundareswar B, Vijayan V: Trace elemental analysis of adenoma and carcinoma thyroid by PIXE method. Nucl Instrum Methods Phys Res B: Beam Interactions with Materials and Atoms 196(3-4): 333-339, 2002.

[67] Boulyga SF, Zhuk IV, Lomonosova EM, Kanash NV, Bazhanova NN: Determination of microelements in thyroids of the inhabitants of Belarus by neutron activation analysis using the k0-method. J Radioanal Nucl Chem 222(1-2): 11-14, 1997.

[68] Zakutinsky DI, Parfyenov YuD, Selivanova LN: Data book on the radioactive isotopes toxicology. State Publishing House of Medical Literature, Moscow, 1962.

[69] Tipton IH, Cook MJ: Trace elements in human tissue. Part II. Adult subjects from the United States. Health Phys 9(2): 103-145, 1963.

[70] Uetani M, Kobayashi E, Suwazono Y, Honda R, Nishijo M, Nakagawa H, Kido T, Nogawa K: Tissue cadmium (Cd) concentrations of people living in a Cd polluted area, Japan. Biometals 19(5): 521-525, 2006.

[71] Stojsavljević A, Rovčanin B, Krstić D, Jagodić J, Borković-Mitić S, Paunović I, Živaljević V, Mitić B, Gavrović-Jankulović M, Manojlović D: Cadmium as main endocrine disruptor in papillary thyroid carcinoma and the significance of Cd/Se ratio for thyroid tissue pathophysiology. J Trace Elem Med Biol 55: 190-195, 2019.

[72] Salimi J, Moosavi K, Vatankhah S, Yaghoobi A: Investigation of heavy trace elements in neoplastic and non-neoplastic human thyroid tissue: A study by proton – induced X-ray emissions. Int J Radiat Res 1(4): 211-216, 2004.

[73] Reitblat MA, Kropachyev AM: Some trace elements in thyroid of the Perm Pricam'ya residents. Proceedings of Perm Medical Institute 78: 157-164, 1967.

[74] Yamagata N: The concentration of common cesium and rubidium in human body. J Radiation Res 3(1): 9-30, 1962.

[75] Katoh Y, Sato T, Yamamoto Y: Determination of multielement concentrations in normal human organs from the Japanese. Biol Trace Elem Res 90(1-3): 57-70, 2002.

[76] Ataullachanov IA: Age changes in the content of manganese, cobalt, copper, zinc and iron in the endocrine glands of women. Probl Endocrinol (Mosk) 15(2): 98-102, 1969.

[77] Belozerov EC: Gallium contents in some human tissues. Zdravookhranenie Turkmenii 4: 15, 1965.

[78] Remiz AM: Endemic goiter and trace elements in Kabardino-Balkaria ASSR In: All-Union conference on endocrinology, Medgiz, Moscow, 1962, 330-331.

[79] Boulyga SF, Becker JS, Malenchenko AF, Dietze H-J: Application of ICP-MS for multielement analysis in small sample amounts of pathological thyroid tissue. Microchimica Acta 134(3-4): 215-222, 2000.

[80] Kvicala J, Havelka, Zeman J, Nemec J: Determination of some trace elements in the thyroid gland by INAA. J Radioanal Nucl Chem 149(2): 267-274, 1991.

[81] Stojsavljević A, Rovčanin B, Krstić D, Borković-Mitić S, Paunović I, Kodranov I, Gavrović-Jankulović M, Manojlović D: Evaluation of trace metals in thyroid tissues: Comparative analysis with benign and malignant thyroid diseases. Ecotoxicol Environ Saf 183: 109479, 2019.

[82] Forssen A: Inorganic elements in the human body. Ann Med Exp Biol Fenn 50(3): 99-162, 1972.

[83] Soman SD Joseph KT, Raut SJ, Mulay CD, Parameshwaran M, Panday VK: Studies of major and trace element content in human tissues. Health Phys 19(5): 641-656, 1970.

[84] Predtechenskaya VC. Nucleic acids and trace elements in thyroid pathology. Proceedings of the Voronezh Medical Faculty 94: 85-87, 1975.

[85] Kovalev MM: Trace element contents in normal and goitrous glands. Vrach Delo 12: 107-111, 1960.

[86] Ianchur NM, Elenevskaia NS, But-Gusaim AM, Nikhamkin LI. The content of manganese, aluminum, copper and zinc in the blood and the thyroid gland of patients with goiter. Klin Khir 4: 27-30, 1967.

[87] Błazewicz A, Dolliver W, Sivsammye S, Deol A, Randhawa R, Orlicz-Szczesna G, Błazewicz R: Determination of cadmium, cobalt, copper, iron, manganese, and zinc in thyroid glands of patients with diagnosed nodular goitre using ion chromatography. J Chromatogr B Analyt Technol Biomed Life Sci 878(1): 34-38, 2010.

[88] Zaripov C: Contents of some trace elements in normal and goitrous thyroid. In: Republic conference of young sientists and specialists of Tadzhik SSR. Dushanbe, 1975, 26-28.

[89] Pavlyuchenkova EG, Sorokina AN: Spectrographic determination of chromium in thyroid. In: Trace Elements in Agriculture and Medicine. Buryatia publishing-house, Ulan-Ude, 1963, 23-27.

[90] Kaya G, Avci H, Akdeniz I, Yaman M: Determination of Trace and Minor Metals in Benign and Malign Human Thyroid Tissues. Asian J Chem 21(7): 5718-5726, 2009.

[91] Petrov IC, Alyab'ev GA, Dmitrichenko MM: Contents of iodine, manganese, and cobalt in thyroid and blood in the local residents and migrants of Irkutsk region. In: Trace Elements in Agriculture and Medicine. Buryatia publishing-house, Ulan-Ude, 1968, 648-651.

[92] Antonova MV, Elinova VG, Voitekhovskaya YaV: Some trace element contents in thyroid and water in endemic goiter region. Zdravookhranenie BSSR 9: 42-44, 1966.

[93] Boulyga SF, Petri H, Zhuk IV, Kanash NV, Malenchenko AF: Neutron-activation analysis of trace elements in thyroids. J Radioanal Nucl Chem 242(2): 335-340, 1999.

[94] Bredikhin LM, Soroka VP. Trace element metabolism in patients with goiter during therapy. Vrach Delo 51(6): 81-84, 1969.

[95] Zagrodzki P, Nicol F, Arthur JR, Słowiaczek M, Walas S, Mrowiec H, Wietecha-Posłuszny R: Selenoenzymes, laboratory parameters, and trace elements in different types of thyroid tumor. Biol Trace Elem Res 134(1): 25-40, 2010.

[96] Schroeder HA, Tipton IH, Nason AP: Trace metals in man: strontium and barium. J Chron Dis 25(9): 491-517, 1972.

[97] Zaichick V: Sampling, sample storage and preparation of biomaterials for INAA in clinical medicine, occupational and environmental health. In: Harmonization of Health-Related Environmental Measurements Using Nuclear and Isotopic Techniques. IAEA, Vienna, 1997, 123-133.

[98] Zaichick V: Losses of chemical elements in biological samples under the dry aching process. Trace Elements in Medicine 5(3): 17-22, 2004.

[99] Lansdown AB: Critical observations on the neurotoxicity of silver. Crit Rev Toxicol 37(3): 237-250, 2007.

[100] Lansdown AB: Silver in health care: antimicrobial effects and safety in use. Curr Probl Dermatol 33: 17-34, 2006.

[101] Drake PL, Hazelwood KJ: Exposure-related health effects of silver and silver compounds: a review. Ann Occup Hyg 49(7): 575-585, 2005.

[102] Krewski D, Yokel RA, Nieboer E, Borchelt D, Cohen J, Harry J, Kacew S, Lindsay J, Mahfouz AM, Rondeau V: Human health risk assessment for aluminium, aluminium oxide, and aluminium hydroxide. J Toxicol Environ Health Part B 10: 1-269, 2007.

[103] Mohan R: Green bismuth. Nature Chem 2: 336-336, 2010.

[104] Noori Jassim AM, Mohammed Al Kazazz FF, Khalaf Ali A: Biochemical study for bismuth oxide and tellurium nanoparticles on thyroid hormone levels in serum and saliva of patients with chronic renal failure. Int J Chem Sci 11(3): 1299-1313, 2013.

[105] Thomas F, Bialek B, Hensel R: Medical use of bismuth: the two sides of the coin. J Clinic Toxicol S3: 004, 2012.

[106] Buha A, Matovic V, Antonijevic B, Bulat Z, Curcic M, Renieri EA, Tsatsakis AM, Schweitzer A, Wallace D: Overview of cadmium thyroid disrupting effects and mechanisms. Int J Mol Sci 19(5): 1501, 2018.

[107] Jancic SA, Stosic BZ: Cadmium effects on the thyroid gland. Vitam Horm 94: 391-425, 2014.

[108] Zaichick S, Zaichick V, Karandashev V, Nosenko S: Accumulation of rare earth elements in human bone within the lifespan. Metallomics 3: 186-194, 2011.

[109] Pagano G, Siciliano A, Gravina M, Palumbo A, Castellano I, Migliaccio O, Thomas PJ, Guida M, Tommasi F, Trifuoggi M: Heavy rare earth elements affect early life stages in *Paracentrotus lividus* and *Arbacia lixula* sea urchins. Environ Res 154: 240-246, 2017.

[110] Järup L: Hazards of heavy metal contamination. Br Med Bull 68: 167-182, 2003.

[111] Qureshi IZ, Mahmood T: Prospective role of ascorbic acid (vitamin C) in attenuating hexavalent chromium-induced functional and cellular damage in rat thyroid. Toxicol Ind Health 26(6): 349-359, 2010.

[112] Petrosino V, Motta G, Tenore G, Coletta M, Guariglia A, Testa D: The role of heavy metals and polychlorinated biphenyls (PCBs) in the oncogenesis of head and neck tumors and thyroid diseases: a pilot study. Biometals 31(2): 285-295, 2018.

[113] Nigam A, Priya S, Bajpai P, Kumar S: Cytogenomics of hexavalent chromium (Cr 6+) exposed cells: a comprehensive review. Indian J Med Res 139(3): 349-370, 2014.

[114] Manz DH, Blanchette NI, Paul BT, Torti FM, Torti SV: Iron and cancer: recent insights. Ann N Y Acad Sci 1368(1): 149-161, 2016.

[115] Torti SV, Torti FM: Iron and cancer: 2020 vision. Cancer Res 80(24): 5435-5448, 2020.

[116] Selby JV, Friedman GD: Epidemiologic evidence of an association between body iron stores and risk of cancer. Int J Cancer 41: 677–682, 1988.

[117] Meneghini R: Iron homeostasis, oxidative stress, and DNA damage. Free Radic Biol Med 23: 783-792, 1997.

[118] Ivanoff CS, Ivanoff AE, Hottel TL: Gallium poisoning: A rare case report. Food Chem Toxicol 50(2); 212-215, 2012.

[119] Chitambar CR: Gallium and its competing roles with iron in biological systems. Biochimica et Biophysica Acta (BBA) - Molecular Cell Research 1863(8): 2044-2053, 2016.

[120] Clarkson TW, Magos L: The toxicology of mercury and its chemical compounds. Crit Rev Toxicol 36: 609-662, 2006.

[121] Hazelhoff MH, Bulacio RP, Torres AM: Gender related differences in kidney injury induced by mercury. Int J Mol Sci 13: 10523-10536, 2012.

[122] Malandrino P, Russo M, Ronchi A, Minoia C , Cataldo D, Regalbuto C, Giordano C, Attard M, Squatrito S, Trimarchi F: Increased thyroid cancer incidence in a basaltic volcanic area is associated with non-anthropogenic pollution and biocontamination. Endocrine 53(2): 471-479, 2016.

[123] Abnoos H, Fereidoni M, Mahdavi-Shahri N, Haddad F, Jalal R: Developmental study of mercury effects on the fruit fly (Drosophila melanogaster). Interdiscip Toxicol 6(1): 34-40, 2013.

[124] Crespo-López ME, Macêdo GL, Pereira SI, Arrifano GPF, Picanço-Diniz DLW, do Nascimento JLM, Herculano AM: Mercury and human genotoxicity: critical considerations and possible molecular mechanisms. Pharmacol Res 60(4): 212-220, 2009.

[125] Anke M, Arnhold W, Schäfer U, Müller R: Recent progress in exploring the essentiality of the ultratrace element lithium to the nutrition of animals and man. Biomed Res Trace Elements 16(3): 169-176, 2005.

[126] Czarnywojtek A, Zgorzalewicz-Stachowiak M, Czarnocka B, Sawicka-Gutaj N, Gut P, Krela-Kazmierczak I, Ruchala M: Effect of lithium carbonate on the function of the thyroid gland: mechanism of action and clinical implications. J Physiol Pharmacol 71(2): 191-199, 2020.

[127] Soldin OP, Aschner M: Effects of manganese on thyroid hormone homeostasis. Neurotoxicology 28: 951-956, 2007.

[128] Sardesai VM: Molybdenum: an essential trace element. Nutr Clin Pract 8: 277-281, 1993.

[129] Luca E, Fici L, Ronchi A, Marandino F, Rossi ED, Caristo ME, Malandrino P, Russo M, Pontecorvi A, Vigneri R, Moretti F: Intake of boron, cadmium, and molybdenum enhances rat thyroid cell transformation. J Exp Clin Cancer Res 36: 73, 2017.

[130] Takir M, Turkoglu O, Turkoglu Z: Thyroid hormone and ultrasonographical analyses in patients with nickel allergy. European Journal of Medicine and Oncology 1(3): 145-148, 2017.

[131] Mohammadi-Bardbori A, Rannug A: Arsenic, cadmium, mercury and nickel stimulate cell growth via NADPH oxidase activation. Chemico-Biological Interactions 224: 183-188, 2014.

[132] Aaseth J, Frey H, Glattre E, Norheim G, Ringstad J, Thomassen Y: Selenium concentrations in the human thyroid gland. Biol Trace Elem Res 1990; 24(2-3):147-152.

[133] Nagy L, Szorcsik A, Kovács K: Tin compounds in pharmacy and nutrition. Acta Pharm Hung 70(2): 53-71, 2000.

[134] Arakawa Y, Tomiyama K: Biological functions of tin and disease. Nihon Rinsho 74(7):1199-1206, 2016.

[135] Emsley J: Thallium. The element of murder. A history of poison. Oxford University Press Inc, New York, 2005.

[136] Kathren RL, Tolmachev SY: Natural uranium tissue content of three Caucasian males. Health Phys 109(3): 187-197, 2015.

[137] Van Gerwen M, Alpert N, Lieberman-Cribbin W, Cooke P, Ziadkhanpour K, Liu B, Genden E: Association between uranium exposure and thyroid health: A National Health and Nutrition Examination Survey analysis and ecological study. Int J Environ Res Public Health 17(3): 712, 2020.

[138] Bozym RA, Chimienti F, Giblin LJ, Gross GW, Korichneva I, Li Y, Libert S, Maret W, Parviz M, Frederickson CJ, Thompson RB: Free zinc ions outside a narrow concentration range are toxic to a variety of cells in vitro. Exp Biol Med (Maywood) 235(6): 741-750, 2010.

[139] Blok LJ, Grossmann ME, Perry JE, Tindall DJ: Characterization of an early growth response gene, which encodes a zinc finger transcription factor, potentially involved in cell cycle regulation. Mol Endocrinol 9(11): 1610-1620, 1995.

[140] Kontargiris E, Vadalouka A, Ragos V, Kalfakakou V: Zinc inhibits apoptosis and maintains NEP downregulation, induced by Ropivacaine, in HaCaT cells. Biol Trace Elem Res 150: 460-466, 2012.

Regular article https://metallomicsresearch.brte.org

Structural analysis of chemically synthesized selenophosphate, a donor for selenocysteine biosynthesis

Noriyuki Suzuki, Marcelo Verdugo†, Teppei Hatakeyama, Yasumitsu Ogra*

Laboratory of Toxicology and Environmental Health, Graduate School of Pharmaceutical Sciences, Chiba University, Chuo, Chiba 260-8675, Japan

† Current affiliation: Laboratorio de Química Analítica y Ambiental, Instituto de Química y Bioquímica, Facultad de Ciencias, Universidad de Valparaíso, Valparaíso, Chile

Abstract

Selenophosphate is an important intermediate for selenoprotein synthesis. Despite its biological significance, the existence of selenophosphate in *in vivo* samples has not been corroborated by instrumental analyses, such as NMR spectroscopy and mass spectrometry. In this study, we synthesized selenophosphate and subjected it to detailed structural analyses, including ^{31}P NMR, ^{77}Se NMR, and LC-ICP-MS/MS analyses. We confirmed that the structural information of the chemically synthesized selenophosphate was consistent with that of the product biologically synthesized by SelD, a bacterial selenophosphate synthetase. Based on these results, the structure of the SelD product was confirmed.

Key words: selenium, selenophosphate, ICP-MS/MS, NMR, selenoprotein

Statements about COI: The authors declare no conflict of interest associated with this manuscript.

Introduction

Selenium (Se) is an element belonging to the same group on the periodic table as oxygen, sulfur, and tellurium, i.e., group 16, and has biologically ambivalent characteristics. Se is an essential element in animals but can be highly toxic when the amount ingested exceeds the nutritional level. Se is required as the active center of such proteins as glutathione peroxidase (GPx), thioredoxin reductase, thyroid hormone deiodinase, and selenoprotein P (Sel P) [1]. These proteins, called selenoproteins, not only function as an anti-oxidant but also participate in thyroid hormone production, DNA synthesis, and fertilization [2–5]. The active center of selenoproteins consists of a selenol group (-SeH) on a selenocysteine (SeCys) residue in a selenoprotein sequence [1, 6]. Thus, animals have very unique translational machinery for SeCys, which is called the "21st amino acid" [7, 8].

A unique mechanism for selenoprotein synthesis is known [7, 9]. Exogenous SeCys, being a free amino acid, is not incorporated into selenoproteins and hence, SeCys is *de novo* synthesized on tRNA by the reaction of activated Se, selenophosphate, and

*Correspondence:
Yasumitsu Ogra, Ph.D. Professor
Laboratory of Toxicology and Environmental Health
Graduate School of Pharmaceutical Sciences Chiba University
1-8-1 Inohana, Chuo, Chiba 260-8675, Japan
Tel./Fax: +81 43 226 2944
E-mail: ogra@chiba-u.jp

Received: August 24, 2021
Accepted: September 10, 2021
Released online: October 15, 2021

activated serine bound to tRNA, and SeCys-binding tRNA (SeCys-tRNA^{SeCys}) carries SeCys to the SeCys translation complex on mRNA [10]. Then, SeCys is incorporated into a protein by the UGA codon, one of the most common stop codons [11, 12]. It is known that ingested Se is utilized for selenoprotein synthesis after it is activated to selenophosphate [13]. Therefore, selenophosphate is an important intermediate for selenoprotein synthesis [14, 15].

Selenophosphate is an enigmatic compound. Although the biological significance of selenophosphate has been clearly established [13, 16], its existence in *in vivo* samples has not been corroborated by instrumental analyses, such as NMR spectroscopy and mass spectrometry. Selenophosphate is highly reactive and sensitive to oxidation. In fact, the half-life of selenophosphate at 0°C in air is 32 hr [17]. Stadtman's group obtained the ^{31}P NMR spectrum of selenophosphate produced by bacterial selenophosphate synthetase, a product of *selD* [18–20]. However, their data indicated that the SelD product contained phosphorus (P) having a unique chemical shift (δ = 23.4), differing from the chemical shifts of P in ATP, ADP, and AMP. In other words, there is no evidence that the *selD* product contains Se and P at the molar ratio 1:1 in its molecule. To confirm the structure of the *selD* product, the simultaneous detection of Se and P in the molecule is mandatory.

Although inductively coupled plasma mass spectrometry (ICP-MS) is the most sensitive and robust technique for Se detection to date [21], it is less sensitive to P than Se due to the low ionization efficiency of P and the large interference. Thus, it is difficult to detect P at the same detection level as Se. Recently, an inductively coupled plasma tandem mass spectrometer (ICP-MS/MS) has been developed and is commercially available. As ICP-MS/MS can effectively remove the interference and has a unique detection mode using oxygen, it is able to simultaneously detect Se and P.

NMR measurement is also applicable to the simultaneous detection of Se and P because both elements have NMR-active isotopes, i.e., ^{77}Se and ^{31}P (natural abundance is 7.6% and 100%, respectively) [22]. In a previous work, the structure of the SelD product was presumed by ^{31}P NMR measurement [19]. However, the simultaneous detection of Se and P by ^{77}Se NMR measurement would be more reliable for the identification of the structure of the SelD product than the ^{31}P NMR measurement, namely, if a direct magnetic coupling of ^{77}Se nuclei with ^{31}P nuclei is observed, the coupling constant calculated by NMR would provide solid evidence of the existence of a Se=P double bond in its molecule [23]. In this study, we chemically synthesized selenophosphate and identified it by ^{31}P NMR, ^{77}Se NMR, and ESI-MS measurements, in comparison with the reported data of the enzymatic product by SelD. Then, we measured the molar ratio of P and Se in the chemically synthesized compound identified as an equivalent to the SelD product by simultaneous detection using LC-ICP-MS/MS.

Materials and methods

Chemicals

Se (metal, powder), tris(trimethylsilyl)phosphite, sodium hydroxide, dithiothreitol, and dimethyl sulfoxide were purchased from Wako Pure Chemical Industries, Ltd. (Osaka, Japan). All other reagents used in this study were of the highest or analytical grade.

NMR analysis

^{31}P and ^{77}Se NMR spectra were obtained by JEOL JNM ECP400 (9.4 T) or JEOL JNM ECP600 (14.1 T) with ^{1}H decoupled. The Larmor frequencies for ^{31}P nuclei were 162 MHz (9.4 T) and 243 MHz (14.1 T), and those for ^{77}Se nuclei were 76.3 MHz (9.4 T) and 114 MHz (14.1 T).

Synthesis of *O,O,O*-tris(trimethylsilyl)selenophosphate **2**.

Elemental Se (powder, 0.66 g) was suspended in liquid tris(trimethylsilyl)phosphite **1** (2.4 g) under nitrogen atmosphere, and the suspension was stirred at 50 °C for 12 hr. The reaction mixture was filtered to afford 3.0 g (quantitative yield) of *O,O,O*-tris(trimethylsilyl)selenophosphate. The chemical purity of the product was confirmed by ^{31}P NMR, ^{77}Se NMR, and ESI-MS analyses. ^{31}P NMR (162 MHz, $CDCl_3$) δ 22.3 (s, relative intensity 0.92), δ 22.3 (d, relative intensity 0.08, $J_{^{31}P\text{-}^{77}Se}$ = 926 Hz). ^{77}Se NMR (76.3 MHz, $CDCl_3$) δ −158.9 (d, $J_{^{77}Se\text{-}^{31}P}$ = 926 Hz). HRMS (ESI) calcd. for $C_9H_{28}O_3PSeSi_3^+$ $[M+H]^+$: 379.0244, found: 379.0248.

Synthesis of trisodium selenophosphate

An aqueous solution of NaOH (10 M, 1 mL) was added to a mixture of **2** (0.30 g) and dithiothreitol (0.77 g) in 10 mL of

DMSO under nitrogen atmosphere, and the reaction mixture was stirred at room temperature for 3 min. 1-Propanol (30 mL) was added, and the reaction mixture was stored at 4 °C for 1 hr. The white precipitate obtained by centrifugation (1,500 x g, 10 min) was resuspended in 1-propanol (30 mL), and the suspension was subjected to centrifugation (1,500 x g, 10 min) to remove the supernatant. This process was repeated twice. The resulting precipitate was dried *in vacuo* to obtain a white powder of purified trisodium selenophosphate (190 mg, y. 78%). The chemical purity of the product was confirmed by ^{31}P NMR, ^{77}Se NMR, and ESI-MS analyses. ^{31}P NMR (243 MHz, Tris-HCl buffer, pH 7.2) δ 23.5 (s, relative intensity was 0.92), δ 23.5 (d, relative intensity was 0.08, $J_{^{31}P-^{77}Se}$ = 538 Hz). ^{77}Se NMR (114 MHz, Tris-HCl buffer, pH 7.2) δ −177.2 (d, $J_{^{77}Se-^{31}P}$ = 538 Hz). HRMS (ESI) calcd. for $H_4O_3PSe^+$ $[M+H]^+$: 162.9058, found: 162.9062.

LC-ICP-MS/MS analysis

An Agilent 8800 ICP-MS/MS (Agilent Technologies, Hachioji, Tokyo, Japan) was used. The operating conditions are summarized in **Table 1**. The ICP-MS/MS was coupled to an HPLC system as the detector for the simultaneous speciation of Se and P. The HPLC system consisted of an on-line degasser, an HPLC pump (Prominence, Shimadzu, Kyoto, Japan), a Rheodyne six-port injector with a 20 μL sample loop, and a column. A multi-mode gel filtration column, Shodex Asahipak GS-320HQ (7.5 i.d. x 300 mm, with a guard column, 7.5 i.d. x 75 mm, Showa Denko, Tokyo, Japan), was used. The column was injected with a 20-μL aliquot of sample and then eluted with 50 mmol/L ammonium acetate, pH 6.5, at the flow rate of 0.6 mL/min. The eluate was introduced directly into the nebulizer of the ICP-MS/MS, and Se and P distributions were monitored at *m/z* 94 and 47 under the O_2 mass shift mode as SeO^+ and PO^+, respectively.

Table 1. ICP-MS/MS operating conditions for the speciation of Se and P

Plasma setting	
RF power (W)	1,550
Nebulizer type	MicroMist
Nebulizer gas flow (L min^{-1})	0.90
Make-up gas flow (L min^{-1})	0.25
Plasma gas flow (L min^{-1})	14.0
Reaction/Collision cell	
O_2 gas flow (mL min^{-1})	0.3
Data acquisition	
m/z monitored	94 shifted from 78 for Se as $^{78}Se^{16}O^+$
	47 shifted from 31 for P as $^{31}P^{16}O^+$

Results and discussion

Synthesis and identification of selenophosphate

Chemically synthesized selenophosphate was obtained on the basis of the synthetic sequence shown in **Scheme 1.** Selenophosphate precursor **2** protected by trimethylsilyl groups was generated by the direct oxidation of **1** using elemental Se, and selenophosphate was obtained as a trisodium salt by the hydrolysis of **2** under basic condition. Each product was appropriately identified by NMR and ESI-MS measurements, as described in Materials and methods.

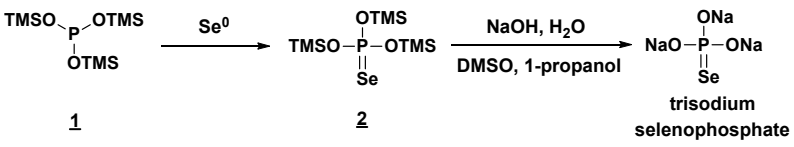

Scheme 1. Synthesis of trisodium selenophosphate.

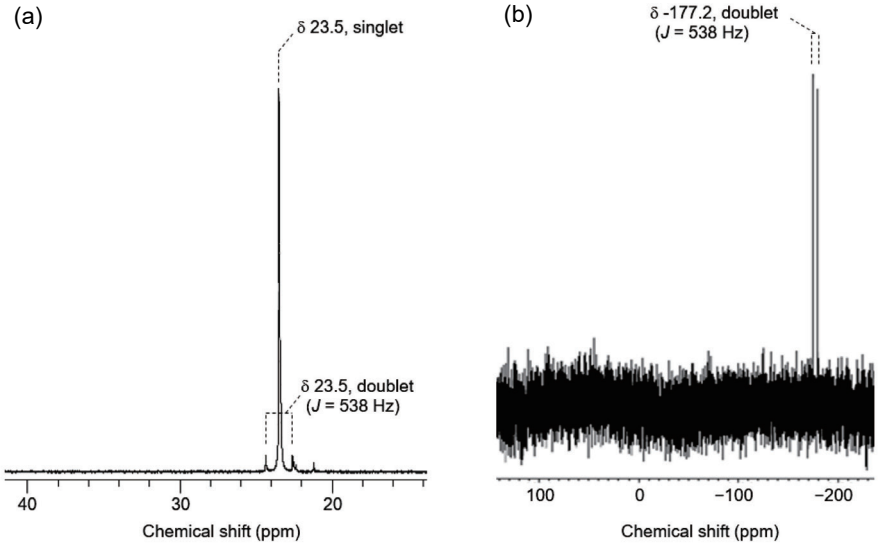

Figure 1. NMR spectra of selenophosphate in Tris-HCl buffer (100 mM, pH 7.2).
(a) ^{31}P NMR spectrum of purified trisodium selenophosphate (3 mM).
(b) ^{77}Se NMR spectrum of purified trisodium selenophosphate (200 mM).

The ^{31}P and ^{77}Se NMR spectra of chemically synthesized selenophosphate in Tris-HCl buffer are shown in **Figure 1**. The chemical shift of ^{31}P in this compound was consistent with that of the *selD* product previously reported by Stadtman's group [19]. The ^{31}P spectrum in **Figure 1(a)** contains a singlet with a relative intensity of 0.92, and a doublet with a relative intensity of 0.08 derived from the coupling with ^{77}Se nuclei. This doublet demonstrated the presence of ^{77}Se adjacent to the ^{31}P nuclei, and the relative intensity of this signal was consistent with the natural abundance of ^{77}Se (7.6%). The ^{77}Se spectrum in **Figure 1(b)** shows a doublet derived from the coupling with ^{31}P nuclei. Because the coupling constants of these doublets matched ($J_{^{31}P\text{-}^{77}Se}$ = 538 Hz), the existence of a Se=P double bond was confirmed.

Speciation of chemically synthesized selenophosphate

Chemically synthesized selenophosphate was subjected to LC-ICP-MS/MS analysis. Se and P in the chemically synthesized selenophosphate were simultaneously eluted on the GS-320HQ column at the retention time of 14.5 min, and no other Se and P peaks were detected (**Figure 2**). We have reported the retention times of many low molecular weight selenium metabolites of microorganisms, plants, and animals under the same elution conditions. However, none of the retention times of the hitherto reported selenometabolites matched the unique retention time of Se and P. Based on the peak heights, the Se/P molar ratio at the retention time of 14.5 min was 0.91 ± 0.05. Phosphate was eluted at the retention time of 14.7 min under the same conditions as those for selenophosphate (data not shown), indicating that the compound composed of Se and P at the molar ratio of approximately 1 had a similar molecular structure to phosphate according to the chromatographic behavior. Hence, we conclude that highly purified selenophosphate was successfully synthesized on the basis of LC-ICP-MS/MS data. As red elemental Se appeared in the solution

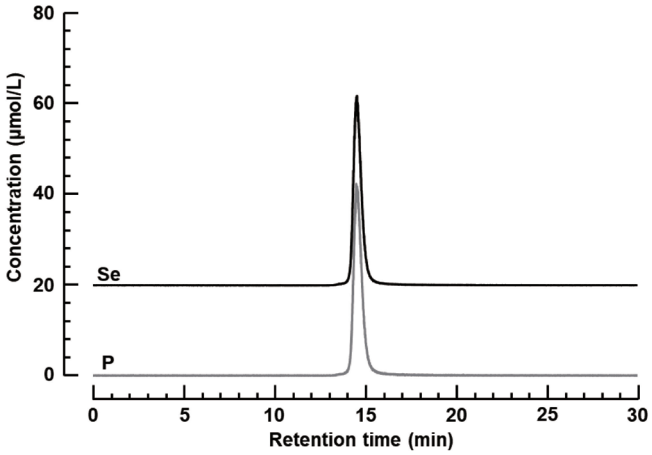

Figure 2. Elution profiles of Se and P in the solution of chemically synthesized selenophosphate. A 20-μL aliquot of the solution was injected into a GS-320HQ column, and the eluate was monitored for Se and P by ICP-MS/MS at *m/z* 94 and 47 as $^{78}Se^{16}O^{+}$ and $^{31}P^{16}O^{+}$, respectively.

of the chemically synthesized selenophosphate during 48-hr preservation, we evaluated the stability of the selenophosphate under ambient condition.

Under ambient condition for 48 hr, the peak height of selenophosphate at the retention time of 14.5 min was markedly decreased to 2.6% of the original height (**Figure 3**). In addition to the decrease in the peak height of selenophosphate, the peak at the retention time of 16.2 min was increased in the 48-hr selenophosphate solution. Selenate and selenite authentic standards were detected at the retention times of 14.0 and 16.2 min, respectively. The oxidation numbers of Se in selenophosphate, elemental Se, and selenite are -II, 0, and +IV, respectively. Hence, selenophosphate was decomposed, namely, oxidized to form elemental Se and selenite under ambient condition. These results indicated that selenophosphate was susceptible to oxidation under ambient condition, and this susceptibility seemed to contribute to its being a selenium donor in the *de novo* synthesis of selenocysteine.

In conclusion, chemically synthesized selenophosphate was subjected to detailed structural analyses by ^{31}P and ^{77}Se NMR and LC-ICP-MS/MS measurements in comparison with the reported data of the enzymatic product, and as a result, the structure of the SelD product was confirmed.

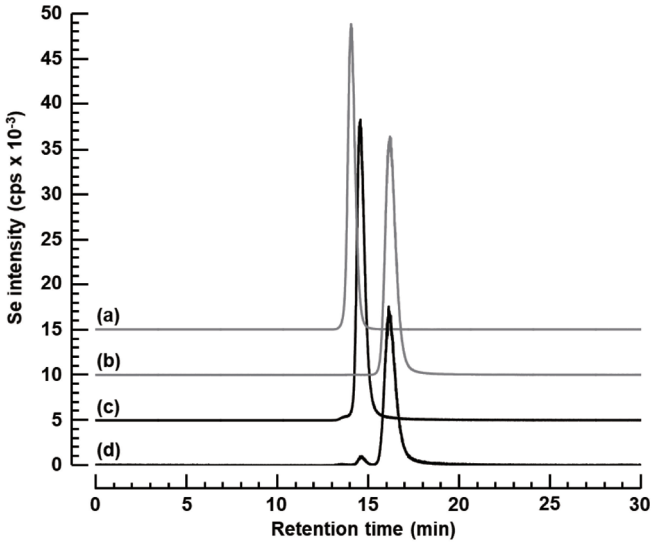

Figure 3. Elution profiles of Se in the solution of chemically synthesized selenophosphate and inorganic Se authentic standards. A 20-μL aliquot of the solution of selenate (a), selenite (b), chemically synthesized selenophosphate immediately after dissolution (c), and chemically synthesized selenophosphate 48 hr after dissolution (d), each at the concentration of 1,000 ng/mL was injected into a GS-320HQ column, and the eluate was monitored for Se by ICP-MS/MS at *m/z* 94 as $^{78}Se^{16}O^{+}$.

Acknowledgements

This study was supported by grants from JSPS KAKENHI (Grant Numbers 19H01081, 19H05772, and 21H04920).

References

[1] Reeves MA, Hoffmann PR: The human selenoproteome: recent insights into functions and regulation. Cell Mol Life Sci 66: 2457-2478, 2009.

[2] Suzuki KT, Ogra Y: Metabolic pathway for selenium in the body: speciation by HPLC-ICP MS with enriched Se. Food Addit Contam 19(10): 974-983, 2002.

[3] Whanger PD: Selenocompounds in plants and animals and their biological significance. J Am Coll Nutr 21: 223-232, 2002.

[4] Bock A, Flohe L, Kohrle J: Selenoproteins - biochemistry and clinical relevance. Biol Chem 388(10): 985-986, 2007.

[5] Burk RF, Hill KE: Selenoprotein P: an extracellular protein with unique physical characteristics and a role in selenium homeostasis. Annu Rev Nutr 25: 215-35, 2005.

[6] Lu J, Holmgren A: Selenoproteins. J Biol Chem 284: 723-727, 2009.

[7] Squires JE, Berry MJ: Eukaryotic selenoprotein synthesis: mechanistic insight incorporating new factors and new functions for old factors. IUBMB Life 60(4): 232-235, 2008.

[8] Mehta A, Rebsch CM, Kinzy SA, Fletcher JE, Copeland PR: Efficiency of mammalian selenocysteine incorporation. J Biol Chem 279(36): 37852-37859, 2004.

[9] Hatfield DL, Berry MJ, Gladyshev VN: Selenium: its molecular biology and role in human health. 2nd ed. Springer-Verlag New York Inc, New York, 2006.

[10] Hoffmann PR, Berry MJ: Selenoprotein synthesis: a unique translational mechanism used by a diverse family of proteins. Thyroid 15: 769-775, 2005.

[11] Hatfield D, Portugal FH: Seryl-tRNA in Mammalian Tissues: Chromatographic Differences in Brain and Liver and a Specific Response to the Codon, UGA. Proc Natl Acad Sci USA 67: 1200-1206, 1970.

[12] Chambers I, Frampton J, Goldfarb P, Affara N, McBain W, Harrison PR: The structure of the mouse glutathione peroxidase gene: the selenocysteine in the active site is encoded by the 'termination' codon, TGA. EMBO J 5(6): 1221-1227, 1986.

[13] Veres Z, Tsai L, Scholz TD, Politino M, Balaban RS, Stadtman TC: Synthesis of 5-methylaminomethyl-2-selenouridine in tRNAs: ^{31}P NMR studies show the labile selenium donor synthesized by the selD gene product contains selenium bonded to phosphorus. Proc Natl Acad Sci USA 89(7): 2975-2979, 1992.

[14] Veres Z, Kim IY, Scholz TD, Stadtman TC: Selenophosphate synthetase. Enzyme properties and catalytic reaction. J Biol Chem 269(14): 10597-603, 1994.

[15] Veres Z, Stadtman TC: A purified selenophosphate-dependent enzyme from Salmonella typhimurium catalyzes the replacement of sulfur in 2-thiouridine residues in tRNAs with selenium. Proc Natl Acad Sci USA 91(17): 8092-6, 1994.

[16] Leinfelder W, Forchhammer K, Veprek B, Zehelein E, Bock A: In vitro synthesis of selenocysteinyl-tRNA(UCA) from seryl-tRNA(UCA): involvement and characterization of the selD gene product. Proc Natl Acad Sci USA 87(2): 543-547, 1990.

[17] Mizutani T, Kanaya K, Tanabe K: Selenophosphate as a substrate for mammalian selenocysteine synthase, its stability and toxicity. Biofactors 9(1): 27-36, 1999.

[18] Ehrenreich A, Forchhammer K, Tormay P, Veprek B, Bock A: Selenoprotein synthesis in E. coli. Purification and characterisation of the enzyme catalysing selenium activation. Eur J Biochem 206(3): 767-73, 1992.

[19] Kim IY, Veres Z, Stadtman TC: Escherichia coli mutant SELD enzymes. The cysteine 17 residue is essential for selenophosphate formation from ATP and selenide. J Biol Chem 267(27): 19650-19654, 1992.

[20] Kim IY, Stadtman TC: Selenophosphate synthetase: detection in extracts of rat tissues by immunoblot assay and partial purification of the enzyme from the archaean *Methanococcus vannielii.* Proc Natl Acad Sci USA 92(17): 7710-7713, 1995.

[21] Połatajko A, Jakubowski N, Szpunar J: State of the art report of selenium speciation in biological samples. J Anal At Spectrom 21: 639-654, 2006.

[22] Suzuki N, Ogra Y: ^{77}Se NMR spectroscopy for speciation analysis of selenium compounds. Ogra Y, Hirata T (ed): Metallomecs. Springer, Berlin, 2017, 147-155.

[23] Silva MS, Alves D, Hartwig D, Jacob RG, Perin G, Lenardão EJ: Selenium-NMR spectroscopy in organic synthesis: From structural characterization toward new investigations. Asian J Org Chem 10: 91-128, 2021.

Regular article https://metallomicsresearch.brte.org

Effect of Phytic Acid Administration on the Zinc concentration, Uric Acid Biosynthesis, and Serum Lipid Components in Rats

Ziwen Jin, Ryota Hosomi, Kenji Fukunaga, Munehiro Yoshida*

Laboratory of Food and Nutritional Sciences, Faculty of Chemistry, Materials and Bioengineering, Kansai University

Summary

The effects of phytic acid on the absorption of several minerals including zinc, iron, copper, calcium, magnesium, manganese and molybdenum, the biosynthesis of uric acid, and the serum lipid components were examined. Weaning male Wistar rats were fed a basal AIN93G diet or the basal diet supplemented with 0.5% or 1.0% sodium phytate for 4 weeks. Phytic acid administration reduced the serum and femur zinc levels in a dose-dependent manner but did not affect the liver and kidney zinc levels. In addition, significant reductions with phytic acid administration were observed in the liver iron, serum and liver copper, liver and kidney calcium, kidney magnesium, and liver and kidney manganese concentrations. In phytic-acid-administered rats, the molybdenum concentration and xanthine oxidase activity in the liver and the serum uric acid decreased in a dose-dependent manner. In addition, phytic acid administration also reduced the serum lipid components including triacylglycerol and total cholesterol. Since phytic acid is hardly absorbed, these results indicate that phytic acid inhibits the absorption of several dietary components including minerals, and that the decrease in the serum uric acid concentration that occurs when phytic acid is ingested is due to the decrease in molybdenum absorption. When utilizing the functionality of phytic acid for health promotion, it is necessary to pay sufficient attention to the intake of minerals.

Key words: phytic acid, zinc, uric acid, molybdenum, xanthine oxidase, serum lipid components

Statements about COI: The authors have no conflicts of interest directly relevant to the content of this article.

*Correspondence:
Yamate 3-3-35, Suita, Osaka 564-8680, Japan
Tel: 81-6-6368-0970 (cell phone number: +81-90-9990-1853)
E-mail: hanmyou4@kansai-u.ac.jp

Received: August 11, 2021
Accepted: September 29, 2021
Released online: October 15, 2021

Introduction

Phytic acid (inositol hexaphosphate) is a major phosphorus storage form present in plant tissues, such as seeds, and is often present as phytin, which is a mixed salt of calcium and magnesium [1]. Therefore, a high intake of beans and unrefined grains leads to a high intake of phytic acid. Phytic acid strongly chelates to many metal ions, which may inhibit their intestinal absorption [2]. In particular, it was believed that a large intake of phytic acid causes zinc deficiency, as Egyptian boys who had growth inhibition due to zinc deficiency ate whole grain breads

high in phytic acid on a daily basis [3]. However, zinc deficiency caused by phytic acid occurs only in the case of insufficient zinc intake, and it is not necessary to worry about zinc deficiency associated with phytic acid when the zinc intake is sufficient [4].

In recent years, there have been increasing reports that phytic acid intake has a positive effect on maintaining good health [5]. Epidemiological studies and animal experiments have shown that phytic acid is effective in preventing neurodegenerative diseases [6], renal stones [7], several types of cancer [8-10], and fatty liver [11]. Furthermore, it has been reported that phytic acid lowers the serum uric acid concentration [12, 13].

Thus, phytic acid is now expected to be a functional ingredient that has a positive effect on health, rather than an antitrophic factor that inhibits mineral absorption. However, many studies examining the effects of phytic acid intake are one-sided, and few examine both positive and unfavorable effects at the same time. In this study, in order to re-evaluate the health effects of phytic acid, phytic acid was administered to rats, and the effects on the concentrations of several minerals including zinc, as well as the serum uric acid and lipid components were examined at the same time. In addition, the effects of phytic acid administration on the liver xanthine oxidase (XOX) activity involved in the production of uric acid [14] and the concentration of molybdenum, which is an essential component of XOX [15], were also investigated.

Materials and methods

Animal feeding

The experimental protocol followed the Guide for the Care and Use of Experimental Animals issued by the Prime Minister's Office of Japan and was reviewed and approved by the Animal Ethics Committee of Kansai University (Approval No. 2005).

Eighteen 4-week-old male Wistar rats (SHIMIZU Laboratory Supplies Co., Kyoto) were divided into 3 groups. One group (control group) was fed a basal AIN93G diet [16], and the other two groups (0.5PA group and 1.0PA group) were fed the basal diet containing 0.5 or 1.0% sodium phytate (Sigma-Aldrich, St. Louis), respectively. Sodium chloride was added to the diets of the control group and the 0.5PA group in order to equalize the sodium intake of each group. During the feeding period, the animals ingested the diets and water (tap water) *ad libitum*. After feeding for 4 weeks, the liver, kidney, femur, and blood were collected under isoflurane (Fujifilm Wako Pure Chemical Co., Tokyo) anesthesia. The blood was centrifuged at 1500 x g for 15 minutes to obtain the serum. The livers, kidneys and femurs were frozen in liquid nitrogen and stored at −30°C until analysis.

Analysis

Analysis of metals. Approximately 1 g of liver, kidney, and femur were heated with 5 mL of nitric acid until there were no solids. The obtained solution was filtered through a 0.45 μm filter, and the concentrations of zinc, iron, copper, manganese, molybdenum, calcium, and magnesium were determined using an atomic absorption spectrophotometer (AA-7000, Shimadzu, Kyoto) or an inductively coupled plasma mass spectrometer (ICPMS-2030, Shimadzu, Kyoto). In the analysis with ICPMS, ^{45}scandium was used as an internal standard. The serum zinc and copper levels were measured using a commercial kit (Metalloassay LS, Metallogenics Co., Chiba).

Assay of hepatic xanthine oxidase (XOX) activity. About 1 g of liver was homogenized with 9 mL of saline. The homogenate was centrifuged at 8000 x g for 20 minutes and the XOX activity in the supernatant was measured as follows [17]. To 200 μL of the homogenate, 800 μL of 0.5 mM xanthine solution and 3 mL of 0.1 M Tris-HCl buffer (pH 7.4) were added, and the mixture was incubated for 20 minutes at 37°C. After the incubation, 1 mL of 30% perchloric acid was added and centrifuged, and the uric acid contained in the supernatant was determined by high performance liquid chromatography (HPLC). The condition of HPLC was as follows: equipment, LC-20Ai (Shimadzu, Kyoto); column, Develosil ODS-HG (4.6 mm φ x 250 mm, Nomura Kagaku, Seto); mobile phase, 20 mM sodium phosphate buffer (pH 3.0)/acetonitrile=99/1 (v/v); column oven, 30°C; flow rate: 1.0 mL/minute; detection, absorbance at 292 nm (SPD-20A, Shimadzu, Kyoto). The activity of XOX that produces 1 μmol of uric acid per minute was defined as 1 unit. Protein in the supernatant of the liver homogenate was determined by Lowry's method [18].

Determination of serum components. The serum calcium, magnesium, iron, uric acid, triacyl glycerol (TAG), total lipid (TL), total cholesterol (TCHOL) and HDL-cholesterol (HDL-CHOL) concentrations were measured with an automatic biochemistry

analyzer (Olympus AU5431; Olympus Co., Tokyo) by Japan Medical Laboratory Co. (Kaizuka).

Statistics

For each measurement, the differences among the groups were tested by one-way ANOVA followed by Tukey-Kramer's multiple comparison test. GraphPad Prism 7.0 (GraphPad Software, Inc., San Diego) was used as the statistical analysis application.

Results

There was no difference in growth among the experimental groups, and the body weight (mean ± SEM) after the end of the feeding period was 287 ± 7 in the control group, 253 ± 18 in the 0.5PA group, and 282 ± 13 g in the 1.0PA group.

Table 1 shows the zinc concentrations in the serum and organs of each experimental group. There was no difference in the zinc concentrations in the liver and kidney among the experimental groups, but the zinc concentrations in the serum and femur were significantly lower in the two groups administered phytic acid than in the control group. Increased phytic acid doses tended to lower the serum and femoral zinc levels.

Table 2 summarizes the concentrations of several metals in the serum, liver, and kidney. As with zinc, the concentration of some metals was reduced by phytic acid administration. Significant reductions with phytic acid administration were observed in the liver iron, serum and liver copper, liver and kidney calcium, kidney magnesium, and liver and kidney manganese concentrations.

Figure 1 shows the serum uric acid concentration, liver XOX activity, and molybdenum concentration. All of these three parameters were significantly lower in a dose-dependent manner after the administration of phytic acid.

Table 3 summarizes the concentrations of the serum lipid components (TAG, TL, TCHOL, HDL-CHOL) in each group. Phytic acid administration significantly reduced the values for all the measured components. However, unlike the serum and femoral zinc or serum uric acid, no further decrease was observed when the dose of phytic acid was increased.

Discussion

Since phytic acid is abundant in unrefined grains and legumes, its intake level varies depending on the content of the dish. In a recent review, phytic acid intake is roughly divided into three types according to eating habits [1]: (i) general Western-style diets low in phytate rich plant foods results in a low intake level of 200 to 350 mg/d, (ii) Western-style diets with enhanced portions of whole grain products or other phytate rich foods results in a higher intake level of 500 to 800 mg/d, and (iii) diets dominated by legumes and unrefined grains such as vegetarian diets or some diets in developing countries in Asia, Africa, and Latin America result in a high intake level of >1000 mg/d. The diets eaten by Egyptian boys with zinc deficiency [3] would fall into this category (iii). In some developing countries corresponding to category (iii), phytic acid intakes in excess of 2000 mg/d have been reported [19-22]. Regarding East Asia, where the Westernization of eating habits is progressing, the daily phytate intake for adult males (21–70 years) was 839 ± 400 mg and for females 752 ± 407 mg in the Republic of Korea [23]. However, phytic-acid-enriched foods and supplements are designed for phytic acid intakes of more than 500 mg/d [12]. Therefore, even in East Asia including Japan, where Westernization is progressing, it can be estimated that there are cases where the phytic acid intake falls into category (iii) due to the intake of phytic-acid-enriched foods. Since the amount of human diet is 400 to 500 g/d by dry weight, the phytic acid dose in this experiment corresponds to 2000 to 5000 mg/d; that is, it corresponds to the phytic acid intake of category (iii).

In this experiment, the serum and femur zinc levels were significantly reduced in rats fed diets supplemented with phytic acid (**Table 1**). This strongly suggests that phytic acid inhibited the absorption of zinc. However, the zinc concentration in the liver and kidney did not change even after the administration of phytic acid, and a decrease in food intake and growth inhibition associated with zinc deficiency did not occur. That is, phytic acid did inhibit zinc absorption, but did not cause a serious deficiency. This is probably because the AIN93G used as the basal diet contains 30 μg/g of zinc, which is sufficient for growth.

The concentrations of some minerals other than zinc in serum and organs also decreased (**Table 2**), and it can be inferred that phytic acid also inhibited the absorption of minerals other than zinc. Similarly to zinc, reduced absorption of these minerals did not lead to the manifestation of a severe deficiency. For example, in the case of iron, administration of phytic acid decreased the iron concentration in the liver, but did not decrease the hemoglobin concentration or the transferrin saturation rate of serum (data not shown). That is, because the iron concentration in the basal AIN93G diet was sufficiently high, the decrease of iron absorption by phytic acid did not lead to the development of iron deficiency.

Table 1. | Effect of phytic acid administration on the zinc concentration in experimental animals

	Zinc concentration		
	Control	**0.5PA**	**1.0PA**
Serum (μg/mL)	2.94 ± 0.20^{b}	2.38 ± 0.10^{a}	2.20 ± 0.05^{a}
Liver (μg/g)	22.9 ± 0.7^{a}	23.7 ± 1.0^{a}	24.8 ± 0.5^{a}
Kidney (μg/g)	24.7 ± 0.6^{a}	24.6 ± 0.4^{a}	23.0 ± 0.6^{a}
Femur (μg/g)	109.2 ± 6.1^{b}	82.8 ± 7.6^{ab}	60.5 ± 8.1^{a}

Values are means ± SEM (n=6).
[a,b)] Means in the same row not sharing a common superscript differ significantly ($p < 0.05$)

Table 2. | Effect of phytic acid administration on several metal concentrations in the serum, liver, and kidney

	Control	**0.5PA**	**1.0PA**
Iron			
Serum (μg/mL)	2.93 ± 0.21^{a}	2.74 ± 0.16^{a}	2.51 ± 0.13^{a}
Liver (μg/g)	76.1 ± 4.5^{b}	58.4 ± 5.2^{a}	60.5 ± 3.5^{ab}
Kidney (μg/g)	46.9 ± 1.3^{a}	45.2 ± 1.2^{a}	42.5 ± 1.1^{a}
Copper			
Serum (μg/mL)	2.34 ± 0.26^{b}	1.56 ± 0.10^{a}	1.87 ± 0.05^{a}
Liver (μg/g)	3.35 ± 0.11^{ab}	3.52 ± 0.13^{b}	3.08 ± 0.08^{a}
Kidney (μg/g)	8.62 ± 0.67^{a}	7.66 ± 0.21^{a}	7.93 ± 0.97^{a}
Calcium			
Serum (μg/mL)	107 ± 2^{a}	106 ± 2^{a}	109 ± 2^{a}
Liver (μg/g)	53.4 ± 2.5^{b}	46.1 ± 2.1^{ab}	38.8 ± 1.2^{a}
Kidney (μg/g)	61.1 ± 0.3^{b}	59.6 ± 2.5^{ab}	52.3 ± 2.8^{a}
Magnesium			
Serum (μg/mL)	18.9 ± 0.5^{a}	18.3 ± 0.2^{a}	18.3 ± 0.4^{a}
Liver (μg/g)	267 ± 7^{a}	247 ± 7^{a}	244 ± 7^{a}
Kidney (μg/g)	201 ± 2^{b}	199 ± 2^{b}	166 ± 2^{a}
Manganese			
Liver (μg/g)	2.36 ± 0.08^{b}	1.97 ± 0.06^{a}	1.74 ± 0.08^{a}
Kidney (μg/g)	0.76 ± 0.01^{b}	0.84 ± 0.02^{b}	0.59 ± 0.01^{a}

Values are means ± SEM (n=6).
[a,b)] Means in the same row not sharing a common superscript differ significantly ($p < 0.05$)

Table 3. | Effect of phytic acid administration on serum lipid components

Components	**Control**	**0.5PA**	**1.0PA**
TAG (mg/dL)	71 ± 12^{b}	42 ± 6^{a}	54 ± 2^{ab}
TL (mg/dL)	305 ± 19^{b}	226 ± 8^{a}	252 ± 7^{a}
TCHOL (mg/dL)	86 ± 6^{b}	71 ± 4^{a}	74 ± 5^{a}
HDL-CHOL (mg/dL)	56 ± 3^{b}	47 ± 1^{a}	45 ± 2^{a}

Values are means ± SEM (n=6).
[a,b)] Means in the same row not sharing a common superscript differ significantly ($p < 0.05$)

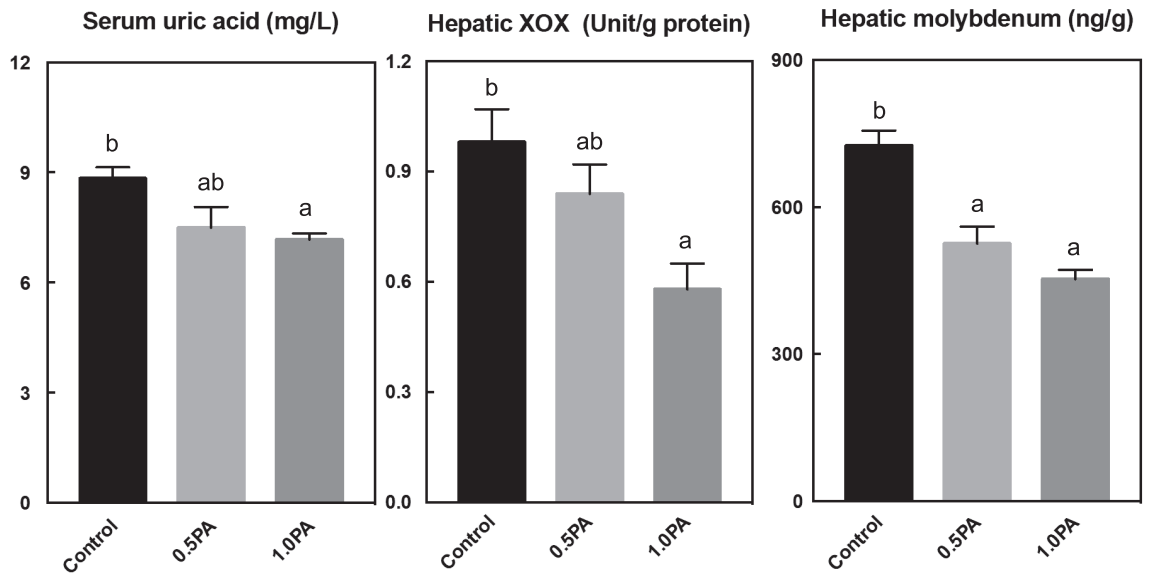

Figure 1. Effect of phytic acid administration on the serum uric acid concentration, hepatic XOX activity, and hepatic molybdenum concentration

Heights of the bars and vertical lines indicate means and SEM (n=6), respectively.

[a,b] Heights of bars in the same frame not sharing a common superscript differ significantly ($p < 0.05$)

It has been reported that the intake of phytic acid reduces serum uric acid in humans [12, 13]. In the present study as well, it was confirmed that the serum uric acid concentration was decreased in the rats to which phytic acid was administered (**Fig. 1**). For the decrease in serum uric acid caused by phytic acid, a mechanism has been proposed in which the intestinal absorption of a purine base that is the source of the serum uric acid is reduced because phytic acid inhibits the conversion of nucleic acids in the diet to purine bases [24]. However, in the present study, rats were fed a nucleic-acid-free diet. Therefore, the decrease in the serum uric acid concentration cannot be explained by the decrease in the amount of purine base absorbed. It has been reported that phytic acid itself inhibits the XOX activity involved in uric acid production [25], but since phytic acid is hardly absorbed, it is unlikely that it will reach a concentration that inhibits the XOX activity in the liver.

We measured the liver XOX activity and molybdenum concentration, and found that both decreased depending on the dose of phytic acid (**Fig. 1**). Since molybdenum has a strong affinity for phosphate [26], it is quite possible that the phosphate group of phytic acid binds to molybdenum in the intestinal tract in phytic-acid-administered rats, and the absorption of molybdenum is reduced. It is considered that as a result of phytic acid inhibiting molybdenum absorption, the biosynthesis of XOX, which is a molybdenum-containing enzyme, decreased, and the production of uric acid decreased. In this regard, we have observed that a decrease in the liver molybdenum concentration leads to a decrease in the XOX activity in rats administered tungsten, which antagonizes molybdenum *in vivo* [27].

Administration of phytic acid reduced the serum lipid components in addition to serum uric acid (**Table 3**). The mechanism by which phytic acid lowers the serum lipid content is unknown. In the small intestine of monogastric animals, phytic acid forms an insoluble complex with divalent or trivalent cations, and its phosphate ester is not hydrolyzed, so that neither the inositol moiety nor the phosphate is absorbed [28, 29]. In fact, in this experiment, no change was observed in the serum inorganic phosphate concentration of the rats to which phytic acid was administered (data not shown), and it can be estimated that there was almost no release of phosphate from phytic acid. Thus, since phytic acid is hardly absorbed, it is most likely that phytic acid interfered with the absorption of several dietary components including lipids and carbohydrates in the gastrointestinal tract. If so, phytic acid also inhibits the absorption of dietary components other than minerals.

If many of the functions of phytic acid depend on the inhibition of absorption of dietary components in the gastrointestinal tract, phytic acid has a positive effect on people who are overeating. However, on the contrary, it can be said that it has an unfavorable effect on people who have an insufficient intake of nutritional components such as minerals. When considering the function of phytic acid, it is important to fully understand the dietary intake status of each individual.

Soluble sodium phytate was used in this experiment. It is necessary to investigate whether the same result can be obtained by using calcium phytate, which is insoluble in water.

References

[1] Schlemmer U, Frølich W, Prieto RM, Grases F: Phytate in foods and significance for humans: food sources, intake, processing, bioavailability, protective role and analysis. Mol Nutr Food Res 53: S330-375, 2009.

[2] Gibson RS, Bailey KB, Gibbs M, Ferguson EL: A review of phytate, iron, zinc, and calcium concentrations in plant-based complementary foods used in low-income countries and implications for bioavailability. Food Nutr Bull 31: S134-146, 2010.

[3] Prasad AS. Deficiency of zinc in man and its toxicity. Prasad AS (ed): Trace elements in human health and disease (vol I, Zinc and copper). Academic Press, New York, 1976, 1-20.

[4] Forbes RM, Parker HM, Erdman JW: Effects of dietary phytate, calcium and magnesium levels on zinc bioavailability to rats. J Nutr 114: 1421-1425, 1984.

[5] Silva EO, Bracarense APFRL: Phytic acid: From antinutritional to multiple protection factor of organic systems. J Food Sci 81: R1357-1362, 2016.

[6] Anekonda TS, Wadsworth TL, Sabin R, Frahler K, Harris C, Petriko B, Ralle M, Woltjer R, Quinn JF: Phytic acid as a potential treatment for Alzheimer's pathology: evidence from animal and in vitro models. J Alzheimer's Dis 23: 21-35, 2011.

[7] Grases F, Garcia-Ferragut L, Costa-Bauzá A, March JG: Study of the effects of different substances on the early stages of papillary stone formation. Nephron 73: 561-568. 1996.

[8] Shamsuddin AM, Yang GY: Inositol hexaphosphate inhibits growth, and induces differentiation of PC-3 human prostate cancer cells. Carcinog 16: 1975-1979, 1995.

[9] Somasuddar P, Riggs DR, Jackson BJ, Cunningham C, Vona-Davis L, McFadden DW: Inositol hexaphosphate (IP6): a novel treatment for pancreatic cancer. J Surg Res 126: 199-203, 2005.

[10] Schroterová L, Haková P, Rudolf E, Cervinka M: Effect of phytic acid and inositol on the proliferation and apoptosis of cells derived from colorectal carcinoma. Oncol Rep 23: 787-789, 2010.

[11] Katayama T: Hypolipidemic action of phytic acid (IP6): prevention of fatty liver. Anticancer Res 19: 3695-3698, 1999.

[12] Ikenaga T, Kakumoto K, Kohda N, Yamamoto T: Effect of inositol hexaphosphate (IP6) on serum uric acid in hyperuricemic subjects: a randomized, double-blind, placebo-controlled, crossover study. Plant Foods Hum Nutr 74: 316-321, 2019.

[13] Ikenaga T, Noguchi H, Kakumoto K, Kohda N, Tsukikawa H, Matsuguma K, Yamamoto T: Effect of phytic acid on postprandial serum uric acid level in healthy volunteers: a randomized, double-blind, crossover study. Nucleosides Nucleotides Nucleic Acids 39: 504-517, 2020.

[14] Watts RW: Uric acid production with particular reference to the role of xanthine oxidase and its inhibition. Proc R Soc Med 59: 287-292, 1966.

[15] Rajagopalan KV: Molybdenum: an essential trace element in human nutrition. Annu Rev Nutr 8: 401-427, 1988.

[16] Reeves PG, Nielsen FH, Fahey GC Jr: AIN-93 purified diets for laboratory rodents: final report of the American Institute of Nutrition ad hoc writing committee on the reformulation of the AIN-76A rodent diet. J Nutr 123: 1939-1951, 1993.

[17] Yoshihara K, Fukunaga K, Yoshida M: Effect of dietary molybdenum level on tissue and serum molybdenum concentrations in rats. Trace Nutr Res 24: 120-123, 2007.

[18] Lowry OH, Rosebrough NJ, Farr AL, Randall RJ: Protein measurement with the Folin phenol reagent. J Biol Chem 193: 265-275, 1951.

[19] Harland BF, Oke OL, Felix-Philips R: Preliminary studies on the phytate content of Nigerian foods. J Food Compos Anal 1: 202-205, 1988.

[20] Fitzgerald SL, Gibson RS, Serrano JQ, Portocarrero L, Vasquez A, Zepeda E, Lopez-Palacios CY, Thompson LU, Stephen AM, Solomons NW: Trace-element intakes and dietary phytate/Zn and Ca x phytate/Zn millimolar ratios of periurban Gatemalan women during the 3rd trimester of pregnancy. Am J Clin Nutr 57: 195-201, 1993.

[21] Khokhar S, Pushpanjali A, Fenwick GR; Phytate content in Indian foods and intakes by vegetarian Indians of Hissar region, Haryana state. J Agric Food Chem 42: 2440-2444, 1994.

[22] Murphy SP, Calloway DH, Beaton GH: Schoolchildren have similar predicted prevalences of inadequate intakes as toddlers in village populations in Egypt, Kenya, and Mexico. Eur J Clin Nutr 49: 647-657, 1995.

[23] Lee J, Shim E, Paik Y: Bioavailable zinc intake of Korean adults in relation to the phytate content of Korean foods. J Food Compos Anal 17: 713-724, 2004.

[24] Ikenaga T, Noguchi H, Ishiyama T, Ishida H, Kakumoto K, Kohda N, Sugimura H, Yamamoto T: Effect of soymilk fermented with lactic acid bacteria on postprandial serumuric acid level and its active ingredients. Jpn Pharmacol Ther 47: 637–645, 2019.

[25] Muraoka S, Miura T: Inhibition of xanthine oxidase by phytic acid and its antioxidative action. Life Sci 74: 1691-1700, 2004.

[26] Adams F. Interaction of phosphorus with other elements in soil and plants. Khasawneh FE, Sample EC, Kamprath EJ (eds): The role of phosphorus in agriculture. Soil Science Society of America, Madison, 1981, 665-680.

[27] Yoshida M, Nakagawa M, Hosomi R, Nishiyama T, Fukunaga K: Low molybdenum state induced by tungsten as a model of molybdenum deficiency in rats. Biol Trace Elem Res 165: 75-80. 2015.

[28] Cheryan M: Phytic acid interactions in food systems. Crit Rev Food Sci Nutr 13: 297-335, 1980.

[29] NR Reddy, SK Sathe, DK Salunkhe: Phytates in legumes and cereals. Adv Food Res 28:1-92,1982.

Regular article https://metallomicsresearch.brte.org

Quantitative imaging analysis of nanoparticles and dissolved forms using laser ablation-single particle-ICP-mass spectrometry

Shuji Yamashita[1], Kumiko Ogawa[2], Takafumi Hirata[1*]

[1] Geochemical Research Centre, The University of Tokyo, 7-3-1 Hongo, Bunkyo-ku, Tokyo 113-0033, Japan
[2] Division of Pathology, National Institute of Health Sciences,3-25-26 Tonomachi, Kawasaki-ku, Kawasaki, Kanagawa 210-9501, Japan

Summary

Laser ablation-single particle-ICP-mass spectrometry (LA-spICP-MS) was applied to define the size, position of silver nanoparticles (Ag NPs), and the concentration of ionic Ag (dissolved Ag) on a frozen section of mouse liver (6 hours after intraperitoneal administered 60 nm Ag NPs (0.2 mg per mouse)). For the accurate size calibration of Ag NPs and quantitative analysis of ionic Ag, a cellulose filter paper doped with Ag NPs suspension and a custom-made photocurable resin reference material containing ionic Ag were prepared in this study. From the imaging results of liver sample, preferential accumulation of the Ag NPs in certain regions was observed. Ionic Ag was also accumulated at regions where Ag NPs are. This suggests that there is a possible contribution of dissolution of Ag NPs through cell activity. This is supported by the detection of small Ag NPs (8–20 nm). The simultaneous imaging analyses of both Ag NPs and ionic Ag can become a useful tool to understand the mechanism of incorporation or metabolism of the NPs.

Key words: nanoparticle, imaging analysis, quantitative analysis, laser ablation, single particle-inductively coupled plasma-mass spectrometry

Statements about COI: The authors declare no conflict of interest associated with this manuscript.

Introduction

Various inorganic nanoparticles (NPs) are widely used in many research fields such as biochemical, material, and environmental sciences[1-3]. Among inorganic NPs, silver NPs (Ag NPs) are the major NPs found in cosmetics, deodorizer, electronic devices, and medicine[4-6]. In addition, Ag, either in ionic or particulate form, are well-known to exhibit strong antimicrobial activity[7,8]. Despite Ag NPs having remarkable physicochemical or biochemical features, these NPs can potentially bring risks to both human health and the environment[9].

Many biochemists are increasingly interested in the mechanism of toxicity of the NPs: how the NPs interact with cells, or what is the critical size of NPs that contribute to cytotoxicity. Smaller sized NPs can pass through the cell membrane[10]. and it is widely believed that reactivities with cellular components such as nucleic acids, proteins, and fatty acids would increase in the small NPs due to their larger surface area. Recently, Cho *et al.*

*Correspondence:
Geochemical Research Centre, The University of Tokyo, 7-3-1 Hongo, Bunkyo-ku, Tokyo 113-0033, Japan
Tel: +81 3 5841 4621
E-mail: E-mail: hrt1@eqchem.s.u-tokyo.ac.jp

Received: August 31, 2021
Accepted: November 18, 2021
Released online: January 6, 2022

evaluated the size-dependent toxicity of Ag NPs through intraperitoneal administration of Ag NPs of varying sizes (10, 60, and 100 nm) into BALB/c mice [11]. For the mice which were administered with 10 nm Ag NPs, a reduction in activity was observed, and histopathological changes such as congestion, vacuolation, single cell necrosis, and focal necrosis in the liver were also found. The size and the distribution of Ag NPs within the sample, can control the toxicity of the Ag NPs. To unveil the biological effects of the NPs, and also to investigate the mechanism of the removal of the NPs (*i.e.,* fate of the incorporated NPs), sensitive analytical techniques for imaging of both the elements and NPs are highly desired.

For the evaluation of toxicity and transport mechanisms of NPs, many analytical techniques such as optical and dark-field microscopy[12], scanning electron microscopy (SEM)[13], surface-enhanced Raman scattering (SERS)[14], and photothermal microscopy[15] have been widely used. For the elucidation of distribution of NPs, many analytical techniques including atomic force microscopy (AFM) or secondary ion mass spectrometry (SIMS) have been adopted[16]. However, these analytical techniques are not capable for quantitative imaging of both elements and NPs from biological tissue samples.

Recently, laser ablation-ICP-mass spectrometry (LA-ICP-MS) is described as a fast, sensitive, and quantitative analytical tool for in-situ elemental analysis or elemental imaging[17,18]. With the LA-ICP-MS, visualization of elemental distributions with spatial resolution in the μm-range can be achieved from biological tissues being >1 mm. Moreover, LA-ICP-MS technique offers reliable quantitative data by using matrix-matched standard materials[19-21]. In recent years, ICP-MS technique designed for detection of single nanoparticle (single particle-ICP-MS: spICP-MS) technique is developed. With the spICP-MS technique, various information on the size, number concentrations, and elemental composition of the NPs can be derived[22,23]. By combining the spICP-MS technique and laser ablation sampling technique, rapid and sensitive imaging of NPs in solid samples can be made. Recent studies have demonstrated that the LA-spICP-MS has great potential for size and distribution analysis of NPs as well as imaging analysis of ionic form in biomaterials[24-26].

This study focuses on the establishment of an analytical methodology using the LA-spICP-MS for simultaneous determinations of (a) size of NPs, (b) concentrations of ionic form (dissolved form), and (c) distributions of NPs and ionic form in biological samples. To do this, the spatial distributions of Ag (NPs and ions) in frozen liver sections collected from a mouse was investigated using the LA-spICP-MS. For accurate calibrations of the size of Ag NPs, a cellulose filter paper, which mimics the matrix of biological tissue samples, containing size-calibrated Ag NPs were used. Moreover, for the determination of Ag concentration, a custom-made photocurable resin reference material containing ionic Ag was used. To evaluate the reliability of the resulting Ag concentration, the Ag concentration was separately measured by solution-based ICP-MS technique after the sample decomposition and dissolution procedures.

Experimental section

Preparation of tissue samples

Our previous study focused on the toxicity of Ag NPs on seven-week-old female BALB/c mice (body weight: 16.3–20.2 g) [11]. Details of the preparation of the tissue sample are as follows: citrate-coated Ag NPs of 60 nm (59.8 ± 6.2 nm) in diameter purchased from NanoComposix (San Diego, CA, USA) were used. 0.2 mg of the 60 nm Ag NPs were intraperitoneally injected in the mice. The mice were then anesthetized with isoflurane (Mylan Inc., Tokyo, Japan) 6 hours after administration. A liver sample from one mouse was resected and subjected to analysis. The total Ag concentration of part of its liver was measured by solution-based ICP-MS. The resulting Ag concentration of the liver sample for this analysis was 35.8 $\mu g\ g^{-1}$[11].

The collected livers were stored at −80°C. The frozen liver sample was embedded in optimal cutting temperature compound, and was sliced into 10-μm-thick sections with a cryotome (Leica Microsystems, Wetzlar, Germany), and then placed on glass slides. No staining procedures were made on the analyzing sliced samples. There was an interval between the preparation of the sliced samples and the time of imaging analysis.

The major problem associated with the present LA-spICP-MS instrument is that the technique is not sensitive enough to monitor the size of the Ag NPs being diameters <10 nm. To demonstrate the capability of the size analysis of the LA-spICP-MS technique, we focused the size and mapping analyses of 60 nm Ag NPs in the mouse liver tissues. Moreover, from the previous study, dark brown pigmentation in the thoracic lymph nodes was confirmed at 6 hours in the 60 nm administration group, suggesting that Ag NPs are in the lymphatic flow and bloodstream[11]. From this result, the mice administered with 60 nm Ag NPs after 6 hours was used for imaging analysis.

Imaging analysis of the frozen section of mouse liver

Simultaneous imaging analysis of both the Ag NPs and ionic Ag was carried out by the LA-spICP-MS technique. The ICP-MS instrument used in this study was a magnetic sector-based ICP-MS (AttoM, Nu Instruments, Wrexam, UK). Neither isobaric nor polyatomic interferences were found on $^{107}Ag^{+}$ signals (*m/z* of 107 u), mass resolving power of about 300 was used throughout the study to maximize the instrument sensitivity. Ag ions were detected by a pulse counting mode with an attenuator system. The attenuator system which can attenuate the ion flux down to about 1/500 level by passing through the platinum grid. This was done to ensure the ion beam with count rates of 50 Mcps is reduced to 100 kcps, obviating the risk of erroneous measurements due to the counting loss of analyte ions[27]. Switching on/off the attenuator device is made automatically within 1 ms, and thus, detection of ion beam with wider dynamic range covering 8 orders of magnitude (*i.e.,* from 1 to 10^8 cps) is achieved by the present system setup. The attenuator system is very important to extend the range of size analysis of NPs[28].

For the laser ablation, a Nd:YAG laser (FQSS-266Q, CryLas, Berlin, Germany) operating at UV wavelength (266 nm) with a pulse duration of 1 ns was employed. The laser operating conditions were set to fluence of 0.4 J cm^{-2}, repetition rate of 1 kHz, and ablation pit size of 4 μm. Imaging analysis was made based on the repeated line profiling analysis with scanning speed of 2 μm s^{-1} and 0 μm for the distance between the lines. In this study, a low laser fluence (*i.e.,* <1 J cm^{-2}) was adopted because of smaller contribution of the disintegration of NPs[25,29,30]. The laser induced sample aerosols were transported into the ICP with a mixed flow of He and Ar gases (He flow rate: 0.7 L min^{-1}, Ar flow rate: 0.85 L min^{-1}).

The instrument was operated in time resolved analysis mode of an output signal intensity (cps) versus time. The duration time for each line was set at 50 s, with a dwell time of 50 μs per reading. The signal intensity data obtained by the spICP-MS system were stored in the csv format. The resulting time-dependent signal intensity profiles were converted to the position-dependent signal intensity data based on the elapsed time and the raster rate, and then, the distributions of NPs and ionic form were visualized using in-house imaging software "iQuantNP"[24].

Separation of signals from NPs and ionic forms

For the separation of signals originating from Ag NPs and signals from ionic Ag, discrimination level (threshold) was defined. Threshold of $\mu + n\sigma$ (μ: mean of the whole dataset, n: an integer multiple times (3 or 5), and σ: standard deviation) was used[23,31]. For the imaging analysis, however, this approach cannot be applied because the contents of Ag can vary largely within the samples. Recently, Metarapi *et al.* reported guidelines for analysis of NPs using LA-spICP-MS by processing the computational data via an "outlier" filter to differentiate between metal NPs and dissolved form[25,32]. In this study, referring to this reported protocol, the particle events were identified apart from instrumental background or dissolved form applying a moving median filter that replaces each data point in the raw data with the median of a certain number of adjacent data points. The threshold was calculated based on counting statistics in each median data point S, associated with the counts in the time slice: $S + 5\sqrt{S}$.

Size calibration of NPs

For an accurate size analysis for NPs, a matrix-matched size calibration standard material is required[25,33,34]. For most biological samples, the main component is carbon. Thus, we have selected a cellulose filter paper to prepare the matrix-matched size calibration standard material. Commercially available citrate-coated 60 nm Ag NPs (59 ± 6 nm) from NanoComposix (San Diego, CA, USA) was used. A 100 μL of solution containing Ag NPs with the number concentration of 1.8×10^{10} particles mL^{-1} was dropped onto the cellulose filter paper (qualitative filter paper No. 1, ADVANTEC, Tokyo, Japan). The Ag NPs solution was left to dry for 1 hour at room temperature, and then used for size calibration. The aggregation of citrate-coated Ag NPs can occur in a biological solution, and thus, the sample matrix containing Gamble's solution[35,36] or artificial lysosomal fluid buffer[35,36] was not used in this study.

The measured ion counts from single particle event reflect the total mass (*i.e.,* total number of Ag atoms) of the NPs, and thus, the size of the NPs can be calculated by the total ion counts of single particle events. The size of NPs was calibrated based on comparing the total ion counts of single NPs and those for the size standard material (60 nm Ag NPs)[37]. Hence, the size of Ag NPs was calculated based on the assumption that the Ag NPs present in the cell tissues had spherical shape. Total ion counts of the individual particle events were calculated by integrating the ion counts between starting and terminal channels[38]. The calibration factor was defined by the mean ion counts of single particle events obtained from about 1000 particles.

Matrix-matched reference material for quantitative imaging analysis of ionic Ag

For the quantitative imaging analysis of ionic Ag, a matrix-matched reference material was prepared. In this study, a photocurable resin was used. Photocurable resins have advantages as follows; (a) including carbon as a major component, (b) easy handling, and (c) long shelf life. About 6 μL of 1000 mg L^{-1} of silver atomic absorption standard solution ($AgNO_3$·HNO_3 (0.1mol L^{-1}), Kanto Chemical Co., Inc., Tokyo, Japan) was diluted by 100 μL of ethanol, and then, 10 μL of the diluted solution was added to 100 mg of the photocurable resin (Acryl-one type:# 2100N, Maruto Instrument Co., Ltd, Tokyo, Japan). The resulting mixture of photocurable resin and Ag solution was mixed well with the stirrer for 5 minutes for homogenization. Then, about 1 mg of the resulting mixture resin were dropped onto glass slides, and then pressed by another glass slide to make thin films. The pressed mixture resins were then left for 1 hour for polymerization under a lamp. The resulting calibration reference materials were square-shaped films with a size of 10 mm with a thickness of ca.10 μm.

The homogeneity of Ag resin reference material was evaluated by laser ablation of 1000 × 1000 μm through the laser ablation with fluence of 6.3 J cm^{-2}, repetition rate of 1 kHz, scanning speed of 100 μm s^{-1}, repeated 15 line scans, and dwell time of 0.2 s. The resulting RSD value was 4.8%, and this is significantly smaller than the uncertainties in the spot analysis (*e.g.,* 10%) achieved in this study.

Validation of Ag concentration in the resulting reference material was carried out with the solid mixing calibration using a multiple spot-LA-ICP-MS[39]. For the calibration using the solid mixing, an ultraviolet femtosecond laser equipped with a galvanometric scanner (wavelength of 257 nm; pulse duration of 290 fs: Jupiter Solid Nebulizer, ST Japan INC., Tokyo, Japan) coupled to a triple quadrupole-based ICP-MS (iCAP TQ, Thermo Fisher Scientific, Bremen, Germany) was used. Glass standard reference material NIST SRM 612 and NIST 614 SRM were used as calibration standards. Laser sampling from wide area with short time duration (0.1 s) was conducted with both the high repetition rate (10 kHz) and fast laser scan achieved by the Galvano scanner. Ablation pit size of 10 μm with fluence of 6.3 J cm^{-2} was used here. Signal intensity data were acquired through 100 cycles repeated ablation from same area. The total ablated zone in three solid materials was 100 × 700 × 1 μm for both the NIST SRM 612 and 614, and 100 × 700 × 7 μm for photocurable resin reference material. Solid mixing was conducted by fast switching of the laser ablation (<1 ms) with high-repetition rate laser (10 kHz) on three materials: the resin and two NIST glass standard materials. The mixing ratios of three materials were controlled with the number of laser shots onto the solid materials. Total time for the laser ablation was fixed at 10 seconds, and stable signal intensities for 8 s were integrated, and the resulting signal data were used for further calculations. The nominal photocurable resin was calculated to contain 7.75 ± 0.42 μg g^{-1} of Ag.

Calibration of ionic Ag concentration

Concentration of the ionic Ag (μg g^{-1}) in the frozen section of mouse liver can be calibrated by signal intensity (I in counts), volume of ablation zone (V in cm^3), and the density (ρ in g cm^{-3}) of the resin and liver sample using Eq. (1):

$$C_{\mathrm{sample}} = C_{\mathrm{standard}} \times \frac{I_{\mathrm{sample}}}{I_{\mathrm{standard}}} \times \frac{V_{\mathrm{standard}}}{V_{\mathrm{sample}}} \times \frac{\rho_{\mathrm{standard}}}{\rho_{\mathrm{sample}}} \qquad (1)$$

The main composition of the photocurable resin was triethylene glycol dimethacrylate, hence the ρ_{standard} was estimated to be 1.1 g cm^{-3}. In contrast, density of the biological samples can vary remarkably among the samples and/or positions. Typical density values of the biological samples are 1.06 g cm^{-3} for muscle, 0.902 g cm^{-3} for fat, 1.03 g cm^{-3} for blood, and 1.05 g cm^{-3} for cell[40,41], suggesting that the density can change about 10% among tissues and analysis points. In-situ and non-destructive analysis of density directly from the frozen sample is difficult, and thus, we take the density of liver tissues (ρ_{sample}) as 1.00 g cm^{-3} as a representative value. The volumes of ablation zone for samples (V_{sample}) were calculated by the resulting volume of ablation zone based on length, width, and depth of the ablation zone, whereas the volume of standard (V_{standard}) was calculated based on the measured area (100 × 300 μm), and depth (2.3 μm) using the digital microscope (Leica VZ 700C, Leica Microsystems, Wetzlar, Germany).

Results and disucussion

Evaluation for occurrence of disintegration of NPs with low laser fluence

To obtain accurate size data of Ag NPs in solid samples, disintegration of the Ag NPs during laser ablation was carefully

investigated in this study. The signal intensity (counts) of each particle event was converted into cubic root of the signal intensity (counts$^{1/3}$). The measured size of the NPs should be correlated with cubic root of the total counts (counts$^{1/3}$) for individual particle events.

The signal intensity distribution obtained from 60 nm Ag NPs using solution-based spICP-MS is shown in **Figure 1** (gray columns). The average signal intensity and variations defined as two standard deviations were 8.0 ± 3.0 counts$^{1/3}$ (N = 4703). The resulting signal intensity distribution obtained by the LA-spICP-MS technique is also given in **Figure 1** as black columns. The 60 nm Ag NPs placed on the cellulose filter paper were measured by the LA-spICP-MS technique. The very low laser fluence of 0.4 J cm^{-2} was adopted. The average signal intensity and variations (2SD) were 8.3 ± 3.6 counts$^{1/3}$ (N = 1173). For an easier

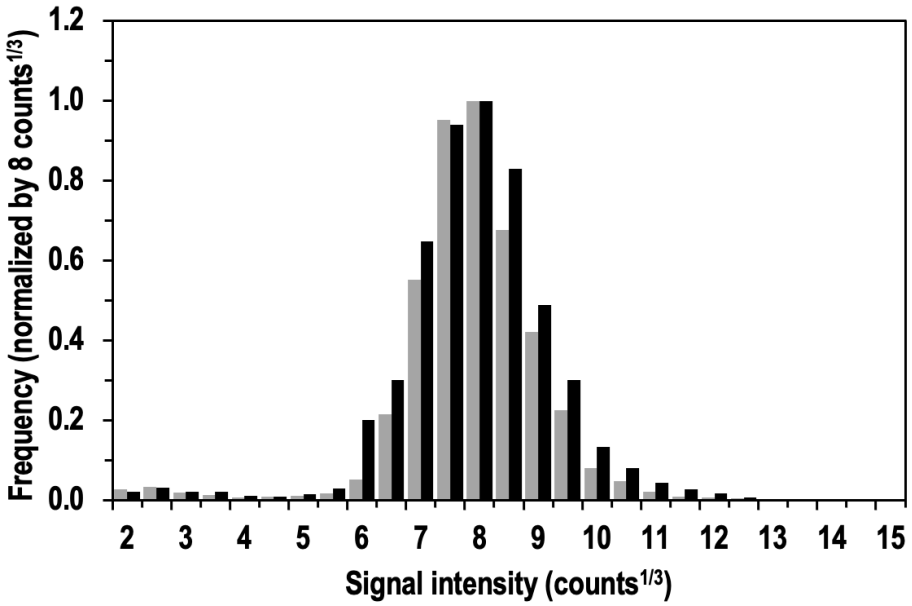

Figure 1. Signal intensity distributions obtained from 60 nm Ag NPs using solution-based spICP-MS (gray columns) and LA-spICP-MS (black columns).

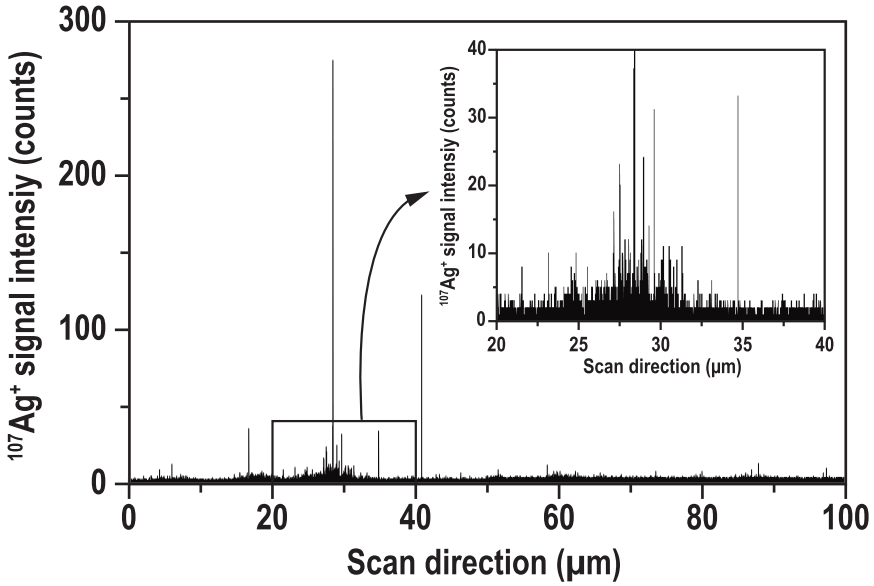

Figure 2. Single line scan data obtained from the second line of the mouse liver (marked with white arrows in Figs. 3(A)–3(I)).

comparison, the frequency normalized by 8 counts$^{1/3}$, rather than the absolute number of particles. The results demonstrated that the LA-spICP-MS technique was in good agreement with the solution-based spICP-MS within analytical uncertainty. The distribution pattern obtained by the LA-spICP-MS technique did not vary significantly from that obtained by the solution-based spICP-MS technique. Moreover, no significant increase in the Ag NPs with smaller signal intensities (<5 counts$^{1/3}$) can be found, suggestive of very small contribution of laser-induced disintegration through laser ablation sampling with low fluence.

Simultaneous imaging analysis of Ag NPs and ionic Ag

Figure 2 shows the signal intensity profile obtained from the second line of the mouse liver (marked with white arrows in **Figure 3(A)–3(I)**). The pulsed signal and low signal intensity data (baseline) represent particle and ionic form of Ag, respectively. This data suggests that the ionic forms of Ag were present around the NPs. In this study, data acquisition was conducted through line profiling analysis under the ablation pit size of 4 μm, scanning speed of 2 μm s^{-1}, and no gap between the lines. Under these conditions, size of the image (henceforth, we refer this as pixel) was 1 μm in horizontal (x) and 4 μm in vertical (y) directions. This high spatial resolution enables the detection of NPs and ions in cells.

The resulting concentration of ionic Ag, together with locations of ionic Ag were visualized by the iQuantNP software. **Figure 3(A)** illustrates the photographic image of the unstained frozen section of the mouse liver, and **Figure 3(B)** shows the distribution and concentration of ionic Ag, calculated based on eq. (1). The color reflects the concentration of ionic Ag as shown in the color bar (**Figure 3(B)**). The ionic Ag concentration in the frozen section of mouse liver varied from 1 to 70 μg g^{-1} per pixel. The overall averaged Ag concentration calculated based on the total signal counts from Ag NPs and ionic Ag, was 30.2 μg g^{-1}, and this is consistent with the bulk Ag content which were separately measured by solution-based ICP-MS technique through chemical decomposition and dissolution processes (*i.e.,* 35.8 μg g^{-1}). It is noted that the measured Ag concentration was different, reflecting sampling volume or weight through laser ablation. The variation of volume of ablation zone was not greater than 6% for the fabricated reference material. Moreover, since the sliced sample was ablated totally in this study, the ablation depth can be kept constant (10 μm). Therefore, the variation of volume of ablation zone cannot account for the discrepancy in the Ag concentrations (*i.e.,* 17%) obtained by the solution-based ICP-MS (35.8 μg g^{-1}) and LA-spICP-MS (30.2 μg g^{-1}) techniques. Another possible explanation of the discrepancy is a density of the biological samples. Typical densities for muscle, fat, blood, and whole cell, were about 1.06 g cm^{-3}, 0.90 g cm^{-3}, 1.03 g cm^{-3}, and 1.05 g cm^{-3}, respectively[40,41], demonstrative of nearly 15% variations. In this study, the bulk Ag concentrations were calculated by assuming that the ρ_{sample} being 1.00 g cm^{-3} as a representative value of the whole tissues, and thus, the Ag concentration obtained the solution-based ICP-MS involved principal uncertainties being >15%. We believe that the present discrepancy in the measured Ag concentrations using the solution-based ICP-MS and LA-spICP-MS techniques can be attributed to the empirical assumption that there was no variation in the density of the sample.

The good agreement with the measured Ag content through the imaging analysis and bulk analysis suggests that the calibration protocol based on the photocurable resin standard material is very promising for the quantitative imaging analysis. Moreover, the heterogeneous distribution of the ionic Ag found in the resulting imaging data suggests that the ionic Ag accumulates preferentially in certain region within the liver tissue (*e.g.,* sinusoid, Kupffer cell, or hepatocyte). This finding was consistent with histopathological feature, demonstrating detection of black granular pigment deposition (*i.e.,* Ag NPs) in the cytoplasm of Kupffer cells along the sinusoids in H&E-stained sections[11].

The imaging results of Ag NPs of various sizes are shown in **Figure 3(C)–3(I)**, in increments of 10 nm. A single Ag particle was indicated as a yellow-dot. Although the size of the dots is linearly correlated with the size of Ag NPs, the size of the dots does not reflect the actual size of Ag NPs. The only exception is the imaging results for Ag NPs of 8–20 nm. The color of the 8–20 nm Ag NPs image (**Figure 3(C)**) represents number of NPs per pixel. In **Figure 3(D)–3(I)**, imaging results of ionic Ag, as well as yellow dots for the Ag NPs, were also shown in gray-colored scale in background. Several interesting features can be derived through the comparison of the resulting images of ionic Ag and Ag NPs. First of all, the number of the smaller size Ag NPs increased. Second point is the heterogeneous distribution of both the ionic Ag and Ag NPs within the liver tissue. The ionic Ag and Ag NPs showed similar distribution patterns within the sample. Concentration of ionic Ag were high at areas where Ag NPs were enriched. From the **Figure 3 (C)** and **(D)** data (*i.e.,* imaging data of 8–20nm and 20–30 nm Ag NPs, respectively), these sizes distributed more densely and widely than the other sizes. This suggests that Ag NPs smaller than 30 nm can be incorporated in not only Kupffer cells in the sinusoids, but also hepatocytes.

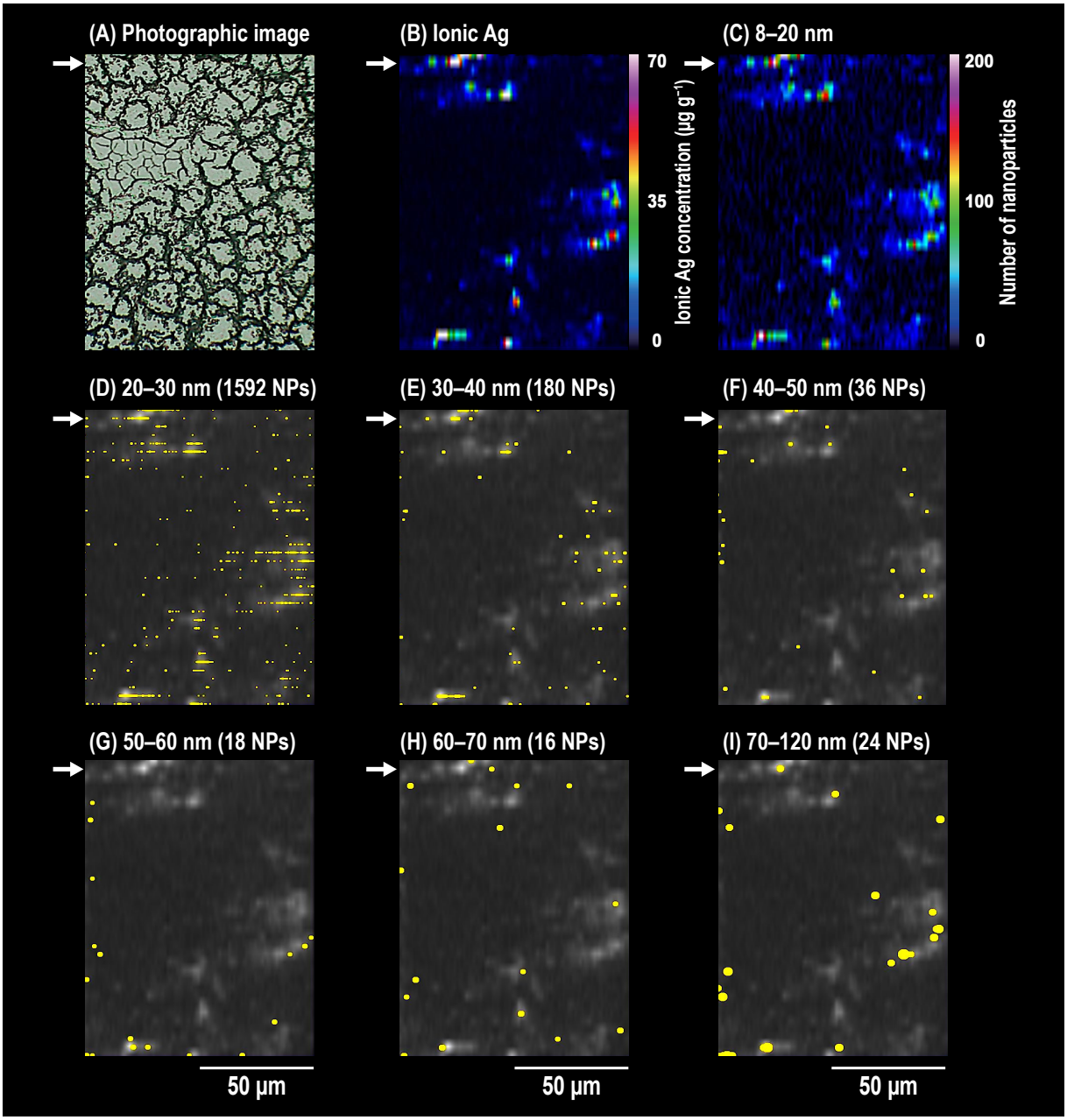

Figure 3. Resulting imaging data for both the ionic Ag and Ag NPs.
(A) Photographic image of the frozen section of mouse liver (administered 60 nm Ag NPs (0.2 mg per mouse)).
(B) Mapping data of the ionic Ag.
(C)–(I) Resulting distribution images of Ag NPs for size range from ≥8 nm to <120 nm, in increments of 10 nm. Background color represents the gray-colored scale of (B) ionic Ag data. In figure (C), the color reflects the number of NPs per pixel. In figure (D)–(I), the yellow-dot represents the single Ag NP.

Figure 4 illustrates the size distribution of Ag NPs found in the frozen section of mouse liver. The inserted figure shows the enlarged-scale of size distribution of the Ag NPs for size range of 40–120 nm. The measured sizes of the Ag NPs were significantly smaller than the administrated Ag NPs (59.8 ± 6.2 nm). The number of detected small particles (<20 nm) were >1,000 times higher than the number of 60 nm Ag NPs. The most plausible explanation for the detection of Ag NPs is that this is due to dissolution of Ag NPs through cellular activity. Moreover, the size distribution data also revealed the presence of the Ag NPs with larger sizes (*e.g.*, >60 nm). A wide size distribution of the detected Ag NPs in the liver tissue suggests there are both the dissolution and aggregation of the Ag NPs occurring in the tissue.

Imaging and size distribution data (**Figure3** and **4**) revealed the accumulation of Ag NPs and ionic Ag in certain positions of

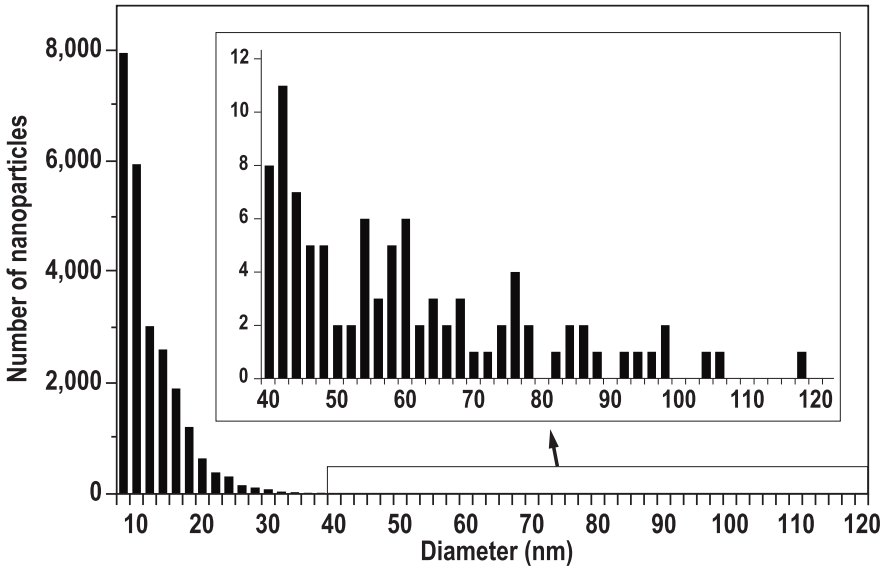

Figure 4. Measured size distribution for Ag NPs obtained from the frozen section of mouse liver (administered 60 nm Ag NPs (59.8 ± 6.2 nm). The insert shows the size distribution of the Ag NPs for size range from 40–120 nm.

the liver. These data suggest that the Ag NPs is likely to be dissolved through cell activity. Singh *et al.* reported that Ag NPs were internalized via scavenger receptor-mediated phagocytic uptake and trafficked into the cytoplasm in macrophages[42]. After the incorporation of Ag NPs into the cells, Ag NPs degrades within the cells to release ionic Ag. Navarro *et al.* also reported that H_2O_2, a metabolite of algae, reacts with Ag NPs to form hydroxyl radicals and this forms ionic Ag as a byproduct[43]. However, there is no clear evidence on the region where the occurrence of Ag NPs dissolution after intraperitoneal administration. It is feasible that the dissolution of Ag NPs could have occurred by the time Ag NPs reached the liver. As for the aggregation of Ag NPs, the aggregation of the Ag NPs can occur under exposure to acidic environment and/or with high ionic strength containing divalent cations (*e.g.,* Ca^{2+})[44,45]. These can be the cause of agglomeration of Ag NPs observed in this frozen section of mouse liver.

Previous studies reported that NPs, which are not immediately trapped by Kupffer cells, are translocated through the fenestrated vascular endothelium into the Dissé spaces to be taken up by hepatocytes and processed into biliary canaliculi[46]. Hirn *et al.* observed through transmission electron microscopy (TEM) that 18 nm Au NPs were predominantly found in not only Kupffer cells, but also endothelial cells and hepatocyte[47]. They also reported that both the small and large agglomerates of Au NPs were observed in Kupffer cells. From this research, Ag NPs can be incorporated into the Kupffer cells and hepatocytes. Despite these observations, the mechanisms of accumulation of NPs in hepatocytes remain unclear. For future studies, we hope that the LA-spICP-MS technique can provide important clues to understand the mechanism of metabolic process of the Ag NPs in the liver tissue.

Conclusion

Simultaneous determinations of (a) size of Ag NPs, (b) concentrations of ionic Ag (dissolved form), and (c) distributions of both the Ag NPs and ionic Ag in a frozen section of mouse liver was carried out by the spICP-MS coupled with laser ablation sampling technique. The size of Ag NPs was calibrated by a matrix-matched reference material prepared through the addition of NPs suspension onto a cellulose filter paper. For the quantitative analysis of Ag concentration, a calibration reference material using the photocurable resin spiked with the ionic Ag (7.75 ± 0.42 $\mu g\,g^{-1}$) was used. The resulting Ag concentration obtained by averaging the overall analysis area was 30.2 $\mu g\,g^{-1}$. This was consistent with the bulk concentration (*i.e.,* 35.8 $\mu g\,g^{-1}$) obtained by solution-based ICP-MS technique, suggestive of high reliability of the present analysis protocol.

The imaging data of the frozen section of mouse liver showed that both the ionic Ag and Ag NPs were heterogeneously distributed within the liver tissue. The number of the smaller size Ag NPs increased. Another important information derived from the imaging data was the similarity between the distribution of ionic Ag and the distribution of the Ag NPs, suggesting that

the Ag NPs can be dissolved through cell activity. This is also supported by the changes in the size distribution of the Ag NPs. Moreover, based on the size distribution of the Ag NPs, both the dissolution and aggregation has occurred. The data obtained in this study demonstrate that the combination of two high spatial resolution images of both the NPs and ionic forms using the LA-spICP-MS technique can provide key information concerning the transport, interaction, and decomposition features of the NPs.

Acknowledgement

We are grateful to Tetsuya Tamaki (Next Lab, Tokyo, Japan) for technical supports. We are also grateful to Hui Hsin Khoo (The Univ. of Tokyo) for scientific advice and critical reading of the manuscript. This work was financially supported by a Grant-in-Aid for Scientific Research (JP19H01081 and JP 21H04511) from the Ministry of Education, Culture, Sports, Science and Technology, Japan.

References

[1] Kessler R: Engineered nanoparticles in consumer products: under-standing a new ingredient. Environ Health Perspect 119(3): A120-A5, 2011.

[2] Weir A, Westerhoff P, Fabricius L, Hristovski K, Van Goetz N: Titanium Dioxide Nanoparticles in Food and Personal Care Products. Environ. Sci. Technol 46: 2242-2250, 2012.

[3] Wei Y, Yan B: Nano products in daily life: to know what we do not know. Natl. Sci. Rev 3: 414-415, 2016.

[4] Ahamed M, Alsalhi MS, Siddiqui MK: Silver nanoparticle applications and human health. Clin Chim Acta 411: 1841-1848, 2010.

[5] Larguinho M, Baptista PV: Gold and silver nanoparticles for clinical diagnostics—Fromgenomics to proteomics. J. Proteomics 758(10): 2811-2823, 2012.

[6] Schluesener JK, Schluesener HJ: Nanosilver: application and novel aspects of toxicology. Arch Toxicol 87: 569-576, 2013.

[7] Mijnendonckx K, Leys N, Mahillon J, Silver S, Van Houdt R: Antimicrobial silver: uses, toxicity and potential for resistance. Biometals 26: 609-621, 2013.

[8] Morones JR, Elechiguerra JL, Camacho A, Holt K, Kouri JB, Ramírez JT, Yacaman MJ: The bactericidal effect of silver nanoparticles. Nanotechnology 16: 2346-2353, 2005.

[9] Schäfer B, Brocke JV, Epp A, Götz M, Herzberg F, Kneuer C, Sommer Y, Tentschert J, Noll M, Günther I, Banasiak U, Böl GF, Lampen A, Luch A, Hensel A: State of the art in human risk assessment of silver compounds in consumer products: a conference report on silver and nanosilver held at the BfR in 2012. Arch Toxicol 87: 2249-2262, 2013.

[10] Pan Y, Neuss S, Leifert A, Fischler M, Wen F, Simon U, Schmid G, Brandau W, Jahnen-Dechent W: Size-dependent cytotoxicity of gold nanoparticles. Small 3: 1941-1949, 2007.

[11] Cho YM, Mizuta Y, Akagi JI, Toyoda T, Sone M, Ogawa K: Size-dependent acute toxicity of silver nanoparticles in mice. J. Toxicol. Pathol 31: 73-80, 2018.

[12] Aaron J, Travis K, Harrison N, Sokolov K: Dynamic imaging of molecular assemblies in live cells based on nanoparticle plasmon resonance coupling. Nano Lett 9(10): 3612-3618, 2009.

[13] Beveridge JS, Stephens JR, Williams ME: Differential magnetic catch and release: experimental parameters for controlled separation of magnetic nanoparticles. Analyst 136(12): 2564-2571, 2011.

[14] Kneipp J, Kneipp H, Rice WL, Kneipp K: Optical probes for biological applications based on surface-enhanced Raman scattering from indocyanine green on gold nanoparticles. Anal Chem 77(8): 2381-2385, 2005.

[15] Nam J, Won N, Jin H, Chung H, Kim S: pH-induced aggregation of gold nanoparticles for photothermal cancer therapy. J Am Chem Soc. 131(38): 13639-13645, 2009.

[16] Mourdikoudis S, Pallares RM, Thanh NTK: Characterization techniques for nanoparticles: Comparison and complementarity upon studying nanoparticle properties. Nanoscale 10: 12871-12934, 2018.

[17] Reifschneider O, Wehe CA, Raj I, Ehmcke J, Ciarimboli G, Sperlingae M, Karst U: Quantitative bioimaging of platinum in polymer embedded mouse organs using laser ablation ICP-MS. Metallomics 5: 1440-1447, 2013.

[18] Limbeck A, Galler P, Bonta M, Bauer G, Nischkauer W, Vanhaecke F: Recent advances in quantitative LA-ICP-MS analysis: challenges and solutions in the life sciences and environmental chemistry. Anal Bioanal Chem 407: 6593-6617, 2015.

[19] Zoriy M, Matusch A, Spruss T, Becker JS: Laser ablation inductively coupled plasma mass spectrometry for imaging of copper, zinc, and platinum in thin sections of a kidney from a mouse treated with cis-platin. Int. J. Mass Spectrom 260(2): 102-106, 2007.

[20] Šala M, Šelih VS, Van Elteren JT: Gelatin gels as multi-element calibration standards in LA-ICP-MS bioimaging: fabrication of homogeneous standards and microhomogeneity testing. Analyst 142: 3356-3359, 2017.

[21] Köppen C, Reifschneider O, Castanheira I, Sperling M, Karst U, Ciarimboli G: Quantitative imaging of platinum based on laser

ablation-inductively coupled plasma-mass spectrometry to investigate toxic side effects of cisplatin. Metallomics 7(12): 1595-1603, 2015.

[22] Degueldre C, Favarger PY: Colloid analysis by single particle inductively coupled plasma-mass spectroscopy: a feasibility study. Colloids Surfaces A Physicochem. Eng. Asp 217(1-3): 137-142, 2003.

[23] Pace HE, Rogers NJ, Jarolimek C, Coleman VA, Higgins CP, Ranville JF: Determining transport efficiency for the purpose of counting and sizing nanoparticles via single particle inductively coupled plasma mass spectrometry. Anal. Chem 83: 9361-9369, 2011.

[24] Yamashita S, Yoshikuni Y, Obayashi H, Suzuki T, Green D, Hirata T: Simultaneous determination of size and position of silver and gold nanoparticles in onion cells using laser ablation-ICP-MS. Anal. Chem 91(7): 4544-4551, 2019.

[25] Metarapi D, Šala M, Vogel-Mikuš K, Šelih VS, Van Elteren JT: Nanoparticle analysis in biomaterials using laser ablation–single particle–inductively coupled plasma mass spectrometry. Anal. Chem 91: 6200-6205, 2019.

[26] Nordhorn ID, Dietrich D, Verlemann C, Vennemann A, Schmid R, Elinkmann M, Fuchs J, Sperling M, Wiemann M, Karst U: Spatially and size-resolved analysis of gold nanoparticles in rat spleen after intratracheal instillation by laser ablation-inductively coupled plasma-mass spectrometry. Metallomics 13: 2021, mfab028.

[27] Sakata S, Hattori K, Iwano H, Yokoyama TD, Danhara T, Hirata T: Determination of U–Pb ages for young zircons using laser ablation-ICP-mass spectrometry coupled with an ion detection attenuator device. Geostand. Geoanal. Res 38(4): 409-420, 2014.

[28] Yamashita S, Miyake A, Hirata T: Size analysis of large-sized gold nanoparticles using single particle ICP-mass spectrometry. J. Anal. At. Spectrom 35: 2834-2839, 2020.

[29] Benesŏva I, Dlabkova K, Zelenak F, Vaculovic T, Kanicky V, Preisler J: Direct analysis of gold nanoparticles from dried droplets using substrate-assisted laser desorption single particle-ICPMS. Anal. Chem 88(5): 2576-2582, 2016.

[30] Metarapi D, Van Elteren JT, Šala M: Studying gold nanoparticle degradation during laser ablation–single particle-inductively coupled plasma mass spectrometry analysis. J. Anal. At. Spectrom. 2021, Advance Article.

[31] Tuoriniemi J, Cornelis G, Hassellöv M: Size discrimination and detection capabilities of single-particle ICPMS for environmental analysis of silver nanoparticles. Anal. Chem 84: 3965-3972, 2012.

[32] Metarapi D, Van Elteren JT: Fundamentals of single particle analysis in biomatrices by laser ablation-inductively coupled plasma mass spectrometry. J. Anal. At. Spectrom 35: 784-793, 2020.

[33] Drescher D, Zeise I, Traub H, Guttmann P, Seifert S, Büchner T, Jakubowski N, Schneider G, Kneipp J: In situ characterization of SiO_2 nanoparticle biointeractions using BrightSilica. Adv. Funct. Mater 24(24): 3765-3775, 2014.

[34] Arakawa A, Jakubowski N, Koellensperger G, Theiner S, Schweikert A, Flemig S, Iwahata D, Traub H, Hirata T: Quantitative imaging of silver nanoparticles and essential elements in thin sections of fibroblast multicellular spheroids by high resolution laser ablation inductively coupled plasma time-of-flight mass spectrometry. Anal. Chem 91: 10197-10203, 2019.

[35] Stebounova LV, Guio E, Grassian VH: Silver nanoparticles in simulated biological media: a study of aggregation, sedimentation, and dissolution. J Nanopart Res 13: 233-244,2011.

[36] Zhong L, Yu Y, Lian H, Hu X, Fu H, Chen Y: Solubility of nano-sized metal oxides evaluated by using in vitro simulated lung and gastrointestinal fluids: implication for health risks. J Nanopart Res 19: 375, 2017.

[37] Laborda F, Jiménez-Lamana J, Bolea E, Castillo JR: Selective identification, characterization and determination of dissolved silver(I) and silver nanoparticles based on single particle detection by inductively coupled plasma mass spectrometry. J. Anal. At. Spectrom 26: 1362-1371, 2011.

[38] Suzuki T, Yamashita S, Yoshikuni Y, Hirata T: Development of data analysis software for nanoparticle measurements by ICP-mass spectrometry. J. Mass Spectrom. Soc. Jpn 67: 147-153, 2019.

[39] Makino Y, Kuroki Y, Hirata T: Determination of major to trace elements in metallic materials based on the solid mixing calibration method using multiple spot-laser ablation-ICP-MS. J. Anal. At. Spectrom 34: 1794-1799, 2019.

[40] Huang HK, Wu SC: The evaluation of mass densities of the human body in vivo from CT scans. Comput. Biol. Med. Pergamon Press 6: 337-343, 1916.

[41] Bryan AK, Hecht VC, Shend W, Payer K, Grover WH, Manalis SR: Measuring single cell mass, volume, and density with dual suspended microchannel resonators. Lab Chip 14(3): 569-576, 2014.

[42] Singh RP, Ramarao P: Cellular uptake, intracellular trafficking and cytotoxicity of silver nanoparticles. Toxicol Lett 213: 249-259, 2012.

[43] Navarro E, Piccapietra F, Wagner B, Marconi F, Kaegi R, Odzak N, Sigg L, Behra R: Toxicity of silver nanoparticles to Chlamydomonas reinhardtii. Environ. Sci. Technol 42(23): 8959-8964, 2008.

[44] El Badawy AM, Luxton TP, Silva RG, Scheckel KG, Suidan MT, Tolaymat TM: Impact of environmental conditions (pH, ionic strength, and electrolyte type) on the surface charge and aggregation of silver nanoparticles suspensions. Environ. Sci. Technol 44: 1260-1266, 2010.

[45] Stebounova LV, Guio G, Grassian VH: Silver nanoparticles in simulated biological media: a study of aggregation, sedimentation, and dissolution. J Nanopart Res 13: 233-244, 2011.

[46] Johnston HJ, Hutchison G, Christensen FM, Peters S, Hankin S, Stone V: A review of the in vivo and in vitro toxicity of silver and gold particulates: particle attributes and biological mechanisms responsible for the observed toxicity. Critical Reviews in Toxicology 40: 328-346, 2010.

[47] Hirn S, Semmler-Behnke M, Schleh C, Wenk A, Lipka J, Schäffler M, Takenaka S, Möller W, Schmid G, Simon U, Kreyling WG: Particle size-dependent and surface charge-dependent biodistribution of gold nanoparticles after intravenous administration. European Journal of Pharmaceutics and Biopharmaceutics 77: 407-416, 2011.

Metallomics Research 2021 (1) #MR202107

Regular article https://metallomicsresearch.brte.org

Imaging Analysis of Amino Acids and Sugar using a Dielectric Barrier Discharge Ionisation-Mass Spectrometer coupled with Laser Ablation Sampling Technique

Hui Hsin Khoo[1], Haruo Shimada[2], Hidekazu Miyahara[1], Takafumi Hirata[1*]

[1] Geochemical Research Center, School of Science, The University of Tokyo, 7-3-1 Hongo, Bunkyo-ku, Tokyo 113-0033, Japan
[2] BioChromato, Inc., 1-12-19 Honcho, Fujisawa, Kanagawa, Japan

Summary

Distribution and concentration of certain organic compounds in drugs or biological tissue samples can provide key information to understand the behaviour and effect of that chemical species. In this study, we developed an analytical technique to perform mass spectrometry imaging for organic compounds under atmospheric pressure. The laser ablation technique was used as a sample introduction method to ablate a small amount of sample by focusing laser light onto the sample surface. Laser-induced sample particles were transferred by an argon gas stream to a newly developed plasma-based ion source for ionisation. The capability of this analytical method was demonstrated with the analysis of amino acids. Either protonated ($[M+H]^+$) or ammoniated ($[M+NH_4]^+$) ions, with slight fragments, were observed for the amino acids and sugar, suggesting a fairly soft ionisation was achieved. Analytical repeatability defined by nine times repeated analysis was better than 10%. More importantly, linear correlations between the signal intensities and concentration of analytes were obtained for three amino acids (valine, methionine, and phenylalanine). With the present analytical technique, imaging analysis of several amino acids and sugar was carried out with a tablet sample. The resulting imaging can be used to evaluate the homogeneity of drug components both the within and among the tablets.

Key words: Laser ablation, Imaging mass spectrometry, Dielectric barrier discharge, Soft ionisation, Amino acids, Sugar

Statements about COI: The authors declare no conflict of interest associated with this manuscript.

*Correspondence:
Takafumi Hirata
Geochemical Research Center, The University of Tokyo
7-3-1 Hongo, Bunkyo-ku, Tokyo 113-0033, Japan
Tel: +81-3-5841-4621
E-mail: hrt1@eqchem.s.u-tokyo.ac.jp

Received: August 31, 2021
Accepted: January 17, 2022
Released online: January 31, 2022

Introduction

The distribution and concentration of a chemical species within a solid sample is important to understand and elucidate the behaviour and effect of that chemical species on the sample. Spatial distribution of organic compounds in samples provides information to scientists to investigate the relation between spatial organisation, structure and function of molecules[1-3]. Imaging mass spectrometry is a sensitive approach to obtain spatial distribution information in solid samples. Imaging using mass spectrometry is conventionally performed by matrix-assisted laser/desorption ionisation-mass spectrometry (MALDI-MS)

and secondary ionisation mass spectrometry (SIMS)[4, 5]. Although soft ionisation can be achieved by these techniques, signal intensities of the target molecules can vary largely, as ionisation depend heavily on the sample preparation conditions and the choices of surface coating (matrix). Thus, these techniques are not suitable for quantitative analysis of organic compounds. Moreover, prior to the analysis, samples should be placed into the vacuum chamber, resulting in the analytical difficulty for biological tissues or tablet samples.

The scope of contemporary analytical mass spectrometry is expanded by a class of atmospheric pressure ionisation sources. Sample preparation requirement can be reduced, providing a significant advantage for real-time and in situ chemical analysis. In addition, samples can be preserved in their native environment. Desorption electrospray ionisation (DESI) has been applied as an imaging method for biological samples at ambient conditions[6]. However, the use of solvent in DESI can be a problematic for samples that are sensitive to solvents. Meanwhile, plasma-based ionisation techniques such as direct analysis in real time (DART), flowing atmospheric pressure afterglow (FAPA), dielectric barrier discharge ionisation (DBDI) and low-temperature plasma (LTP) has proven to be successful in analysing compounds directly from untreated surfaces[7-10]. Plasma-based ionisation techniques have advantages including simplicity, portability and absence of solvents. Although these plasma-based ionisation techniques prove to be useful in analysing a variety of low-molecular-weight compounds, such as volatile organic compounds (VOCs), obtaining spatial information of the compounds in a solid sample still remains an issue.

Since sensitivity is crucial for the detection of small amounts organic compounds, an ion source that ionise compounds efficiently while generating a stable plasma is needed. Plasma sources in the corona discharge region are atmospheric pressure chemical ionisation (APCI) and direct analysis in real time (DART)[7, 11]. These ion sources can only generate a limited number of reagent ions due to the low current used for corona discharges[12]. Plasma sources that are produced at the normal glow regime (*i.e.,* DBDI and LTP) have a dielectric barrier acting as a current-limiting device, which in-turn helps produce a more stable plasma[12]. Nevertheless, the use of DBDI and LTP for quantitative studies are seldom reported. Lastly, plasma sources produced in the abnormal glow region (*i.e.,* FAPA) produces more reagent ions than corona and glow discharges[8]. However, they are not usually used for analytical purposes due to their instability[12].

Laser ablation is widely known as a method for sample introduction of solid samples. Laser ablation is routinely combined with inductively coupled plasma-mass spectrometry (ICP-MS) for elemental analysis[13]. LA-ICP-MS has advantages such as analysis of solid materials at atmospheric pressure, high spatial resolution and high sensitivity[14-16]. Wang *et al.* reported the first application of LA-ICP-MS on the imaging of elemental distribution in biological samples[17]. Since then, LA-ICP-MS has flourished as a technique for imaging analysis of various solid samples. The ICP is a powerful ionisation source, allowing for reproducible results, which leads to good quantification capabilities. However, this property of the ICP is a trade-off with the lack of ability to obtain molecular information. Toward the goal of performing molecular imaging at atmospheric pressure, the laser ablation sampling method can be a useful tool when combined with a soft ionisation method.

Hence, in the present work, our aim is to develop an analytical method that has the ability to analyse solid samples under atmospheric pressure conditions, with minimal sample preparation, and without the use of matrices and solvents. Here, we develop an ion source, DBDI that can produce a stable and homogeneous plasma using glow discharge. We combine a UV femtosecond laser with the DBDI source as a soft ionisation method for organic compounds. Femtosecond laser was reported to reduce thermal diffusion into solid samples, producing smaller and stoichiometric aerosols[18-21]. The reduction in thermal degradation and vaporisation is important, especially when analysing biological samples, to preserve the integrity of the samples during analysis time and to ensure the highest possible resolution during imaging analysis. Here, we explore the use of LA-DBDI-MS in the direct analysis of low-molecular-weight compounds in solid samples. Low-molecular-weight compounds such as amino acids and sugars were analysed to demonstrate the potentials of this analytical technique. The characteristics of ions generated and the demonstration of reproducibility of the system, as well as imaging of organic compounds will be reported in this study.

Experimental Section

Reagents and Sample Preparation

Operational settings were optimised by maximising the ion signal of L-valine, L-methionine and L-phenylalanine. All reagents used were analytical grade, purchased from FUJIFILM Wako Pure Chemical Industries, Ltd. (Osaka, Japan). Table sugar, sold as stick packets (Mitsui Sugar Co., Ltd.), were purchased from the local supermarket. Prior to the analysis, powdered samples of the

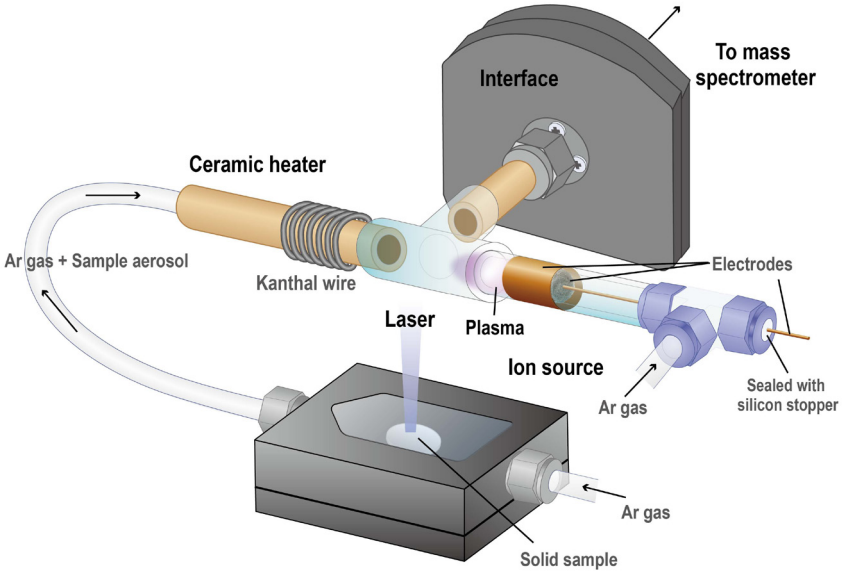

Figure 1. | Schematic diagram of instrumental setup.

amino acids and sugar were pelletised for the laser sampling. About 50 mg of the amino acids were loaded onto a 7 mm-diameter die chamber and a pressing force of 1 ton (*i.e.,* 250 MPa) was applied for 5 minutes using a hydraulic press (PIKE Technologies, Madison, USA) to form pellets. These powder pellets were directly subjected to laser ablation sampling.

Instrumentation

A femtosecond laser, equipped with Galvanometric mirrors (Jupiter Solid Nebulizer, ST Japan, Tokyo, Japan) was used as the laser ablation system in this study. The laser ablation technique was used as the sample introduction method to ablate a small amount of sample by focusing laser light onto the sample surface. Aerosols produced were transferred by an Ar gas stream at 0.3 L/min through a Tygon tube with FEP inner lining (Versilon™ SE-200, Saint-Gobain Performance Plastics, NJ, USA) to the ion source. The tube was 1 m in length, with a 6.4 mm o.d. and 3.2 mm i.d.

The ion source was an in-house atmospheric pressure plasma ion source. A schematic diagram of the instrumental setup is depicted in **Figure 1**. Plasma was produced by a dielectric barrier discharge (DBD). A quartz glass tube (o.d. 6 mm, i.d. 4 mm) was used as the body of the ion source. To produce a stable and homogeneous plasma, steel wool (internal electrode), acting as discharge stabiliser, was stuffed into the quartz tube, and 20 mm copper foil tape (external electrode) was wrapped around periphery of the quartz glass tube where the steel wool is. A copper wire (1 mm diameter), acting as cathode, was passed through the quartz tube and met with the steel wool. A high-voltage AC power supply, with frequency of 15–25 kHz (PCT-DFMJ-02AN, Plasma Concept Tokyo, Tokyo, Japan) was used to produce a plasma. A current of 20 mA and a peak-voltage of 10 kV was applied to the electrodes, while 0.6 L/min argon gas was flowed through the quartz tube, producing a plasma.

Prior to the ionisation by the atmospheric pressure plasma, laser induced sample particles were heated to evaporate the target molecules by passing through a heater made of a ceramic tube (o.d. 6 mm, i.d. 4 mm) with a Kanthal wire coiled around it. Organic molecules were evaporated and then ionised by collision with the reagent ions produced at the plasma. The resulting ions were then introduced into a hybrid dual quadrupole linear ion trap mass spectrometer (QTRAP 5500, AB SCIEX, Framingham, MA, USA). Vapur® interface (IonSense, Inc., Saugus, MA, USA) was applied to the mass spectrometer. A diaphragm vacuum pump (LABOPORT® N 810.3 FT.18, KNF Neuberger Inc., NJ, USA) was connected to the vacuum port of the Vapur® interface to introduce more ions into the mass spectrometer. All analyses were acquired in positive ion mode at 650 K.

Imaging Analysis

For the imaging analysis, a commercially available Animalin L pharmacetical tablet (Taisho Pharmaceutical Co., Ltd., Tokyo, Japan) was used. The tablet was embedded in a photocurable resin (Acryl-one #2100N, Maruto Instrument Co., Ltd., Tokyo

Japan) and exposed to light for one hour at room temperature. When the resin hardened, the sample was sectioned into half using IsoMet® 1000 (Buehler Ltd., IL, USA) and subjected to imaging analysis.

Analytical Procedure and Data Processing

Mass spectra were collected at a rate of 1000 Da/s, in the mass range of *m/z* 10–1000 using full scan mode (Q1). Galvanometric mirrors were used for fast repeated line scanning of the sample to give 15 s for each signal. The ablation area for each signal was 200 × 200 μm. Since high-purity samples were used, low laser conditions: fluence 1.5 J/cm^2, repetition rate 100 Hz were used to prevent contamination of the mass spectrometer. Data processing was performed using Analyst (Version 1.7.1). Background correction was made by subtraction of the signal intensity data obtained without sample introduction (gas blank).

For repeatability and reproducibility experiments, quantitative evaluation experiments, and imaging analysis, signal intensities at the specific *m/z* values were monitored using selected ion monitoring (SIM) mode to obtain time-resolved signal intensity profiles. Analytical procedure and laser conditions when conducting repeatability and reproducibility experiments were the same (fluence 1.5 J/cm^2, repetition rate 100 Hz, ablation area 200 × 200 μm). Dwell time per *m/z* was 100 ms. The measured signal intensities of each ablation area did not change much across the signal profile, thus, the signal intensity for each signal were calculated by integrating 10 s data.

For quantitative evaluation, solid mixing calibration method by implementing Galvanometric mirrors for fast-scanning of the laser on multiple solid materials was used[22, 23]. Two powder pellets were placed side-by-side in the laser cell: a target analyte (amino acid) and a TiO_2 (Kanto Chemical Co., Inc., Tokyo, Japan) pellet, for dilution purposes, were used to construct a calibration curve for each analyte. Laser ablation of the two materials was achieved with multiple laser ablation at different spots within very short time intervals. The mixing ratio of the two materials was adjusted by laser ablation with different proportion of number of laser shots onto the sample materials. This calibration protocol is explained in detail in previous studies[22, 23]. Fluence of 1.5 J/cm^2, repetition rate 1000 Hz was used. High repetition rate (*e.g.,* >1000 Hz) is needed for the resulting aerosols of the two samples to be mixed well within the laser ablation cell. The total number of laser shots was 1000 shots, ablation cycle was within 1 s and repeated 15 times. The number of shots were adjusted as follows: ratio of target analyte and TiO_2 ratios were 0/1000, 1/999, 2/998, 5/995 and 10/990. Analysis was repeated three times. Total time for the laser ablation was fixed to 15 s, and signal intensities for 10 s were integrated. The ablated zones for the target analyte and TiO_2 were measured by laser scanning confocal microscope (LEXT OLS3100, Olympus Corporation, Tokyo, Japan). Calibration curves were constructed based on the obtained signal intensities against the corrected concentration of the analyte.

Imaging analysis was conducted based on repeated line-profiling analysis across the sample with a raster speed of 50 μm/s. Fluence 1.2 J/cm^2 and repetition rate 2000 Hz was used for analysis. Data was acquired in SIM mode and dwell time per *m/z* was 50 ms. The raw data were exported as text files (.txt) and converted to comma separated values (CSV) formatted files. The data saved as the CSV format were then transported to an in-house software, iQuant2 for visualisation of the distribution of ingredients in the tablet[24]. Background correction was also carried out using the iQuant2 software.

Results and Discussion

Characterisation of Ionisation Process

Representative mass spectra of the LA-DBDI-MS are shown in **Figure 2**. **Figures 2(a)–(c)** show the mass spectra of three amino acids and table sugar (sucrose). The base peaks of $[M + H]^+$ were observed for the amino acids. Fragments such as $[M - HCOOH + H]^+$ were also observed. The fragments observed in the mass spectra were consistent with fragmentation mechanism of amino acids reported in previous studies[25,26]. Moreover, the patterns of the mass spectra were similar with those obtained experimentally with dielectric barrier discharge by analysing amino acids deposited on filter paper[9].

As for the mass spectrum of sucrose (**Figure 2(d)**), the dominant ion was the ammonium adduct $[M + NH_4]^+$ of the parent molecule instead of being protonated. Similar to the mass spectra of amino acids, fragments were observed. Polar molecules are known to form ammonium adducts[27]. Since sucrose is a polar molecule, ammonium adduct of the molecule is formed more readily instead of the protonated molecule. All of the obtained mass spectra in **Figure 2** were similar to those obtained by DART-MS[28,29].

This study utilised a femtosecond laser, rather than nanosecond lasers usually used in previous studies for atmospheric pressure

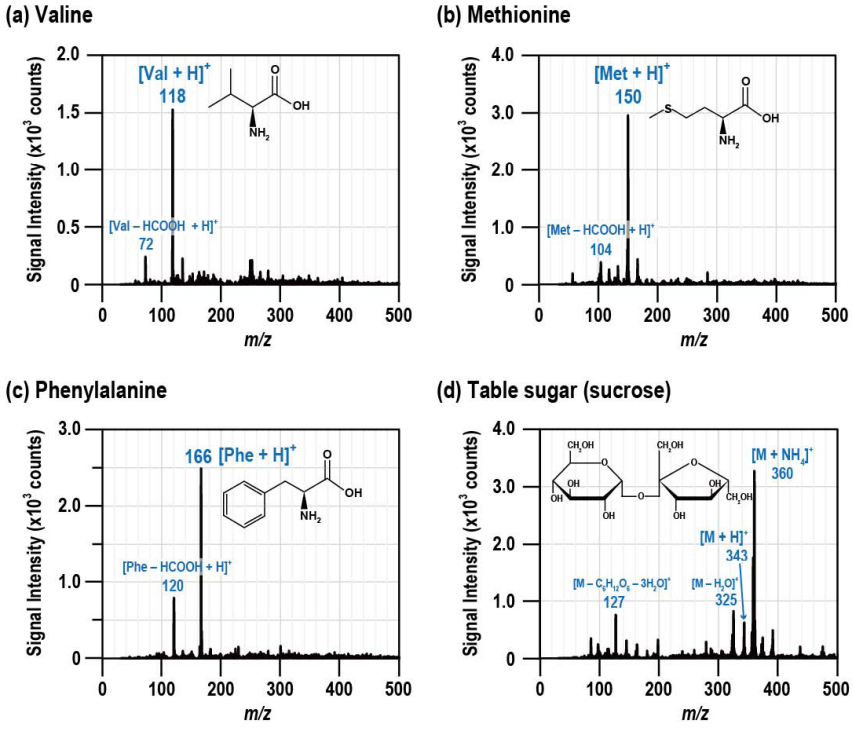

Figure 2. Mass spectra of different analytes, (a) valine, (b) methionine, (c) phenylalanine and (d) table sugar (sucrose) recorded by LA-DBDI-MS. Laser conditions were as follows: fluence 1.5 J/cm^2, repetition rate 100 Hz and ablation area being 200 × 200 µm.

plasma-based ion source (*i.e.,* FAPA, APCI, DBDI, and DART)[30,33]. The mass spectra obtained in this study had a similar trend with the previous studies, *i.e.,* protonated molecules or ammonium adducts of the molecules are detected as base peaks, with slight fragmentation. This shows that the degree of fragmentation was independent on the pulse width of the laser. Instead, neutral molecules and small particles are mainly produced during the laser ablation process[34]. Meanwhile, the tendency of the production of fragments increases as the supplemental heating temperature increases[32].

Repeatability

To test the repeatability of the measurements, the signal intensity profile was acquired by the repeated-analysis from separated nine areas on a valine pellet. **Figure 3** illustrates the signal intensity profile of valine at *m/z* 118. The washout time for each signal was long, due to the low Ar carrier gas flow rate for aerosols, preventing the aerosols to be efficiently flushed out of the laser cell. The use of a higher carrier gas flow rate was hindered due to the configuration of the instrumental setup, which can be improved with further modifications to the system.

The mean counts of ion signals at *m/z* 118 was (197.3 ± 12.6) × 10^3 counts (N = 9, SD), suggesting that the repeatability of 6% could be achieved. The major cause of the variation of the signal intensities could be due to difference in the sampling mass of the sample powder through laser ablation. In fact, magnitude of variation found in this study was comparable with those obtained by elemental analysis of powder pellet with LA-ICP-MS[35]. There could also be other causes of variations in the measured signal intensity, such as discharge current of the DBDI, temperature of the ceramic heater, or stability of mass spectrometer. Unfortunately, the evaluation of stability for these parameters are difficult, so these must be left as a possibility. In this study, we take the repeatability of signal intensity profile defined by the repeated analysis as the stability of overall system setup.

Signal Output Linearity

A correlation between signal intensity of the analytes and concentration is required to achieve accurate quantitative analysis. In this study, signal intensities of various concentrations were monitored for (a) valine, (b) methionine, and (c) phenylalanine (**Figure 4**). The concentration of the analytes was adjusted by the dilution with TiO_2 through the solid sample mixing using

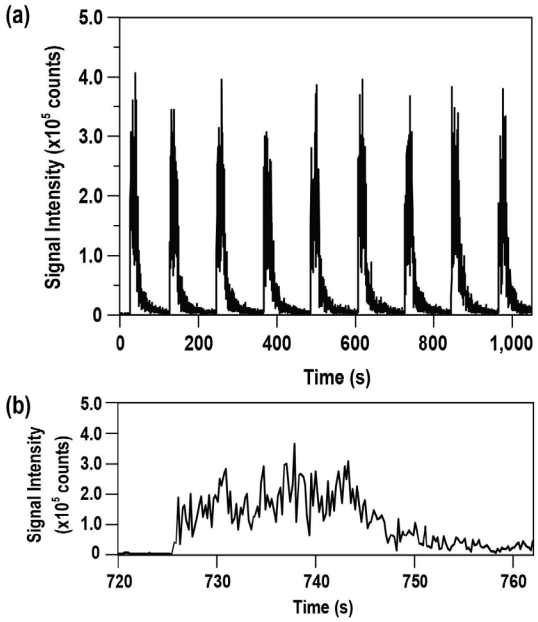

Figure 3. Signal intensity profile of valine measured at *m/z* 118: (a) signal intensity profile obtained from nine different areas, and (b) an enlargement figure of a signal. Laser was irradiated on the sample for 15 s to create a signal.

the multiple-spot ablation[18, 19]. Mass of the analyte and TiO_2 was separately defined from the volume of each analysis, and the sampling mass was calculated based on equation (1), under the assumption that the density of each pellet is equal to the density of their respective bulks.

$$m = C \times V \times \rho \quad (1)$$

Here, m, C, and V represent the mass of the ablated material (g), concentration of the analyte (g/g), and volume of the ablated material (cm^3), respectively. ρ denotes the density of the analyte (g/cm^3). Concentration of the analyte was assumed to be >0.99 g/g for all samples based on their purity provided by the manufacturer. The volumes of the ablated materials were obtained by a laser scanning confocal microscope. The calculated mass of the target analyte was then divided by total ablated mass (mass of target analyte + mass of TiO_2) to calculate the concentration values. The resulting signal intensity were plotted against concentration to obtain the calibration curves. Each data point was repeated for three times, and errors bars were 2SD. Good linear correlations were found for all the amino acids. Moreover, the small error bars indicate that the aerosols of both materials (*i.e.,* target analyte and TiO_2) were mixed well within the laser ablation cell. Variation in hardness of pellets resulted in the difference in the final concentrations of each target analyte even though the same number of laser shots were used on all the three analytes. Besides that, the difference in ablation efficiency between the target analyte and TiO_2, as well as the variation in transport efficiency of the ablated material into the mass spectrometer may have resulted in the deviation of the data points from the calibration lines and the ion detection response. The limits of detection for each analyte were determined as follows: 626 μg/g for valine, 668 μg/g for methionine, and 612 μg/g for phenylalanine. The above findings indicate that quantification is possible with the present LA-DBDI-MS system. Furthermore, our results are the first example of successfully constructing calibration lines of signal intensity response against concentration, compared to previous studies where laser ablation was coupled with a DBD ion source[32, 36, 37].

Imaging Analysis

Finally, LA-DBDI-MS was applied for the imaging analysis of solid materials. A commercially-available Animalin L tablet was used as the sample. The cross section of the severed tablet (**Figure 5(a)**) has a boiled-egg-like structure, showing a white outer shell and a yellow inner core. This tablet is a sugar-coated tablet, which explains the white outer shell. The yellow inner core is

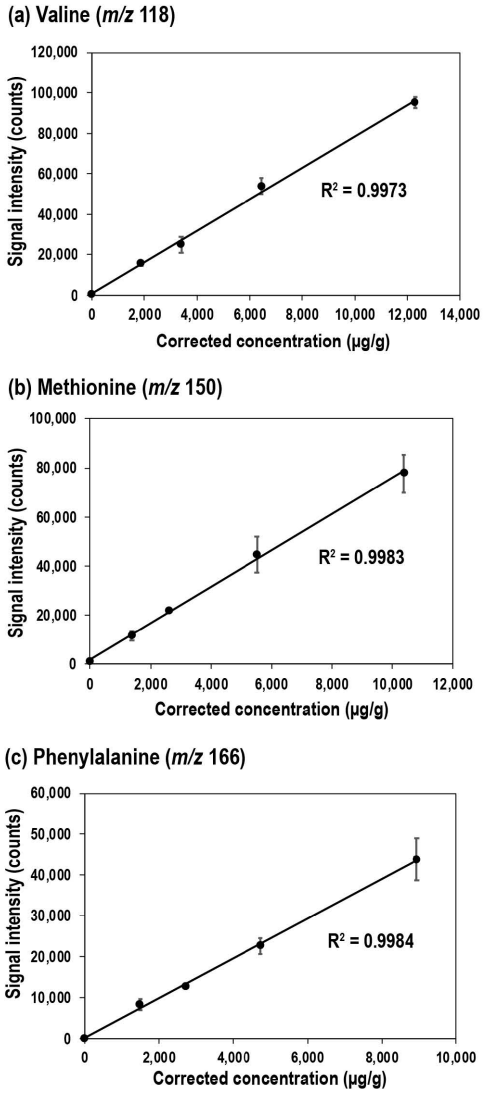

Figure 4. Calibration curve of different analytes obtained with the solid mixing protocol. Analytes are (a) valine, (b) methionine and (c) phenylalanine. The concentration of each analyte was changed by mixing the aerosols of different proportions of analyte and TiO_2 pellet using solid mixing protocol. Number of replicates per data point was three and error bars represent two standard deviations.

the active ingredients, containing amino acids and vitamins.

Prior to the imaging analysis, peak identification was carried out. **Figures 6(a)** and **6(b)** illustrate the mass spectrum obtained from the centre and edge of the tablet, respectively. The mass spectrum of the shell (**Figure 6(a)**) has a similar pattern with table sugar (sucrose) from **Figure 2(d)**, as well as reports from pharmaceutical manufacturers stating that the ingredient used in sugar-coated tablets is mainly sucrose[38]. For the mass spectrum obtained from central part of the tablet (**Figure 6(b)**), several peaks at 118, 120, 132, 266, and 377 were detected. Based on the ingredients list by the manufacturer, these peaks originated from valine, threonine, leucine/isoleucine, vitamin B_1, and vitamin B_2, respectively. Other amino acids, such as methionine (*m/z* 150), phenylalanine (*m/z* 166), and tryptophan (*m/z* 205) were detected as well (imaging results not shown). Unfortunately, we were unable to distinguish between leucine and isoleucine due to these amino acids being isomers (both having molecular weight of 131.17). Peak assignment of the various ingredients is summarised in **Table 1**.

Next, the imaging analyses of sucrose, valine, threonine, leucine/isoleucine, vitamin B_1, and vitamin B_2 were carried out by the present system setup. The resulting imaging analysis are shown in **Figures 5(b)–5(g)**. Based on the imaging results, sucrose (detected as *m/z* 360) was distributed at the outer edges of the tablet, whereas all ingredients were heterogeneously distributed within the tablet, suggesting of formation of preferential enrichment of the ingredients within the tablet. The total analysis time

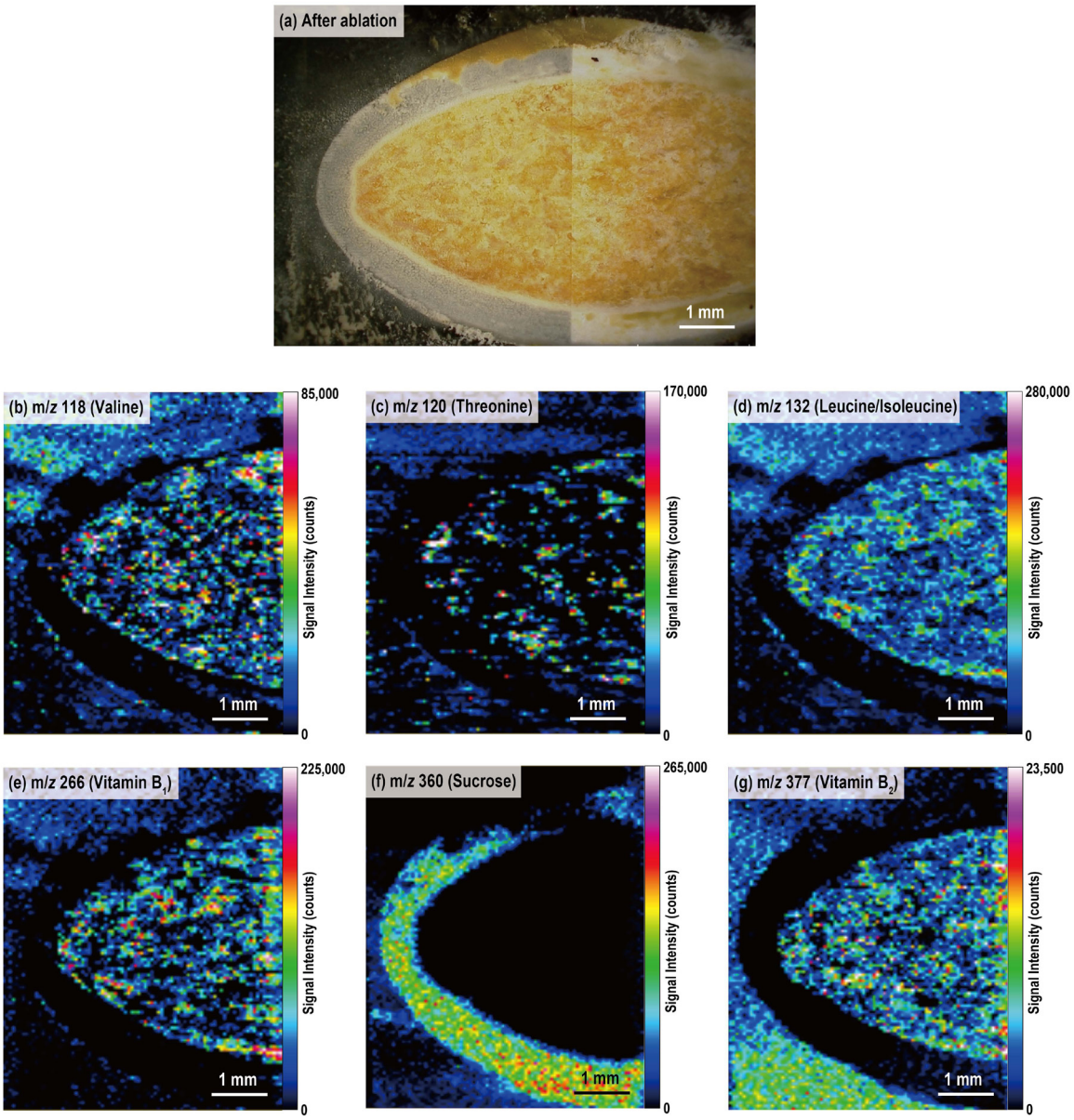

Figure 5. Imaging results of Animalin L tablet. Cross-section of tablet (a) after imaging analysis. Ablation area was (W) 4.8 mm × (H) 5.5 mm. (b)–(g) shows the distribution of ingredients within the tablet.

for the imaging analysis was around 2.5 hours, with the time lengthen due to long washout time. Analysis time can be further shortened when improvements to the system is made.

Amino acids are an important class of metabolites which are involved in cell signalling, nutrition and disease therapy[40, 41]. On the other hand, sucrose is an essential biomarker to assess sugar uptake associated with diseases such as metabolic syndrome, obesity, and cardiovascular problems[41]. Knowledge of the spatial distribution of these molecules enhances our understanding of pharmacology and toxicology mechanisms, contributing to drug development. The above results demonstrated that LA-DBDI-MS can be an analytical method to study the distribution of low-molecular-weight compounds in solid samples.

Conclusion

This work has demonstrated that coupling laser ablation with an atmospheric pressure plasma-based ion source is possible for mass spectrometry imaging of organic compounds. Mass spectra of organic compounds obtained in this study showed that the ion source developed primarily ionises sample material into protonated molecular ions and ammonium adducts of the molecular

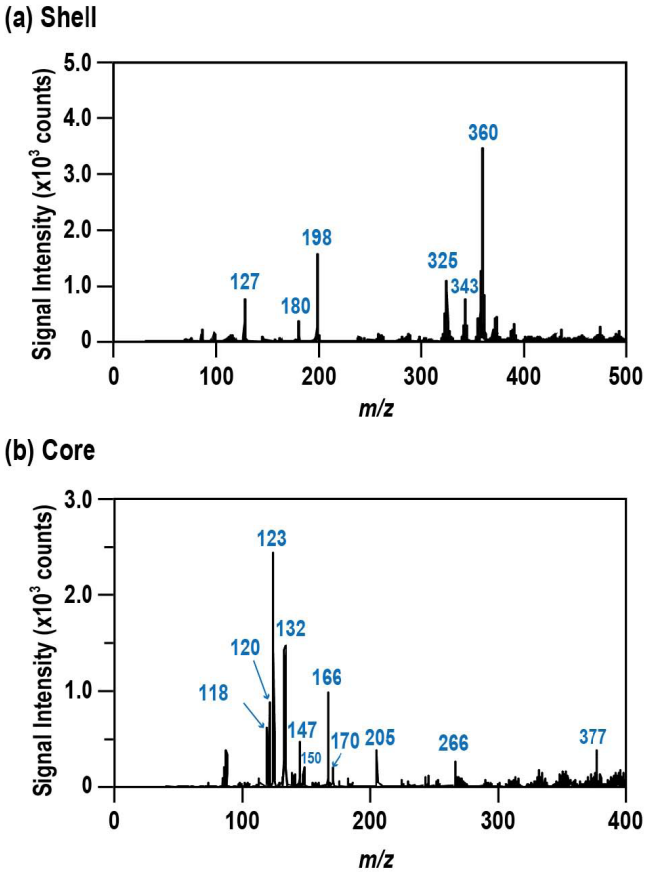

Figure 6. | Mass spectra of the (a) shell and (b) core of the tablet.

Table 1. | List of ions at the core of the tablet and their corresponding ingredients.

Detected *m/z*	Ingredient	Molecular weight
118	Valine	117.15
120	Threonine	119.12
123	Nicotinamide (Vitamin B_3)	122.12
132	Leucine Isoleucine	131.17
147	Lysine	146.19
150	Methionine	149.21
166	Phenylalanine	165.19
170	Pyridoxine (Vitamin B_6)	169.18
205	Tryptophan	204.22
266	Thiamine (Vitamin B_1)	265.35
377	Riboflavin (Vitamin B_2)	376.36

ions with few fragments. This indicates that although DBDI is not as soft as ionisation methods such as MALDI or electrospray ionisation (ESI), it is definitely softer than electron impact (EI). LA-DBDI-MS gives good stability and repeatability, as well as good quantitative capability. Limits of detection were rather high, at above 600 μg/g for all measured analytes, but sensitivity could be improved by using helium to generate plasma or modifying the configuration of the laser ablation and ion source. Finally, this preliminary work shows that rapid imaging analysis of pharmaceuticals is promising, which does not require any solvent or matrices, allowing us to analyse solid samples in their native state. Future works will involve combining the current instrumentation with LA-ICP-MS to simultaneously obtain spatial information on elements through a single analysis. We hope that through this future work, we will be able to provide visualised data on the distribution of elements and organic compounds, as well as provide a metallomics perspective on the interaction of elements with organic compounds within biological samples.

Acknowledgements

We are grateful to the following people for their support, without whose help this work would never have been possible: Takahiro Kanamori and Yoshihiro Ichido from Eurofins Analytical Science Laboratories, Inc. for providing the mass spectrometer as well as scientific advice, Tetsuya Tamaki (Next Lab) for technical assistant of the laser system, Takao Nishiguchi (BioChromato, Inc.) for technical support on the Vapur® interface used in this study, Prof. Hiroyuki Kagi (The Univ. of Tokyo) for scientific advice and technical assistance of the laser scanning confocal microscope, and Shuji Yamashita (The Univ. of Tokyo) for critical reading the manuscript. This work was financially supported by a Grant-in-Aid for Scientific Research (JP 19H01081 and JP 21H04511) from the Ministry of Education, Culture, Sports, Science and Technology, Japan.

References

[1] Hanash S: Disease proteomics. Nature 422: 226–232, 2003.

[2] Roher AE, Weiss N, Kokjohn TA, Kuo Y, Kalback W, Anthony J, Watson D, Luehrs DC, Sue L, Walker D, Emmerling M, Goux W, Beach T: Increased Aβ Peptides and Reduced Cholesterol and Myelin Proteins Characterize White Matter Degeneration in Alzheimer's Disease. Biochemistry 41(37): 11080–11090, 2002.

[3] Niziol J, Sunner J, Beech I, Ossolinski A, Ossolinski T, Plaza A, Ruman T: Localization of Metabolites of Human Kidney Tissue with Infrared Laser-Based Selected Reaction Monitoring Mass Spectrometry Imaging and Silver-109 Nanoparticle-Based Surface Assisted Laser Desorption/Ionisation Mass Spectrometry Imaging. Anal. Chem. 92(6): 4251–4258, 2020.

[4] Caprioli RM, Farmer TB, Gile J: Molecular Imaging of Biological Samples: Localization of Peptides and Proteins Using MALDI-TOF MS. Anal. Chem. 69(23): 47514760, 1997.

[5] Pacholski ML, Winograd N: Imaging with Mass Spectrometry. Chem. Rev. 99(10): 2977–3005, 1999.

[6] Takáts Z, Wiseman JM, Gologan B, Cooks RG: Mass spectrometry sampling under ambient conditions with desorption electrospray ionisation. Science 306: 471–473, 2004.

[7] Cody RB, Larameé JA, Durst HD: Versatile new ion source for the analysis of materials in open air under ambient conditions. Anal. Chem. 77(8): 2297–2302, 2005.

[8] Andrade FJ, Shelley JT, Wetzel WC, Webb MR, Gamez G, Ray SJ, Hieftje GM: Atmospheric Pressure Chemical Ionisation Source. 1. Ionisation of Compounds in the Gas Phase. Anal. Chem. 80(8): 2646–2653, 2005.

[9] Na N, Zhao M, Zhang S, Yang C, Zhang X: Development of a dielectric barrier discharge ion source for ambient mass spectrometry. J. Am. Soc. Mass Spectrom. 18(10): 1859–1862, 2007.

[10] Harper JD, Charipar NA, Mulligan CC, Zhang X, Cooks RG, Ouyang Z: Low-temperature plasma probe for ambient desorption ionisation. Anal. Chem. 80(8): 9097–9104, 2008.

[11] Horning EC, Horning MG, Carroll DI, Stillwell RN: New Pictogram Detection System Based on a Mass Spectrometer with an External Ionisation Source at Atmospheric Pressure. Anal. Chem. 45(6): 936–943, 1973.

[12] Molnar BT, Shelley JT: Modern Plasma-based Desorption/Ionisation: From Atoms and Molecules to Chemical Synthesis. Mass Spectrom. Rev. 40(5): 609–627, 2020.

[13] Gray AL: Solid Sample Introduction by Laser Ablation for Inductively Coupled Plasma Source Mass Spectrometry. Analyst 110: 551–556, 1985.

[14] Becker JS, Zoriy M, Matusch A, Wu B, Salber D, Palm C, Becker JS: Bioimaging of metals by laser ablation inductively coupled plasma mass spectrometry (LA-ICP-MS). Mass Spectrom. Rev. 29(1): 156–157, 2010.

[15] Koch J, Günther D: Review of the state-of-the-art of Laser Ablation Inductively Coupled Plasma Mass Spectrometry. Appl. Spectrosc.

65(5): 155A–162A, 2011.

[16] Makino Y, Ohara S, Yamada M, Mukoyama S, Hattori K, Sakata S, Tanaka Y, Suzuki T, Shinohara A, Matsukawa T, Yokoyama K, Hirata T. Quantitative Elemental Bioimaging Protocol using Femtosecond-Laser Ablation-ICP-Mass Spectrometry Coupled with Glass Standard Reference Material. Ogra & Hirata (ed): Metallomics. Recent Analytical Techniques and Applications. Springer, Tokyo, 2017, 93–106.

[17] Wang S, Brown R, Gray DJ: Application of Laser Ablation-ICPMS to the Spatially Resolved Micro-analysis of Biological Tissue. Appl. Spectrosc. 48(11): 1321–1325, 1994.

[18] Koch J, von Bohlen A, Hergenröder R, Niemax K: Particle size distributions and compositions of aerosols produced by near-IR femto-and nanosecond laser ablation of brass. J. Anal. At. Spectrom. 19: 267–272, 2004.

[19] Hergenröder R, Samer O, Hommes V: Femtosecond laser ablation elemental mass spectrometry. Mass Spectrom. Rev. 25: 551–572, 2006.

[20] Fernández B, Claverie F, Pécheyran C, Donard OFX: Direct analysis of solid samples by fs-LA-ICP-MS. Trends in Anal. Chem. 26(10): 951–966, 2007.

[21] Poitrasson F, d'Abzac FX: Femtosecond laser ablation inductively coupled plasma source mass spectrometry for elemental and isotopic analysis: are ultrafast lasers worthwhile? J. Anal. At. Spectrom. 32: 1075–1091, 2017.

[22] Yokoyama TD, Suzuki T, Kon Y, Hirata T: Determinations of Rare Earth Element Abundance and U-Pb Age of Zircons U-Pb Age of Zircons Using Multispot Laser Ablation-Inductively Coupled Plasma Mass Spectrometry. Anal. Chem. 83(23): 8892– 8899, 2011.

[23] Makino Y, Kuroki Y, Hirata H: Determination of major to trace elements in metallic materials based on the solid mixing calibration method using multiple spot-laser ablation-ICP-MS. J. Anal. At. Spectrom. 34(9): 1794–1799, 2019.

[24] Suzuki T, Sakata S, Makino Y, Obayashi H, Ohara S, Hattori K, Hirata T: iQuant2: Software for Rapid and Quantitative Imaging using Laser Ablation-ICP Mass Spectrometry. J. Mass Spectrom. 7(1): A0065, 2018.

[25] Klassen JS, Kebarle P: Collision-Induced Dissociation Threshold Energies of Protonated Glycine, Glycinamide, and Some Related Small Peptides and Peptide Amino Amides. J. Am. Chem. Soc. 119(28): 6552–6563, 1997.

[26] O'Hair RA, Broughton PS, Styles ML, Frink BT, Hadad CM: The Fragmentation Pathways of Protonated Cycline: A Computational Study. J. Am. Chem. Soc. 11(8): 687– 696, 2000.

[27] Cody RB: Observation of Molecular Ions and Analysis of Nonpolar Compounds with the Direct Analysis in Real Time Ion Source. Anal. Chem. 81(3): 1101–1107, 2009.

[28] Sekimoto K, Sakakura M, Kawamukai T, Hike H, Shiota T, Usui F, Bando Y, Takayama M: Ionisation characteristics of amino acids in direct analysis in real time mass spectrometry. Analyst 139: 2589–2599, 2014.

[29] Wang Y, Liu L, Ma L, Liu S: Identification of saccharides by using direct analysis in real time (DART) mass spectrometry. Int. J. Mass. Spectrom. 357: 51–57, 2014.

[30] Shelley JT, Ray SJ, Hieftje GM: Laser Ablation Coupled to a Flowing Atmospheric Pressure Afterglow for Ambient Mass Spectral Imaging. Anal. Chem. 80(21): 8308–8313, 2008.

[31] Herdering C, Reifschneider, Wehe CA, Sperling M, Karst U: Ambient molecular imaging by laser ablation atmospheric pressure chemical ionisation mass spectrometry. Rapid Commun. Mass Spectrom. 27(23): 2595–2600, 2013.

[32] Gilber-López B, Schilling M, Ahlmann N, Michels A, Hayen H, Molina-Díaz A, García-Reyes, Franzke J: Ambient Diode Laser Desorption Dielectric Barrier Discharge Ionisation Mass Spectrometry of Nonvolatile Chemicals. Anal. Chem. 85(6): 3174–3182, 2013.

[33] Fowble KL, Teramoto K, Cody RB, Edwards D, Guarrera D, Musah RA: Development of "Laser Ablation Direct Analysis in Real Time Imaging" Mass Spectrometry: Application to Spatial Distribution Mapping of Metabolites Along the Biosynthetic Cascade Leading to Synthesis of Atropine and Scopolamine in Plant Tissue. Anal. Chem. 89(6): 3421–3429, 2017.

[34] Conzemius RJ, Capellen JM: A review of the applications to solids of the laser ion source in mass spectrometry. Int. J. Mass Spectrom. Ion Phys. 34(3–4): 197–271, 1980.

[35] Kon Y, Hirata T: Determination of 10 major and 34 trace elements in 34 GSJ geochemical reference samples using femtosecond laser ablation ICP-MS. Geochem. J. 49(4): 351–375, 2015.

[36] Bierstedt A, Riedel J: High-repetition rate laser ablation coupled to dielectric barrier discharge postionisation for ambient mass spectrometry. Methods 104: 3–10, 2016.

[37] Funke SKI, Brückel VA, Weber M, Lützen E, Wolf JC, Haisch C, Karst U: Plug-and-play laser ablation-mass spectrometry for molecular imaging by means of dielectric barrier discharge ionisation: Analytica Chimica Acta 1177: 338770, 2021.

[38] Hogan JE. Sugar Coating. Cole G (ed): Pharmaceutical Coating Technology. Taylor & Francis, London, 1995, 53–64.

[39] Wu G: Functional Amino Acids in Growth, Reproduction, and Health. Adv. Nutr. 1(1): 31–37, 2010.

[40] Huang C, McConathy J: Radiolabeled Amino Acids for Oncologic Imaging. J. Nucl. Med. 54(7): 1007–1010, 2013.

[41] Tasevska N: Urinary sugar – a biomarker of total sugars intake. Nutrients 7: 5816–5833, 2015.

Editor's note

We are delighted to introduce the first issue of *Metallomics Research* as a new official journal of the Japan Society for Biomedical Research on Trace Elements. In this first issue, Prof. Yasumitsu Ogra, a president of the Japan Society for Biomedical Research on Trace Elements, contributed an introduction about the start of *Metallomics Research*. Prof. Hiroki Haraguchi, the founder of "metallomics", contributed the historical overviews and future perspectives about metallomics. Furthermore, many scientists have kindly contributed to this issue in their various fields including medicine, biology, toxicology, analytical chemistry, environmental science, pharmaceutical science, and so on. We thank all of the authors, reviewers, and executive office members for their significant contribution about this new journal. *Metallomics Research* is a small seed at the present time, however, we hope *Metallomics Research* will grow up into a big tree which connects numerous scientists in various research field and provide a good platform. We kindly ask to submit your valuable results to *Metallomics Research*.

Masahiro KAWAHARA, Ph D.
Editor in Chief
Metallomics Research